Mining bacteria for hopanoids and genomic insights of hopanogenesis; A critical analysis of global transcriptional response of *shc* mutant of *Rhodopseudomonas palustris* TIE-1

A Thesis Submitted

to

UNIVERSITY OF HYDERABAD

Hyderabad, India

For the Degree of

DOCTOR OF PHILOSOPHY

By

TUSHAR LODHA

(Reg. No. 11LPPH08)

Department of Plant Sciences
School of Life Sciences
University of Hyderabad
Hyderabad-500 046
Telangana, India

MARCH 2017

University of Hyderabad
(A central University established in 1974 by Act of Parliament)
School of Life Sciences
Department of Plant Sciences
Hyderabad-500046

DECLARATION

I, Tushar Lodha hereby declare that this thesis entitled "**Mining bacteria for hopanoids and genomic insights of hopanogenesis; A critical analysis of global transcriptional response of *shc* mutant of *Rhodopseudomonas palustris* TIE-1**" submitted by me under the supervision of **Prof. Ch. Venkata Ramana** is an original and independent research work. I also declare that it has not been submitted previously in part or in full to this University or any other University or Institution for the award of any degree or diploma. The particulars given in this thesis are true to the best of knowledge and belief.

Supervisor
Prof. Ch. Venkata Ramana

Name: Tushar Lodha
Reg. No.:11LPPH08

University of Hyderabad
(A central University established in 1974 by Act of Parliament)
School of Life Sciences
Department of Plant Sciences
Hyderabad-500046

CERTIFICATE

This is to certify that this thesis entitled "**Mining bacteria for hopanoids and genomic insights of hopanogenesis; A critical analysis of global transcriptional response of *shc* mutant of *Rhodopseudomonas palustris* TIE-1**" submitted by Tushar Lodha, bearing registration number 11LPPH08 in partial fulfillment of the requirements for award of Doctor of Philosophy in the School of Life Sciences is a bonafide work carried out by him under my supervision and guidance.

This thesis is free from plagiarism and has not been submitted previously in part or in full to this or any other University or Institution for award of any degree or diploma.

Parts of this thesis have been published in the following journals;

1. Antonie van Leeuwenhoek (1 publication)
2. Archives of Microbiology (1 publication)
3. DNA Research (1 publication)
4. Genome announcements (2 publications)
5. International Journal of Systematic and Evolutionary Microbiology (17 publications)
6. Systematic and Applied Microbiology (1 publication)

Further, the student has passed the following courses towards fulfillment of coursework reqirements for Ph.D

Course Code	Name	Credits	Pass/Fail
1. PL 801	Seminar	1	Pass
2. PL 802	Research Ethic & Mangment	2	Pass
3. PL 803	Biostatics	2	Pass
4. PL 804	Analytical Techiques	3	Pass
5. PL 805	Lab Work	4	Pass

Supervisor **Head of the Department** **Dean of the School**

ACKNOWLEDGEMENT

As the no work on the mother earth is a solo effort and this work is also not the exception! I take this opportunity to thank everyone who helped me in the journey of Ph.D.

I express my overwhelming sense of gratitude to my supervisor ***Prof. Ch. Venkata Ramana,*** *for his acceptance to my request and allowing me to work in his lab. His continuous encouragement, stimulating guidance and moral support enabled me to complete research work successfully. The blessing, help and advice given by him time to time shall carry me a long way in the journey of life on which I am about to embark.*

I would like to thank Doctoral Committee members, ***Prof. Appa Rao Podile*** *and* ***Prof. K.P.M.S.V. Padmasree****, for their cordial support, valuable suggestions and guidance throughout my research work.*

I extend my sincere and heartfelt gratitude to present Head of the Department of Plant Sciences ***Prof. Ch. Venkata Ramana*** *and former Head,* ***Prof. A. R. Reddy*** *for providing the necessary departmental facilities for the smooth conduction of research work.*

I feel privileged to be a part of this prestigious University. I am thankful to the Dean, ***Prof. P Reddanna,*** *and former Deans,* ***Prof. M. Ramanadham, Prof. A. S. Raghavendra, Prof. Aparna Dutta Gupta,*** *School of Life Sciences, University of Hyderabad, for giving me the opportunity and support throughout my work.*

My greatest gratitude goes to ***Prof. Ch. Sasikala****, JNTU, Hyderabad, for sharing bacterial cultures, generous support extending her lab facilities to utilize during my research work.*

I extend my sincere thanks to all the ***faculty members*** *of School of Life Sciences, for permitting me to use the research facilities.*

I am extremely grateful to ***my teachers****, who taught me just not science, also ethics and morals in life.*

My special thanks to all ***non-technical staffs****, for their co-operation throughout my study.*

*I am extremely happy to gratefully acknowledge **my present and former lab mates** for their friendly association, encouragement, suggestions, care and help offered to me.*

*I am thankful to **Prof. D.K. Newman,** Division of Geological and Planetary Sciences, California Institute of Technology, California and **Dr. Paula Welander**, Earth System Science, Stanford University, California for sharing hopanoid biosynthetic mutants with us.*

*I acknowledge **Dr. M. Blumenberg,** Geoscience Centre, University of Gottingen, Germany and **Mr. Prashanth Bitla,** NIPER, Hyderabad for timely advising in the identification of hopanoids.*

*I extend my sincere and heartfelt thanks to **Dr. Nagalakshmi N**, Melaka Manipal Medical College, Manipal for providing clinical isolates of Staphylococcus spp.*

*I acknowledge the **UGC** for providing me research fellowship. **CSIR**, **DST-FIST, UGC-SAP, DBT-CREEB** are acknowledged for school and departmental facilities.*

*My heartfelt thanks to all **my friends** for their care, support and encouragement throughout research work.*

*I have no words to put across gratefulness to **my parents**; this work should serve as a small token for their unconditional love, encouragement and support. I never would have made it this far without them. I would also like to apologize for all the inconvenience caused to them during my research work.*

*My deepest gratitude goes to **my brothers** and **family members** for their co-operation, love, support and inspiration throughout my life.*

All that I cherish today is the grace of God. I thank the Almighty God for answering my prayers, for granting me the strength, wisdom, knowledge and showering his blessings upon me during research work.

I am thankful to one and all who helped me directly or indirectly at every stage of my research work.

I dedicate this thesis to my mother, family members and supervisor.

Tushar Lodha

CONTENTS

LIST OF ABBREVIATIONS

Abbreviations	Expansion
µl	Microliter
µM	Micromolar
^{0}C	Degree Celsius
^{0}C.min^{-1}	Degree Celsius per minute
aminotriol	35-aminobacteriohopane-32, 33, 34-triol
ATCC	American Type Culture Collection
ATP	Adenosine triphosphate
BHD	Bacteriohopane derivative
BHP	Bacteriohopanepolyol
BHT	Bacteriohopanetetrol
BLAST	Basic Local Alignment Search Tool
bp	Base pair
CCBAU	Culture Collection of Beijing Agricultural University
CCCP	Carbonyl cyanide m-chlorophenyl hydrazine
cDNA	Complementary deoxyribonucleic acid
CDP-ME	4-diphosphocytidyl-2C-methyl-D-erythritol
CDP-ME2P	4-diphosphocytidyl-2C-methyl-D-erythritol-2-phosphate
CoA	Coenzyme-A
CRAC	Cholesterol recognition amino acid consensus
cRNA	Complementary ribonucleic acid
CTP	Cytidine triphosphate
DAVID	Database for Annotation, Visualization, and Integrated Discovery
DMAPP	Dimethylallyl diphosphate
DMSO	Dimethyl sulfoxide
DNA	Deoxyribonucleic acid
DOXP	1-deoxy-D-xylulose 5-phosphate
DPE	Diploptene
DPL	Diplopterol
DSMZ	Deutsche Sammlung von Mikroorganismen und Zellkulturen GmbH
EDTA	Ethylenediamine tetra-acetic acid
ESI	Electrospray ionization
eV	Electron volt
FAD	Flavin adenine dinucleotide
FC	Fold change

Abbreviations	Expansion
$g.l^{-1}$	Gram per liter
GC-MS	Gas chromatography mass spectrophotometry
GEO	Gene Expression Omnibus
GO	Gene Ontology
h	Hour
H33342	Hoechst 33342
HEPES	4-(2-hydroxyethyl)-1-piperazineethanesulfonic acid
HMG	3-hydroxy-3-methylglutaryl
IPP	Isopentenyl pyrophosphate/ Isopentenyl diphosphate
I-TASSER	Iterative Threading Assembly Refinement
iTOL	Interactive tree of life
kb	Kilo base
kcal/mol	Kilocalorie per mole
KCTC	Korean Collection for Type Cultures
KEGG	Kyoto encyclopedia of genes and genomes
LMG	Laboratorium voor Microbiologie
M	Molar
m/z	Mass-to-charge ratio
MAGUK	Membrane associated guanylate kinase
Mb	Mega base pairs
MECP	2C-methyl-D-erythritol-2,4-cyclodiphosphate
MEGA	Molecular Evolutionary Genetics Analysis
MEP	2-C-methyl-D-erythritol 4-phosphate
MFS	Major facilitator superfamily
mg	Milligram
min	Minute
ml	Milliliter
mM	Millimolar
MPP	Membrane Palmitoylated Protein
mRNA	Messenger Ribonucleic Acid
MS/MS	Mass spectrometry/Mass spectrometry
MVA	Mevalonate
NCBI	National Center for Biotechnology information
nm	Nanometer
NPN	N-phenylnaphthylamine

Abbreviations	Expansion
OD	Optical density
ORF	Open reading frame
PBS	Phosphate buffer saline
PCA	Principal component analysis
PCR	Polymerase chain reaction
PROSESS	Protein Structure Evaluation Suite & Server
qPCR	Quantitative polymerase chain reaction
RAST	Rapid Annotation using Subsystem Technology
Rdv.	*Rhodovulum*
RIN	RNA integrity number
Rmi.	*Rhodomicrobium*
RNA	Ribonucleic acid
RND	Resistance nodulation cell division
Rpl.	*Rhodoplanes*
Rps.	*Rhodopseudomonas*
rRNA	Ribosomal ribonucleic acid
s	Seconds
SD	Standard deviation
shc/SHC	Squalene hopene cyclase gene / Squalene hopene cyclase protein
TBDT	TonB dependent transport system
TRAP	Tripartite ATP-dependent periplasmic
tRNA	Transfer ribonucleic acid
UV	Ultra Violet
V	Volts
v/v	Volume per volume
w/v	Weight per volume
WT	Wild type

ABSTRACT

Hopanoids are isoprenoid lipids, biosynthesized primarily by bacteria as cell membrane component, play a key role in rigidifying membrane and act as analogous to sterols which are components of eukaryotic membranes. Hopanoids are among the most widespread of all complex natural products and are probably essential constituents of many prokaryotes. Though not extensively studied, hopanoids contribute to the membrane stability, membrane permeability, cell cycle, plant microbe interaction, resistance to antibiotics and help in stress tolerance. However, the role of hopanoids is not conclusively elucidated and the extent to which they are sterol surrogate remains an open question. Therefore, a robust interpretation of phylogenetic distribution and cellular function of hopanoid is required to better understand their physiological significance. This part of the work aimed at mining bacteria for the presence of hopanoids and deciphering the hopanoid biosynthetic pathway. In addition, the present study also looked into the cellular response of a hopanoid deficient mutant of *Rhodopseudomonas palustris* TIE-1 using genome-wide transcriptome analysis.

Biohopanoids can be synthesized by bacteria as well as few eukaryotes and can be used as molecular fossils. Therefore, it is significant to know the distribution of hopanoid biomarkers and source specific information. In the present study, 86 bacterial species representing 24 genera were screened for hopanoids. The distribution of hopanoid is heterogeneous among the screened bacteria i.e., few members have hopanoids whereas the phylogenetically close member did not show any detectable hopanoid. But it is too early to conclude about the distribution of hopanoids as still many bacterial members are not screened for hopanoids. Therefore, there is need to screen different genera for hopanoid to establish it as a suitable taxonomic marker for other group of bacteria.

Tremendous development in the sequencing technology leads to generation of enormous genomic data which is available in public database. Screening of genomes was carried out to find the distribution of hopanoid biosynthetic capabilities. Mining genomes of bacteria for hopanoid biosynthetic pathway genes showed that the pathway is present in diverse bacterial taxa. Screening of genomes had revealed that only 10.5% of sequenced organisms have genetic capacity to synthesize pentacyclic triterpenoid of hopane series. Hopanoid biosynthetic pathway is highly conserved in phylum

Cyanobacteria and it might be one of the major contributors for environmental hopanoids. Few members of phylum *Planctomycetes* harbor both hopanoid biosynthetic pathway as well as sterol biosynthetic pathway. As *Planctomycetes* are one of the oldest division of the domain bacteria and harbor hopanoid as well as sterol biosynthetic pathway. It can be postulated that the cenancestor can synthesize both hopanoids and sterol and with the time hopanoid biosynthesis might have been conserved in domain bacteria whereas sterol biosynthesis in eukaryotes.

Information on the hopanoid biosynthetic pathway is limited. In the present study, genome sequence of *Rhodomicrobium udaipurense* JA643^T was carried out to understand the hopanoid biosynthetic pathway. The genome sequence revealed that *Rmi. udaipurense* JA643^T has 18 genes involved in the hopanoid biosynthesis and transport of hopanoids. In *Rmi. udaipurense* JA643^T major hopanoids are diploptene, diplopterol, 2-methyldiploptetrol, tetrahymanol, bacteriohopanetetrol, aminobacteriohopanetriol, N-tryptophanyl-35-aminobacteriohopanetriol. Based on the genes observed, hopanoids detected and the literature available hopanoid biosynthetic pathway was predicted. This part of the work will help to study the hopanoid biosynthesis and its regulation in *Rmi. udaipurense* JA643^T.

Hopanoid deficiency may lead to the weakened structural integrity of cell membrane and may affect the other structures within or spanning cell envelope resulting in impaired lipid ordering which is linked to permeability, fluidity, ion conductivity, cell potential, cell signaling and lateral segregation. Understanding the role of hopanoids in shaping membrane properties would provide an important step towards bridging this gap. Therefore, the present study was undertaken to gain insights into the role of hopanoids in bacteria using genome-wide transcriptome study. *Rhodopseudomonas palustris* TIE-1 was used as a model organism in understanding the role of hopanoids. Microarray experiment showed that 299 genes were upregulated and 306 genes were downregulated in *Δshc* mutant of *Rps. palustris* TIE-1. Genes involved in membrane transport, chemotaxis and signal transductions were differentially expressed in *Δshc* mutant. From the experiments, it was explicit that the energy-dependent multidrug transport is deficient in the hopanoid *Δshc* mutant. Transcriptome data suggest that hopanoid plays an important role in maintaining cellular homeostasis. The hopanoid deficient cell membrane may lead to alteration in signal transduction which may results in affected swimming motility in *Δshc* mutant.

Cholesterol interacts with PDZ domain-containing proteins having CRAC motif and modulates cell signaling and protein network in the eukaryotic cells. The genome of the *Rps. palustris* TIE-1 consist of 34 diguanylate cyclase genes having CRAC motif out of which three got significantly downregulated in *Δshc* mutant. Diguanylate cyclase has a PDZ domain containing CRAC motif which is known to be involved in interaction with cholesterol. The docking study showed that diguanylate cyclase (Rpal_1916 and Rpal_2444) interact with hopanoids (diploptene, diplopterol and tetrahymanol) and might be playing a role in motility and cell signaling in *Rps. palustris* TIE-1. Still, the validation of this docking experiment needs to be performed to find out the interaction between proteins and hopanoids and outcome of this interaction remains an open question.

INTRODUCTION

1.0 Introduction

Membrane lipids are hydrophobic biomolecules which play a vital role in bacterial cell physiology. Initially, it was thought that membrane lipids are a static barrier. But with the advanced findings it is recognized as a complex and dynamic component of the membrane which selectively connects cell with its extracellular environment. Lipids can sense extracellular signals and they support different cell processes, including cell differentiation, cell proliferation, cellular homeostasis and protein secretion (Barak and Muchova, 2013). Membranes are composed of different lipid species (>1000) having distinct physicochemical properties which result in the formation of membrane microdomains (lipid rafts). However, the necessity for this diversity of lipid species is not clear (Bramkamp and Lopez, 2015; van Meer *et al.*, 2008). Based on the structures, lipids are classified as fatty acyl, glycerolipids, phospholipids, sphingolipids, polyketides, saccharolipids and polyprenyl lipids (sterol, hopanoids and prenol lipids; Fahy *et al.*, 2005; Fahy *et al.*, 2009). Fatty acyl, glycerolipids, phospholipids, polyketides, saccharolipids and sphingolipids are extensively studied in bacterial systems, whereas limited reports are available related to the membrane polyprenyl lipids in bacteria (Bramkamp and Lopez, 2015; Cronan and Thomas, 2009; Hannich *et al.*, 2011; Lingwood *et al.*, 2009; Lopez-Lara and Geiger, 2016; Meikle and Summers, 2017; Sohlenkamp and Geiger, 2016; van Meer *et al.*, 2008; Zhang and Rock, 2008). Polyprenyl lipids are synthesized by the condensation of isopentenyl diphosphate and dimethylallyl diphosphate (Fahy *et al.*, 2005). These lipids include quinones, prenol lipids, sterols and hopanoids (Fahy *et al.*, 2009). Sterol lipids (cholesterol and its derivatives) are widely distributed in a eukaryotic system and vital component of membrane lipids along with phospholipids and sphingolipids (Hannich *et al.*, 2011). Sterols are absent in prokaryotic members with few exception but have polyisoprenoid lipid, hopanoid which is analogous to sterols and reported from various bacteria (Rohmer *et al.*, 1984; Saenz *et al.*, 2015; Wei *et al.*, 2016). Hopanoids are among the most widespread of all complex natural products and are probably an essential constituent of many prokaryotes (Blumenberg *et al.*, 2012; Blumenberg *et al.*, 2010; Doughty *et al.*, 2009; Ourisson *et al.*, 1979; Ourisson *et al.*, 1987; Rohmer *et al.*, 1984). Although, hopanoids are one of the largest mass of any single class of organic molecule on the earth, yet, they are unfamiliar to most people, in and out of science.

1.1 Hopanoids

Hopanoids are pentacyclic isoprenoid lipid molecules biosynthesised in many eubacteria as well as few higher plants, protists, ferns, mosses, and fungi (Blumenberg *et al.*, 2009; Cvejic *et al.*, 2000; Hartner *et al.*, 2005; Ourisson *et al.*, 1979; Ourisson *et al.*, 1987; Rohmer *et al.*, 1984; Silipo *et al.*, 2014; Talbot *et al.*, 2008; Tank and Bryant, 2015). The name hopane is derived from the genus *Hopea* (from which they were first isolated as components of the resin) which itself got named after the John Hope, the botanist. Hopanoids [bacteriohopanetetrol (XXII) and diplopterol (VI)] were first reported in 1973 as the compounds inducing the orientation of cellulose microfibrils secreted by *Acetobacter xylinum* (Forster *et al.*, 1973). The hopanoids and sterols both have C_{30} hydrocarbon molecule squalene (I) as a biosynthetic precursor. Hopanoids have four cyclohexane ring and one cyclopentane ring whereas sterols have three cyclohexane ring and one cyclopentane ring. In addition, sterols have a hydroxyl group at a C_3 position which makes it different from hopanoids (Fig. 1). Hopanoids have chair-chair-chair-chair-chair conformations in the cyclohexane ring whereas sterols have chair-boat-chair-boat-open conformations (Kontnik *et al.*, 2008). Both, sterol and hopanoid structures are planar, rigid and hydrophobic with the thickness of half a membrane bilayer; therefore they can easily intercalate into the phospholipid bilayer and interact with adjacent fatty acids (Kannenberg *et al.*, 1985; Saenz *et al.*, 2015). As a result, hopanoids and sterols can modulate the fluidity and the permeability of the membrane.

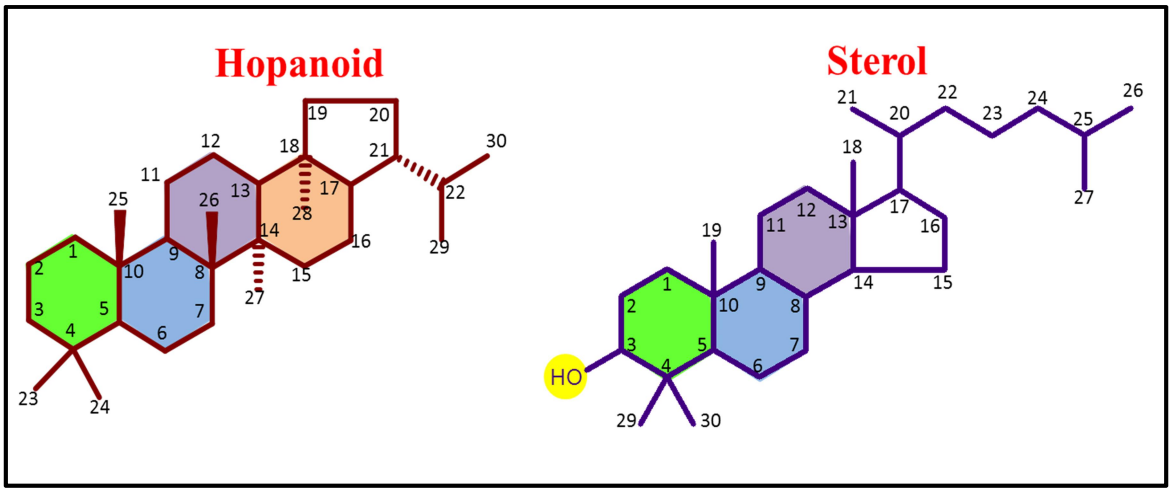

Fig. 1. Structure of hopanoid and sterol skeleton

As hopanoids are primarily derived from the bacteria, they are used as proxies to help decipher the geobiological communities. Hopanoids were reported from the ancient sediments, modern sediments, fossil records, petroleum reservoir and Archean and Proterozoic rocks. Hopanoids are among the ancient molecular biomarkers, which is reported from the late Archean times (>2500 billion years ago) from Mount Bruce Supergroup, Hamersley Basin, Western Australia (Brocks *et al.*, 2003; Brocks *et al.*, 1999). Hopanoid is one of the most abundant class of natural product present on the earth surface and recorded throughout the geological records (Ourisson *et al.*, 1979). The simplest C_{30} hopanoid is diploptene or hop-22(29)-ene (II), and it is usually found with diplopterol or hopan-22-ol (VI). There are various hopanoid structures reported, including the C_{30} compounds such as diploptene (II), diplopterol (VI) and complex hopanoids such as C_{35} bacteriohopanepolyols (BHPs) which have an extended C_5 side chain derived from D-ribose, composite hopanoids in which hopanoids are linked to glycosyl moiety (Hartner *et al.*, 2005; Lombard and Moreira, 2011; Rohmer, 2008; Talbot *et al.*, 2008). The structures referred in the text are given in Fig. 2.

The variations are present in the side chains of hopanoids, with typical BHPs containing four, five or six functional groups. The most common BHP is tetrafunctionalised biohopanoids with the functional variation occurring at C_{35}. C_{35} position can be occupied by hydroxyl group (bacteriohopane-32,33,34, 35-tetrol (XXIII; BHT), or by amino group (35-aminobacteriohopane-32, 33, 34-triol (XXIV; aminotriol). The C_{30} diploptene (II) and diplopterol (VI) are the synthetic precursors of all BHPs and found in low levels in most of the hopanoid producing bacteria (Rohmer *et al.*, 1984). There are two types of hopanoids; biohopanoids and geohopanoids.

1.1.1 Biohopanoids

Biohopanoids are the lipid molecules found in many of the prokaryotic cell membrane, which are buried in the phospholipid bilayer. Hopanoids are similar to sterol molecules found in eukaryotic cells, which play a crucial role in rigidifying and maintaining the integrity of cell membrane (Talbot and Farrimond, 2007). Hopanoids are reported in some of Gram-stain-positive and Gram-stain-negative bacteria, cyanobacteria, purple non-sulfur bacteria, acetic acid bacteria, nitrogen fixing bacteria, methylotrophs methanotrophs, sulphate reducing bacteria (SRB; Blumenberg *et al.*, 2012; Blumenberg *et al.*, 2006; Cvejic *et al.*, 2000; Doughty *et al.*, 2009; Hartner *et al.*,

2005; Kannenberg *et al.*, 1995; Ourisson *et al.*, 1979; Ourisson *et al.*, 1987; Rohmer *et al.*, 1984; Saenz *et al.*, 2012b; Talbot *et al.*, 2008).

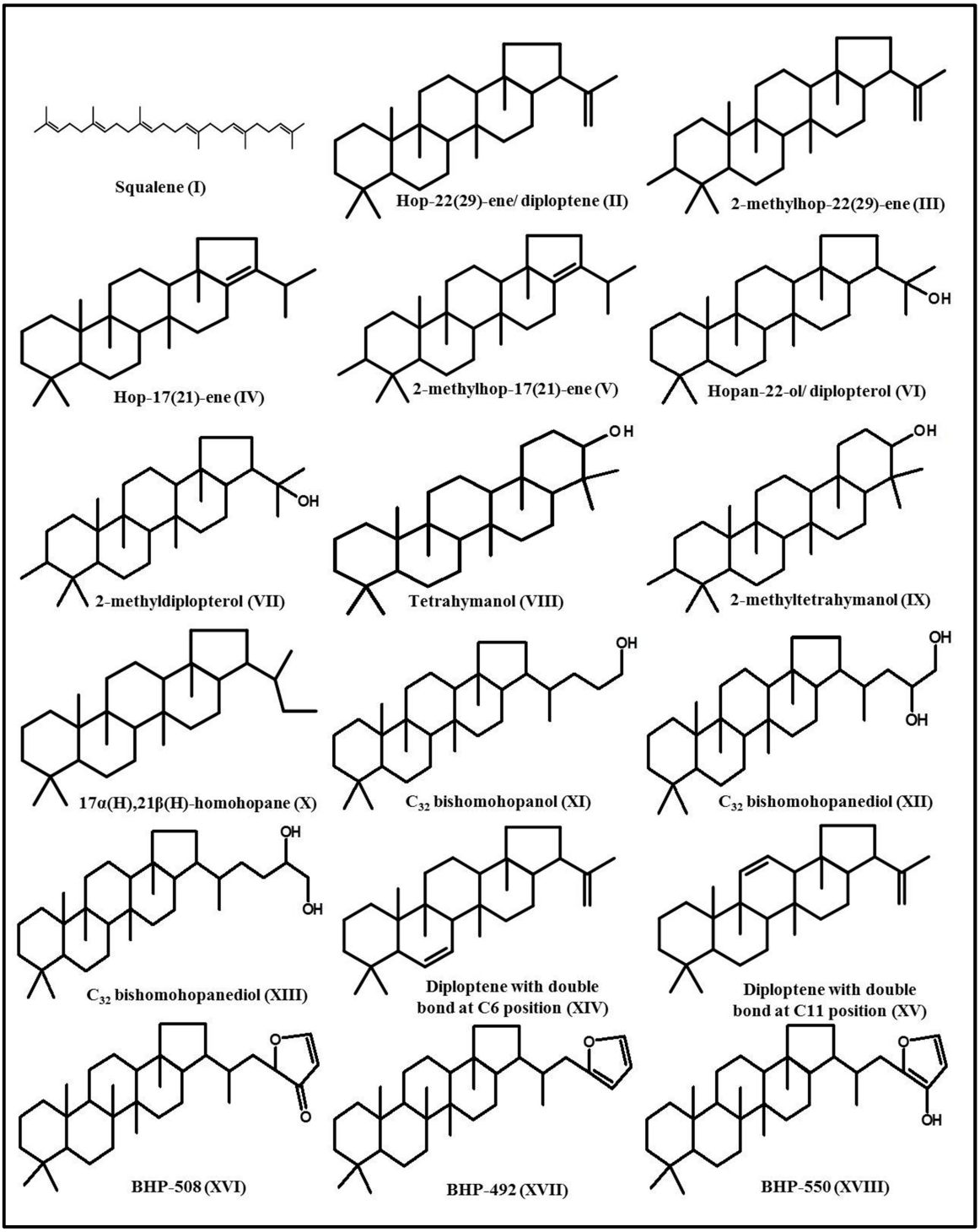

Fig. 2. Hopanoid structures referred in the text. **Continued……**

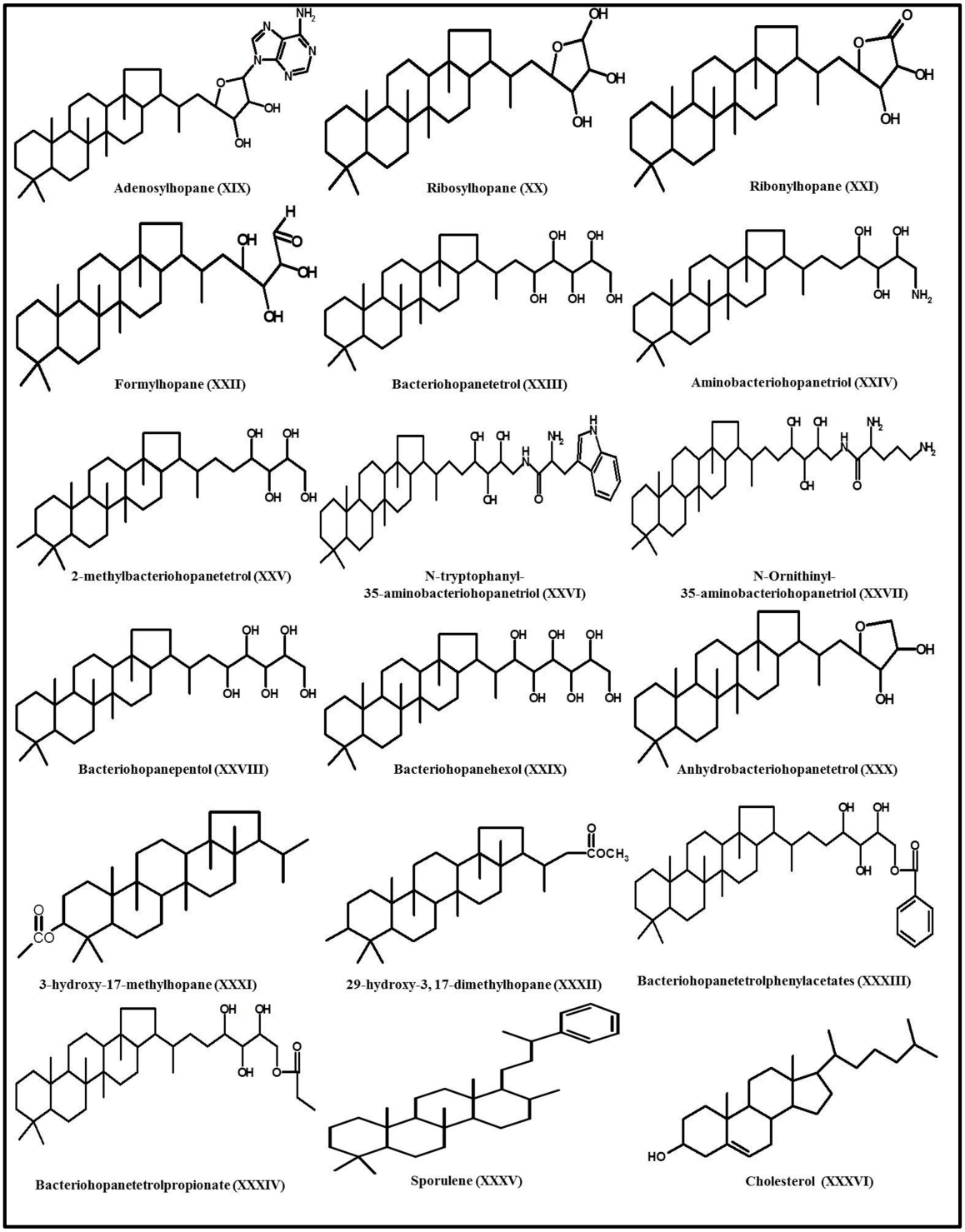

Fig. 2. Hopanoid structures referred in the text. Squalene is not a hopanoid, but it is the substrate in hopanoid biosynthesis and cholesterol (XXXVI) is a sterol molecule. Throughout the text roman number for each structure is given. BHP-508, bacteriohopanepentol with molecular weight 508; BHP-492, bacteriohopanepentol with molecular weight 492, BHP-550, bacteriohopanepentol with molecular weight 550 (These molecular weights are after acetylation)

1.1.2 Geohopanoids

Geohopanoids are the derivatives of biohopanoids which are formed by the diagenesis of biohopanoid (Tritza *et al.*, 1999). Diagenesis is a chemical and physical change occurs during the sedimentary rock formation. Hopanoids are highly stable at extreme conditions like alkali, acidic and high temperature (McGarvey and Croteau, 1995; Shunthirasingham and Simpson, 2006). Therefore they are one of the very few compounds which survived in the process of rock and petroleum formation (Shunthirasingham and Simpson, 2006). The pentacyclic skeletons of the hopanoids are relatively stable. After the release of biohopanoids in nature, the BHPs get converted to a simpler product during sediment diagenesis (hopanols, hopanoic acids, hopanes), but still, they retain the information about their parent compound (Shunthirasingham and Simpson, 2006).

1.2 Distribution of hopanoids in bacteria

Although the biosynthesis of hopanoid does not require dioxygen, it was thought that it is derived from aerobic organisms (Rohmer *et al.*, 1984). Hence, hopanoids were considered as synthesized by bacteria in aerobic condition and indicative for oxygenated environments (Rohmer, 1999). However, few studies reported hopanoids from facultative anaerobic bacteria like *Rhodomicrobium* spp, *Rhodopseudomonas* spp, *Rhodospirillum rubrum* and *Zymomonas mobilis* (Miziorko, 2011; Neunlist *et al.*, 1985; Rohmer *et al.*, 1984; Talbot *et al.*, 2007a). Recent studies showed that anaerobically grown *Geobacter metallireducens*, *G. sulfurreducens* and few species of the genus *Desulfovibrio* had hopanoids, but these bacteria can tolerate some oxygen (Blumenberg *et al.*, 2006; Hartner *et al.*, 2005). The occurrence of hopanoids from strictly anaerobic anammox bacteria which belong to phylum *Planctomycetes* were also reported (Hunter, 2007). These findings help to explain the occurrence of hopanoids in anaerobic environments as well (Banerjee and Sharkey, 2014; Bode *et al.*, 2003; Volkman, 2003).

Literature shows that 280 bacteria which represent 206 species, 117 genera and 10 major phyla were screened for hopanoid production (Berry *et al.*, 1993; Blumenberg *et al.*, 2006; Blumenberg *et al.*, 2009; Hartner *et al.*, 2005; Rohmer *et al.*, 1984). Around 168 bacteria which represents 60% of bacterial taxa tested were comprised of hopanoids (Talbot and Farrimond, 2007). Hopanoids were detected from various species belonging to diverse group such as *Proteobacteria*, *Cyanobacteria*, *Actinobacteria*, *Acidobacteria*,

Planctomycetes, Firmicutes and majority of studies were focused on these groups. (Damsté *et al.*, 2004; Rohmer *et al.*, 1984; Talbot *et al.*, 2007b; Talbot *et al.*, 2008). However, the screening is strongly biased towards the specific taxonomic groups. The distribution of hopanoids is found to be heterogeneous; therefore the extent to which they are sterol surrogates is questionable.

Hopanoids (diploptene (II), diplopterol (VI) and BHPs) were detected at all sampling depth of sediments (Blumenberg *et al.*, 2010). With the increasing in depth of sampling the amount of diagenetic product of hop-17(21)-ene (IV), hop-22(29)-ene (V) and 17β(H),21β-homohopane (X) increases whereas the amount of diplopterol (VI) decreases with the depth. Bacteriohopanepolyols [bacteriohopanetetrol (XXIII) and aminobacteriohopanetriol (XXIV)] are dominant hopanoids in recent sediments. The occurrence of BHPs in sediment remains unchanged with increase in depth of sampling which suggests that BHPs are highly stable to diagenetic breakdown (Blumenberg *et al.*, 2010). The BHPs are the putative precursor for diagenetically formed geohopanoids (hopanoidal alcohols, ketones, acids and hydrocarbons). Anhydrobacteriohopanetetrol (XXX) is abundant in sedimentary samples which are the immediate diagenetic product of other BHPs (Blumenberg *et al.*, 2010). Many bacteria contain characteristic BHPs which are reported from modern and ancient sedimentary rocks and preserve the source specific information (Summons *et al.*, 1999). Hence, hopanoids are used by geologists and paleobiologists for various paleoenvironmental reconstructions. But the knowledge about the source of sedimentary BHPs and changes in marine settings is limited.

1.3 Lipid as biomarker

Biomarker is a characteristic (molecule, gene or any trait) which carry information regarding the specific taxonomic group, metabolic process, physiological process or environmental condition. Various biological metabolites are used as biomarkers as they preserve the source specific information or can be linked to specific taxa. Lipid molecules are one of the important molecular biomarker as it is highly stable to adverse conditions and mining of lipids from numerous species belonging to diverse taxa provide information to link there source of origin in environmental samples and geological records (Benz *et al.*, 1983; Fischer *et al.*, 2005). Therefore, it is important to understand the source of specific lipid and the degree of specificity which will help to assign significance of its environmental distribution. Initially, there was lack of

knowledge about the genes involved in the biosynthesis of a biomarker in question; therefore a survey of diverse taxa for generic compounds and taxonomically unique molecules was used to determine the origins of biomarker lipids. But with next generation sequencing approach thousands of genomes are getting sequenced, so the genomic approach can be used to find out the phylogenetic distribution and origin of these biomarkers.

1.3.1 Hopanoids as biomarker

Polycyclic triterpenoids (sterols and hopanoids) are ringed lipids and are highly stable to adverse conditions like acidic/alkali and elevated temperature as well as withstand the conditions which can destroy the most of the organic compounds present in the sediments (McGarvey and Croteau, 1995; Shunthirasingham and Simpson, 2006). Biohopanoids are the pentacyclic triterpenoid lipids of the hopane series which can be synthesized by bacteria and few eukaryotes (Rohmer *et al.*, 1984). Biohopanoids get converted to some other products during the diagenesis process, but it still retains the information of the number and position of the original functional group. For example, C_{32} and C_{34} hopanediols and novel compounds [C_{32} hopanediol (XI) and C_{33} hopanediol (XIII)] can be related to a restricted number of BHP precursors (Rodier *et al.*, 1999). However, these functionalised geohopanoids will not survive deep burial in the geosphere, and for the longer-term preservation of information the hopanoids in macromolecular sedimentary organic matter must be looked which are bound through the sites of original functionality, and may thus preserve source-specific information (Rodier *et al.*, 1999). Hopanoids are used as molecular fossils by geologists and paleobiologists to study the history of Earth surface environments (Pearson *et al.*, 2007). Hopanoids were also reported from the ancient samples which are >2500 billion years old (Brocks *et al.*, 2003; Brocks *et al.*, 1999).

A survey of hopanoid distribution reveals that specific hopanoids may be linked to specific bacterial taxa (Belin, 2009; Blumenberg *et al.*, 2012; Cvejic *et al.*, 2000; Silipo *et al.*, 2014; Summons *et al.*, 1999). It was established that *Cyanobacteria* are one of the most important producers of BHPs in the environmental samples (Blumenberg *et al.*, 2010). Intact BHPs are reported from the ancient sample as old as 50 million year ago (van Dongen *et al.*, 2006). Methylated C_{35} hopanoid is one the signature hopanoids for *Cyanobacteria* in ancient sedimentary environment, therefore, considered as the

biomarker for oxygenic photosynthesis (Summons *et al.*, 1999). 2-Methylhopanoids were reported from few methylotrophs, symbiotic nitrogen-fixing bacteria and *Rhodopseudomonas palustris* TIE-1, hence 2-methylhopanoids cannot be used as an indicator of cyanobacterial oxygenic photosynthesis (Blumenberg *et al.*, 2006; Cvejic *et al.*, 2000; Silipo *et al.*, 2014; Welander *et al.*, 2009). Type I methanotrophs can produces hexafunctionalized BHPs (XXIX) as major hopanoids and similarly type II methanotrophs produces tetra (XXIII) and pentafunctionalized BHPs (XXVIII) as major hopanoids (Cvejic *et al.*, 2000; Silipo *et al.*, 2014). It was observed that freshwater sediments are having an abundant quantity of penta- (XXVIII) and hexafunctionalized (XXIX) hopanoids, which can be linked to enriched methanotrophs in these environment sites (Blumenberg *et al.*, 2006; Silipo *et al.*, 2014).

1.4 Isoprene biosynthesis

The important biosynthetic precursor of hopanoid biosynthesis is isopentenyl diphosphate which is also a precursor for all the isoprenoid group of molecules. Isopentenyl pyrophosphate (IPP) and its isomer dimethylallyl diphosphate (DMAPP) get oligomerised to yield isoprenoid molecules. Isoprenoids are a diverse class of organic molecule studied and >35000 different isoprenoids were reported from all the three domains of life (archaea, bacteria and eukarya; Heuston *et al.*, 2012). Isoprenoids are one of the essential constituent for the cell survival and involved in various vital functions such as electron transport, photosynthesis, membrane architecture, micronutrient as vitamin, peptidoglycan biosynthesis, regulation of transcription, signal transduction, protein degradation, steroid hormones and plant defence compounds (Heuston *et al.*, 2012; Lombard and Moreira, 2011; McGarvey and Croteau, 1995; Rohmer, 2008). There are two independent and non-homologous pathways for the synthesis of isopentenyl pyrophosphate; mevalonate (MVA) pathway and methylerythritol phosphate (MEP) pathway (Lombard and Moreira, 2011).

1.4.1 Mevalonate pathway

Mevalonate pathway is usually present in archaea and eukarya, whereas it is also reported from some bacteria which is considered as a result of horizontal gene transfer from the eukaryotic or archaeal origin (Heuston *et al.*, 2012; Lombard and Moreira, 2011). Six enzymes are needed to synthesize IPP in eukaryotes whereas in archaea only three enzymes carry out the synthesis of IPP through mevalonate pathway (Heuston *et*

al., 2012; Lombard and Moreira, 2011). Mevalonate pathway starts with the synthesis of 2-hydroxy-3methylglytaryl-Co-A (HMG-CoA) from acetyl-CoA and acetoacetyl-CoA. HMG-CoA gets reduced to mevalonate which inturn gets phosphorylated to phosphomevalonate. Mevalonate pyrophosphate decarboxylase converts phosphomevalonate to IPP through a formation of mevalonate diphosphate as an intermediate product (Fig. 3; Miziorko, 2011).

1.4.2 Methylerythritol phosphate pathway

Methylerythritol phosphate (MEP) pathway was reported and elucidated in early 21st century (Hunter, 2007; Rohmer, 1999). The investigation of the hopanoid biosynthesis in bacteria expedites the discovery of novel and alternate pathway for IPP biosynthesis that is MEP pathway (Rohmer, 2008). MEP pathway was reported from bacteria and plastid-containing eukaryotes. MEP pathway in eukaryotes might be originated from the endosymbionts of cyanobacterial origin which gave rise to plastids (Lombard and Moreira, 2011). The first step in the MEP pathway is condensation of pyruvate and glyceraldehyde-3-phospahte which results in the formation of 1-deoxy-D-xylulose 5-phosphate (DOXP), the reaction is catalysed by DOXP synthase (Hunter, 2007). As DOXP is the first intermediate product, the pathway is also known as DOXP pathway. A-ketol rearrangements of DOXP lead to the formation of methylerythritol phosphate which is catalysed by DOXP reductoisomerase (Banerjee and Sharkey, 2014; Hunter, 2007). DOXP reductoisomerase is a potential target for antimicrobial compounds like fosmidomycin (Hunter, 2007). The reaction between cytidine triphosphate (CTP) and MEP results in the formation of 4-diphosphocytidyl-2C-methyl-D-erythritol (CDP-ME). Phosphorylation of CDP-ME leads to formation of 4-diphosphocytidyl-2C-methyl-D-erythritol-2-phosphate (CDP-ME2P). In the next step, cytidine monophosphate moiety is cleaved off from CDP-ME2P to form 2C-methyl-D-erythritol-2,4-cyclodiphosphate (MECP). MECP undergo reduction and elimination to form IPP (Hunter, 2007). Isomerisation of IPP to more electrophile DMAPP is catalysed by isopentenyl-diphosphate isomerase (Fig. 3; Hunter, 2007). Condensation of IPP and DMAPP leads to the formation of farnesyl Pyrophosphate, geranyl pyrophosphate, geranylgeranyl pyrophosphate, squalene and various other oligomerized isoprene molecules (Banerjee and Sharkey, 2014; Heuston *et al.*, 2012; Hunter, 2007; Lombard and Moreira, 2011; Rohmer, 2008).

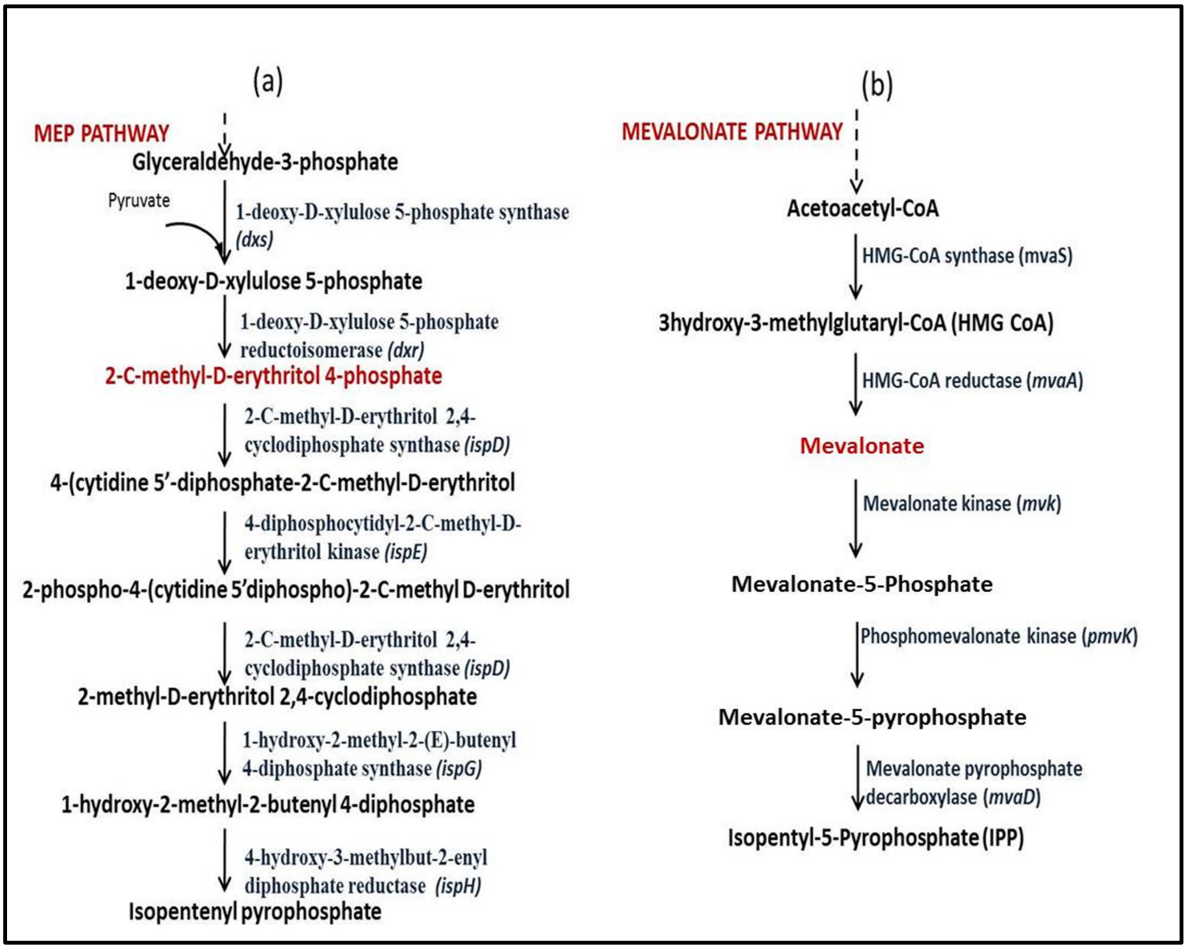

Fig. 3. IPP biosynthetic pathway; (a) Methylerythritol phosphate pathway commonly present in most of the prokaryotes and plastid-containing eukaryotes. (b) Mevalonate pathway present in eukaryotes, archaea and few bacteria.

1.5 Sterol biosynthesis in bacteria

Sterols are tetracyclic terpenoid ubiquitously present in the eukaryotic system and perform various functions such as cell signaling, protein networking, protein transport, stress tolerance, phagocytosis, maintain membrane rigidity and regulate fluidity (Listowski *et al.*, 2015; Pearson *et al.*, 2003; Wei *et al.*, 2016). Even though sterols are reported from eukaryotes, there are few reports which show the occurrence of sterols in bacteria, but there is no report of sterols from archaea (Bode *et al.*, 2003; Pearson *et al.*, 2003; Volkman, 2003; Wei *et al.*, 2016). Recently the biosynthetic pathway of sterols in diverse bacteria was studied (Pearson *et al.*, 2003; Wei *et al.*, 2016). Similar to hopanoids, sterols are also synthesized from the C_{30} hydrocarbon molecule, squalene (I). The basic difference between sterol biosynthesis and hopanoid biosynthesis is the involvement of molecular oxygen in sterol biosynthetic pathway. As sterol biosynthetic pathway is the only known biological pathway which needs molecular oxygen, it is of immense interest for an evolutionary biologist to understand the origin and evolution of sterol biosynthesis (Wei *et al.*, 2016). Cyclization of squalene (I) into sterols is carried out by two enzymes; squalene monooxygenase and oxidosqualene cyclase. The first step in the sterol biosynthesis is epoxidation of squalene into squalene epoxide which is catalysed by squalene monooxygenase (Volkman, 2003). The genome search for squalene monooxygenase in bacteria has given a significant match for *Methylococcus capsulatus* and *Gemmata obscuriglobus* (Pearson *et al.*, 2003). BLAST search detected that *Burkholderia mallei* have a FAD-binding monooxygenase which is homologous to squalene monooxygenase, but till today sterols are not detected from it (Pearson *et al.*, 2003).

Oxidosqualene cyclase catalyses the cyclization of squalene epoxide into sterol molecule that is lanosterol (Wei *et al.*, 2016). Oxidosqualene cyclase is homologous to squalene hopane cyclase involved in hopanoid biosynthetic pathway. Comparison of all the bacterial genome has shown that only *Methylococcus capsulatus* and *Gemmata obscuriglobus* have oxidosqualene cyclase. The major sterols in *G. obscuriglobus* are lanosterol and parkeol (Pearson *et al.*, 2003). Sterols are reported from the myxobacteria (*Stigmatella aurantiaca* and *Nannocyctis excedens*) but genes involved in the sterol biosynthesis is not detected yet, which suggest that there is need for further sequencing of myxobacteria (Pearson *et al.*, 2003). Reports suggest that bacteria and ancient eukaryotes might have exchanged the sterol biosynthetic pathway through gene transfer

(Wei *et al.*, 2016). Similarly, stable isotope study showed that mycobacteria produce sterols but the homologs squalene monooxygenase and oxidosqualene cyclase are not present in the genome of mycobacteria which suggest that there might be the alternate route of sterol biosynthesis in these bacteria (Pearson *et al.*, 2003; Wei *et al.*, 2016).

1.6 Role of hopanoids

1.6.1 Membrane integrity and rigidity

In the eukaryotic cell, sterols play a key role in membrane fluidity, stability and help in tolerating ethanol stress and temperature stress (Swan and Watson, 1998). Therefore, it is always a topic of interest that whether the sterol surrogate, bacterial hopanoids also performed the same role in a bacterial cell membrane. It was observed that hopanoids have condensing effect on the artificial membrane and in liposome it results in increased viscosity (Benz *et al.*, 1983). Hopanoid deficient mutant of *Rps. palustris* TIE-1 became sensitive to bile salt which is the indicator of outer membrane damage and antibiotic like rifampicin and erythromycin which suggest that hopanoids similar to sterol play important role in membrane rigidity and decreases membrane permeability (Welander *et al.*, 2009). Hopanoid intercalate in phospholipid bilayer and pack the hydrophobic centres of bilayers. This architecture helps in inhibiting the loss of protons and important in protecting the cell in extreme pH conditions (Welander *et al.*, 2009).

1.6.2 Lipid Ordering

The ordered plasma membrane is an important property shared by all the three domains of life (Saenz *et al.*, 2015). Lipid ordering gives the property of freedom of motion and lateral segregation of lipids without losing the integrity of a membrane which contributes to membrane fluidity, membrane permeability and signal transduction (Saenz *et al.*, 2015). The property of planner geometry and interaction with sphingomyelin endows natural tendency to sterols to form the ordered lipid phase (Saenz *et al.*, 2015). Lipid A in bacteria is analogous to sphingomyelin and it is reported that hopanoid can covalently linked to lipid A molecule which will enhance the outer membrane resistance (Silipo *et al.*, 2014).

In a model membrane, it was observed that diplopterol (VI) can interact with saturated lipids and form ordered lipid phase (Saenz *et al.*, 2012a). Reports showed that

hopanoid might play a crucial role in lipid ordering but the mechanism and significance of lipid ordering in bacteria is poorly understood. Still, there are various bacteria which do not produce hopanoids, so how lipid ordering will be maintained in the absence of hopanoids remains an open question.

1.6.3 Plant microbe interaction

Symbiosis is the mutual interaction between two organisms from which both the organisms get benefited. *Bradyrhizobium diazoefficiens* is nitrogen fixing bacterium shows symbiotic association with legume *Aeschynomene afraspera* and soybean (Kulkarni *et al.*, 2015). *ΔhpnP* and *ΔhpnH* mutants of *B. diazoefficiens* were unable to synthesize methylated hopanoids and C_{35} hopanoids respectively. In *B. diazoefficiens* methylated hopanoids and C_{35} hopanoids are important in microaerobic growth. It was observed that C_{35} hopanoids are important in outer membrane rigidity, aerobic growth and stress tolerance (Kulkarni *et al.*, 2015). *ΔhpnP* and *ΔhpnH* mutants of *B. diazoefficiens* induce fewer nodules on soybean and nitrogenase activity was also reduced. But on the other hand, when *A. afraspera* was infected with *ΔhpnH* mutants of *B. diazoefficiens,* it was able to induce nodule organogenesis but plant shows typical nitrogen starvation symptoms like reduced plant growth, a decrease in acetylene reduction activity and foliage chlorosis (Kulkarni *et al.*, 2015). In conclusion, it was reported by Kulkarni *et al.*, that C_{35} hopanoids are essential for growth in symbiotic microenvironment and symbiosis between *B. diazoefficiens* and *A. afraspera* (Kulkarni *et al.*, 2015).

1.6.4 Spore formation

In liquid media under different growth conditions *Streptomyces coelicolor* A3(2) does not produce any detectable hopanoids. But when *S. coelicolor* A3(2) was grown in solid media it produces hopanoids. Solid media allow differentiation of *S. coelicolor* A3(2) and process of sporulation (Poralla *et al.*, 2000). In *S. coelicolor* A3(2), only during the transition period from a substrate to aerial hyphae hopanoids will be formed and protect spores from dehydration (Poralla *et al.*, 2000). In contract to this, *Streptomyces scabies* 87-22 produces hopanoids both in solid and lipid media but the process of sporulation in *S. scabies* 87-22 is different and it produces spores both in solid and liquid media (Seipke and Loria, 2009). *Bacillus subtilis* produces the sporulene (XXXV) using enzyme squalene hopene cyclase. Sporulene (XXXV) in *B. subtilis* is

produced only in sporulating stage which protect spores from oxidative stress (Kontnik *et al.*, 2008).

1.6.5 Cell cycle

hpnN is the RND-family transporter homologous to the protein involved in eukaryotic steroidal trafficking. The knockout of the *hpnN* gene from *Rps. palustris* TIE-1 results in mislocalization of hopanoids in the cell (Doughty *et al.*, 2011). There is an asymmetric distribution of hopanoids in daughter cell and mother cell (Doughty *et al.*, 2011). At high temperature (38^{o}C), *ΔhpnN* mutant cells remains connected by their cell wall, forming a long filament. Hopanoid mislocalization rather than the absence of hopanoids in the outer membrane is responsible for the filamentation phenotypes. The asymmetric hopanoid distribution promotes cell division at elevated growth temperatures by participating in the formation of protein-lipid microdomains, resulting in the recruitment of cell division machinery to the proper subcellular region (Doughty *et al.*, 2011).

1.7 Definition of problem

Hopanoids are among the most widespread of all complex natural products and are probably essential constituents of many prokaryotes. Though not extensively studied, hopanoids contribute to the membrane stability, membrane permeability, cell cycle, plant microbe interaction, resistance to antibiotics and help in stress tolerance. However, the role of hopanoids is not conclusively elucidated and the extent to which they are sterol surrogate remains an open question. A robust interpretation of phylogenetic distribution and cellular function of hopanoid is required to better understand their physiological significance. Therefore, to gain insights into the distribution of hopanoids in bacteria, deciphering hopanoid biosynthetic pathway and the role of hopanoids in bacteria, study was taken up with following objectives;

1.8 Objectives of this study

1. Mining bacteria for hopanoids

    I. Mining for hopanoids in cultured bacteria

    II. Mining genomes for genes involved into hopanogenesis

2. Genomic insights of hopanogenesis in *Rhodomicrobium udaipurense* JA643^T

3. Genome-wide transcriptional response of hopanoid deficient *Rhodopseudomonas palustris* TIE-1

MATERIALS AND METHODS

2.0 Materials and Methods

2.1 Glassware, chemicals and devices

2.1.1 Glassware and cleaning

All glassware used in this study which includes all the test tubes, measuring cylinders, pipettes, culturing flasks, Petri dishes, reagent bottles, screw cap test tubes were of Duran or Borosil brand. The glassware used in this study were soaked in the diluted chromic acid solution (potassium dichromate and sulphuric acid) for overnight and washed with tap water and teepol detergent. The glassware were rinsed with deionized water and dried in hot air oven.

2.1.2 Deionized water

Deionized water was obtained from deionizer plant (ion exchange India Ltd. Model-CA20/U). Distilled and double distilled water were obtained from the distillation plant (Millipore) and used to prepare media, stock solutions and reagents.

2.1.3 Chemicals

All the chemicals used in this study were of analytical grade obtained from HiMedia, Sigma-Aldrich, Merck solvents, Fermentas and Thermo Fisher Scientific.

2.1.4 Determination of pH

pH of the culture media and stock solutions were determined using a digital pH meter (Digisun Electronics, India model DI-707) and the pH meter was calibrated with standard buffer solutions (pH 4.2, 7 and 9.2).

2.1.5 Buffers and standard solutions

Deionised water was used for buffer solutions preparation. Standard operating procedure was used to prepare buffer solutions and pH was adjusted at room temperature.

Phosphate buffer saline (PBS) buffer (composition $g.l^{-1}$): NaCl-8, KCl-0.2, Na_2HPO_4-1.44 and KH_2PO_4-0.24; pH was adjusted to 7.4 and sterilized by autoclaving.

HEPES buffer (5 mM): 1.12 grams of HEPES in 1000 ml of deionised water; pH was adjusted to 7.2 and sterilized by autoclaving.

N-phenylnaphthylamine (NPN; 1 mM): 219.28 grams of N-phenylnaphthylamine in 1000 ml of acetone.

H33342 (100 µM): 56.2 mg of H33342 in 1000 ml of sterilized water.

Carbonyl cyanide m-chlorophenyl hydrazone (CCCP; 10% v/v): 10 ml of CCCP in 90 ml of DMSO.

2.1.6 Sterilization

Sterilization of culture media, glassware and microtips was done by autoclaving at 120°C for 15 min. Thermolabile solutions were filter sterilized through 0.22 µm membrane filter (Millipore).

2.2 Media preparation

2.2.1 Mineral salt media (composition $g.l^{-1}$)

KH_2PO_4-0.5, $MgSO_4.7H_2O$-0.2, NaCl-20.0, NH_4Cl-0.6, $CaCl_2.2H_2O$-0.05 and 5 ml of ferric citrate solution (0.1%, w/v)] with 22 mM pyruvate; pH was adjusted to 7.0 and sterilized by autoclaving.

2.2.2 Yeast malt broth (composition $g.l^{-1}$)

Yeast extract-3.0, malt extract-3.0, peptone-5.0 and glucose-10.0; pH was adjusted to 6.2 and sterilized by autoclaving.

2.2.3 Nutrient broth (composition $g.l^{-1}$)

Peptone-3.0, yeast extract-3.0, NaCl-5; pH was adjusted to 7.0 and sterilized by autoclaving.

2.2.4 Zobell marine broth 2216 (composition $g.l^{-1}$)

Added 40.25 grams of dehydrated powder **(**Marine broth 2216, M385; HiMedia) in 1000 ml distilled water. Heated it to dissolve in the water (prepared as per the manufacture's instruction); pH was adjusted to 7.6 and sterilized by autoclaving.

2.2.5 Nutrient medium (composition g.l^{-1})

KH_2PO_4-0.2, NH_4Cl-0.25, KCl-0.5, $CaCl_2.2H_20$-0.15, NaCl-1.0, $MgCl_2.6H_2O$-0.62, Na_2SO_4-2.84, HEPES-2.83, yeast extract-3.0, peptone-3.0, casamino acid-0.5, glucose-0.5 and sodium pyruvate-3.0; pH was adjusted to 7.2 and sterilized by autoclaving.

2.2.6 Alkaline medium II (composition g.l^{-1})

$NaHCO_3$-15.0, Na_2CO_3-10.0, NaCl-10.0, $MgCl_2.6H_2O$-0.2 and starch-5.0; pH was adjusted to 9 and sterilized by autoclaving.

2.2.7 Alkaline basic medium (composition g.l^{-1})

Na_2CO_3-2.0, $NaHCO_3$-4.5, NaCl-48, NH_4Cl-0.5, KH_2PO_4-0.3, $MgCl_2.6H_2O$-0.2, resazurin-0.001, yeast extract-0.5, sucrose-5.0, 1 ml SL_7 [trace elements solution (mg.l^{-1}): HCl-(25%, v/v)-1 ml, $ZnCl_2$-70, $MnCl_2.4H_2O$-100, H_3BO_3-60; $CoCl_2.6H_2O$-200, $NiCl_2.6H_2O$-20, $Na_2MoO_4.2H_2O$-40 and $CuCl_2.2H_2O$-20] and 10 ml of vitamin solution. Autoclaved $Na_2S.9H_2O$-0.5 (g.l^{-1}) was added separately after sterilization; pH was adjusted to 10.8.

2.2.8 YPP media (composition g.l^{-1})

Yeast extract-3, peptone-3, pyruvate-0.88; pH was adjusted to 7.0 and sterilized by autoclaving.

2.2.9 Clostridial medium (composition g.l^{-1})

Added 38 grams of dehydrated powder (M443; HiMedia, with 2% NaCl) in 1000 ml distilled water. Heated it to dissolve in the water (prepared as per the manufacture's instruction); pH was adjusted to 6.8 and sterilized by autoclaving.

2.3 Organisms and growth conditions

Details of the bacterial strains studied in the present study and their growth conditions are listed in Table 1. Few bacterial strains were isolated in our laboratory and others were shared as freeze-dried samples by Prof. Ch. Sasikala, Jawaharlal Nehru Technological University, Hyderabad. Biomass of clinical isolates of *Staphylococcus* spp. was shared by Dr. Nagalakshmi N., Melaka Manipal Medical College, Manipal.

Rhodopseudomonas palustris TIE-1 was shared by Dr. Paula V. Welander, Earth System Science, Stanford University, California. *Δshc* mutant of *Rps. palustris* TIE-1 was shared by Prof. D.K. Newman, Division of Geological and Planetary Sciences, California Institute of Technology, California. *Rps. palustris* strains were grown photoheterotrophically at 30°C in light with 2,400 lux in YP medium maintaining micro-aerobic condition in the screw cap test tube. The growth analysis of *Δshc* mutant and wild type strain of TIE-1 was carried out in YP media with different carbon source (succinate, malate, acetate and malate at 10 mM concentration). Exponential growth phase cells normalised to 0.5 at OD_{660nm} were inoculated (2% inoculum) in triplicate into the appropriate medium. The growth was monitored over the time by measuring absorbance at 660 nm. Pyruvate (YPP media) as carbon source was selected for further study. All the stock cultures were maintained as agar slants. For long time preservation, 30% glycerol stock cultures were maintained for 6 months at -80°C.

2.4 Mining of hopanoids in bacteria

2.4.1 Extraction of Hopanoids

0.1-0.2 grams of lyophilized cells were sonicated for 1 hour in 30 ml of chloroform:methanol (2:1). 25 ml of chloroform:methanol:water (3:1:1) was added to the extract and centrifuged at 5000g for 10 min. The organic layer was collected and pellet was re-extracted in chloroform and both the organic layers were mixed together. The extract was evaporated to dryness. 3 ml of periodic acid (100 mg) in tetrahydrofuran:water (95:5; v/v) was added and stirred for one hour and evaporated to dryness over anhydrous sodium sulphate. Sodium borohydride (Na_2BH_4) was added in excess and stirred for 1 hour. The reaction was stopped by adding 15 ml of potassium dihydrogen phosphate (100 mM) and the sample was extracted by adding 15 ml of petroleum ether. Petroleum ether extract was collected and concentrated by rotary flash evaporator for thin layer chromatography. Two-dimensional thin layer chromatography was run in dichloromethane which was stained with 0.1% alcoholic solution of berberine hydrochloride and bands were visualized at 360 nm.

Table 1. List of bacteria used in this study and their growth conditions

Bacterial strains	Growth conditions
Alcanivorax balearicum DSM23776^T	Mineral salt media with pyruvate as carbon source, pH-7, 28^{o}C
Alcanivorax dieselolei DSM16502^T	
Alcanivorax xenomutans JC109^T	
Bacillus sp. JC325	Nutrient broth, pH-7, 30^{o}C
Bacillus sp. JC326	
Ciceribacter lividus MSSRFBL^T	Yeast malt broth, pH-7, 30^{o}C
Cohaesibacter haloalkalitolerance JC131^T	Zobell marine broth, pH-7.5, 30^{o}C
Cohaesibacter marisflavi NCCB100300^T	
Ensifer adhaerens LMG20216^T	Yeast malt broth, pH-7, 30^{o}C
Ensifer kostiensis DSM13372^T	
Erythrobacter longus CIP104268^T	Nutrient medium, pH-7, 30^{o}C
Erythrobacter odishensis JA747^T	
Falsirhodobacter halotolerans JA144^T	
Jeotgalibacillus alimentarius JCM 10872^T	Marine broth, pH-7, 30^{o}C
Jeotgalibacillus alkaliphilus JC303^T	
Jeotgalibacillus malaysiensis KCTC 33550^T	
Jeotgalibacillus salarius KCTC 13257^T	
Jeotgalibacillus terrae KCTC 13528^T	
Litoribacter alkaliphilus JC166^T	Nutrient medium,pH-7, 30^{o}C
Litoribacter ruber KCTC 22899^T	
Mongoliicoccus roseus KCTC 19808^T	
Mongoliicoccus alkaliphilus JC165^T	
Paraclostridium benzoelyticum JC272^T	Clostridial medium
Pontibacter actiniarum LMG23027^T	Nutrient medium, pH-7, 30^{o}C
Pontibacter korlensis NRRL B-51097^T	
Pontibacter odishensis JC130^T	
Rhizobium alkalisoli CCBAU01393^T	Nutrient broth, pH-7, 30^{o}C
Rhizobium endophyticum JC140^T	
Rhizobium vignae CCBAU05176^T	
Rhizobium yanglingense LMG19592^T	
Rhodobacter aestuarii JA296^T	Mineral salt media with pyruvate as carbon source, pH-7, 28^{o}C
Rhodobacter capsulatus ATCC11166^T	
Rhodobacter sphaeroides DSM158^T	
Rhodobacter viridis JA737^T	
Rhodomicrobium udaipurense JA643^T	
Rhodomicrobium udaipurense JA755	
Rhodomicrobium vannielii DSM162^T	
Rhodoplanes elegans DSM11907^T	
Rhodoplanes oryzae JA793^T	
Rhodoplanes piscinae JA266^T	
Rhodoplanes pokkaliisoli JA415^T	
Rhodoplanes roseus DSM5909^T	
Rhodopseudomonas palustris ATCC17100	
Rhodopseudomonas palustris TIE-1	
Rhodopseudomonas pentothenatexigens JA575^T	

Table 1. List of bacteria used in this study and their growth conditions

Bacterial strains	Growth conditions
Rhodovulum adriaticum DSM16428^T	Zobell marine broth medium pH-7.6, 30^{o}C
Rhodovulum algae JA877^T	
Rhodovulum bhavnagarense JA738^T	
Rhodovulum euryhalinum DSM4868^T	
Rhodovulum imhoffii JA125^T	
Rhodovulum kholense JA297^T	
Rhodovulum marinum JA128^T	
Rhodovulum phaeolacus JA580^T	
Rhodovulum robiginosum N2^T	
Rhodovulum salis JA756^T	
Rhodovulum steppense A-20s^T	
Rhodovulum strictum MB G2^T	
Rhodovulum sulfidophilum DSM 1374^T	
Rhodovulum viride JA756^T	
Rhodovulum visakhapatnamense JA181^T	
Salinicoccus alkaliphilus T8^T	Nutrient broth, pH-7, 30^{o}C
Salinicoccus halitifaciens JC90^T	
Salinicoccus kekensis K164^T	
Sinorhizobium americanum DSM15007^T	
Spirochaeta alkalica Z-7491^T	Alkaline basic medium pH-10.8, 30^{o}C
Spirochaeta americana ASpG1^T	
Spirochaeta bajacaliforniensis DSM16054^T	
Spirochaeta sphaeroplastigenes JC133^T	
Staphylococcus aureus ATCC25923	Nutrient broth, pH-7, 37^{o}C
Staphylococcus aureus ATCC43300	
Staphylococcus sp. N1	
Staphylococcus sp. N2	
Staphylococcus sp. N3	
Staphylococcus sp. N5	
Staphylococcus sp. N5	
Staphylococcus sp. S74	
Staphylococcus sp. S75	
Staphylococcus sp. S76	
Staphylococcus sp. S90	
Staphylococcus sp. S91	
Streptomyces sp. JC322	
Streptomyces sp. JC323	
Vogesella alkaliphila JC141^T	Nutrient medium, pH-7, 30^{o}C
Vogesella lacus LMG24504^T	
Vogesella perlucida LMG24214^T	
Vogesella indigofera LMG6867	

2.4.2 Extraction of total lipids

0.1-0.2 grams of lyophilized cells were sonicated for 1 hour in 10 ml of methanol:dichloromethane:water (10:5:4). The extract was centrifuged at 5000g for 10 min. Supernatant was collected in a new tube and again pellet was sonicated in methanol: dichloromethane:water (10:5:4) and the supernatants were pooled together. Ten ml of dichloromethane and water was added to the supernatant. The mixture was centrifuged at 5000g for 10 min. The dichloromethane layer was collected and evaporated to dryness. Dichloromethane extract was further used for the characterization of hopanoids by GC-MS analysis.

2.4.3 Characterization of hopanoid by GC-MS

Hopanoids were derivatized by 100 µl of acetic anhydride:pyridine (1:1) and incubated at 80^{o}C for 30 min. Acetylated extract was analysed by GC-MS (Agilent 7890). Separation was achieved using DB-1HT column (30m X 0.25mm i.d.; 0.1 µm film thickness) with helium as carrier gas. Ramping program was started with 100^{o}C hold for 2 min then ramped from 100^{o}C to 200^{o}C at 10^{o}C.min^{-1} followed by 200-360^{o}C at 6^{o}C.min^{-1} (held for 10 min). System was operated with the following parameters; electron voltage 70eV, source temperature 200^{o}C, interface temperature 350^{o}C, acquisition delay was for 120s. Mass spectrometer was operated in full scan mode (m/z 30-1000).

2.4.4 Statistical analysis of GC-MS data

Statistical analysis was done using a web based tool MetaboAnalyst server (http://www.metaboanalyst.ca/MetaboAnalyst/). Heat map which is a graphical representation of data where the individual variables are represented in colours was also generated using MetaboAnalyst. Principal component analysis (PCA) was used to represent whether each species is having variations compared to other species. Based on hopanoid data dendrogram was constructed using MetaboAnalyst server.

2.5 Mining of genomes for hopanoid biosynthetic pathway proteins

In the NCBI database total available SHC protein sequences were retrieved. Homologs of SHC protein were identified by BLAST and aligned by using ClustalW. The MEGA6 was used to construct phylogenetic tree and 242 sequences representing all sequences were selected based on phylogenetic affiliation. In the selected organisms

hopanoid biosynthetic proteins were searched in NCBI database. iTOL (interactive tree of life) server was used to draw to pictorial representation of occurrence of hopanoid biosynthetic pathway in microorganisms.

2.6 Genomic insights of hopanogenesis in *Rmi. udaipurense* JA643^T

2.6.1 DNA isolation

DNA was isolated using QIAamp DNA mini kit (Qiagen) according to the manufacture's protocol. The late log phase culture of *Rmi. udaipurense* JA643^T was pelleted down by centrifugation at 5000g for 10 min. Pellet was resuspended in 180 µl of ATL buffer with 10 µl of lysozyme (10 mg/ml) and incubated at 37^{o}C for 15 min. After incubation, 20 µl of proteinase K was added and mixed by pulse vortexing. The mixture was incubated at 56^{o}C for 2 hours. RNase A (4 µl) treatment was given and incubated at 70^{o}C for 10 min. 200 µl of ethanol was added and loaded into QIAamp Mini spin column. Column was washed with 500 µl buffer AW1 followed by second washing with 500 µl buffer AW2 and centrifuge at 20,000g for 3 min. To dry the column, it was centrifuged at high speed for 1 min. Added 200 µl of deionised water into the column and incubated for 2 min at room temperature and DNA was eluted by centrifugation at 6000g for 1 min. The quality of DNA was checked on 0.8% agarose gel. DNA was stored in -80^{o}C.

2.6.2 Genome sequencing and annotations

Genome sequencing was carried out using Illumina Hiseq platform which was outsourced from NxGenBio Life Sciences, New Delhi, India. Covaris system was used to fragment the genomic DNA to a mean size range of 300-350 bp and run on Agilent 2100 Bioanalyzer system to check the fragmentation results. The peak at 200 bp indicated that the fragmentation was successful and desired. Standard Illumina TruSeq protocol was used to prepare DNA shortgun library. Illumina Hiseq 2X100 bp paired end chemistry was utilized for sequencing. Two sequencing runs were carried out. FastQC tool was used to check the quality of raw reads (www.bioinformatics.babraham.ac.uk/ projects/fastqc). Using fastx tool kit the raw reads were trimmed (www.hannonlab.cshl.edu/fastx_toolkit). The raw reads were assembled into contigs using Newbler assembly software. Annotations were performed with the RAST (Rapid Annotation using Subsystem Technology) server. tRNA and rRNA were predicted using

RNAmmer. *In silico* DNA–DNA hybridization was carried out using formula 2 of GGDC website server (http://ggdc.dsmz.de/).

2.7 Genome-wide transcriptional response of *Δshc* mutant of *Rps. palustris* TIE-1

2.7.1 Whole-genome microarray construction

The genome sequence of *Rps. palustris* TIE-1 having accession number CP001096.1 was retrieved from NCBI. 5245 unique number of genes available in the genome of strain TIE-1. 8×15k array chip was used for experiment. The probes were designed as follow; three probes per coding genes; two probes per genes coding for hypothetical protein and a probe for genes (89 genes) showing cross-hybridisation. Each probe is 60 mer in length.

2.7.2 RNA isolation and microarray experiment

The experiment was carried out in triplicate, each with three biological replicates. Three biological replicates from individual experiment was pooled together to minimize biological variation. The cells were harvested from the mid-log growth phase for microarray experiment. By harvesting cells in mid log phase, the variability between the strains due to different growth rates and morphologies was minimized (Welander *et al.*, 2009). Cells (10 ml each) were harvested by centrifugation (4^{o}C, 2000g for 10 min) and washed twice with PBS buffer. The cell pellet was snap freeze immediately in liquid nitrogen and stored in -80^{o}C until further process. RNA was isolated using Qiagen RNeasy Mini kit and RNA quality (integrity and DNA contamination) was checked by Agilent 2100 bioanalyser. Isolated RNA was treated with DNase using on column DNase treatment as per manufacturer's instructions. The RNA was eluted with 20 µl of nuclease free water and stored at -80^{o}C until further use.

2.7.3 RNA quality and quantity assessment

The isolated RNA was quantified using a NanoDrop spectrophotometer (ND-2000, Thermo fisher scientific, USA). The quantity was measured by absorbance at 260 nm and the purity was assessed using ratio 260/230 and 260/280 for salt/organic solvents and protein/phenol/other contaminants respectively. The isolated total RNA integrity was analysed with an Agilent 2100 Bioanalyzer (Agilent Technologies, Palo Alto, CA) according to the manufacturer's instructions. The 16S and 23S rRNA ratio was obtained

from 2100 Expert software (Agilent Technologies) and RNA integrity number (RIN) was obtained from RIN Beta version software (Agilent Technologies).

2.7.4 Labeling and microarray hybridization

The RNA samples were labelled using Agilent Quick-Amp labeling Kit (Agilent Technologies) as per manufacturer's instructions. In brief, 500 ng each of total RNA were reverse transcribed using oligo-dT primer tagged to a T7 polymerase promoter and converted to double stranded cDNA. The cRNA was generated by *in vitro* transcription during which, the dye Cy3 CTP (Agilent Technologies) was incorporated. The labelled cRNA was cleaned up using Qiagen RNeasy Mini kit columns as per manufacturer's instructions (Qiagen, USA). The yield and specific activity was measured using NanoDrop spectrophotometer.

2.7.5 Hybridization and scanning

The fragmentation of labelled cRNA and hybridization were carried out using the Gene Expression Hybridization kit (Agilent Technologies). In brief, the 600 ng of labelled cRNA samples were fragmented at 60^{o}C and hybridized on to Agilent *Rhodopseudomonas palustris*_GXP_8X15k (AMADID: 75878) array format. Hybridization was carried out in Agilent's Surehyb chamber at 65^{o}C for 16 hours. The hybridized slides were washed using Agilent Gene Expression wash buffers (Agilent Technologies) and scanned using the Agilent Microarray Scanner (Agilent Technologies).

2.7.6 Feature extraction

Data extraction from images were carried out using Feature Extraction software version 11.5 (Agilent Technologies).

2.7.7 Microarray data analysis

Images were quantified using Feature Extraction software version 11.5 (Agilent Technologies). Feature extracted raw data was analysed using GeneSpring GX software version 13.0 (Agilent Technologies). Normalization of the data was done in GeneSpring GX using the 75th percentile shift (Percentile shift normalization is a global normalization, where the locations of all the spot intensities in an array are adjusted). Differential expression patterns were identified among the samples. Fold change was

calculated as logarithmic values with log_2. Significant genes upregulated (fold change> 0.6 which corresponds to 1.5 fold change) and downregulated (fold change <-0.6 which corresponds to -1.5 fold change) in the test samples with respect to control sample were identified. Statistical student t-test and p-value among the replicates was calculated based on volcano plot algorithm. Differentially regulated genes were clustered using hierarchical clustering based on Pearson coefficient correlation algorithm to identify significant gene expression patterns. Pathway analysis for the differentially regulated genes was performed using DAVID database (http://david.abcc.ncifcrf.gov/home.jsp).

2.7.8 Microarray data submission

Microarray data were deposited in the GEO database under project identifier GSE84950.

2.7.9 Network construction, visualization and analysis

PheNetic is an algorithm which selects the sub-network from selected gene list between genetic perturbation (a cause) and differentially expressed genes (its effect). PheNetic was used with a path length of 4, cost 0.1 fold change 1.5 and p-value 0.05. No adjustments of the probabilities in the network based on network centrality were performed. Visualization and analysis of the network was performed by using Cytoscape 3.0. Gene Ontology (GO) annotation for *Rps. palustris* TIE-1 was downloaded from UniProt website (ww.uniprot.org).

2.8 Swimming and swarming motility assay

To understand whether weaken cell membrane in hopanoid deficient mutant affect the cell motility swimming and swarming motility assays were performed according to Schmerk *et al.*, 2011. For swimming assays, 2 µl of overnight grown culture, adjusted to OD_{660nm} of 0.5, was inoculated within the agar of swim plate (YPP and YP media with 0.3% agar). For swarming assays, 2 µl of culture adjusted to OD_{660nm} of 0.5 was spotted on top of the swarm plate agar (YPP and YP media with 0.5% agar and 0.2% glucose). The plates were incubated at 30°C for 96 hours, after which the diameter of the swimming and swarming zones were measured.

2.9 NPN uptake assay

To test whether hopanoid deficiency leads to defected membrane permeability and transport, NPN uptake assay was carried out. *Rps. palustris* strains (WT and *Δshc* mutant) cultures were grown for 96 hours and harvested by centrifugation (5,000g for 10 min) under sterile condition. The pellet was washed with media and final OD_{660nm} was adjusted to 0.5. 180 µl of cells was transferred to 96-wells microtiter plate. The background signal was measured for 5 min before NPN was added to a final concentration of 5 µM (5 µl of 185 µM NPN solution) per well. The uptake of dye was recorded for 300 min by measuring its emission under the same conditions. The emission of NPN was recorded using a plate reader [Perkins Elmer EnVision; filters (wavelength/bandwidth): excitation = 340/25 nm, emission = 450/8 nm]. Readouts were taken after every 5 min, with 25s of shaking before every readout. The entire assay was performed at room temperature. Pyruvate was added at 10 mM concentration whereas control was without carbon source.

2.10 H33342 ATP-dependent efflux assay

ATP-dependent efflux assay was performed to test whether energy dependent multidrug transport was impaired in *Δshc* mutant. *Rps. palustris* strains (WT and *Δshc* mutant) were grown for 96 hours at 30°C. Cells were harvested by centrifugation (5,000g for 10 min) and washed once with YP media without supplement of an utilizable carbon source. All the following wash steps and resuspensions were performed in YP media containing 5 µM H33342 (8,000g for 2 min). The OD_{660nm} was adjusted to 1.0 before freshly prepared CCCP in DMSO was added to a final concentration of 100 µM [~1% (vol/vol) DMSO] to abolish ATP synthesis. The 1% DMSO did not inhibit growth of strain TIE-1 or *Δshc* mutant. The mixtures were incubated in darkness for 1hour, washed twice to remove CCCP, and then resuspended in YP media and adjusted to OD_{660nm} of 1.0. Bacterial suspension (180 µl) was transferred to wells of a 96-well microtiter plate. The initial uptake/equilibrium of H33342 was recorded using a plate reader for 60 min [filters (wavelength/ bandwidth): excitation = 340/25 nm, emission = 405/8 nm], and readings were taken after every 5 min, with 25s of shaking before readouts. Afterward, pyruvate was added to a final concentration of 20 mM (5 µl of 740 mM solution) per well and the change in H33342 emission was recorded for an additional 240 min. All steps of the assay were performed at room temperature.

2.11 Protein modelling and docking experiments

Protein sequence for Rpal_1916 and Rpal_2444 was retrieved from the NCBI database. TMHMM2 (http://www.cbs.dtu.dk/services/TMHMM/) were used for the prediction of transmembrane helices from the protein sequences. Cholesterol recognition amino acid consensus (CRAC) and CRAC-like motifs in proteins were searched using EMBOSS: fuzzpro (emboss.bioinformatics.nl/cgi/emboss/fuzzpro). A sequence given as a search pattern were: CRAC motif: [LV]-X(1,5)-Y-X(1,5)-[RK]; [RK]-X(1,5)-Y-X-(1,5)-[LV] and CRAC-like motif: [LV]-X(1,5)-F-X(1,5)-[RK]; [RK]-X(1,5)-F-X(1,5)-[LV]. The hydrophobicity plot was plotted using ProtScale server (http://web.expasy.org/protscale/). The pdb (protein data bank) structure of MPP1 protein was shared by Prof. Aleksander F. Sikorski and the homology model for Rpal_1916 and Rpal_2444 was generated using I-TASSER server (http://zhanglab.ccmb.med.umich.edu/I-TASSER/). The quality of generated model was assessed using PROSESS server (http://www.prosess.ca). The docking of cholesterol, diplopterol, diploptene and tetrahymanol was carried out using PyRx software and docking was visualized using discovery studio software and PyMol software.

RESULTS

3.0 Results

3.1 Mining of hopanoids in bacteria

Newly isolated bacterial species from the Bacterial Discovery Laboratory, Jawaharlal Nehru Technological University, Hyderabad and its phylogenetically nearest members were selected to find out the distribution and chemotaxonomic importance of hopanoids. Mining of hopanoids was carried out for 86 bacterial species which belong to 24 different genera. Out of 86 bacterial species screened, 60 species were shown to be containing detectable hopanoid which represents 19 genera, whereas 26 bacterial species (representing 5 genera) didn't show any detectable hopanoid. Mining of hopanoids was carried out using thin layer chromatography or GC-MS analysis. Distribution of hopanoids in screened bacteria is given in Table 2, Table 3 and Table 4. The bacteria which were not containing any detectable hopanoid are listed in Table 5.

3.1.1 Distribution of hopanoids among the members of genus *Rhodomicrobium*

Three strains of genus *Rhodomicrobium* (*Rmi. udaipurense* JA643^T, *Rmi. udaipurense* JA755 and *Rmi. vannielii* DSM162^T) were screened using thin layer chromatography. All three strains had bacteriohopane derivatives (BHD1, 2), diplopterol and unidentified hopanes (UH1, 2 and 4) as major hopanoids (Fig. 4). Diploptene and an unidentified hopane (UH5) were present only in strains JA643^T and JA755. An unidentified hopane (UH3) was present in strain JA755 and *Rmi. vannielii* DSM 162^T. As *Rmi. udaipurense* JA643^T had wide variety of hopanoids, it was selected for further study and genome sequencing. Hopanoids of *Rmi. udaipurense* JA643^T were identified using GC-MS analysis. In *Rmi. udaipurense* JA643^T squalene (I), hop-22(29)-ene (II), diplopterol (VI), tetrahymanol (VIII), 2-methyldiploptetrol (VII), adenosylhopane (XIX), bacteriohopanetetrol (XXIII), aminobacteriohopanetriol (XXIV), N-tryptophanyl aminobacteriohopanetriol (XXVI) were identified using GC-MS analysis (Fig. 5) and their structures are shown in Fig. 2.

3.1.2 Distribution of hopanoids among the members of genus *Rhodovulum*

Fifteen species of the genus *Rhodovulum* were screened for the presence of hopanoids using GC-MS analysis. Six strains (*Rdv. adriaticum* DSM2781^T, *Rdv. phaeolacus* JA580^T, *Rdv. euryhalinum* DSM4868^T, *Rdv. robiginosum* DSM12329^T, *Rdv.*

strictum DSM11289^T and *Rdv. steppense* VKM B-2489^T) showed the presence of hopanoids (Table 3). *Rdv. algae* JA877^T, *Rdv. viride* JA756^T, *Rdv. sulfidophilum* DSM1374^T, *Rdv. visakhapatnamense* JA181^T, *Rdv. salis* JA756^T, *Rdv. imhoffii* JA125^T and *Rdv. bhavnagarense* JA738^T contained choles-5-en-3ol-like molecule whereas, in *Rdv. kholense* JA297^T and *Rdv. marinum* JA128^T there was no detectable hopanoid or cholesterol-like molecules (Table 3).

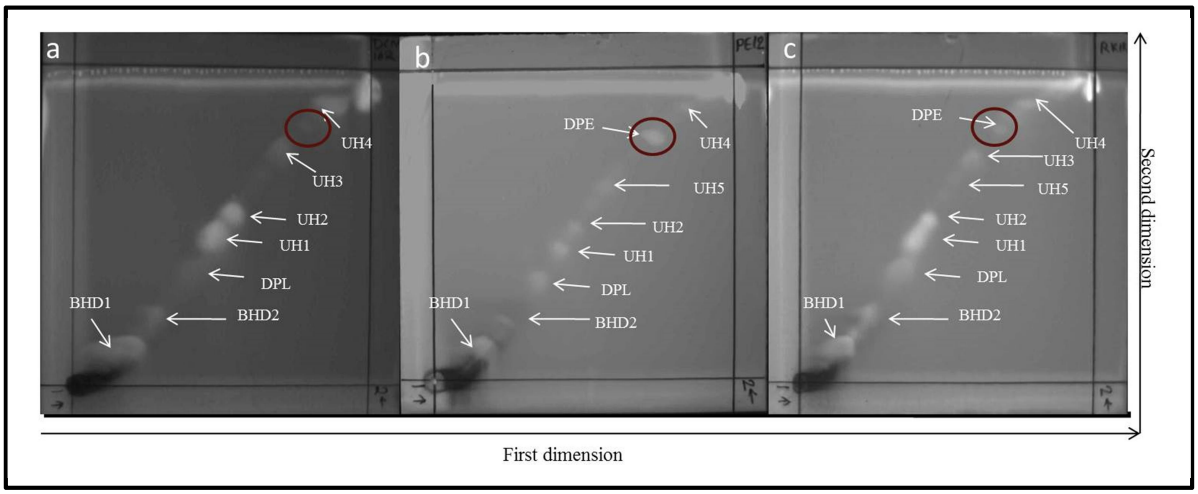

Fig. 4. Two-dimensional thin-layer chromatogram of whole-cell hopanoids from members of the genus *Rhodomicrobium*. Hopanoids were double developed in dichloromethane (DCM); BHD1,2, bacteriohopane derivatives; DPL, diplopterol; DPE, diploptene; UH1–5, unidentified hopanes. Hopanoid profile of (a) *Rmi. vannielii* DSM162^T; (b) *Rmi. udaipurense* JA643^T and (c) *Rmi. udaipurense* JA755 is shown in figure.

Table 2. Distribution of hopanoids in screened bacteria which was carried out by thin layer chromatography.

Bacteria having hopanoids	Name of the hopanoids									
	DPL	BHD1	BHD2	DPE	UH1	UH2	UH3	UH4	UH5	UH6
Alcanivorax xenomutans JC109^T	+	+	+	-	+	-	-	-	-	+
Alcanivorax dieselolei DSM16502 ^{T}	+	+	+	-	+	-	-	-	-	+
Alcanivorax balearicum DSM23776 ^{T}	+	+	+	-	+	-	-	-	-	+
Ciceribacter lividus MSSRFBL ^{T}	+	+	+	+	-	+	+	+	-	-
Cohaesibacter haloalkalitolerance JC131^T	+	+	+	+	-	-	-	-	-	+
Cohaesibacter marisflavi NCCB100300^T	+	+	+	+	-	-	-	-	-	-
Ensifer kostiensis DSM13372^T	+	+	+	+	-	-	+	+	-	-
Ensifer adhaerens LMG20216^T	+	+	+	+	-	+	+	+	-	-
Erythrobacter longus CIP104268^T	+	+	+	-	+	+	-	-	+	-
Erythrobacter odishensis JA747^T	+	+	+	+	-	-	-	-	-	-
Falsirhodobacter halotolerans JA144^T	+	+	+	+	-	-	-	-	-	-
Litoribacter alkaliphilus JC166^T	+	+	-	+	+	+	-	+	-	-
Litoribacter ruber KCTC 22899^T	+	+	+	+	+	+	-	+	-	-
Mongoliicoccus alkaliphilus JC165^T	+	+	+	+	-	-	-	+	+	-
Mongoliicoccus roseus KCTC 19808^T	+	+	+	+	-	-	-	+	+	-
Pontibacter odishensis JC130^T	+	+	+	+	-	-	-	-	-	-
Pontibacter actiniarum LMG23027^T	+	+	+	+	-	-	-	-	-	-
Pontibacter korlensis NRRL B-51097^T	+	+	+	+	+	-	-	-	-	-
Rhizobium endophyticum JC140^T	+	-	+	-	+	+	-	-	-	-
Rhizobium yanglingense LMG19592^T	-	-	+	-	+	+	-	-	-	-
Rhizobium alkalisoli CCBAU 01393^T	+	+	+	+	+	+	-	-	+	-
Rhizobium vignae CCBAU 05176^T	-	-	+	+	+	+	-	-	+	-
Rhodomicrobium udaipurense JA755	+	+	+	+	+	+	+	+	+	-
Rhodomicrobium udaipurense JA643^T	+	+	+	+	+	+	-	+	+	-
Rhodomicrobium vannielii DSM162^T	+	+	+	-	+	+	+	+	-	-
Sinorhizobium americanum DSM15007^T	+	+	+	+	-	+	+	+	-	-
Salinicoccus alkaliphilus T8^T	+	+	+	+	+	-	-	-	-	-
Salinicoccus halitifaciens JC90^T	+	+	+	+	+	+	-	-	-	-
Salinicoccus kekensis K164^T	+	+	+	+	+	-	-	-	-	-

Note: Screening was done using thin layer chromatography which was stained with 0.1% alcoholic solution of berberine hydrochloride. The bands were visualized at 360 nm.

DPL-diplopterol; BHD1-bacteriohopane derivative-1; BHD2-bacteriohopane derivative 2; DPE-diploptene; UH1 to 6 unidentified hopanoids.

Table 3. Distribution of hopanoids or cholesterol-like molecules among the members of genus *Rhodovulum*

Cyclic triterpenoids	1	2	3	4	5	6	7	8	9	10	11	12	13	14	15
Hopanoids															
2-Methylhop-21-ene (V)	-	-	-	-	-	-	-	+	+	-	-	-	-	+	-
Diplopterol (VI)	-	-	-	-	-	-	-	+	+	-	-	-	-	-	-
2-Methyldiplopterol (VII)	-	-	-	-	-	-	-	+	+	-	-	-	-	-	-
Hop-21-ene (IV)	-	-	-	-	-	-	-	-	-	+	-	+	+	-	-
Bacteriohopanetetrol (XXIII)	-	-	-	-	-	-	-	-	-	+	-	+	-	-	-
H1	-	-	-	-	-	-	-	-	+	-	-	-	-	-	-
H2	-	-	-	-	-	-	-	-	+	-	-	-	-	-	-
Cholesterol															
Cholest-5-en-3-ol-like molecule	+	+	+	+	-	+	+	-	-	-	-	-	-	-	+

Note: Screening was carried out using GC-MS; + represents the presence; – represents absence; H- Unidentified hopanoid (H1 and H2)

1-*Rdv. algae* JA877^T; 2-*Rdv. viride* JA756^T; 3-*Rdv. sulfidophilum* DSM 1374^T; 4-*Rdv. visakhapatnamense* JA181^T; 5-*Rdv. kholense* JA297^T; 6-*Rdv. salis* JA756^T; 7-*Rdv. imhoffii* JA125^T; 8-*Rdv. adriaticum* DSM2781^T; 9-*Rdv. phaeolacus* JA580^T; 10-*Rdv. euryhalinum* DSM4868^T; 11-*Rdv. marinum* JA128^T; 12-*Rdv. robiginosum* N2^T; 13-*Rdv. strictum* MB G2^T; 14-*Rdv. steppense* A-20s^T; 15-*Rdv. bhavnagarense* JA738^T

Table 4. MS/MS Fragmentation patterns of hopanoids and comparative distribution of hopanoids among the members of genus *Rhodoplanes*

Hopanoids	Mass fragmentation (m/z) pattern	*Rhodoplanes* sp.				
		1	2	3	4	5
2-Methyldiplopterol (VII)	189 205 220 213 249 343 369 389 410 424 470 484	+	+	+	+	+
2-Methylhop-21-ene (V)	161 189 191 205 231 285 355 381 410 424	-	+	-	-	-
2-Methylhop-22(29)-ene (III)	191 205 218 245 313 368 381 424	+	-	-	-	-
2-Methyltetrahymanol (IX)	189 205 220 249 339 368 381 410 424 484	+	+	+	+	+
Hop-22(29)-ene (II)	191 203 218 231 255 299 341 367 410	+	-	+	+	+
AnhydroBHT (XXX)	191 213 287 369 391 534 612	+	-	-	-	-
Aminobacteriohopanetriol (XXIV)	191 219 229 231 253 317 369 403 413 492 558 639 713	-	-	+	-	-
Bacteriohopanetetrol (XXIII)	191 208 282 317 369 397 414 433 461 493 562 620 714	+	-	-	-	-
BHP-492 (XVII)	191 211 239 271 328 356 381 407 467 492	-	-	+	+	+
BHP-508 (XVI)	191 213 229 269 287 343 369 453 508	-	-	-	+	+
BHP-550 (XVIII)	153 191 213 287 329 369 493 508 550	+	-	-	+	+
Diplopterol (VI)	191 207 249 279 347 367 449 470	+	+	+	+	+
Hop-17(21)-ene (IV)	161 191 203 217 231 367 395 410	-	-	+	+	+
Tetrahymanol (VIII)	191 206 231 249 369 410 455 470	+	+	+	+	+
H1	191 207 217 231 353 384 396 413 428	-	+	-	-	+
H2	151 177 189 205 219 329 442	-	+	-	-	-
H3	136 191 275 314 350 400 434 486 517 556 596 640	-	+	-	-	-
H4	147 191 217 249 381 410	+	-	-	-	-
H5	191 217 225 263 304 347 442 607 669 732	+	-	-	-	-
H6	133 191 271 313 369 402 669 852	-	+	-	-	-
H7	191 209 281 391 490 537 606 665	-	-	-	+	-
H8	192 207 241 281 305 361 397 431 466	-	-	-	+	-
H9	191 208 251 295 369 396 433 452 466 545 697 788	-	-	-	+	+
H10	191 222 257 269 369 415 506 690	+	-	-	-	-

Note: Screening was carried out using GC-MS; + represents the presence; – represents absence; H- Unidentified hopanoid (H1 to H10)

1-*Rpl. oryzae* JA793^T, 2-*Rpl. elegans* DSM11907^T, 3-*Rpl. piscinae* JA266^T, 4-*Rpl. pokkaliisoli* JA415^T, 5-*Rpl. roseus* DSM5909^T

Table 5. Bacteria not having any detectable hopanoids

Bacteria not having detectable hopanoids	
Jeotgalibacillus alimentarius JCM 10872^T	*Spirochaeta sphaeroplastigenens* JC133^T
Jeotgalibacillus alkaliphilus JC303^T	*Staphylococcus aureus* ATCC25923
Jeotgalibacillus malaysiensis KCTC 33550^T	*Staphylococcus aureus* ATCC43300
Jeotgalibacillus salarius KCTC 13257^T	*Staphylococcus* sp. N1
Jeotgalibacillus terrae KCTC 13528^T	*Staphylococcus* sp. N2
Paraclostridium benzoelyticum JC272^T	*Staphylococcus* sp. N3
Rhodobacter aestuarii JA296^T	*Staphylococcus* sp. N5
Rhodobacter capsulatus ATCC11166^T	*Staphylococcus* sp. N5
Rhodobacter sphaeroides ATH2.1^T	*Staphylococcus* sp. S74
Rhodobacter viridis JA737^T	*Staphylococcus* sp. S75
Spirochaeta alkalica Z-7491^T	*Staphylococcus* sp. S76
Spirochaeta americana ASpG1^T	*Staphylococcus* sp. S90
Spirochaeta bajacaliforniensis DSM16054^T	*Staphylococcus* sp. S91

Note: Screening was done using thin layer chromatography which was stained with 0.1% alcoholic solution of berberine hydrochloride. The bands were visualized at 360 nm.

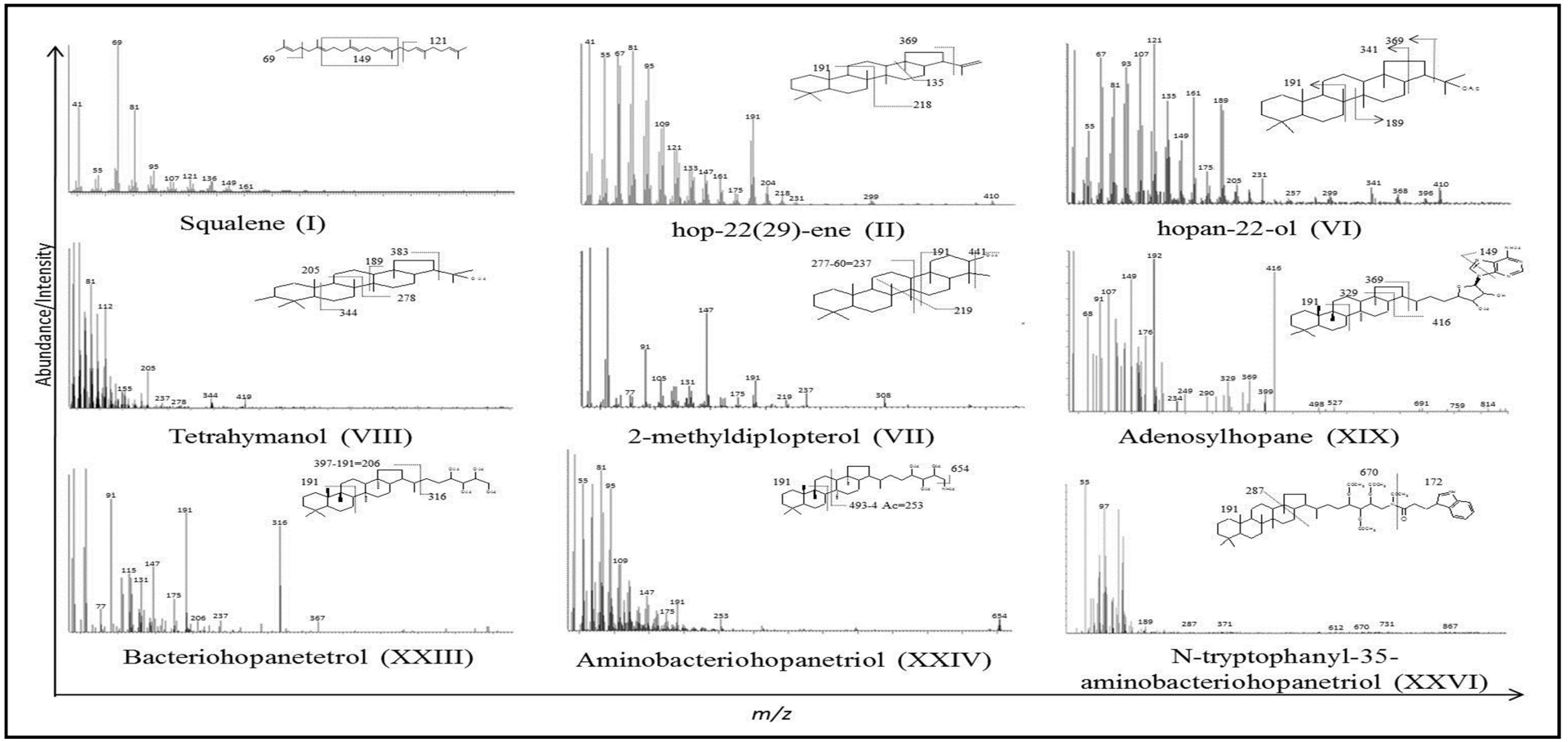

Fig. 5. Mass spectra and fragmentation pattern of hopanoids detected by GC-MS analysis of acetylated total lipid extract from the *Rmi. udaipurense* JA643^{T}. Hopanoids were identified by comparing fragmentation patterns with previously published data. Squalene (I), hop-22(29)-ene (II), hopan-22-ol (VI), tetrahymanol (VIII), 2-methyldiplopterol (VII), adenosylhopane (XIX), bacteriohopanetetrol (XXII), aminobacteriohopanetriol (XXIV)) and N-tryptophanyl-35-aminobacteriohopanetriol (XXVI).

3.1.3 Distribution of hopanoids among the members of genus *Rhodoplanes*

Acetylated total lipid extract of five species which belongs to genus *Rhodoplanes* contain 2-methyldiplopterol (VII), 2-methylhop-21-ene (V), 2-methylhop-22(29)-ene (III), 2-methyltetrahymanol (IX), hop-22(29)-ene (IV), anhydrobacteriohopanetetrol (XXX), aminobacteriohopanetriol (XXIV), bacteriohopanetetrol (XXIII), BHP-492 (XVII), BHP-508 (XVI), BHP-550 (XVIII), diplopterol (VI), hop-17(21)-ene (IV) and tetrahymanol (VIII; Table 4). Additionally, there were peaks with hopanoid like fragmentation pattern which might be unidentified hopanoids (H1-10). Fragmentation pattern and distribution of hopanoids in the genus *Rhodoplanes* is given in Table 4.

Rpl. oryzae JA793^T has 3.3% hopanoid in total lipid extract which is higher compared to the other four species of *Rhodoplanes* used in this study. This species has tetrahymanol (VIII) as the major hopanoid lipid which is approximately 38% of the total hopanoids (Fig. 6). The majority of the hopanoids of *Rpl. piscinae* JA266^T are diplopterol (VI) and 2-methyldiplopterol (VII). Diplopterol (VI) and its methylated product 2-methyldiplopterol (VII) comprise around 89% of total hopanoids in strain JA266^T. It has BHP-492 (XVII) and aminobacteriohopanetriol (XXIV) as the elongated hopanoids. The total hopanoids represents approximately 1.76% of total lipids. *Rpl. elegans* DSM11907^T has low content (~1.28%) of hopanoids compared to other *Rhodoplanes* spp. Polyfunctionalized elongated hopanoids were not present in *Rpl. elegans* DSM11907^T in detectable quantities. *Rpl. pokkaliisoli* JA415^T contains tetrahymanol (VIII) and its methylated product 2-methyltetrahymanol (IX) as its major part of hopanoids. *Rpl. pokkaliisoli* JA415^T has elongated hopanoids as BHP-492 (XVII), BHP-550 (XVIII) and BHP-508 (XVI; Fig. 6). Total hopanoids represent approximately 1.82% of total lipids. The bulk hopanoids of *Rpl. roseus* DSM5909^T were tetrahymanol (VIII) and its methylated product 2-methyltetrahymanol (IX). Tetrahymanol (VIII) and 2-methyltetrahymanol (IX) comprises around 80% of total hopanoids in strain DSM5909^T (Fig. 6). Principle component 2D score plot, heatmap and dendrogram were generated using MetaboAnalyst tool for the hopanoid data obtained in this study (Fig. 7).

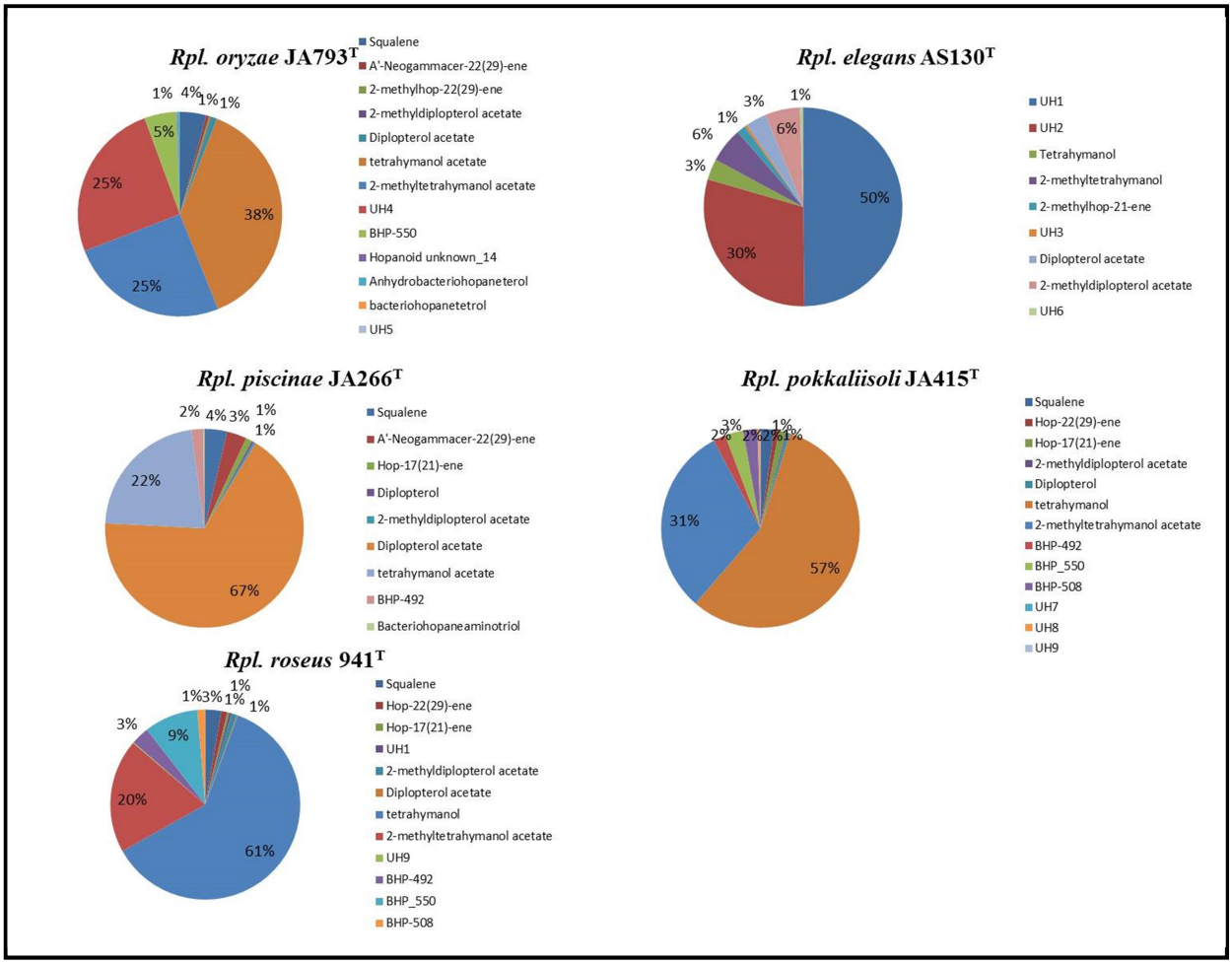

Fig. 6. Distribution of hopanoids among the members of the genus *Rhodoplanes*.

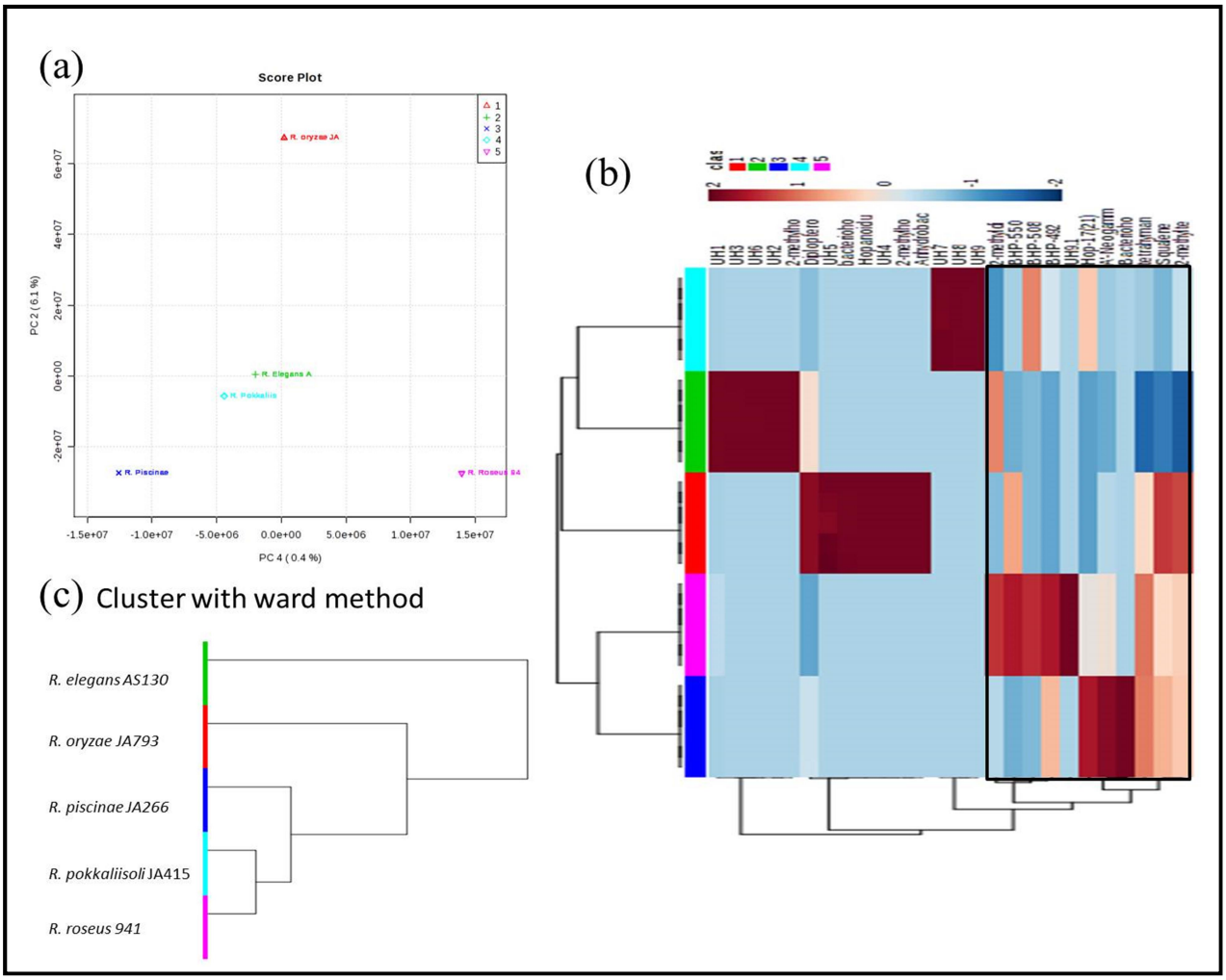

Fig. 7. (a) Principal component plot (2D score plot); (b) Heat map and (c) dendrogram (based on cluster ward method) generated based on hopanoid distribution using MetaboAnalyst server, which indicates that there is a clear difference in the hopanoid content between the species of genus *Rhodoplanes*.

3.2 Mining genomes for hopanoid biosynthetic pathway proteins

To determine the distribution of hopanoid biosynthetic pathway among the members of domain Bacteria, mining of the NCBI database for proteins involved in hopanoid biosynthesis was carried out. Squalene hopene cyclase (SHC) is the first enzyme in the hopanoid biosynthetic pathway. The NCBI database contained 8272 SHC protein sequences as on when the study was carried out. SHC protein is present among the members of the phylum *Actinobacteria*, *Cyanobacteria*, *Firmicutes*, *Proteobacteria*, *Planctomycetes*, *Verrucomicrobia*, *Nitrobacter*, *Solibacter*, *Chloroflexi*, *Armatimonadetes*, *Nitrospinae*, *Bacteroidetes* and *Acidobacteria* (Fig. 8). From the database, 222 bacterial SHC enzymes representing all genera were selected based on their phylogenetic affiliation. Few eukaryotic members were also possess squalene hopene cyclase protein out of which 21 members were selected for further study. The selected organisms include 26 members of phylum *Actinobacteria*, 42 members of phylum *Cyanobacteria*, 35 members of phylum *Firmicutes*, 85 members of phylum *Proteobacteria*, 10 members of phylum *Planctomycetes*, 8 members of phylum *Verrucomicrobia*, 3 members of phylum *Nitrobacter*, 2 members of phylum *Solibacter*, 11 members represented the remaining phyla and 21 members representing the kingdom *Fungi*. In the selected organisms hopanoid biosynthetic pathway proteins [glycosyl transferase family 2 (hpnB), 5-methylthioadenosine nucleosidase (hpnG), radical SAM protein required for addition of adenosine to hopane skeleton (hpnH), acetylornithine aminotransferase (hpnO), squalene associated FAD dependent desaturase (hpnE), squalene synthase (hpnC/hpnD) and sterol desaturase family protein (hpnX)] were mined from the NCBI database. The list of organisms selected and accession number for the protein which was identified in the respective member is given in Table S1.

3.2.1 Distribution of hopanoid biosynthetic pathway proteins in *Actinobacteria*

The NCBI database contained 1671 members of the phylum *Actinobacteria* which were genome sequenced and 83% (1393) members showed the presence of SHC protein. Few members showed the presence of homologous to SHC protein having different functions like prenyltransferase from *Saccharopolyspora erythraea* NRRL2338 (CAM03917) and *Rubrobacter xylanophilus* DSM9941 (ABG05671), MFS transporter from *Mycobacterium smegmatis* MC2155 (WP003895014). Based on the phylogenetic affiliation of SHC protein, 26 were selected and were screened for hopanoid biosynthetic

pathway proteins (Table S1). All selected members of phylum *Actinobacteria* had SHC protein, hpnH protein, hpnC protein and hpnE protein except for *Thermomonospora curvata* DSM43183 which did not have hpnC and hpnE protein. 5-methylthioadenosine nucleosidase (hpnG), acetylornithine aminotransferase (hpnO), glycosyl transferase family 2 (hpnB) and sterol desaturase family protein (hpnX) was not observed in 33%, 19%, 26% and 37% members out of selected *Actinobacteria* respectively.

3.2.2 Distribution of hopanoid biosynthetic pathway proteins in *Cyanobacteria*

In NCBI database, 142 members of the phylum *Cyanobacteria* were genome sequenced, out of which 42 members were selected for the screening of hopanoid biosynthetic pathway proteins. All the selected cyanobacterial members have all the proteins needed for hopanoids biosynthesis except "*Candidatus* Atelocyanobacterium thalassa isolate ALOHA" which did not have hpnH, hpnO, hpnB and hpnE protein (Table S1).

3.2.3 Distribution of hopanoid biosynthetic pathway proteins in *Firmicutes*

The NCBI database contained 2045 genome sequences of various members of phylum *Firmicutes*. Thirty five members were selected for further screening. Among selected members, hpnH, hpnG, hpnO, hpnB, hpnC, hpnE and hpnX protein were not observed in 26%, 52%, 37%, 26%, 21%, 16% and 39% members respectively (Table S1).

3.2.4 Distribution of hopanoid biosynthetic pathway proteins in *Proteobacteria*

In phylum *Proteobacteria*, 4216 copies of SHC proteins were present in NCBI database out of which 89 members were selected for the screening of hopanoid biosynthetic pathway proteins. The hpnH protein which is a radical SAM protein is present in 93% of the mined *Proteobacteria* members and absent in "*Candidatus* Phaeomarinobacter ectocarpi", *Corallococcus coralloides* ATCC25202, *Cystobacter fuscus* DSM2262, *Komagataeibacter europaeus* LMG18890, *Pseudoalteromonas* sp. Bsw20308 and *Stigmatella aurantiaca* DW4/3-1. The hpnG, hpnO, hpnB, hpnC, hpnE and hpnX proteins were not found in 44%, 53%, 36%, 57%, 32% and 69% of selected members of phylum *Proteobacteria* respectively (Table S1).

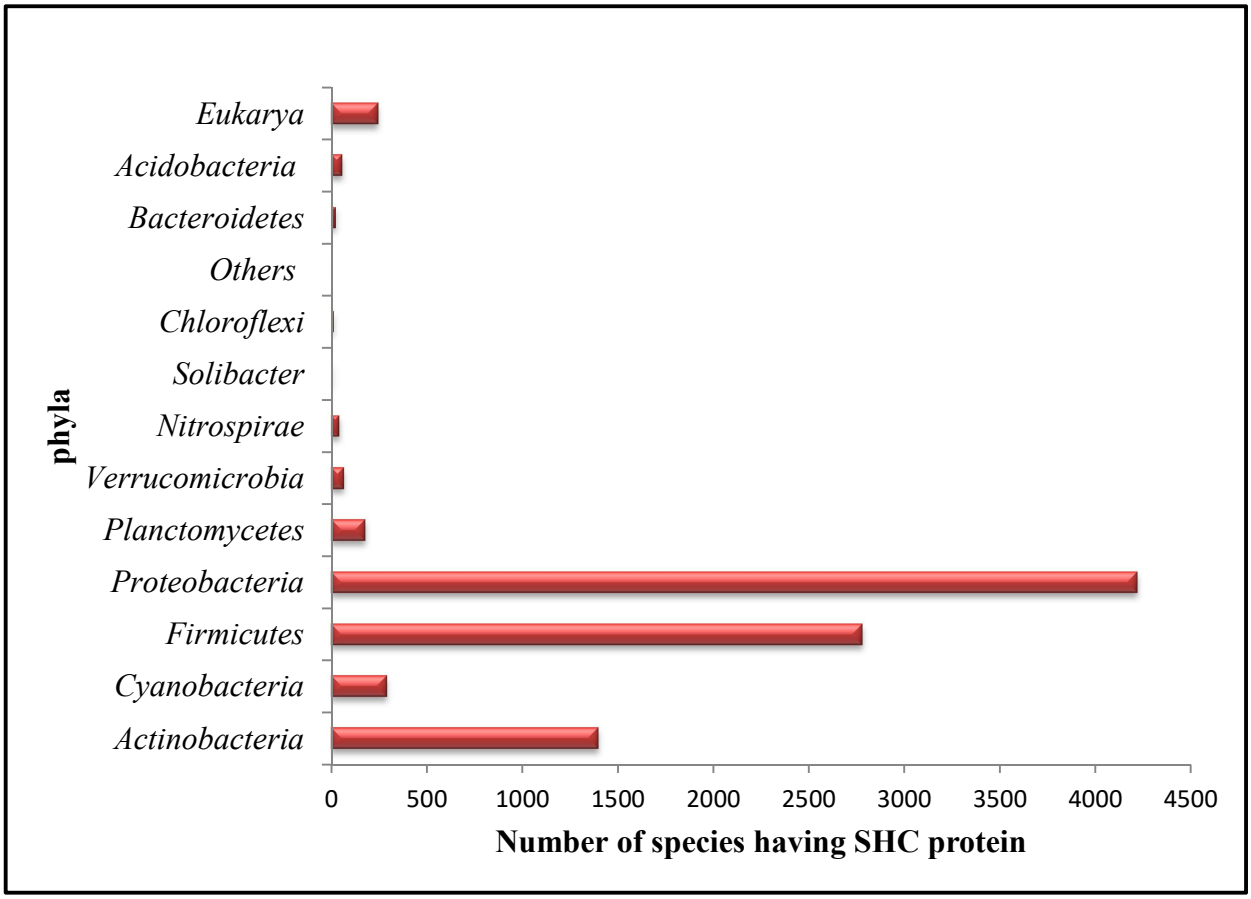

Fig. 8. Distribution of SHC protein in different phyla. The data is collected from the NCBI database.

3.2.5 Distribution of hopanoid biosynthetic pathway proteins in *Planctomycetes*

Out of 97 genomes sequenced *Planctomycetes*, 10 having squalene hopene cyclase protein were selected based on phylogenetic affiliation. Screening of hopanoid biosynthetic pathway proteins in NCBI database revealed that all the selected members have radical SAM protein (hpnH), glycosyl transferase family 2 (hpnB), 5-methylthioadenosine nucleosidase (hpnG) and acetylornithine aminotransferase (hpnO). Squalene synthase (hpnC/hpnD) and squalene associated FAD dependent desaturase (hpnE) were not present in "*Candidatus* Scalindua brodae" and *Planctomycete* sp. KSU-1, whereas sterol desaturase family protein (hpnX) was present only in *Blastopirellula marina* DSM3645, *Gemmata obscuriglobus* UQM2246 and *Schlesneria paludicola* DSM18645 (Table S1).

3.2.6 Distribution of hopanoid biosynthetic pathway proteins in other phyla

Hopanoid biosynthetic pathway proteins were screened among the phyla *Verrucomicrobia*, *Nitrobacter*, *Solibacter*, *Chloroflexi*, *Armatimonadetes*, *Nitrospinae*, *Bacteroidetes* and *Acidobacteria*. The list of all organisms selected and accession number for the protein which was identified in the respective member is given in Table S1.

3.2.7 Distribution of hopanoid biosynthetic pathway proteins in *Fungi*

Out of 154 squalene hopene cyclase proteins in NCBI database from the kingdom *Fungi*, only 21 members having these proteins were selected. Other members were also showed the presence of SHC homologs like animal, plants and protists but these were not included in this study. All the selected fungal members had SHC protein but didn't have other proteins involved in hopanoid biosynthetic pathway.

3.3 Draft genome sequence and hopanoid biosynthetic pathway of *Rmi. udaipurense* JA643^T

3.3.1 Overview of draft genome of *Rmi. udaipurense* JA643^T

Thirteen point seven million reads of 101 bp long were obtained after sequencing the genome of *Rmi. udaipurense* JA643^T. Raw reads were trimmed and assembled into the total genome of length 3,649,277 bp (3.64 Mb). The genome sequence has revealed 95% of its genome length, with average GC content of 62.4% and consists of 2989 open reading frames (ORFs). Out of the total ORFs, 2029 (67.85%) are functionally annotated, 899 (30.06%) hypothetical, 50 are putative and 12 are conserved hypothetical genes. Draft genome of *Rmi. udaipurense* JA643^T has an average gene length of 881 bases, with least as 70 bases to as much as 3326 bases per gene. The protein coding bases were 2,634,947 which are 65.63% of the total bases. It consists of 65 tRNAs, 2 rRNA (Table 6). With most of the protein coding sequences as much as 1367 genes (37%) were involved in metabolic, biosynthetic and other cellular process, 39 genes are involved in cell signaling and regulations, 26 genes are involved in motility and chemotaxis, 109 genes are involved in DNA metabolism, 74 genes are involved in membrane transport, 119 genes involved in RNA metabolism, 83 genes are involved in replication and DNA repair, 46 genes are involved into defence, 168 in protein metabolism, 88 genes are involved into cell wall and capsule formation and 259 which are not categorized into these groups. The remaining 1316 were related to hypothetical and unknown functions (Fig. 9).

Rmi. udaipurense JA643^T shows phototrophic growth and it has a set of homologous gene sequences for bacteriochlorophyll biosynthesis, a set of light harvesting complexes, a set of *puf* L,M,C and Q (Table 7). For N_2 fixation, two types of nitrogenase dimmers are present with all related cofactors and accessory genes for the nitrogenases. The nitrogenases present are molybdenum-dependent and also vanadium-dependent nitrogenase which is an alternative iron nitrogenase. Secondary transport system genes include facilitator superfamily (MFS) transporter, resistance nodulation cell division (RND) pumps, tripartite ATP-dependent periplasmic (TRAP) and organic solvent resistance transporters (Table 7). The heavy metal efflux transporters and organic solvent resistance transporters present in genome may allow the organism to survive in high concentrations of metals and other solvents.

Table 6. General features of *Rmi. udaipurense* JA643^T genome sequence

Total bases	3,649,277 bp (3.64 Mb)
Average gene length	881 bp
Protein coding features	2989
Protein coding bases	2634947 bp (65.63%)
tRNAs	65
rRNAs	2
GC percentage	62.4 % mol
DNA-DNA hybridization (*in vitro*)	46.1%
In silico DNA-DNA hybridization	58.21%

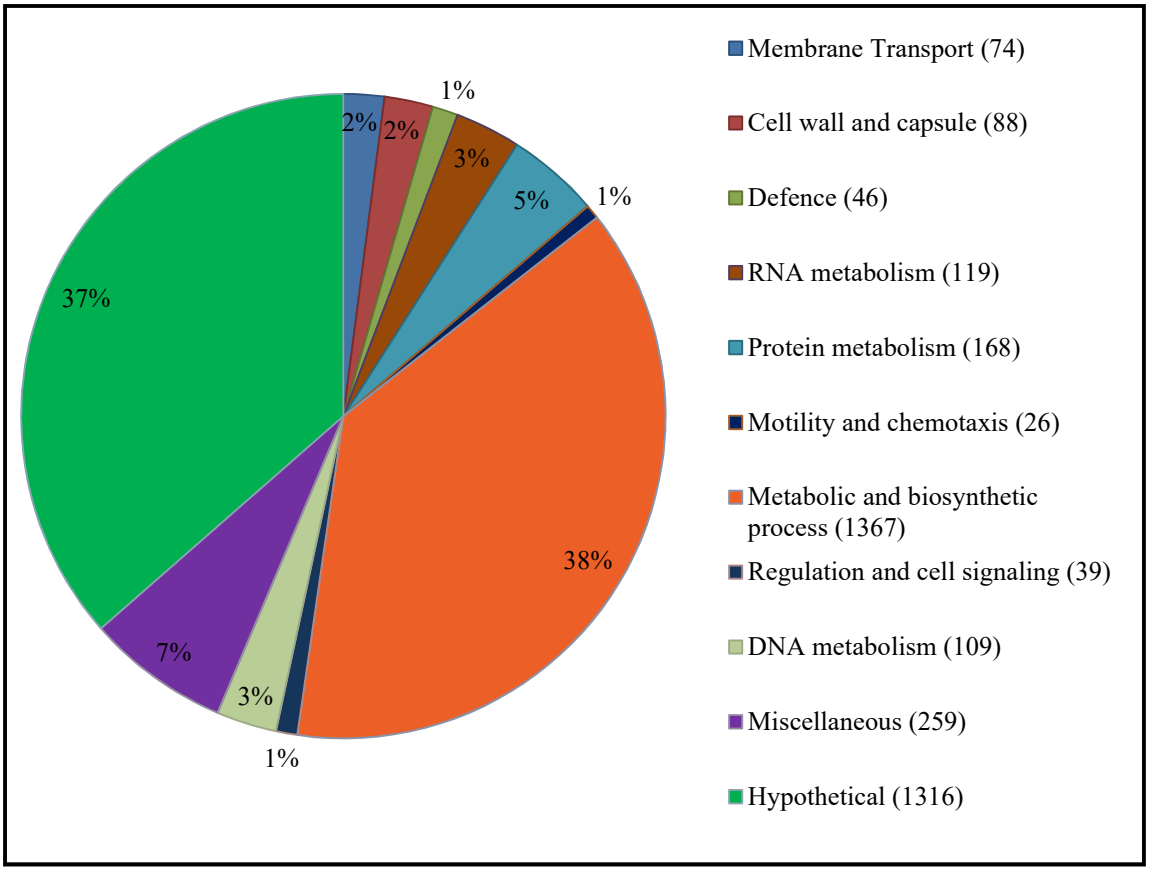

Fig. 9. Distribution of genes present in the genome of *Rmi. udaipurense* JA643^T according to the function.

Table 7. List of few genes present in the draft genome sequence of *Rmi. udaipurense* JA643^T

Name of the gene	Code	Length of gene (bp)
Photosynthetic reaction center		
Photosynthetic reaction center L subunit	*puf* L	594
Photosynthetic reaction center M subunit	*PufM*	978
Photosynthetic reaction center cytochrome c subunit	*pufC*	927
Photosynthetic reaction center H subunit	*pufH*	768
Light Harvesting complex		
Light-harvesting LHI, alpha subunit	*LHI* α	177
Light-harvesting LHI, beta subunit	*LHI* β	219
Nitrogen fixation genes		
AnfR protein, required for Mo- and V-independent nitrogenase	*anfR*	492
AnfO protein, required for Mo- and V-independent nitrogenase	*anfO*	750
Nitrogenase (iron-iron) beta chain (EC 1.18.6.1)	*nifH-β*	1389
Nitrogenase (iron-iron) delta chain (EC 1.18.6.1)	*nifH-δ*	351
Nitrogenase (iron-iron) alpha chain (EC 1.18.6.1)	*nifH-α*	1572
Nitrogenase (iron-iron) reductase and maturation protein AnfH	*anfH*	828
Nitrogenase (iron-iron) transcriptional regulator	*anfA*	1668
probable iron binding protein from the HesB/IscA/SufA family in Nif operon	*Nif*	321
Iron-sulfur cluster assembly scaffold protein NifU	*nifU*	297
Cysteine desulfurase (EC 2.8.1.7), NifS subfamily	*nifS*	1209
Nitrogenase (molybdenum-iron)-specific transcriptional regulator NifA	*nifA*	1848
Nitrogenase molybdenum-iron protein beta chain (EC 1.18.6.1)	*NifK-β*	741
Cysteine desulfurase (EC 2.8.1.7)	*icsS*	1950
NifB-domain protein, type 2	*nifB2*	354
Nitrogenase FeMo-cofactor synthesis FeS core scaffold and assembly protein NifB	*nifB*	936
Homocitrate synthase (EC 2.3.3.14)	*lys*	1284
Nitrogenase stabilizing/protective protein NifW	*nifW*	342
probable iron binding protein from the HesB_IscA_SufA family in Nif operon	*Nif*	354
4Fe-4S ferredoxin, nitrogenase-associated	-	216

Name of the gene	Code	Length of gene (bp)
Nitrogenase FeMo-cofactor synthesis FeS core scaffold and assembly protein NifB	*nifB*	1560
Nitrogenase FeMo-cofactor scaffold and assembly protein NifE	*nifE*	1743
Nitrogenase (molybdenum-iron) beta chain (EC 1.18.6.1)	*NifK-β*	1560
Nitrogenase (molybdenum-iron) alpha chain (EC 1.18.6.1)	*NifK-α*	1458
Nitrogenase (molybdenum-iron) reductase and maturation protein NifH	*nifH*	879
Nitrogenase-associated protein NifO	*nifO*	441
NifT protein	*nifT*	201
Nitrogen regulation protein NtrX	*ntrX*	1398
Nitrogen regulation protein NtrY (EC 2.7.3.-)	*ntrY*	2325
Nitrogenase FeMo-cofactor scaffold and assembly protein NifN	*nifN*	927
Nitrogenase FeMo-cofactor carrier protein NifX	*nifX*	489
NifX-associated protein	*nifX-AP*	465
4Fe-4S ferredoxin, nitrogenase-associated	-	309
Nitrogenase FeMo-cofactor synthesis molybdenum delivery protein NifQ	*nifQ*	669
Nitrogenase subunit NifH paralog, type 1	*nifH-1*	444
Nitrogenase (molybdenum-iron) alpha chain (EC 1.18.6.1)	*nifH-α*	1530
Nitrogen fixation-related protein	-	402
NifZ protein	*nifZ*	249
NifZ protein	*nifZ*	315
Membrane transporter		
Major facilitator superfamily transporter		
Probable MFS transporter precursor	*MFS*	1209
MFS family multidrug efflux protein, similarity to bicyclomycin resistance protein Bcr	*Bcr*	1269
major facilitator superfamily MFS_1	*MFS_1*	1188
major facilitator superfamily MFS_1	*MFS_1*	1218
Resistance nodulation cell division pumps		
RND efflux system, outer membrane lipoprotein CmeC	*cmeC*	1422
Probable RND efflux membrane fusion protein	*RND1*	1122
Hopanoid-associated RND transporter, HpnN	*hpnN*	2667
RND efflux system, inner membrane transporter CmeB	*cmeB*	3165

Name of the gene	Code	Length of gene (bp)
Predicted exporter of the RND superfamily, Rpal_4267	*Rpal_4267*	2397
RND multidrug efflux transporter; Acriflavin resistance protein	*arfP*	3147
Probable RND efflux membrane fusion protein	*RND2*	1230
Tripartite ATP-dependent periplasmic transporter		
TRAP dicarboxylate transporter, DctM subunit, unknown substrate 4	*dctM*	1914
TRAP transporter solute receptor, unknown substrate 4	*TRAP*	1014
Organic solvent resistance transporter		
ABC-type transport system involved in resistance to organic solvents, periplasmic component	*ABC1*	936
ABC-type transport system involved in resistance to organic solvents, permease component USSDB6A	*ABC2*	1158
Heavy metal efflux transporter		
putative efflux protein	*leuE*	3174
Probable Co/Zn/Cd efflux system membrane fusion protein	*cusB*	1398
Cobalt-zinc-cadmium resistance protein CzcA; Cation efflux system protein CusA	*czcA*	3168
Magnesium and cobalt efflux protein CorC	*corC*	960
Probable Co/Zn/Cd efflux system membrane fusion protein	*cusB*	1305
Probable Co/Zn/Cd efflux system membrane fusion protein	*cusB*	1260
Monooxygenase		
monooxygenase, FAD-binding	*MFAD*	1164
Putative ammonia monooxygenase	*amoA*	1089
Ubiquinone biosynthesis monooxygenase UbiB	*ubiB*	1401
Antibiotic biosynthesis monooxygenase	*Amo*	300
Alkane-1 monooxygenase (EC 1.14.15.3)	*alkB*	993
Dioxygenase		
Lignostilbene alphabeta-dioxygenase and related enzymes	*OJ1*	1359
Peroxidase		
Cytochrome c551 peroxidase (EC 1.11.1.5)	*ccpA*	1032
Alkylhydroperoxidase protein D	*ahpD*	534
Cytochrome c551 peroxidase (EC 1.11.1.5)	*ccpA*	330
Cytochrome c551 peroxidase (EC 1.11.1.5)	*ccpA*	1206
hydrolase, haloacid dehalogenase-like family	*hdhG*	672

Name of the gene	Code	Length of gene (bp)
Benzoate degradation related genes		
Benzoate-CoA ligase (EC 6.2.1.25)	*bclA*	975
2-hydroxymuconic semialdehyde hydrolase (EC 3.1.1.-)	*xylG*	777
4-hydroxybenzoate polyprenyl transferase (EC2.5.1.39)	*ubiA*	996
2,3-dihydro-2,3-dihydroxybenzoate dehydrogenase (EC 1.3.1.28) of siderophore biosynthesis	-	687
Benzoate transport protein	*benK*	735
Muconate cycloisomerase (EC 5.5.1.1)	*catB*	162
4-hydroxybenzoyl-CoA thioesterase family active site	*fcbC*	465
Benzoyl-CoA reductase subunit BadG (EC 1.3.99.15)	*badG*	843
Benzoyl-CoA reductase subunit BadF (EC 1.3.99.15)	*badF*	1293
Benzoyl-CoA reductase subunit BadE (EC 1.3.99.15)	*bade*	1184
Benzoyl-CoA reductase subunit BadD (EC 1.3.99.15)	*bad*	1164
putative 4-hydroxybenzoyl-CoA thioesterase	-	453
Benzoate transport, ATP binding protein	*btp*	717
Benzoate transport, ATPase component / Benzoate transport, inner membrane transport component	*btpA*	1794
Benzoate transport, inner-membrane translocator	*btimp*	867
Benzoate transport, extracellular ligand-binding receptor	*btpe*	1185
Unique homologues sequences		
sterol desaturase family protein	*hpnX/SD*	777
Putative hemolysin	*Hem*	969
COG1272: Predicted membrane protein hemolysin III homolog	*hemIII*	669
Hemolysins and related proteins containing CBS domains	*CBS*	1287
67 kDa Myosin-cross-reactive streptococcal antigen	*MCRSP*	1611
Sporulation domain protein	*spo0A*	1950
Chromosome (plasmid) partitioning protein ParB / Stage 0 sporulation protein J	*parB*	927
Chromosome (plasmid) partitioning protein ParA / Sporulation initiation inhibitor protein Soj	*parA*	819
Peptidyl-tRNA hydrolase (EC 3.1.1.29)	*tRNA*	2139
Spermidine synthase	*speE*	855
Spermidine N1-acetyltransferase (EC 2.3.1.57)	*Sat1*	570

Rmi. udaipurense JA643^T has genes involved in benzoate degradation. Benzoate degradation takes place by two known pathways; degradation by -CoA ligation and hydroxylation (Harwood *et al.*, 1999). *Rmi. udaipurense* JA643^T has genes involved in both the pathways. In most of the phototrophs anaerobic benzoate degradation proceeds via benzoyl-CoA formation. Benzoate CoA ligase, benzoyl CoA reductase are the key enzyme in anaerobic benzoate degradation which are functionally annotated in the genome of *Rmi. udaipurense* JA643^T and other 12 genes were also present in the genome. Six genes involved in the benzoate degradation via hydroxylation were present in the genome of *Rmi. udaipurense* JA643^T. However, RAST subsystem classifies these as non-functional in this organism (Aziz *et al.*, 2008). *Rmi. udaipurense* JA643^T have the genes which are involved in the degradation of nitrogen containing compounds like amino acids and heterocyclic aromatic compounds (Table 7). Some of the unique homologous sequences are sterol-binding domain containing protein, hemolysins and related proteins containing CBS domain, putative hemolysin, myosin-cross reactive streptococcal antigen**,** cobalt-zinc-cadmium/protein resistance, sporulation domain protein, spermidine synthase, antibiotic biosynthesis monooxygenase, stage 0 sporulation protein J, sporulation initiation inhibitor protein (Table 7).

3.3.2 Hopanoid biosynthesis

Hopanoids are biosynthesized from the isopentenyl subunits which are synthesized either through mevalonate pathway or methylerythritol phosphate (MEP) pathway (Rohmer, 2008). Genes involved in MEP are present in the *Rmi. udaipurense* JA643^T and the genes are scattered in the genome (Fig. 10). Eight genes involved in the hopanoid biosynthesis are located on contig no. 3 in the region between 3272 kb to 3282 kb including *ispH* which encodes for 4-hydroxy-3-methylbut-2-enyl diphosphate reductase enzyme, which is involved in MEP pathway (Fig. 10). List of seven genes involved in MEP pathway and hopanoid biosynthetic pathway are given in Table 8 and Table 9 respectively. The genes involved in hopanogenesis are radical SAM protein (*hpnH*), adenosine nucleosidase (*hpnG*), squalene hopene cyclase *(shc/hpnF),* squalene associated FAD dependent desaturase *(hpnE/crtI),* squalene synthase *(hpnD* and *hpnC)* and glycosyltransferase family protein *(hpnB).* While a few other genes involved in hopanoid biosynthesis were scattered in the genome. The region having hopanoid biosynthetic genes and there upstream and downstream regions are shown in Fig. 10.

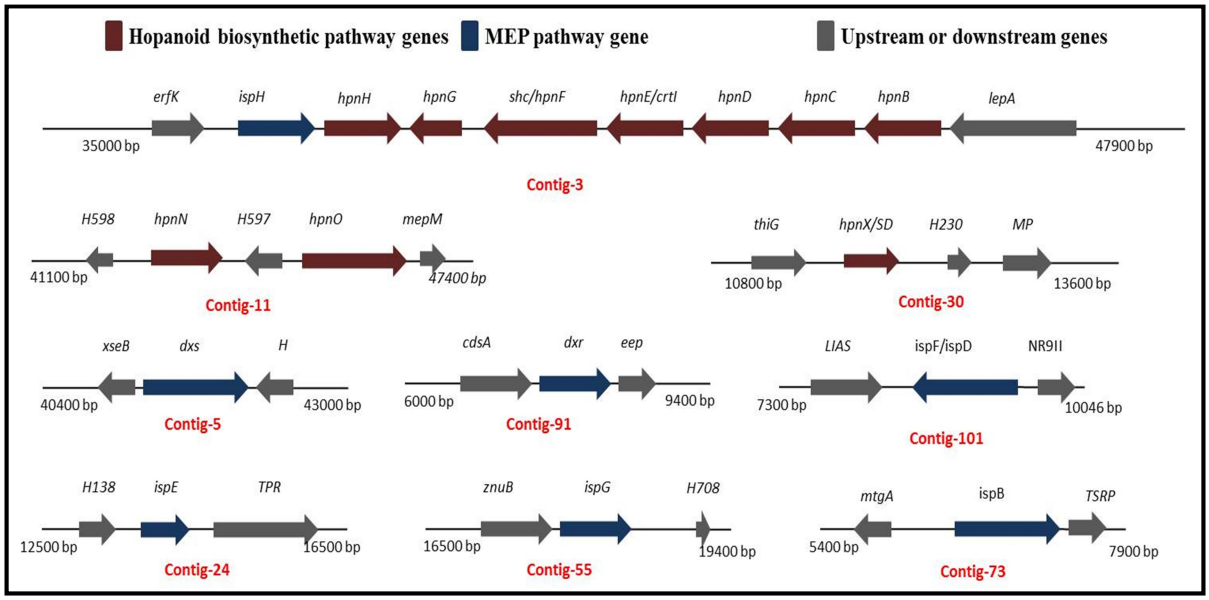

Fig. 10. Location of the hopanoid biosynthetic genes in the genome of *Rmi. udaipurense* JA643^{T}. The representation is not up to the scale. *erfK*:- *ErfK/YbiS/YcfS/YnhG* family gene, *ispH*:- 4-hydroxy-3-methylbut-2-enyl diphosphate reductase, *hpnH*:-Radical SAM protein required for addition of adenosine to hopane skeleton, *hpnG*:- Adenosylhopane nucleoside/hopanoid associated phosphorylase, *shc/hpnF*:- Squalene hopene cyclase, *hpnE/crtI*:- Squalene associated FAD-dependent desaturase/phytoene desaturase, *hpnD*:- Squalene synthase, *hpnC*:- Squalene synthase, *hpnI/hpnB*:- Glycosyltransferase, family 2, *lepA*:- Translation elongation factor LepA, *mepM*:- Murein endopeptidase, *hpnO*:- Acetylornithine aminotransferase, *H597*:- Hypothetical gene-597, *hpnN*:- Hopanoid-associated RND transporter, *H598*:-Hypothetical gene-598, *MP*:- membrane protein , *H230*:- Hypothetical gene-230, *hpnX/SD*:- sterol desaturase family protein , *thiG*:- Thiazole biosynthesis protein, *H*:- Hypothetical protein, *dxs*:- 1-deoxy-D-xylulose-5-phosphate synthase, *xseB*:- Exodeoxyribonuclease VII small subunit, *cdsA*:- Phosphatidate cytidylyltransferase, *dxr*:- 1-deoxy-D-xylulose 5-phosphate reductoisomerase, *eep*:- Membrane-associated zinc metalloprotease, *LIAS*:- Lipoate synthase , *ispF/ispD*:- 2-C-methyl-D-erythritol 2,4-cyclodiphosphate synthase, *NR9II*:- Nitrogen regulation protein NR(II), *TRP*:- TPR domain protein, *ispE*:- 4-diphosphocytidyl-2-C-methyl-D-erythritol kinase, *H138*:- Hypothetical gene-138, *znuB*:- Zinc ABC transporter, *ispG*:- 1-hydroxy-2-methyl-2-(E)-butenyl 4-diphosphate synthase, *H708*:- Hypothetical gene-708, *TSRP*:- Two-component system regulatory protein, *ispB*:- Geranyltranstransferase (farnesyldiphosphate synthase), *mtgA*:- peptidoglycan transglycosylase

Table 8. Genes of *Rmi. udaipurense* JA643^T involved in the MEP pathways

Gene name	Code	EC number	Gene length	Percentage similarity[a]
1-deoxy-D-xylulose 5-phosphate synthase	*dxs*	2.2.1.7	1931	96%
1-deoxy-D-xylulose 5-phosphate reductoisomerase	*dxr*	1.1.1.267	1250	96%
2-C-methyl-D-erythritol 2,4-cyclodiphosphate synthase	*ispD*	2.7.7.60/ 4.6.1.12	1181	95%
4-diphosphocytidyl-2-C-methyl-D-erythritol kinase	*ispE*	2.7.1.148	869	95%
2-C-methyl-D-erythritol 2,4-cyclodiphosphate synthase	*ispF*	2.7.7.60/ 4.6.1.12	1181	95%
1-hydroxy-2-methyl-2-(E)-butenyl 4-diphosphate synthase	*ispG*	1.17.7.1	1265	96%
4-hydroxy-3-methylbut-2-enyl diphosphate reductase	*ispH*	1.17.1.2	962	97%

[a]Simlarity with respective gene from *Rmi. vannielii* ATCC17100^T

Table 9. Genes of *Rmi. udaipurense* JA643^T involved in the hopanoid biosynthesis pathway

Gene name	Code	EC number	Gene length	Percentage similarity[a]
Squalene hopene cyclase	*Shc/hpnF*	5.4.99.17	2039	97%
Glycosyl transferase, family 2, *hpnB*	*hpnI/hpnB*	-	1166	99%
5'-methylthioadenosine nucleosidase / S-adenosylhomocysteine nucleosidase	*hpnG*	3.2.2.16/ 3.2.2.9	701	98%
Radical SAM protein required for addition of adenosine to hopane skeleton	*hpnH*	-	1142	99%
Acetylornithine aminotransferase	*hpnO/argD*	2.6.1.11	1199	98%
Hopanoid-associated RND transporter	*hpnN*	-	2666	98%
Phytoene desaturase /squalene associated FAD dependent desaturase	*hpnE/crtI*	1.14.99.-	1325	99%
Phytoene synthase /squalene synthase	*hpnC*	2.5.1.32	857	97%
Phytoene synthase /squalene synthase	*hpnD*	2.5.1.32	881	98%
sterol desaturase family protein	*erg3/ hpnX*		776	97%
Geranyltranstransferase (farnesyldiphosphate synthase)	*ispB/ ispA*	2.5.1.10	890	95%

[a]Similarity with respective gene from *Rmi. vannielii* ATCC17100^T

3.4 Transcriptional response of *Δshc* mutant of *Rps. palustris* TIE-1

3.4.1 Growth study of wild-type and *Δshc* mutant

To study the physiological response of hopanoid deficiency in *Rps. palustris* TIE-1, growth curve was performed for wild-type (WT) and *Δshc* mutant in different carbon sources. In comparison to WT, *Δshc* mutant showed differential behaviour when grown photoheterotrophically in a media supplemented with different carbon sources (succinate, pyruvate, malate and acetate; Fig. 11). In all the tested carbon sources the growth rate of *Δshc* mutant was retarded. In succinate (YPS) grown culture, the final growth of the *Δshc* mutant was nearly half compared to the WT strain. In YPS media, doubling time for WT strain was 6.1±0.1h, whereas for *Δshc* mutant strain it was increased to 7.6±0.3h (Fig. 11a). In pyruvate (YPP) grown culture, WT strain and *Δshc* mutant attended almost similar growth, with a slight difference in doubling time as 6.2±0.4h and 6.7±0.7h respectively (Fig. 11b). In malate grown cultures, it was observed that there is 48 min difference in doubling time of WT (6.4±0.15h) and *Δshc* mutant (7.2±0.5h), but WT and *Δshc* mutant attended almost same growth (Fig. 11c). In acetate grown cultures, there was least difference in both final growth and doubling time compared to other carbon sources tested but the lag phase for *Δshc* mutant was around 60 hours by the same time WT was in its late log phase (Fig. 11d). Since the behaviour of WT and *Δshc* mutant strains was almost identical in pyruvate as a carbon source, YPP media was used for culturing WT and *Δshc* mutant in further study. To understand the physiological changes of *Rps. palustris* TIE-1 in the absence of hopanoid biosynthesis, genome-wide transcriptome of WT and *Δshc* mutant was studied.

3.4.2 Microarray experiment and statistical analysis

The microarray experiment was carried out for wild type and *Δshc* mutant grown in YPP media. The experiment was carried out in triplicate, each with three biological replicates. Three biological replicates from individual experiment were pooled together to minimize biological variation. For microarray experiment, WT and *Δshc* mutant cells were harvested from the mid-log phase, at 62 hours and 72 hours respectively. By harvesting cells in mid log phase, the variability between the strains due to different growth rates and morphologies was minimized (Welander *et al.*, 2009). The microarray experiment was carried out in duplicate to calculate the statistical significance of the data. To check the quality of replicates statistical analysis was carried out. The scatter

plot was plotted to visualize overall mRNA expression levels within a single hybridization. Most of the genes had equal expression values in replicates and the majority of points are grouped around the diagonal line (Fig. 12a). Principal component analysis (PCA) which is used to visually assess the quality of replicates in a biological sample was carried out and it was observed that WT and mutant separated from each other and respective replicates clustered together (Fig 12b). Once the quality was checked, relative fold changes were calculated by considering WT as a control. Fold change was converted into the $\log_2$ values. Genes having fold change > 0.6 ($\log_2$ 1.5=0.6) was considered to be upregulated and fold change < -0.6 ($\log_2$-1.5 =-0.6) was considered to be downregulated.

3.4.3 Overview of Microarray data analysis

Microarray experiment showed that in hopanoid deficient mutant of *Rps. palustris* TIE-1, 299 genes were upregulated and 306 genes were downregulated with respect to WT (Table S2 and S3). Hundred and five uncharacterised protein coding genes were downregulated whereas 100 uncharacterised genes were upregulated (Table S4 and Table S5). To validate microarray data, 10 genes were selected and qPCR was carried out (Table 10). Out of 10 genes, fold change for 9 genes was in accordance with the with microarray data, whereas *Rpal_2511* gene did not show significant differential expression (Fig. 13).

3.4.4 Functional annotation of differentially expressed genes

In order to obtain deeper insights into the transcriptional response of *Rps. palustris* TIE-1 during hopanoid deficiency, we used the Gene Ontology (GO) classification to check for the enrichment of specific functionally related gene groups within the different sets of correlated genes. The function and pathway analysis were done for the differentially regulated genes using DAVID database. It was observed that genes belonging to processes such as oxidation reduction, cell redox homeostasis, proteolysis, electron carrier activity, ABC transporters, glyoxylate and dicarboxylate metabolism, fatty acid metabolism, signal and monooxygenase were upregulated. It was also found that genes belonging to processes such as regulation of transcription, membrane transport activity, ABC transporters, plasma membrane, two-component system, bacterial chemotaxis, nitrogen metabolism and amino acid metabolism were downregulated.

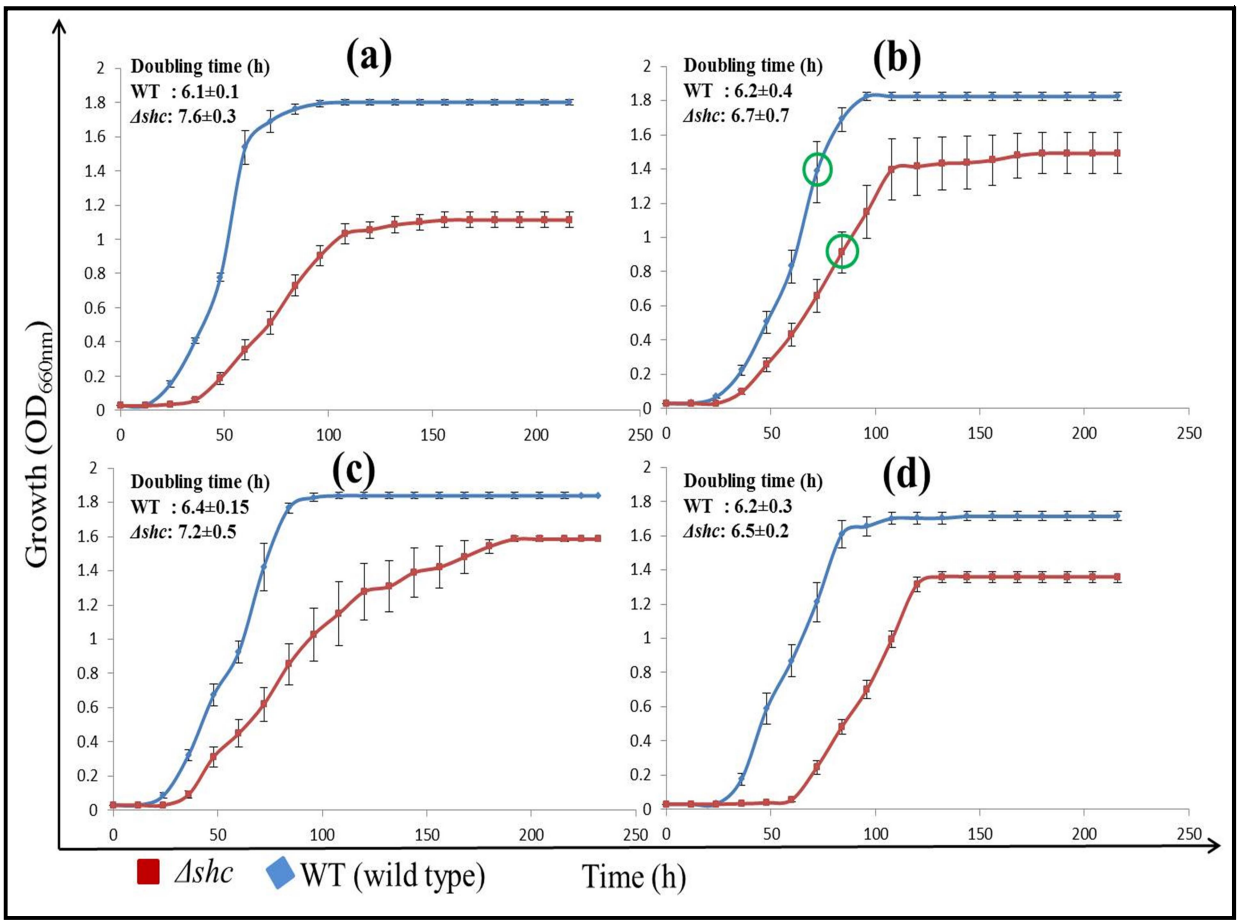

Fig. 11. Photoheterotrophic growth of *Δshc* mutant and WT strain of *Rps. palustris* TIE-1 in different carbon sources given at 10 mM concentration. Shown are the growth curves of the WT and *Δshc* mutant strains in (a) succinate, (b) pyruvate, (c) malate and (d) acetate. Each time point represents the average of three replicate cultures (the error bars represents standard deviation). Each growth curve repeated three times and representative growth curves are shown. Red colour line is for *Δshc* mutant and blue colour line is for wild type of *Rps. palustris* TIE-1. The green colour rings are the time points selected for the expression profiling.

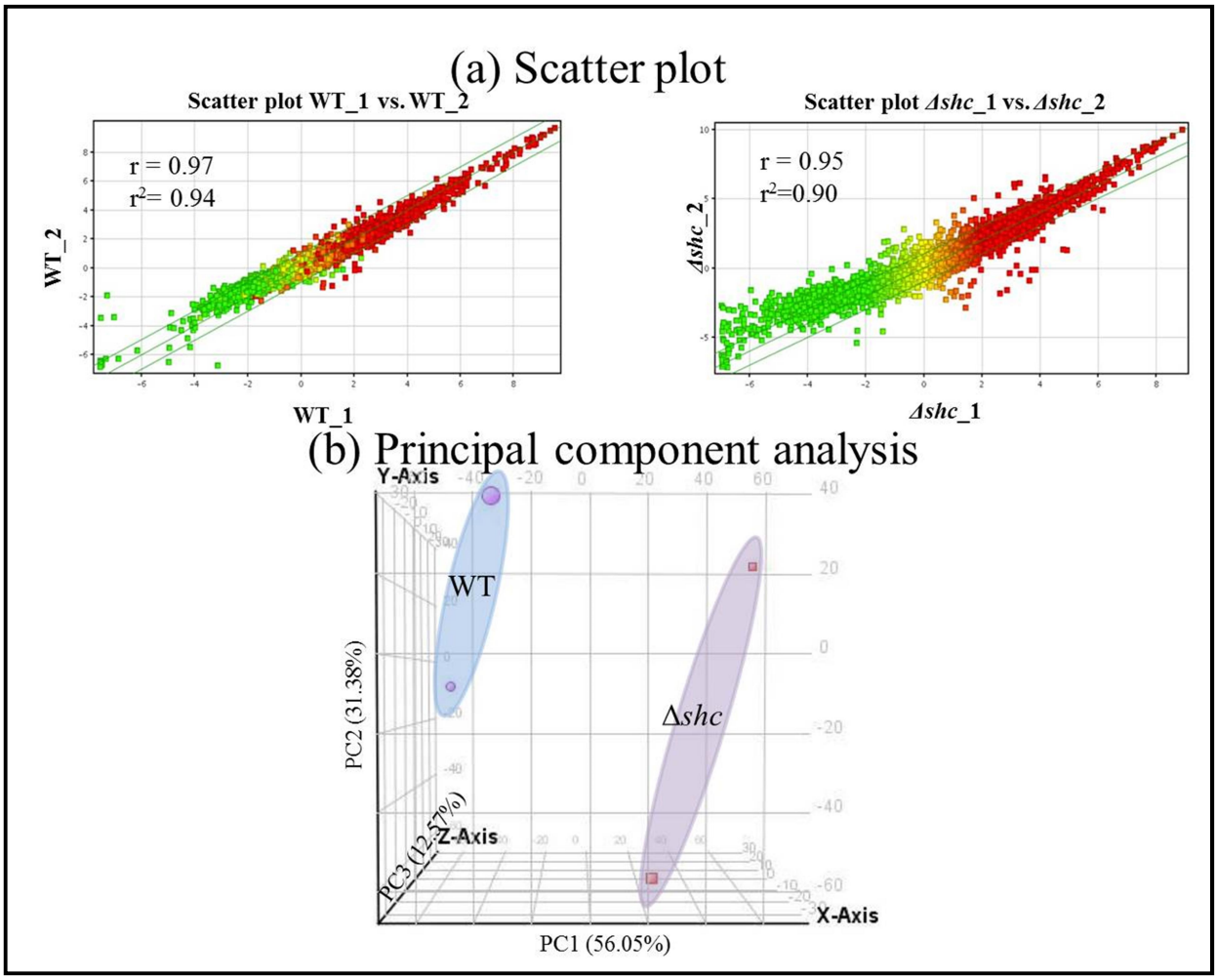

Fig. 12. Statistical analysis of microarray data. (a) Scattered plot showing the overall mRNA expressions in WT and *Δshc* mutant; (b) Principal component analysis visually showing the quality of replicates in biological experiments.

Table 10. List of genes of *Rps. palustris* TIE-1 selected for validation of gene expression by qPCR

Gene Code	Gene name
Oxidoreductase activity	
Rpal_0377	Thioredoxin
Rpal_5257	33 kDa chaperonin
Rpal_2511	Putative monooxygenase protein
Rpal_0425	Cytochrome P450
Rpal_4674	OsmC family protein
Localization	
Rpal_1871	Methyl-accepting chemotaxis sensory transducer with Pas/Pac sensor
Rpal_1916	Diguanylate cyclase
Rpal_2444	Diguanylate cyclase/ phosphodiesterase with PAS/PAC sensor(S)
Transport	
Rpal_3823	Sodium/ hydrogen exchanger
Rpal_2651	TonB dependent receptor

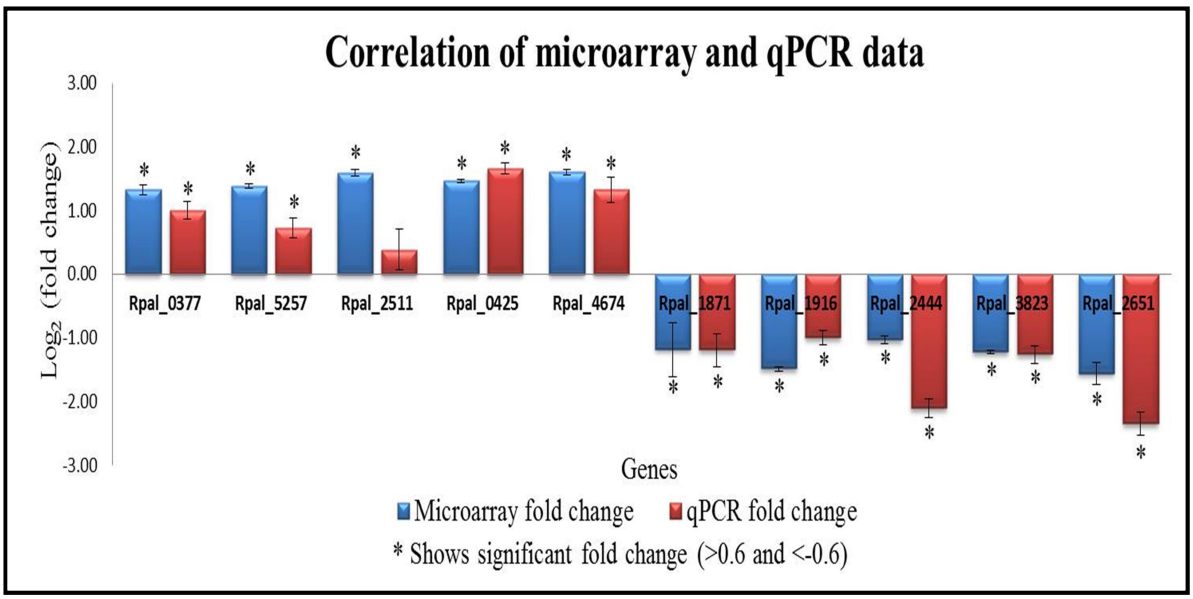

Fig. 13. Correlation of microarray and qPCR data for 10 genes of *Rps. palustris* TIE-1. Blue colour indicates the fold change calculated from microarray data and red colour indicates the fold change from qPCR experiments. Microarray experiment was done in duplicate and qPCR experiment was done in triplicate.

3.4.5 Subnetwork analysis

To understand how the hopanoid deficiency could affect cellular response, a subnetwork selection algorithm, PheNetic, was used to construct subnetwork based on differentially expressed genes. A possible interaction network representing interactome of nearest strain *Rps. palustris* CAG009 was compiled from string actions networks and mapped on *Rps. palustris* TIE-1 genome. Using this network a minimal common subnetwork was constructed by PheNetic algorithm which connects a cause (hopanoid deficiency) to differentially expressed genes (its effect). From the differentially expressed genes subnetwork was constructed which consisted of 266 nodes (genes) and 408 edges (interactions). Out of 605 differentially expressed genes, 219 genes were selected for subnetwork construction and 49 additional intermediately genes were selected by PheNetic algorithm to connect the corresponding differentially expressed genes (Fig. 14).

3.4.6 Cellular response of *Δshc* mutant

3.4.6a Membrane transport

Microarray data revealed that 54 genes involved in various activities of membrane transport were downregulated in *Δshc* mutant compare to WT strain (Table S3). To test whether hopanoid deficiency leads to defected membrane permeability and transport, NPN uptake assay was carried out. In NPN uptake assay it was observed that, in pyruvate (10 mM) containing WT strain fluorescence signal increases up to 130 min after which it started decreasing with time. Similar results were obtained for without carbon source (Fig. 15). In *Δshc* mutant, in both pyruvate and without carbon sources it was observed that fluorescence signal was increased till 120 min and became constant with the time (Fig. 15).

ATP-dependent efflux assay was performed to test whether energy dependent multidrug transport was impaired in *Δshc* mutant. In H33342 ATP dependent assay, after inhibiting ATP synthesis by CCCP in stained cells (stained with H33342 dye), cells were washed to remove excess dye (H33342) and inhibitor (CCCP). Fluorescence readings were taken for 60 min which shows that there is no variation of fluorescence indicating the inhibition of ATP biosynthesis by CCCP. Pyruvate (20 mM) was added in ATP synthesis abolished cultures which restore the ATP biosynthesis. After adding pyruvate,

fluorescence in WT strain initially started increasing and with time as ATP synthesis restored the fluorescence signal decreased with time. In *Δshc* mutant the initial fluorescence was high compared to WT and after adding pyruvate fluorescence started increasing immediately and subsequently started decreasing but did not decrease significantly below the control (Fig. 16). In control without pyruvate where ATP synthesis was not restored, the fluorescence remains constant throughout the experiment (Fig. 16).

3.4.6b Chemotaxis, response to stimulus and flagellar assembly

In response to external stimuli, bacteria show chemotaxis and flagellar motility which helps the bacteria to reach favourable environment. Cell membrane plays a crucial role in sensing and passing the message inside the cell. Therefore, in a compromised cell membrane there might be alteration in signal transduction and motility. Microarray data showed that 38 genes involved in response to external stimuli, chemotaxis and flagellar assembly were downregulated in *Δshc* mutant (Table S3). Seven genes involved in flagellar assembly and motility showed significant downregulation in hopanoid deficient mutant. Therefore swimming assay was carried out to understand the defect in motility. In swimming motility assay, the diameter of motility was same for WT and *Δshc* mutant within the first 48 hours but after 96 hours swimming motility was reduced in *Δshc* mutant (Fig. 17a). In swarming motility assay, there was no significant difference between the motility of WT and *Δshc* mutant (Fig. 17b).

3.4.6c Oxidation reduction and electron carrier activity

Oxidation and reduction reactions play a crucial role in cellular respiration. Nineteen genes which are involved in oxidation reduction process were found to be upregulated in *Δshc* mutant (Table S2). Various enzymes act as electron acceptors as well as donors and take part in electron transport chain generating electrochemical gradient across the cell membrane. In *Δshc* mutant, 21 genes which are involved in electron carrier activity were also upregulated (Table S2). Six genes involved in monooxygenase activity were also upregulated in *Δshc* mutant which also take part in electron carrier activity. These genes includes cytochrome P450 (*Rpal_0425*, *Rpal_1803* and *Rpal_1932*), putative monooxygenase protein (*Rpal_2511*), luciferase-like monooxygenase (*Rpal_4222*) and monooxygenase FAD-binding protein (*Rpal_5156*).

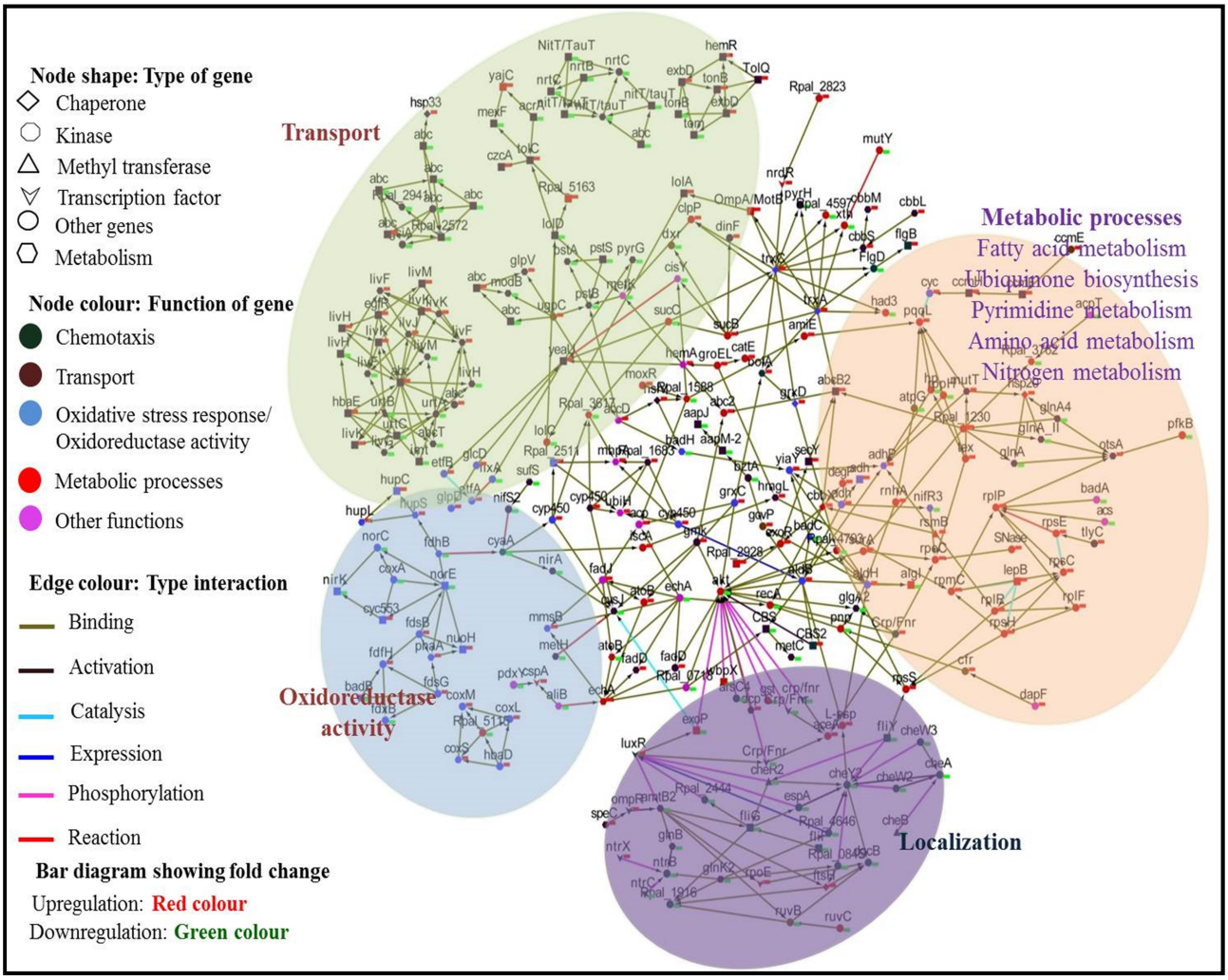

Fig. 14. Hopanoid deficiency triggers transcriptional changes. Shown is selected sub-network based on the differentially expressed genes in the *Δshc* mutant of *Rps. palustris* TIE-1. The PheNetic algorithm was used to select sub-network from 605 differentially expressed genes. Sub-network consists of 262 nodes and 438 nodes, 219 differentially expressed genes and additional 43 intermediate genes which were selected by PheNetic. The shape of the node represents the type of gene, colour of node represents the function of gene, colour of edge represents the type of interaction and bar diagram besides the nodes corresponds to fold change.

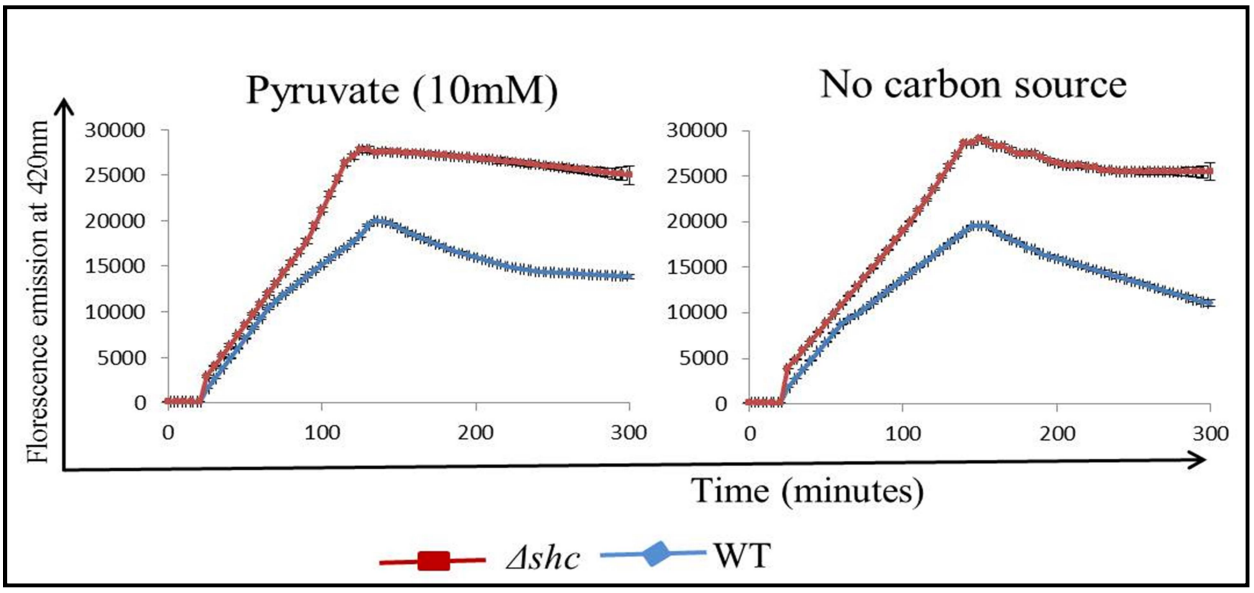

Fig. 15. The membrane permeability was assessed by NPN uptake assay which is monitored by the accumulation of the NPN (lipophilic dye) in the cell. Each reading represents the average of three replicates (the error bars represents standard deviation). NPN uptake assay was repeated three times.

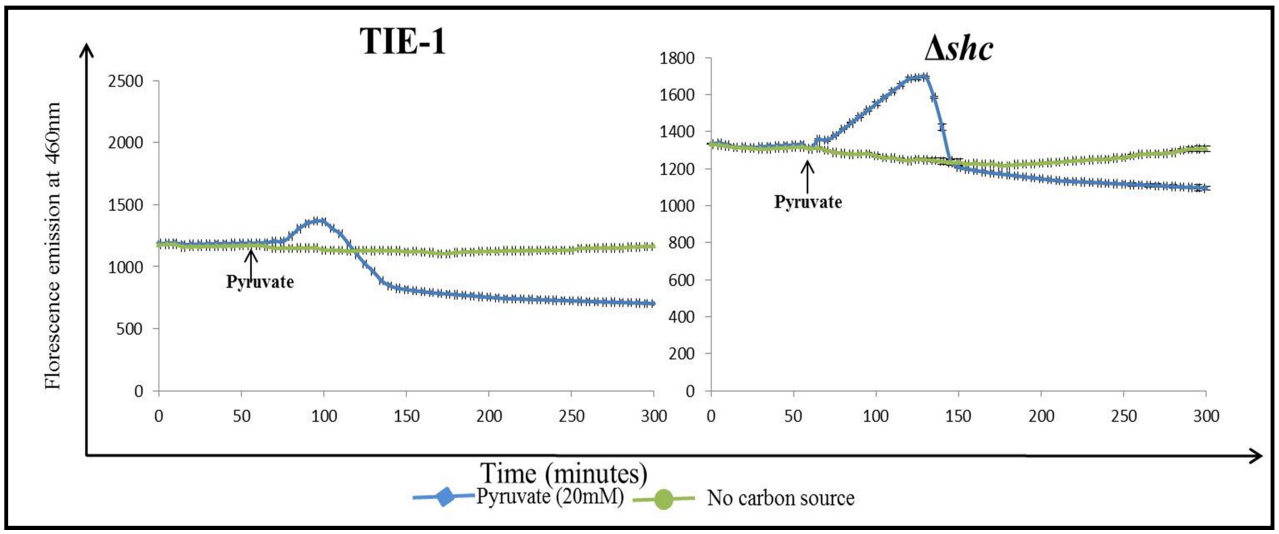

Fig. 16. Energy-dependent multidrug transport was assessed by ATP-dependent efflux assay which is monitored by efflux of fluorescent dye (H33342). Each reading represents the average of three replicates (the error bars represents standard deviation). ATP-dependent efflux assay was repeated three times.

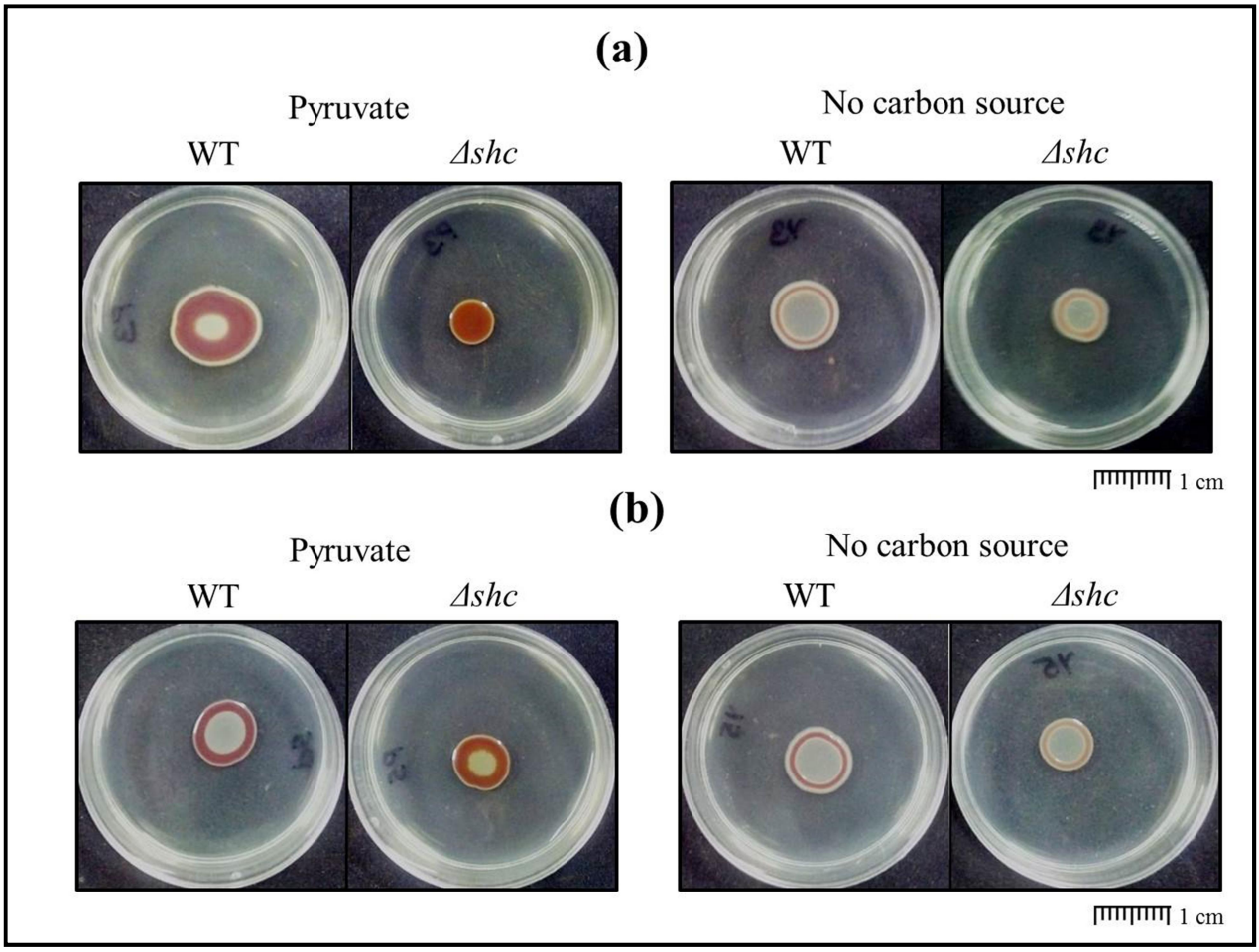

Fig. 17. Visual representation of swimming and swarming motility of *Δshc* and WT of *Rps. palustris* TIE-1 in YP media with pyruvate and no carbon source. (a) Swimming motility of WT and *Δshc* (b) Swarming motility of WT and *Δshc*. Each assay was repeated thrice and representative of each experiment is shown.

3.4.6d Other cellular processes

In *Δshc* mutant, 5 genes of glyoxylate and dicarboxylate metabolism, 4 genes involved in fatty acid metabolism, 8 genes of envelope part, 8 genes involved in proteolysis were upregulated (Table S3). Various other genes are also differentially expressed which all are listed in Table S2, S3, S4 and S5).

3.5 Docking study

3.5.1 Docking of ligands with MPP1

Membrane palmitoylated protein 1 (MPP1) belongs to MAGUK protein family which is membrane associated guanylate kinase. Prof. Aleksander F. Sikorski shared the full model built on the I-TASSER web server with us (Listowski *et al.*, 2015). MPP1 protein has 17 CRAC motifs and 14 CARC motifs (CRAC-like motif) which were predicted using EMBOSS: fuzzpro server. *In silico* docking experiments were performed to test whether cholesterol (XXXVI), diplopterol (VI), diploptene (II) and tetrahymanol (VIII) bind to these motifs. Docking results show that the cholesterol (XXXVI) binds to this sequence motif with a binding energy ranging from -8.3 to -7.1 kcal/mol, diplopterol (VI) binds to these motifs with a binding energy ranging from -9.0 to 8.2 kcal/mol, diploptene (II) binds to these motif with binding energy ranging from -8.4 to -7.8 kcal/mol and tetrahymanol (VIII) binds to these motif with binding energy ranging from -10.1 to -8.6 kcal/mol. The binding site of all four ligands lies in the CRAC motif of MPP1 protein (Table 11). Visualization of docking between ligand and CRAC motif spanning from 258 to 286 amino acids and another spanning from 423 to 435 amino acid of MPP1 protein is shown in Fig. 18.

3.5.2 Docking of ligands with Rpal_1916

Rpal_1916 is diguanylate cyclase gene which catalyses the synthesis of cGDP. The CRAC motif of Rpal_1916 was predicted using EMBOSS: fuzzpro server. Rpal_1916 protein has 15 CRAC motif and 26 CRAC-like motifs (Table 12). TMHMM has shown that in Rpal_1916 protein, there are 8 possible regions which might be buried in the cell membrane (Fig. 19). *In silico* docking experiments were performed to test whether cholesterol (XXXVI), diplopterol (VI), diploptene (II) and tetrahymanol (VIII) binds to these motifs (Table 13). Docking results showed that cholesterol (XXXVI) binds to these sequence motifs with a binding energy ranging from -8.2 to -7.3 kcal/mol,

diplopterol (VI) binds to these motifs with a binding energy ranging from -9.9 to -8.4 kcal/mol, diploptene (II) binding energy ranging from -10.1 to -8.8 kcal/mol and tetrahymanol binding energy ranging from -9.7 to 9.1 kcal/mol. Cholesterol (XXXVI), diplopterol (VI), diploptene (II) and tetrahymanol (VIII) showed binding with Rpal_1916 in CRAC motif spanning from 593 to 619 amino acids and another motif spanning from 593 to 714 amino acids (Fig. 20).

3.5.3 Docking of ligands with Rpal_2444

Rpal_2444 protein has 17 CRAC motif and 18 CRAC-like motifs (Table 12). TMHMM has shown that in Rpal_2444 protein, there is one transmembrane helix (Fig. 21). *In silico* docking experiments were performed to test whether cholesterol (XXXVI) and diplopterol (VI) binds to these motifs (Table 14). Docking results show that cholesterol (XXXVI) binds to these sequence motifs with a binding energy ranging from -7.9 to -6.7 kcal/mol, diplopterol (VI) binds to these motifs with a binding energy ranging from -9.4 to -7.5 kcal/mol, diploptene (II) binds to these motifs with a binding energy ranging from -10.5 to -7.7 kcal/mol and tetrahymanol (VIII) binds to these motif with binding energy ranging from -8.5 to -7.8kcal/mol. Cholesterol (XXXVI) and diplopterol (VI) both showed binding with Rpal_2444 in a pocket spanning from CRAC motif spanning from 269 to 296 amino acids which is in hydrophobic region and might be a part of transmembrane domain (Fig. 22).

Table 11. Molecular docking of ligands with MPP1 protein of *Homo sapiens*.

CRAC motif in MPP1	Docking of ligand with MPP1 protein			
	Cholesterol (XXXVI)	Diplopterol (VI)	Diploptene (II)	Tetrahymanol (VIII)
423-RSQYAHYFDLSLV-435 (3)	+	+	+	+
309-KFVYPVPYTTRPPR-322 (5)	+	-	-	-
258-KHSSIFDQLDVVSYEEVV RLPAFKRKTLV-286 (14)	+	+	+	+
247- KKKKYKDKYL -256 (3)	+	-	-	-
156-LPALQMFMR-176 (2)	+	-	-	-
68- KVRLIQFEKV -77 (4)	+	-	-	-

'+' represents docking is possible in the respective CRAC motif whereas '-' represents no docking of ligands were observed

Docking of ligands against MPP1 protein was done by PyRx software. Grid box was set on entire protein.

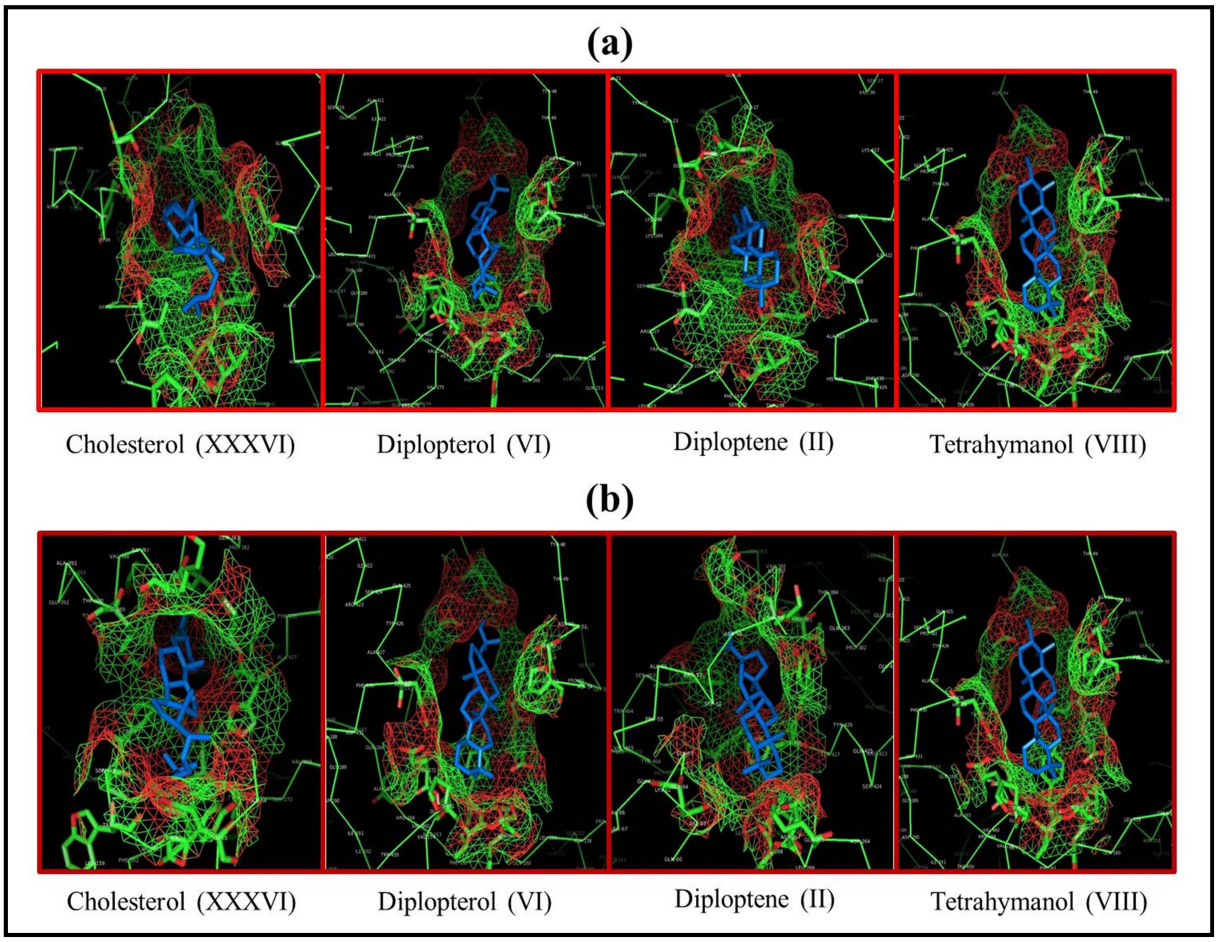

Fig. 18. Visualization of binding between ligands and MPP1 protein of *Homo sapiens*. (a) Binding of ligands with CRAC motif spanning from 258 to 286 amino acids which have fourteen overlapping CRAC motifs; (b) binding of ligands with CRAC motif spanning from 423 to 435 which has three CRAC motifs.

Table 12. Predicted CRAC motif in Rpal_1916 and Rpal_2444 protein of *Rps. palustris* TIE-1

Predicted CRAC motifs	
Rpal_1916	**Rpal_2444**
43-RWIGLFGCV-51 (1)	25- LGVVAAYGGLR-35 (3)
127-KAAARYLL-134	149-LDIYGIPPGR-158
140-VLVAFTAFTGR-150 (3)	130-RGFCLFDAVGRL-141 (3)
229-KLDYPGYSLHLKRQFIGVL-247 (9)	233-KQAEQRFAYLALHDVXXXXLPNRAAFNDRIV -262 (6)
260-LTNYLGEIYR-269 (1)	269-RRFDGSFAVIRLGIDRFKEINDVFGQAV-296 (6)
424-RFDQAFFVV-432 (2)	319-RPGGDEFSIV-328
443-RRDELFRTL-451 (2)	348-LCDTEFEVDGHR-359
460-LQIAEQFGASGR-471 (1)	368-VSVYPR-373
476-REIFGGDWVEFGGRRSYVL-484 (5)	387-VALYRAK-393
511-VKGIFASRLL-518 (3)	397-RGTVCLFEPAMDL-409
533-LFYFFGMDRGVRDRFERQLR-552 (5)	445-VGFEALLR-452
574-LANRMKFDARL-584 (2)	498-LAIAVNFSPLDFRRFDVPAL-517 (4)
593-RSGRPFSLIIFDIDHFKEVNDIYGHPV-619 (4)	574-LSYLQSFPFDKIKIDQAFTRKL-595 (5)
643-RWGGEEFAILL-653 (2)	641-VQGYLIGR-648
704-RADNALYRAKL-714 (1)	

CRAC motif was predicted using EMBOSS: fuzzpro server. The position of CRAC motif in protein is given with amino acid number before and after the motif sequence. In bracket the number of overlapping CRAC motif is given.

Table 13. Molecular docking of ligands with Rpal_1916 protein of *Rps. palustris* TIE-1

CRAC motif residues	**Docking of ligand with MPP1 protein**			
	Cholesterol (XXXVI)	Diplopterol (VI)	Diploptene (II)	Tetrahymanol (VIII)
229-KLDYPGYSLHLKRQFIGVL-247 (9)	+	+	+	+
476-REIFGGDWVEFGGRRSYVL-484 (5)	+	+	+	
511-VKGIFASRLL-518 (3)	-	-	-	-
593-RSGRPFSLIIFDIDHFKEVNDIYGHPV-619 (4)	-	+	+	+
643-RWGGEEFAILL-653 (2)	-	+	+	+
704-RADNALYRAKL-714 (1)	-	+	+	+

'+' represents docking is possible in the respective CRAC motif whereas '-' represents no docking of ligands were observed

The position of CRAC motif in protein is given with amino acid number before and after the motif sequence. In bracket the number of overlapping CRAC motif is given. Docking of ligands against Rpal_1916 protein was done by PyRx software. Grid box was set on entire protein.

Table 14. Molecular docking of ligands with Rpal_2444 protein of *Rps. palustris* TIE-1

CRAC motif residues	Docking of ligand with Rpal_2444 protein			
	Cholesterol (XXXVI)	Diplopterol (VI)	Diploptene (II)	Tetrahymanol (VIII)
149-LDIYGIPPGR-158	-	-	+	-
130-RGFCLFDAVGRL-141 (3)	+	-	+	-
233-KQAEQRFAYLALHDVXXXXLPNRAAFNDRIV-262 (6)	-	+	+	+
269-RRFDGSFAVIRLGIDRFKEINDVFGQAV-296 (6)	+	+	-	-
319-RPGGDEFSIV-328	-	-	-	+
348-LCDTEFEVDGHR-359	-	+	-	-
397-RGTVCLFEPAMDL-409	-	-	+	-
445-VGFEALLR-452	-	-	-	+
498-LAIAVNFSPLDFRRFDVPAL-517 (4)	-	-	+	-
574-LSYLQSFPFDKIKIDQAFTRKL-595 (5)	-	-	-	+
641-VQGYLIGR-648	-	-	-	+

'+' represents docking is possible in the respective CRAC motif whereas '-' represents no docking of ligands were observed

The position of CRAC motif in protein is given with amino acid number before and after the motif sequence. In bracket the number of overlapping CRAC motif is given. Docking of ligands against Rpal_2444 protein was done by PyRx software. Grid box was set on entire protein.

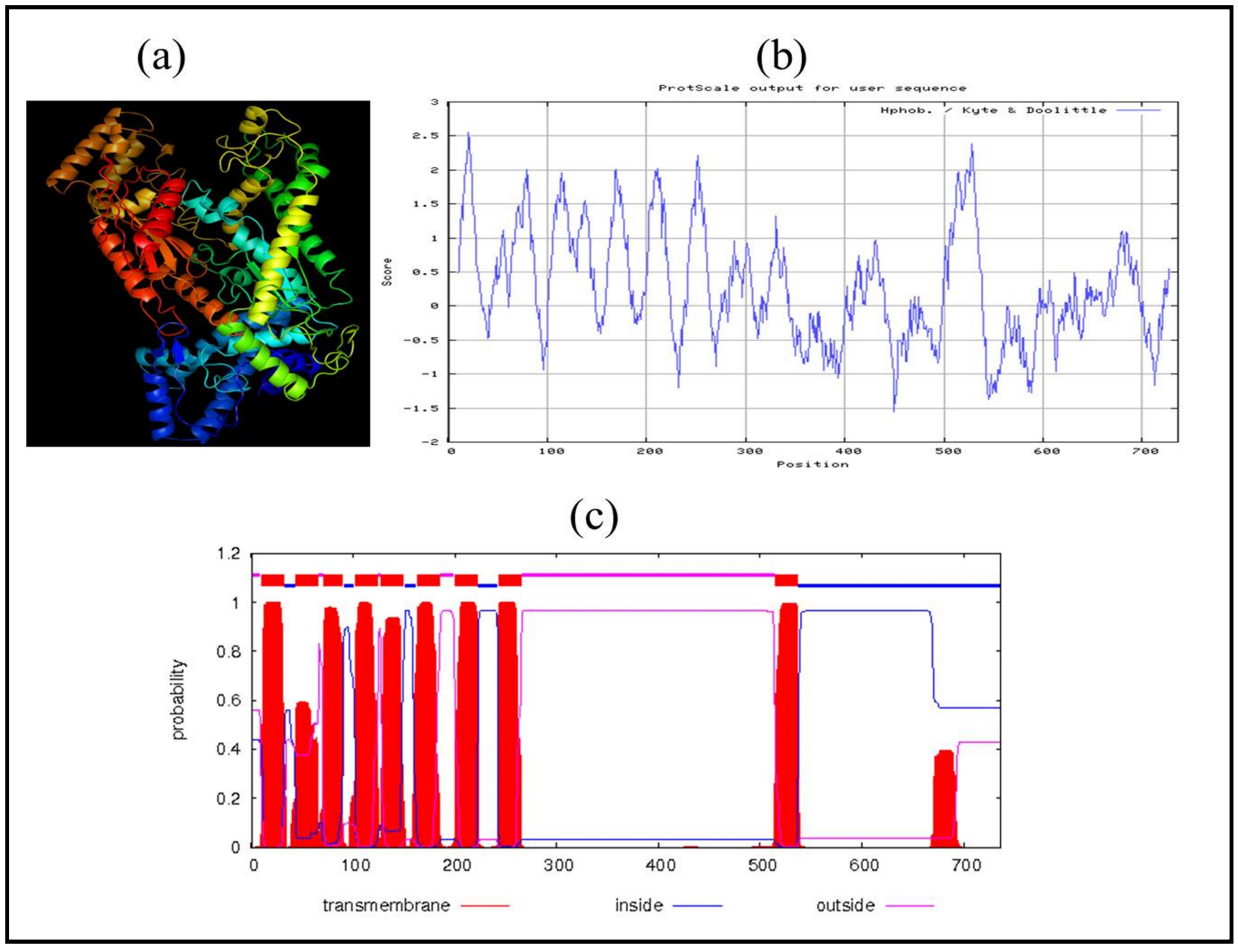

Fig. 19. (a) Protein model of Rpal_1916 built with the I-TASSER web server; (b) Hydropathy plot of Rpal_1916 generated using ProtScale server. (c) Transmembrane helix prediction of Rpal_1916 protein by TMHMM server.

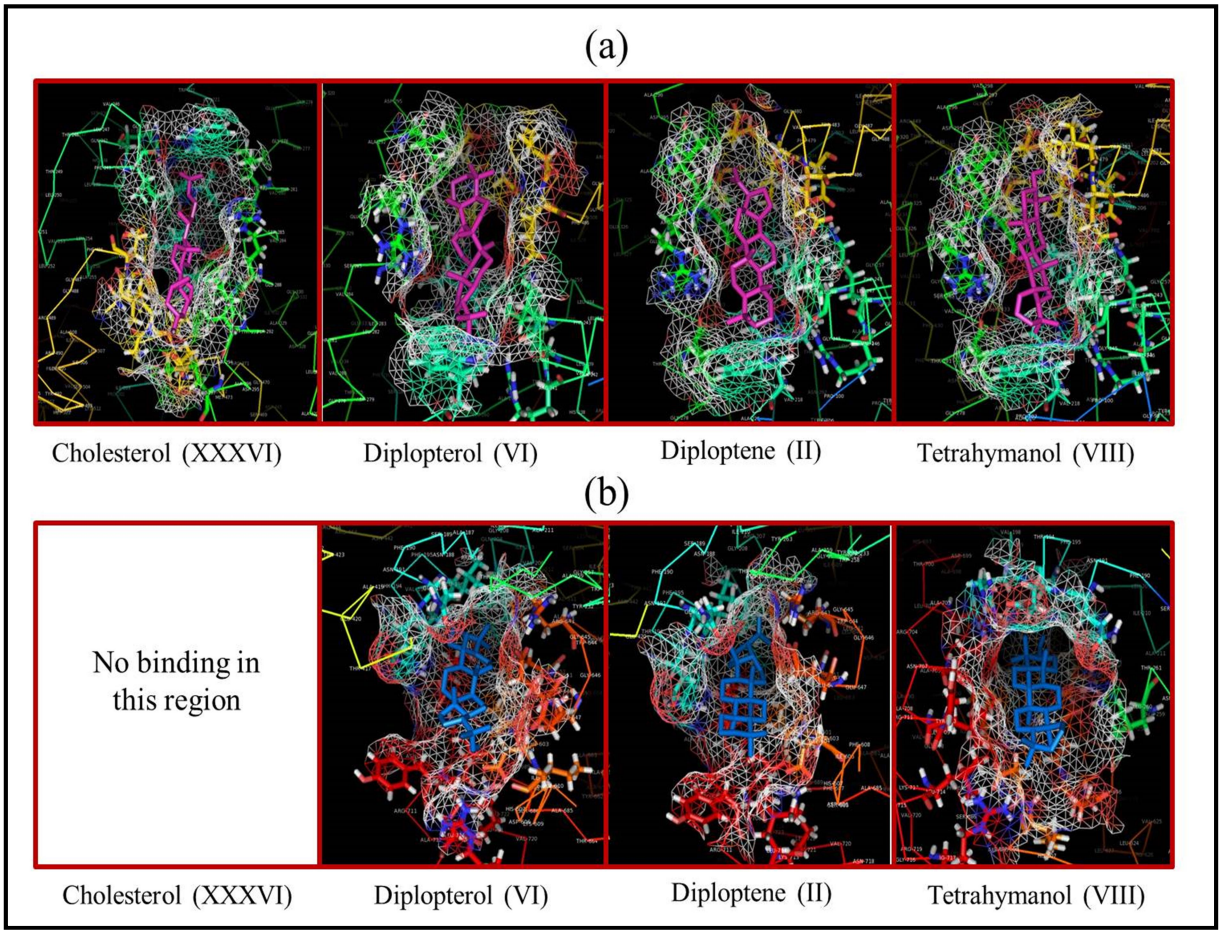

Fig. 20. Visualization of binding between ligands and Rpal_1916 protein (a) binding of ligands with CRAC motif spanning from 593 to 619 amino acids which have nine overlapping CRAC motifs; (b) binding of ligands with CRAC motif spanning from 593 to 714 which has eight CRAC motifs.

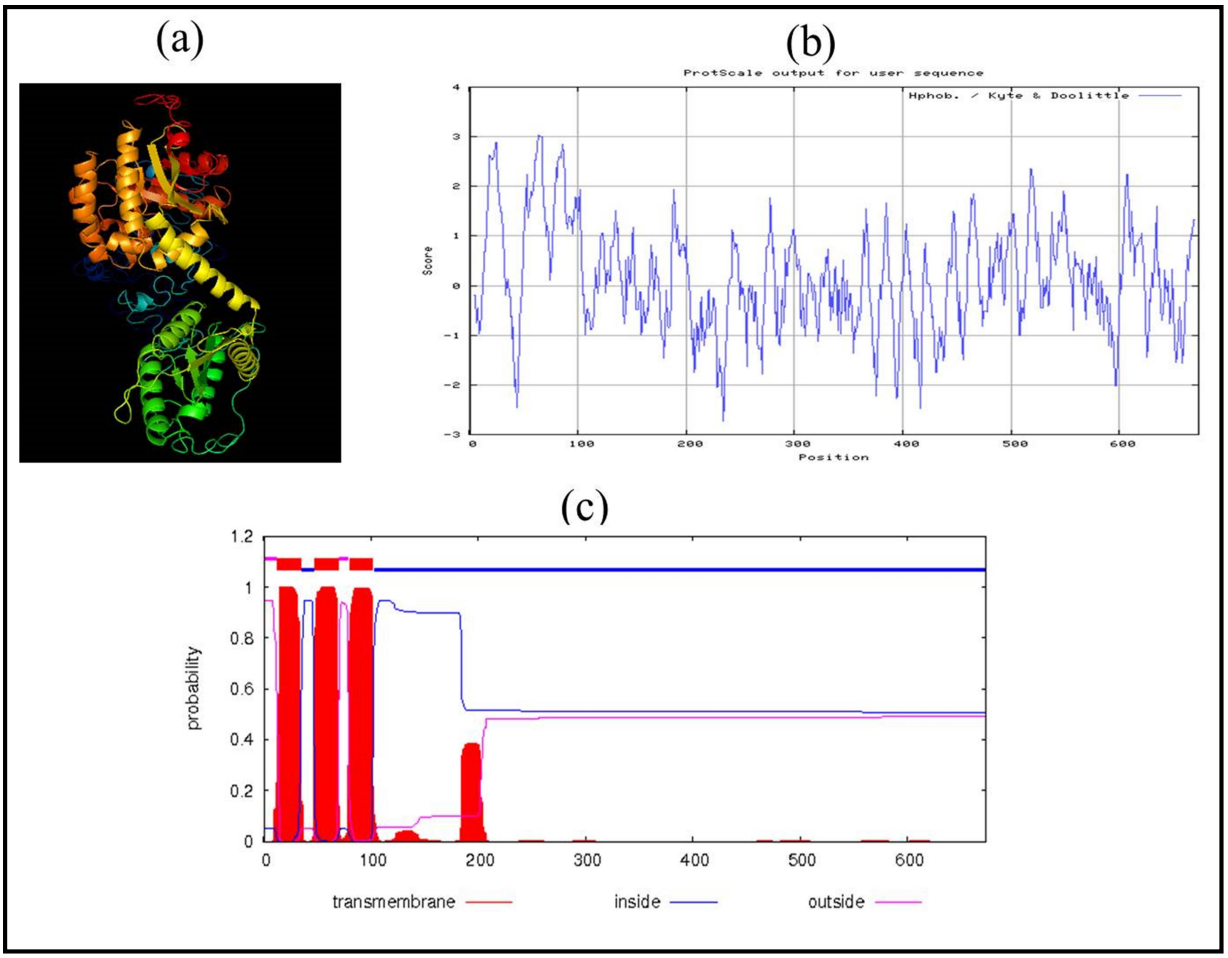

Fig. 21. (a) Protein model of Rpal_2444 built with the I-TASSER web server; (b) Hydropathy plot of Rpal_2444 generated using ProtScale server. (c) Transmembrane helix prediction of Rpal_2444 protein by TMHMM server.

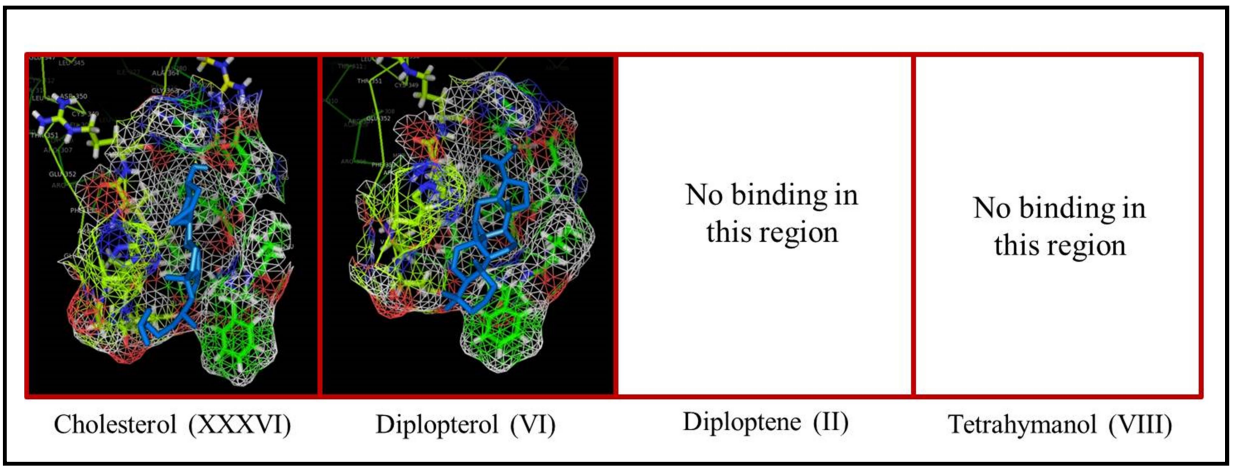

Fig. 22. Visualization of binding between ligands and Rpal_2444 protein with CRAC motif spanning from 269 to 296 amino acids which have six overlapping CRAC motifs.

DISCUSSION

4.0 Discussion

4.1 Mining of bacteria for hopanoids

The investigation of hopanoid biosynthesis is limited to a very few microorganisms which include few members of phylum *Actinobacteria*, *Cyanobacteria*, *Planctomycetes*, *Firmicutes* and other physiological groups like acetic acid bacteria, nitrogen fixing bacteria, methanotrophs, methylotrophs, purple non-sulfur bacteria, sulphate reducing bacteria (Blumenberg *et al.*, 2012; Doughty *et al.*, 2009; Hartner *et al.*, 2005; Neunlist and Rohmer, 1985b; Reipen *et al.*, 1995; Rohmer *et al.*, 1984; Rosa-Putra *et al.*, 2001; Talbot and Farrimond, 2007; Talbot *et al.*, 2007b). Although hopanoids were reported from some phylogenetically related members, no definitive conclusions about their taxonomic importance were drawn from their reported distribution. Therefore, to study the chemotaxonomic importance of hopanoid, mining of bacteria for hopanoid production was carried out. Eighty-six bacterial species representing 24 different genera were screened for hopanoids. Initially, the screening was carried out using thin layer chromatography which was stained with 0.1% alcoholic solution of berberine hydrochloride and bands were visualized at 360 nm. As the hopanoid standard was not available it was difficult to identify complex hopanoids using thin layer chromatography, therefore a more sophisticated and better method for the identification of hopanoids was tried. An attempt was made to identify hopanoids using LC-MS with ESI as ionisation mode with different methods of derivatisation (acetylation, silylation and benzoylation), but the ESI mode was not able to ionize hopanoids, hence couldn't be used to identify hopanoids. Further, GC-MS was carried out for the identification of hopanoid, where acetylated total lipid extract was analysed by GC-MS using DB-1HT column having extended temperature limit of 400^{o}C which makes it possible to identify functionalized hopanoid eluting at high temperature (360^{o}C; Sessions *et al.*, 2013). In the GC-MS analysis, hopanoids were identified based on the fragmentation pattern and previous reports (Sessions *et al.*, 2013; Welander *et al.*, 2009).

Three members of the genus *Rhodomicrobium* were screened for hopanoid. These are *Rmi. vannielii* DSM162^{T}, *Rmi. udaipurense* JA643^{T} and *Rmi. udaipurense* JA755. On the basis of 16s rRNA gene sequence analysis of *Rmi. udaipurense* JA643^{T} and *Rmi. udaipurense* JA755 shared 99% similarity with *Rmi. vannielii* DSM162^{T} (Ramana *et al.*, 2013b). However, Diploptene (DPE; II) and an unidentified hopane (UH5) were present

only in strains JA643^T and JA755 which differentiate between *Rmi. udaipurense* and *Rmi. vannielii* (Table 2; Ramana *et al.*, 2013b). Similarly, *Ciceribacter lividus* MSSRFBL1^T was isolated from chickpea rhizosphere soil from Kannivadi, India (Kathiravan *et al.*, 2013). The highest 16S rRNA gene sequence similarities for strain MSSRFBL1^T were found with the genera *Ensifer*, *Rhizobium*, *Sinorhizobium*, *Shinella* and *Kaistia* (>96.9%; Kathiravan *et al.*, 2013). Hopanoids of strain MSSRFBL1^T share similarity with *Sinorhizobium americanum* DSM15007^T and differs from *Ensifer adhaerens* LMG20216^T and *Ensifer kostiensis* DSM13372^T by the presence of bishomohopanediol (XII; Table 2). Therefore, hopanoid screening can be one of the taxonomic character to distinguish between the species of genus *Rhodomicrobium* (*Rmi. udaipurense* and *Rmi. vannielii*) as well as species and nearest members of genus *Ciceribacter*. Similarly, hopanoid can be used as taxonomic character for the differentiating species of genus *Cohaesibacter*, *Erythrobacter*, *Litoribacter*, *Pontibacter*, *Salinicoccus*, *Vogesella*, *Rhodoplanes*, *Rhodovulum* and *Rhizobium*, whereas species of genus *Mongoliicoccus* as well as species of genus *Alcanivorax* could not be differentiated based on hopanoid (Rahul *et al.*, 2014; Ramana *et al.*, 2013a; Shivani *et al.*, 2015; Srinivas *et al.*, 2014; Subhash *et al.*, 2013a, Subhash *et al.*, 2013b, Subhash *et al.*, 2013c, Subhash *et al.*, 2013d; Vishnuvardhan *et al.*, 2013a; Vishnuvardhan *et al.*, 2013b; Tushar *et al.*, 2015).

Fifteen species of the genus *Rhodovulum* were screened by GC-MS analysis. It was observed that seven species of genus *Rhodovulum* could synthesize cholesterol like molecule, six members could synthesize hopanoid but in *Rdv. kholense* JA297^T and *Rdv. marinum* JA128^T did not contain detectable hopanoid as well as cholesterol-like molecules. Sterol biosynthesis is present in eukaryotes and absent in prokaryotes with few exception (Pearson *et al.*, 2003; Wei *et al.*, 2016). Squalene monooxygenase and oxidosqualene cyclase are necessary for the synthesis of sterols from squalene which is C_{30} hydrocarbon compounds. *Gemmata obscuriglobus* which belongs to the phylum *Planctomycetes* and *Methylococcus capsulatus* which belongs to phylum *Proteobacteria* are reported to have the capacity to synthesize sterols (Wei *et al.*, 2016). In the present study, *Rdv. algae* JA877^T, *Rdv. viride* JA756^T, *Rdv. sulfidophilum* DSM1374^T, *Rdv. visakhapatnamense* JA181^T, *Rdv. salis* JA756^T, *Rdv.* imhoffii JA125^T and *Rdv. bhavnagarense* JA738^T were observed to produce cholesterol-like molecule (Ramaprasad *et al.*, 2016). The genome sequences of *Rdv. viride* JA756^T

(MUAV00000000) and *Rdv. sulfidophilum* DSM1374^T (CP015418.1) were screened for the presence of squalene monooxygenase and oxidosqualene cyclase homologs. But the homologs were not observed in both the genomes. It suggests that either draft genome might not have covered these genes or there might be an alternate pathway of sterol biosynthesis in these organisms.

The five type species of the genus *Rhodoplanes* (*Rpl. elegans* DSM11907^T, *Rpl. roseus* DSM5909^T, *Rpl. pokkaliisoli* JA415^T, *Rpl. piscinae* JA266^T and *Rpl. oryzae* JA793^T) used in this study for hopanoid analysis, which were previously isolated from different geographical regions and are physiologically versatile representing various growth modes (Lakshmi *et al.*, 2009). Members of the genus *Rhodoplanes* are characterized by their phototrophic growth, rod-shaped cells, motile, lamellar type intra-cytoplasmic membranes and are widely distributed in the aquatic habitats (Hiraishi and Ueda, 1994). Hopanoids of *Rhodoplanes* spp. were identified by comparing with hopanoids of *Rmi. udaipurense* JA643^T and fragmentation pattern of standards (Sessions *et al.*, 2013; Tushar *et al.*, 2014). All the five species of *Rhodoplanes* contain considerable amount of hop-22(29)-ene (II), diplopterol (VI), tetrahymanol (VIII), 2-methyldiplopterol (VII) and 2-methyltetrahymanol (IX) which are C_{30}/C_{31} hopanoids also found in most of the hopanoid containing bacteria, except methylated hopanoids which are present in bacteria containing 2-*methyltranferase* gene (Table 4). The structures of the biohopanoids mentioned are shown in Fig. 2. In NCBI database, there was no genomic information available for genus *Rhodoplanes*. Therefore some degenerate primers were designed and few were used from the literature in order to amplify the *shc* gene from these bacteria, but all the attempts were failed to amplify the gene.

Principal component analysis (PCA) converts data obtained from high-throughput instrumental analysis into a quantitative visual presentation (scores plot) and showing the clustering of biological samples into either similar or different grouping. PCA of hopanoids data from different species of genus *Rhodoplanes* distinctly separates all the five species (Fig. 7a) and recognises all five as independent species supporting the 16S rRNA gene based analysis. Heatmap analysis shows that these five species mainly differ in hop-22(29)-ene (II), 2-methylhop-22(29)-ene (III), BHP-550 (XVIII), BHP-492 (XVII), BHP-508 (XVI), aminobacteriohopanetriol (XXIV), hop-17(21)-ene (IV), 2-methylhop-21-ene (V; Fig. 7b) and cluster the data into five different clusters. Based on

hopanoid data dendrogram was constructed (Fig. 7c), which also classified the five species into four different leaves and one out-group of *Rpl. elegans* DSM11907^T. From the above analysis it is clear that hopanoid production can be a taxonomic marker to distinguish between the species of genus *Rhodoplanes*.

It is interesting to find, how wide spread hopanoids are and what their functions are in anoxygenic phototrophic bacteria like *Rhodomicrobium*, *Rhodopseudomonas* and *Rhodoplanes*. N-tryptophanyl-35-aminobacteriohopanetriol (XXVI) is unique to the genus *Rhodomicrobium*, which is not reported from other bacteria screened till today (Neunlist *et al.*, 1985; Tushar *et al.*, 2014), whereas genus *Rhodoplanes* has BHP-492 (XVII), BHP-508 (XVI) and BHP-550 (XVIII) which is reported only from *Rps. palustris* TIE-1 (Sessions *et al.*, 2013). The results presented here show that anaerobically grown bacteria contain hopanoid lipids in functionally significant amounts. Therefore, further analysis of hopanoid structure/function relationships is needed. Whether this difference is important for hopanoid functioning, or whether it is a mere result of the condition of the culture, remains to be seen. The unidentified hopanoids have to be critically studied to confirm their structure.

After screening 86 bacteria for hopanoids, it was observed that the distribution of hopanoid is heterogeneous in the screened bacteria (Fig. 23). The distribution of hopanoids in the nearest members is also heterogeneous i.e., few members have hopanoids whereas the phylogenetically close members did not show any detectable hopanoid. For example, genus *Rhodovulum* and *Rhodobacter* belong to the class *Alphaproteobacteria*, but few members of genus *Rhodovulum* contain hopanoids whereas members of genus *Rhodobacter* did not show any detectable hopanoids. It was observed that even within the genus also there is heterogeneity in the distribution of hopanoids. However it seems too early to conclude about the distribution of hopanoids as still many bacterial members have not yet been screened for hopanoids. Therefore there is a need for further screening of other bacteria for hopanoids so as to establish it as a suitable taxonomic marker. There are few possible explanations for the absence of detectable hopanoids in some strains; (a) These prokaryotes may lack the squalene hopene cyclase gene which is essential for the synthesis of hopanoids (b) hopanoid biosynthesis might be inducible in these organisms and was not induced under the growth conditions used in the present study (c) complex hopanoids might be present which may not be detected using analytical techniques used in this study.

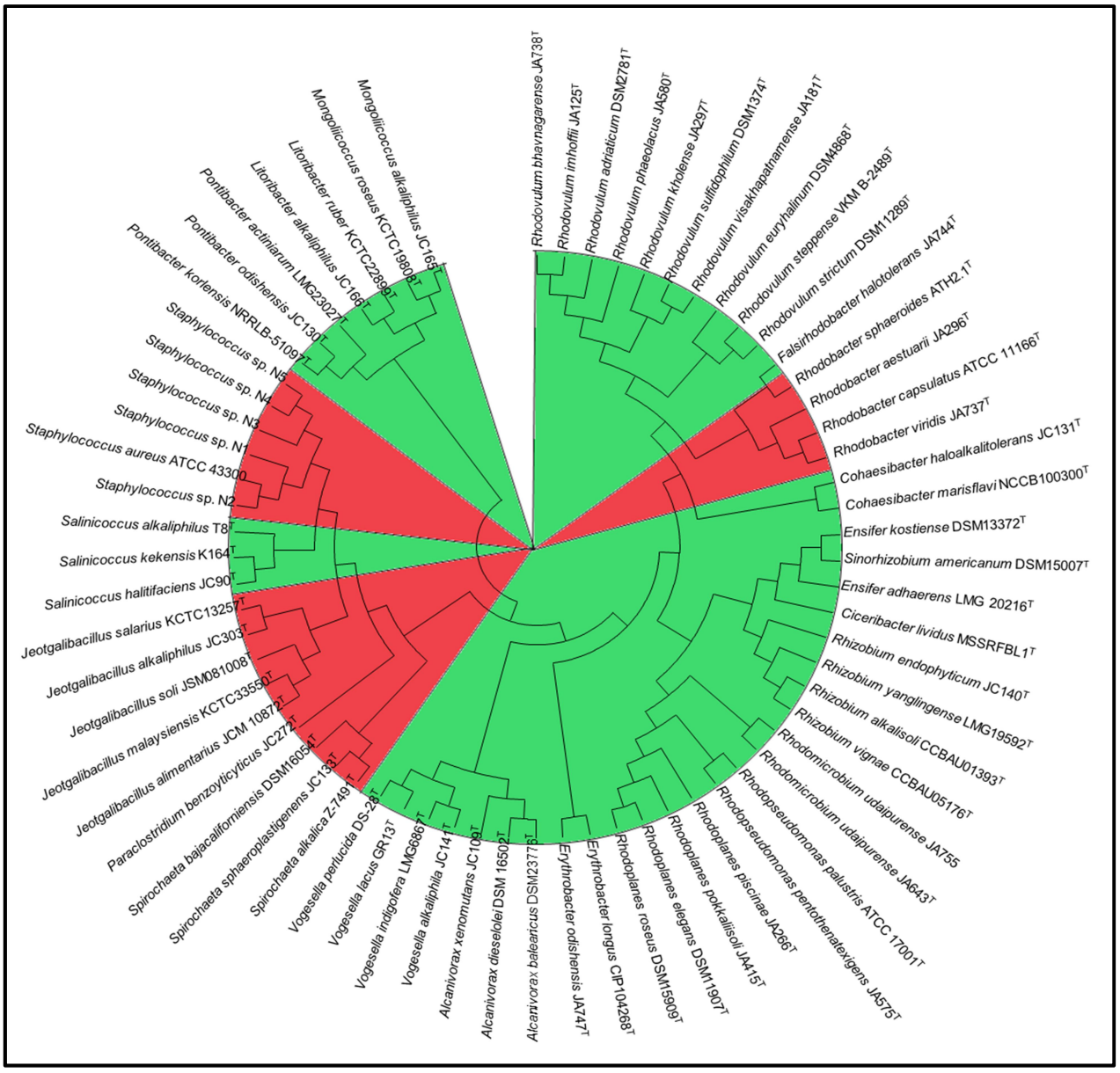

Fig. 23. Phylogenetic tree based 16S rRNA gene sequences of bacteria screened for hopanoids. The phylogenetic tree was constructed by the neighbour-joining method using the MEGA6 software. Green colour represents bacteria having hopanoids and red colour represents the bacteria not having any detectable hopanoids.

4.2 Mining genomes for the hopanoid biosynthetic pathway

Hopanoids are natural products that can be traced to its biological origin, therefore can be used as molecular fossils (Summons *et al.*, 1999). Hence, it is important to understand the distribution of these biomarkers and source specific information. Practically it is difficult to examine the distribution of hopanoids in all organisms and draw a conclusion. Recently, few reports had described about hopanoid biosynthetic pathway and genes involved in it (Tushar *et al.*, 2014; Welander *et al.*, 2012; Welander *et al.*, 2009). But the distribution of hopanoid biosynthetic pathway in bacteria has not yet been studied. With the advancement of next generation sequencing, the enormous genomic data is available in the public database. Therefore, screening of genomes was carried out to find the insight into hopanogenesis and phylogenetic distribution of hopanoid biosynthetic capabilities. Mining genomes of bacteria for hopanoid biosynthetic pathway genes was carried out and it was observed that the pathway is present in diverse bacterial taxa. Screening of genomes had revealed that only 10.5% of sequenced organisms have the genetic capacity to synthesize pentacyclic triterpenoid of hopane series.

Squalene hopene cyclase (SHC) is one of the complex enzymes which catalyse the cyclization of squalene (I) into hopanoids. SHC protein is known to be present in phylum *Actinobacteria*, *Cyanobacteria*, *Firmicutes*, *Proteobacteria*, *Planctomycetes*, *Verrucomicrobia*, *Nitrobacters*, *Solibacter*, *Chloroflexi*, *Armatimonadetes*, *Nitrospinae*, *Bacteroidetes* and *Acidobacteria* (Fig. 8). SHC protein contains eight QW motifs. The definition of QW motif is [K/R][G/A]$X_{2\text{-}3}$[F/Y/W][L/I/V]x_3Q$X_{2\text{-}5}$GXW where only amino acid glutamine (Q) and tryptophan (W) is conserved (Siedenburg and Jendrossek, 2011). In all selected 243 SHC proteins, QW motifs were screened and found to be having QW motif as it is very important for the function of SHC enzyme. This suggests that all these enzymes have capabilities to synthesize hopanoids. Some of the proteins like prenyltransferase from *Saccharopolyspora erythraea* NRRL2338 (CAM03917) and *Rubrobacter xylanophilus* DSM9941 (ABG05671), MFS transporter from *Mycobacterium smegmatis* MC2155 (WP003895014) showed homology with SHC protein. Interestingly, the distribution of hopanoid biosynthesis capability is not concentrated to a specific group of bacteria but non-homogeneously distributed into the domain bacteria and does not follow a systematic pattern (Fig. 24).

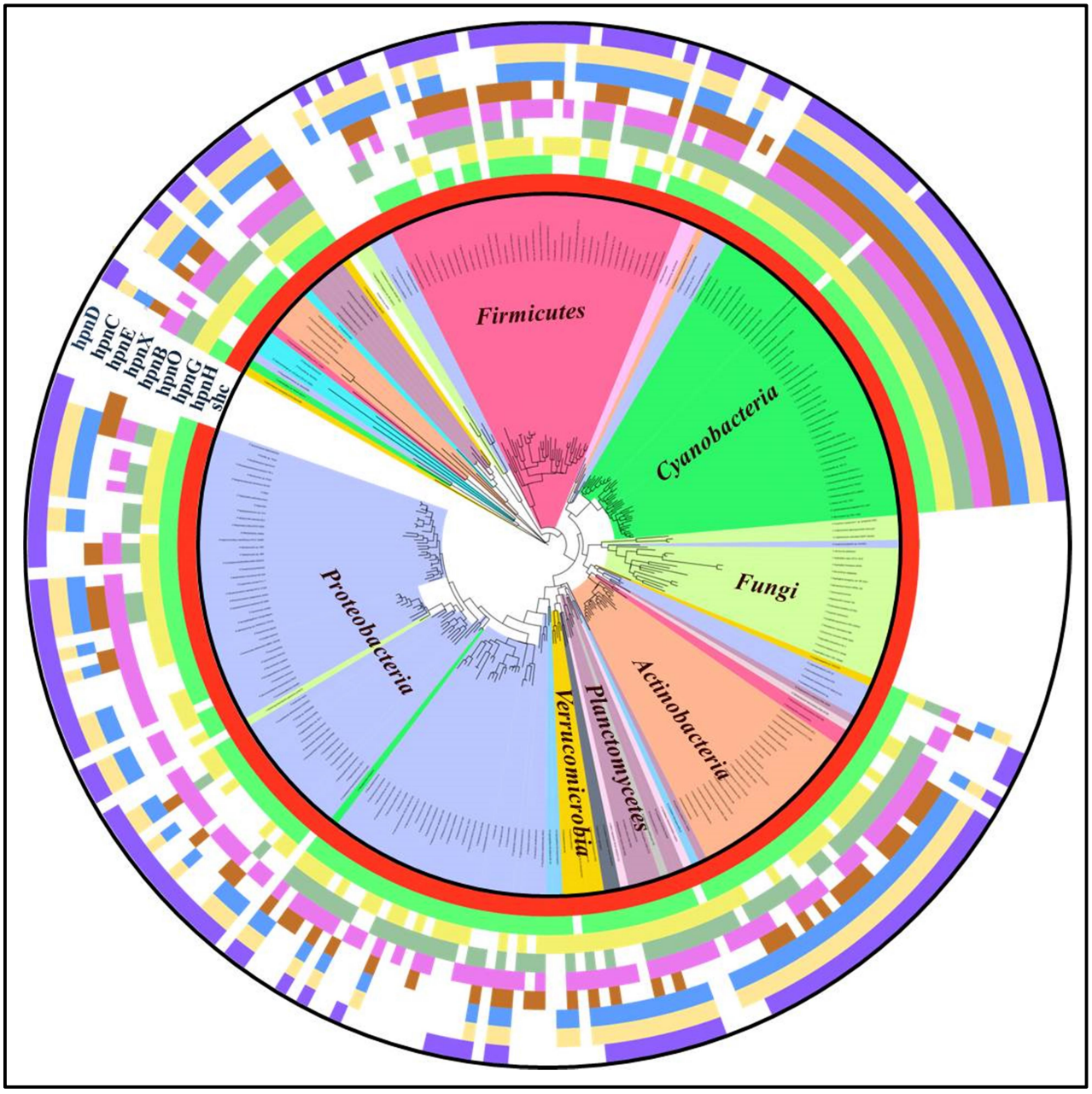

Fig. 24. The occurrence of hopanoid biosynthetic pathway proteins in distinctly related organisms. Total of 243 organisms were selected and the phylogenetic tree was constructed using SHC protein sequence by neighbour joining method using MEGA6 software. Each outer ring represents a protein. Red colour ring indicates SHC protein, green colour indicates hpnG protein, yellow colour indicates hpnH protein, grey colour indicates hpnO protein, pink colour indicates hpnB protein, brown colour indicates hpnX protein, blue colour indicates hpnE protein, light yellow colour indicates hpnC protein and violet colour indicates hpnD protein.

4.2.1 Distribution of hopanoid biosynthetic pathway in *Actinobacteria*

Actinobacteria is one of the economically important bacterial phyla which constitute Gram-stain-positive bacteria with physiologically and metabolically versatile properties (Ventura *et al.*, 2007). Out of genome sequenced *Actinobacteria*, 26% species have the genetic capability to synthesize hopanoids. All the selected *Actinobacteria* have SHC and hpnH protein which shows that they can synthesize diploptene (II), diplopterol (VI), tetrahymanol (VIII) and adenosylhopane (XIX). Nine members didn't have the presence of hpnG protein (adenosylhomocysteine nucleosidase) which is giving the genetic capability to synthesize ribosylhopane (XX). Fifty five percentage of mined *Actinobacteria* have potential to synthesize aminobacteriohopanetriol (XXIV) whereas 74% can synthesize glycosyl group containing hopanoids. The presence of sterol desaturase (hpnX) in 18 mined members suggests that it has the genetic potential to produce double bond containing hopanoids. In *Streptomyces coelicolor* A3(2), hopanoids are biosynthesized during the transition phase of spore formation, whereas in *Streptomyces scabies* 87-22 hopanoid biosynthesis is independent of lifestyle (Poralla *et al.*, 2000; Seipke and Loria, 2009). It suggests that the function of hopanoids vary among different bacterial members. *Frankia* sp., a member of phylum *Actinobacteria* is capable of synthesizing bacteriohopanetetrol (XXIII), bacteriohopanetetrol phenylacetate (XXXIII) and bacteriohopanetetrol propionate (XXXIV), which plays a crucial role in vesicle formation under nitrogen depletion conditions (Nalin *et al.*, 2000). The genes involved in the synthesis of these hopanoids are not yet reported.

4.2.2 Distribution of hopanoid biosynthetic pathway in *Cyanobacteria*

Cyanobacteria are ecologically important phytoplankton of freshwater and marine environment. They are also present in extreme habitats like hot springs, hyper saline lakes and high temperature (Stanier and Cohen-Bazire, 1977). *Cyanobacteria* are one of the significant producers of pentacyclic triterpenoids of hopane series. A survey of hopanoid distribution in phylum *Cyanobacteria* has shown that 89% of cyanobacterial species tested were found to produce hopanoids (Saenz *et al.*, 2012b; Talbot *et al.*, 2008). In the present study, out of 283 cyanobacterial members having SHC protein, 42 were selected based on phylogenetic affiliation. Almost all mined cyanobacterial members have the entire protein set which are involved in the synthesis of functionalized hopanoids, except "*Candidatus* Atelocyanobacterium thalassa isolate ALOHA". Genome

mining showed 41 species have the genetic capability of synthesizing BHPs, glycosylated, methylated and double bond containing hopanoids. Previous reports also found that cyanobacteria are good producers of BHPs and methylated hopanoids (Saenz *et al.*, 2012b; Talbot *et al.*, 2008). *Anabaena variabilis* and *Nostoc muscorum* were already reported to produce double bond containing BHPs (Rohmer *et al.*, 1984). *Prochlorothrix hollandica* and *Synechococcus* PCC 6907 was reported to produce glycosyl group comprising hopanoids (galacturonosyl bacteriohopanetetrol and anhydro-galacturonopyranosyl bacteriohopanetetrol; Simonin *et al.*, 1996). It has been observed that C_{35} hopanoids methylated at the C_2 position was a potential diagnostic marker for phylum *Cyanobacteria* in sedimentary environments (Summons *et al.*, 1999). Distribution of hopanoid biosynthetic pathway in *Cyanobacteria* suggests that hopanoid biosynthetic pathway is highly conserved in phylum *Cyanobacteria* and might be one of the major contributors of environmental hopanoids.

4.2.3 Distribution of hopanoids biosynthetic pathway in *Firmicutes*

Firmicutes are ecologically and industrially important group of bacteria which include 274 different genera as of 2016. So far very few members of phylum *Firmicutes* have been screened for the presence of hopanoids (Kontnik *et al.*, 2008; Rohmer *et al.*, 1984). From the present study, 28 members out of the total mined *Firmicutes* had capability to synthesize adenosylhopane (XIX), whereas only 25% have potential to convert adenosylhopane (XIX) to ribosylhopane (XX). Only 10 mined members can synthesize aminobacteriohopanetriol (XXIV) and 79% can synthesize glycosylgroup containing hopanoids. Unsaturated hopanoids can be synthesized by 59% of the selected *Firmicutes*. SHC protein of thermophile *Alicyclobacillus acidocaldarius* is extensively studied triterpene cyclase (Siedenburg and Jendrossek, 2011). At elevated temperature it produces seven times more hopanoids which suggest the role of hopanoids in high temperature tolerance (Poralla *et al.*, 1984). In *Bacillus subtilis* putative squalene hopene cyclase gene reported to produce the polycyclic skeleton of the sporulenes (XXXV; Kontnik *et al.*, 2008). From this study, it was also observed that solvent tolerant *Bacillus* sp. JC325 which is a phylogenetically close relative of *Bacillus tequilensis* KCTC13622 can also produce sporulene (XXXV) during the spore formation. The phylogenetic tree of SHC protein of few bacteria already known to produce hopanoids revealed that SHC enzyme which produces sporulene formed a different out group (Fig. 25). The possible explanation for the synthesis of sporulene (XXXV) by SHC protein might be the

difference in key amino acid residues at catalytic sites (Fig. 25). Twelve strains of genus *Staphylococcus*, 5 species of genus *Jeotgalibacillus*, and *Paraclostridium benzoelyticum* JC272^T were screened for hopanoids but no detectable hopanoids were observed. Even the genome sequence also did not show the presence of SHC protein in these members (The genomes were mined for those members only for which genomic data is available in NCBI database). It is interesting to investigate that how these members maintain the membrane integrity and rigidity in the absence of hopanoids. Are these bacteria having alternative metabolites which overtake the function of hopanoids? Still a lot needs to be investigated in order to answer these questions.

4.2.4 Distribution of hopanoid biosynthetic pathway in *Proteobacteria*

Proteobacteria is one of the widely screened bacterial phyla for the presence of hopanoids. From the present study, only 7% of mined *Proteobacteria* members did not have genetic capability to synthesize adenosylhopane (XIX), whereas 56% members had potential to produce ribosylhopane (XX). Aminobacteriohopanetriol (XXIV) may be produced by only 30% of the mined *Proteobacteria* whereas 64% can synthesize glycosylgroup containing hopanoids. Only 30% of the mined *Proteobacteria* have the genetic potential to synthesize unsaturated hopanoids. Already the screening of hopanoids in *Proteobacteria* stated that *Alpha*-, *Beta*-, *Gamma*- and *Deltaproteobacteria* can synthesize wide array of hopanoids (Blumenberg *et al.*, 2006; Hartner *et al.*, 2005; Rohmer *et al.*, 1984; Talbot *et al.*, 2007a, Talbot *et al.*, 2007b; Vilcheze *et al.*, 1994). In *Deltaproteobacteria*, few cases of gene duplication events or lateral gene transfer may exist, as it contains two copies of *shc* gene which apparently arose from different origin (Pearson *et al.*, 2007). Reports state that the methyltransferase (*hpnP*) gene which is involved in the synthesis of methylated hopanoid is originated from the *Alphaproteobacteria* (Ricci *et al.*, 2015). *Rps. palustris* TIE-1 is known to produce diploptene (II), 2-methyldiploptene (III), diplopterol (VI), 2-methyldiplopterol (VII), tetrahymanol (VIII), 2-methyltetrahymanol (IX), adenosylhopane (XIX), ribosylhopane (XX), bacteriohopanetetrol (XXIII), 2-methylbacteriohopanetetrol (XXV), aminobacteriohopanetriol (XXIV), anhydrobacteriohopanetetrol (XXX), BHP-508 (XVI), BHP-550 (XVIII) and BHP-492 (XVII; Neunlist and Rohmer, 1985a; Rohmer *et al.*, 1984; Sessions *et al.*, 2013). Similarly, *Rmi. vannielii* is reported to synthesize 3β-hydroxy-17-methylhopane (XXXI), 29-hydroxy-3,17-dimethylhopane (XXXII), N-ornithinylaminobacteriohopanetriol (XXVII) and N-tryptophanyl-35-aminobacterio-

hopanetriol (XXVI; Neunlist *et al.*, 1985). But the enzyme involved in the biosynthesis of bacteriohopanetetrol (XXIII), anhydrobacteriohopanetetrol (XXX), BHP-508 (XVI), BHP-550 (XVIII), BHP-492 (XVII), 3β-hydroxy-17-methylhopane (XXXI), 29-hydroxy-3,17-dimethylhopane (XXXII), N-ornithinylaminobacteriohopanetriol (XXVII) and N-tryptophanyl-35-aminobacteriohopanetriol (XXVI) is not reported.

4.2.5 Distribution of hopanoids biosynthetic pathway in *Planctomycetes*

Planctomycetes inhabit the wide variety of habitat occupying diverse ecological niches, but only a few species can be cultured in the laboratory (Damsté *et al.*, 2004). *Planctomycetes* include few strictly anaerobic group of bacteria capable of oxidizing ammonia under anaerobic conditions known as anammox bacteria (Damsté *et al.*, 2004). Thirteen members have the genetic potential to synthesize diploptene (II), diplopterol (VI), adenosylhopane (XIX), ribosylhopane (XX), aminobacteriohopanetriol (XXIV), bacteriohopanetetrol (XXIII), glycosylgroup containing hopanoids, whereas synthesis of unsaturated hopanoids is constrained to only 30% of *Planctomycetes*. In the study conducted on the environmental distribution of hopanoid biosynthetic genes, it was observed that the *shc* genes in *Planctomycetes* are divergent in nature (Pearson *et al.*, 2007). Members of *Planctomycetes* were reported to synthesize diploptene (II), diplopterol (VI), bacteriohopanetetrol (XXIII), composite-BHPs and C_{27} hopanoid ketone (Damsté *et al.*, 2004). C_{27} hopanoid ketone is unique in *Planctomycetes* and can be used as a biomarker for *Planctomycetes*, whereas the route for synthesis of hopanoid ketone is unexplored. *G. obscuriglobus*, a *Planctomycetes* member can synthesize lanosterol and parkeol, but there is no subsequent modification of these sterols (Pearson *et al.*, 2003). Interestingly, the genome of *G. obscuriglobus* possess all the genes involved in hopanoid biosynthesis, in addition it has squalene monooxygenase and oxidosqualene cyclase which suggest that *G. obscuriglobus* have the genetic capability to synthesize hopanoids as well as sterols. Only few members of *Planctomycetes* harbour both hopanoid biosynthetic pathway as well as sterol biosynthetic pathway. As *Planctomycetes* are one of the oldest division of the domain bacteria and harbour hopanoid as well as sterol biosynthetic pathway it can be postulated that the cenancestor could have synthesized both hopanoids and sterol and with the time hopanoid biosynthesis might have been conserved in domain bacteria whereas sterol biosynthesis in eukaryotes.

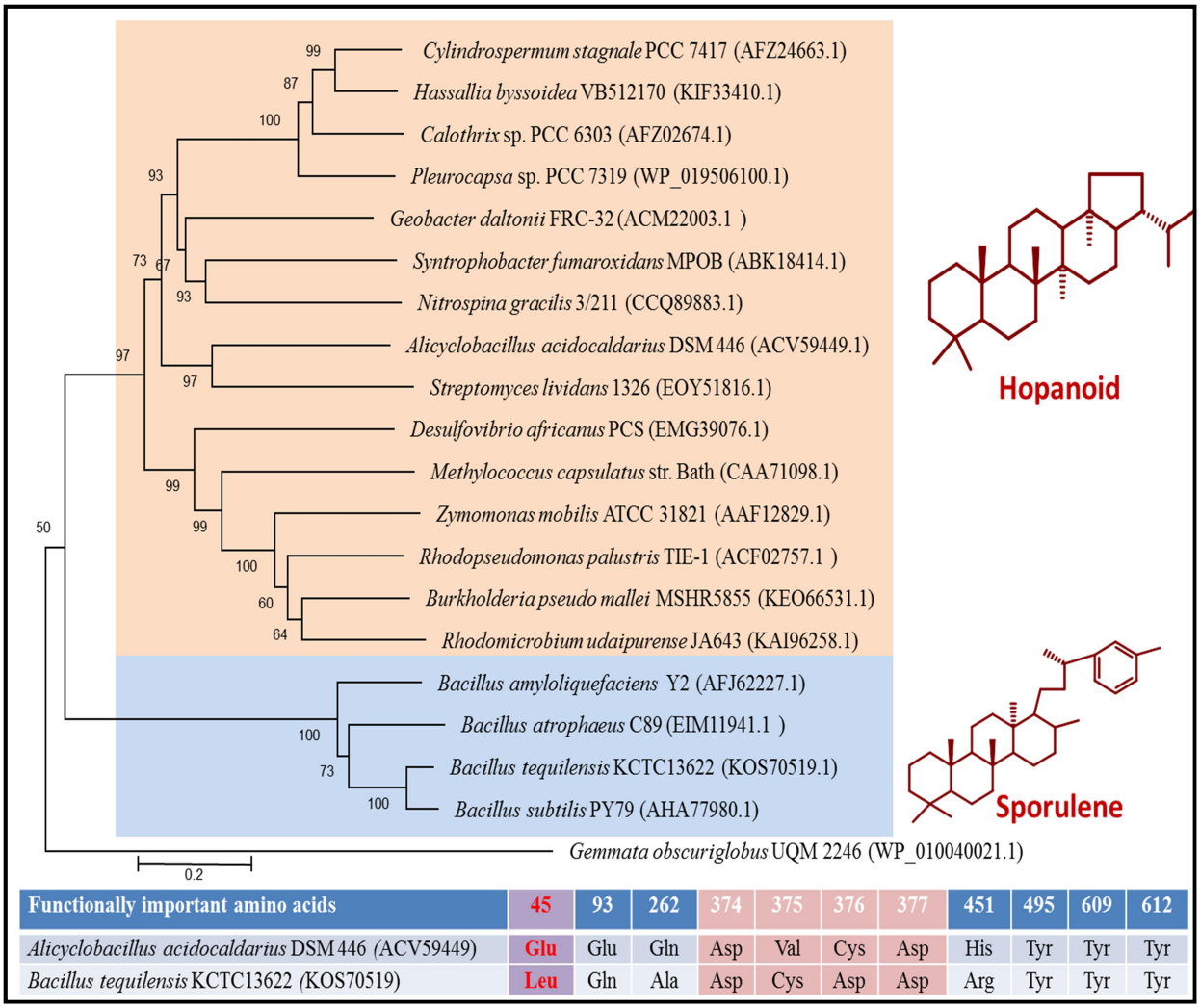

Functionally important amino acids	45	93	262	374	375	376	377	451	495	609	612
Alicyclobacillus acidocaldarius DSM 446 (ACV59449)	Glu	Glu	Gln	Asp	Val	Cys	Asp	His	Tyr	Tyr	Tyr
Bacillus tequilensis KCTC13622 (KOS70519)	Leu	Gln	Ala	Asp	Cys	Asp	Asp	Arg	Tyr	Tyr	Tyr

Fig. 25. Phylogenetic tree constructed using SHC protein sequence available in NCBI database (accession numbers are given in parentheses). Bootstrap values are listed as a percentage at branching points. Multiple sequence alignment and phylogenetic tree was constructed using the MEGA6 software. Bootstrap values based on 100 replications are listed as percentages at the branching points. Clade with brown colour is capable of synthesizing hopanoids where as other clade (blue) have potential to synthesize sporulene (XXXV). Table indicate the differences in amino acid residues at key catalytic positions of SHC protein between standard hopanoid producing species *Alicyclobacillus acidocaldarius* and sporulene producing member *Bacillus tequilensis.*

4.2.6 Distribution of hopanoid biosynthetic pathway in other phyla

So far there is no study conducted for the screening of hopanoids among the members of phylum *Verrucomicrobia*, *Spirochaetes*, *Nitrobacter* and *Solibacter*. But genome sequences suggest that few members of these phyla have the genetic capability to synthesize hopanoids. In the screening of new squalene hopene cyclase genes from acid mine drainage, putative *shc* gene was reported from the *Leptospirillum* group II and *Leptospirillum* group III which belongs to phylum *Nitrobacter* showing a genetic capability to synthesize hopanoids (Pearson *et al.*, 2003). *Chloracidobacterium thermophiles* which belong to the phylum *Acidobacteria* have genetic ability to synthesize diploptene (II), diplopterol (VI), adenosylhopane (XIX), ribosylhopane (XX), aminobacteriohopanetriol (XXIV), glycosyl group containing hopanoids as well as unsaturated hopanoids. *Chloracidobacterium thermophiles* was reported to synthesize diploptene (II), bacteriohopanetetrol (XXIII) and bacteriohopane cyclitol ether (Garcia Costas *et al.*, 2012; Tank and Bryant, 2015), but the gene involved in synthesis of bacteriohopane cyclitol ether is not yet reported. Genome sequence of phylum *Spirochaetes* were mined for hopanoid biosynthetic pathway but in none of the sequenced member SHC protein was observed. Similarly, few *Spirochaetes* member were also mined for hopanoids using GC-MS analysis where no detectable hopanoids were observed. Therefore, it is interesting to investigate that how these members maintain the membrane integrity and rigidity in the absence of hopanoids. Are these bacteria having alternative metabolite which overtakes the function of hopanoids or is it a loss of character in these members which remains an open question?

4.2.7 Distribution of hopanoids biosynthetic pathway in *Fungi*

Among the selected fungal members, only SHC protein was observed and other hopanoid biosynthetic pathway proteins were not present which suggest that few fungal members have genetic capabilities to synthesize hopanoids like diplopterol (VI), diploptene (II) and tetrahymanol (VIII) but don't have genetic capabilities to synthesize complex and poly-functionalized hopanoids. Similarly, simple hopanoids like diploptene (II), diplopterol (VI) and tetrahymanol (VIII) are reported from few higher plants, protists, ferns, mosses, and fungi (Cvejic *et al.*, 2000; Hartner *et al.*, 2005; Ourisson *et al.*, 1979; Ourisson *et al.*, 1987). This support previous findings that the eukaryotic members like plants and fungi can synthesize simple hopanoids but not able to produce

polyfunctionalized hopanoids (Blumenberg *et al.*, 2009; Cvejic *et al.*, 2000; Hartner *et al.*, 2005; Ourisson *et al.*, 1979; Ourisson *et al.*, 1987; Rohmer *et al.*, 1984; Talbot *et al.*, 2008). Still, the role of hopanoids in these eukaryotic members is not studied. The heterogeneous and rare distribution of hopanoid biosynthesis in eukaryotes gives a clue that hopanoid perform an important biological function. Therefore, there is a need to decipher the role of hopanoids in eukaryotes.

4.3 Genome sequence of *Rhodomicrobium udaipurense* JA643^T with special reference to hopanoid biosynthesis

Though *Rmi. udaipurense* JA643^T and *Rmi. vannielii* ATCC17100^T have 99% 16s rRNA gene sequence similarity, based on the genome relatedness (46.1% after DND-DNA hybridization) and phenotypic traits, these were described as two different species (Ramana *et al.*, 2013b). Delineation of the two *Rhodomicrobium* spp. comes from the genome sequence data based on the *in silico* genome to genome distance calculated based on the regression DDH which was estimated to be 58.21% which is much lower than the golden standard value of 70% for delineation of bacterial species (Wayne *et al.*, 1987). Further, SpecI analysis which is based on the forty phylogenetic marker genes (pMGs) also indicated an average identity of 97.24% concludes a clear delineation between the two (Mende *et al.*, 2013). Calculated ANI value of 95.26% between the genomes of *Rmi. udaipurense* JA643^T and *Rmi. vannielii* ATCC17100^T strengthens the separation into two species.

Information on the genes involved in the biosynthesis of hopanoids is limited and our study mainly focuses on genomic insights of the hopanoid biosynthesis in *Rmi. udaipurense* JA643^T. In strain JA643^T, IPP is synthesized through MEP pathway. IPP isomerase catalyzes the conversion of relatively un-reactive IPP to more reactive electrophile dimethylallyl pyrophosphate (DMAPP; Street and Poulter, 1990). Farnesyldiphosphate synthase gene (*ispA/ispB*) product catalyses the formation of (2Z, 6E)-farnesyl diphosphate from three isopentenyl pyrophosphate (Cantera *et al.*, 2002). Squalene synthase (*hpnC/hpnD*) catalyses stepwise tail-to-tail addition of farnesyl diphosphate (C_{15}) which condenses to form presqualene pyrophosphate which is an intermediate product (Siedenburg and Jendrossek, 2011). Presqualene pyrophosphate get converted to squalene (I) by squalene synthase (*hpnC/hpnD*). Squalene synthase is homologous to the phytoene synthase which leads to the production of carotenoids. The

function of *hpnC/hpnD* is poorly understood but its similarity with phytoene synthase suggests that it is involved in squalene synthesis (Kannenberg and Poralla, 1999; Perzl *et al.*, 1998). The product squalene is a C_{30} hydrocarbon which is the biochemical precursor for hopanoid biosynthesis (Siedenburg and Jendrossek, 2011).

Squalene (I) is converted into the hop-22(29)-ene/diploptene (II) or 22-hopanol/diplopterol (VI) by squalene hopene cyclase (*shc*) or squalene hopanol cyclase. Cyclisation of squalene (I) into the pentacyclic triterpenoid is one of the complex processes catalyzed by squalene hopene cyclase (*shc*/*hpnF*). A single enzyme catalyses the stepwise formation of 13 covalent bonds and nine stereo centers (Siedenburg and Jendrossek, 2011). *Δshc* mutant strain shows that there is accumulation of squalene (I) and did not produce hopanoids as well as triterpenoid tetrahymanol (VIII; Welander *et al.*, 2009). This study suggests that *shc* is also involved in the biosynthesis of tetrahymanol (VIII; Welander *et al.*, 2009).

A gene *hpnP* is hopane 2-methyltransferase which is not located in the genome sequence of *Rmi. udaipurense* JA643^T. But the methylated hopanoid, 2-methyldiplopterol (VII) was identified by GC-MS which indicate that the *hpnP* gene might be there but it might not be covered in the genome sequence. The hop-22(29)-ene (II) is further converted to adenosylhopane (XIX) by the radical SAM protein (*hpnH*) required for addition of adenosine to hopane skeleton. *hpnH* gene product is a B12 binding radical SAM protein. *ΔhpnH* mutant results in the production of C_{30} hopanoids (diploptene (II) and diplopterol (VI); Walender *et al.*, 2012). The next step in the biosynthesis is removal of adenine moiety from adenosylhopane (XIX) which is carried out by adenosylhopane nucleoside/hopanoid associated phosphorylase which is encoded by *hpnG* gene, a putative nucleoside hydrolase which leads to the formation of ribosylhopane (XX). In *ΔhpnG* mutant bacteriohopanetetrol (XXIII) and aminobacteriohopanetriol (XXIV) were not found and accumulation of intermediate adenosylhopane (XIX) was observed (Welander *et al.*, 2012).

A lactone hopanoid, ribosylhopane (XX) were identified as an intermediate in the biosynthesis of C_{35} hopanoids (Seeman *et al.*, 1999). The lactone ring of this hopanoid could be opened via a lactone hydrolase in a reaction similar to the hydrolysis of the quorum sensing molecule acylhomoserine lactone (AHL) by acylhomoserine lactonase (Wang *et al.*, 2010). However, O-acylhomoserine lactonase was not observed in the

genome of *Rmi. udaipurense* JA643^T. The lactone hopanoid might be oxidized to putative ribonylhopane (XXI) precursor (Duvold and Rohmer, 1999). The presence of ribonylhopane (XXI) in some *Rps. palustris* mutant extracts suggests that the biosynthesis of the C_{35} hopanoids would require an oxidation of the ribosylhopane (XX) produced by the *hpnG* to form ribonylhopane (XXI; Welander *et al.*, 2012). There might be an interconversion of ribonylhopane (XXI) to formylhopane (XXII), because ribonylhopane (XXI) is less reactive while, formylhopane (XXII) is more reactive. In GC-MS analysis ribosylhopane (XX), ribonylhopane (XXI) and formylhopane (XXII) were not detected. The gene involved in the interconversion of ribosylhopane (XX) to formylhopane (XXII) is not yet known.

Reductive amination of formylhopane (XXII) may lead to the production of aminobacteriohopanetriol (XXIV; Rohmer, 1993). Knock out study of Ornithine: oxo-acid aminotransferase (*hpnO)* showed that it is involved in the formation of aminobacteriohopanetriol (XXIV; Welander *et al.*, 2012). *hpnO* bears homology with N-acetylornithine aminotransferase (*ArgD*). *ArgD* acts on an aldehyde rather that a hydroxyl group supporting the idea that the formylhopane (XXII) is more likely the correct substrate. The hopanoid having amino acid residue linked to amino group of aminobacteriohopanetriol [N-tryptophanyl-35-aminobacteriohopanetriol (XXVI)] was observed which indicate the modification of aminobacteriohopanetriol in *Rmi. udaipurense* JA643^T. The gene involved in the synthesis of bacteriohopanetetrol (XXIII) and N-tryptophanyl-35-aminobacteriohopanetriol (XXVI) is not yet identified but products were identified in GC-MS analysis.

Sterol desaturase (*erg32*/*hpnX*) gene is present in the genome of *Rmi. udaipurense* JA643^T from 959672 to 958896 bp and upstream and downstream region is shown in Fig. 10. Sterol desaturase family protein known to catalyzes the formation of a C-5 double bond in the B ring of ergosterol. *erg32* is involved in the biosynthesis of ergosterol which is important for plasma membrane structure, function and for localization of plasma membrane proteins (Volkman, 2003). But in prokaryotes sterols are not present with few exceptions (Wei *et al.*, 2016). As hopanoids are the sterol surrogates and some hopanoids with double bond at C_6 and C_{11} position were reported previously (XIV and XV; Simonin *et al.*, 1994), it is hypothesized that sterol desaturase (*hpnX*) might be responsible for the incorporation of double bond in the hopanoids.

hpnI/hpnB genes are associated with hopanoid glycosyltransferase and glycosylated hopanoids were identified with *Geobacter sulfurreducens* and *G. metallireducens* (Eickhoff *et al.*, 2013; Methe *et al.*, 2003). Hopanoids with glycosyl moiety is expected in the *Rmi. udaipurense* JA643^T since *hpnI/hpnB* gene was observed in the genome of this organism, however no glycosyl containing hopanoids were detected in the GC-MS analysis. *hpnC*, *hpnD* and *hpnE* genes are involved in the modification of squalene. *hpnE* is squalene-associated FAD-dependent desaturase which has oxidoreductase activity. Perzl *et al.*, suggested that it might be involved as an oxidoreductase in hopanoid or terpenoid biosynthesis pathways (Perzl *et al.*, 1998). But its role in hopanoid biosynthesis is not understood. *hpnA* is NAD-dependent nucleoside diphosphate-sugar epimerase/dehydrates protein, which is not observed in the genome of *Rmi. udaipurense* JA643^T. Based on the genes observed, hopanoids detected and literature available hopanoid biosynthetic pathway is predicted which is shown in Fig. 26 (Cantera *et al.*, 2002; Duvold and Rohmer, 1999; Eickhoff *et al.*, 2013; Kannenberg and Poralla, 1999; Malott *et al.*, 2012; Methe *et al.*, 2003; Perzl *et al.*, 1997; Perzl *et al.*, 1998; Rohmer, 1993; Rohmer, 2008; Seeman *et al.*, 1999; Simonin *et al.*, 1996; Street and Poulter, 1990; Walender *et al.*, 2012; Wang *et al.*, 2010; Welander *et al.*, 2009).

Apart from these genes involved in the biosynthesis of hopanoid there are few genes which play a key role in the localization of hopanoids. Some of the genes are involved in hopanoid regulation or transport of the hopanoid to its correct place. One such reported gene is *hpnN* which encodes a RND-like transporter that helps to localize hopanoids to the outermembrane (Doughty *et al.*, 2011). *hpnN* and *hpnO* is located close together with a hypothetical protein in between. *ΔhpnN* mutant no longer contains any hopanoids in the outermembrane. *hpnN* mutant produces more 2-methylhopanoids, possibly indicating some role for *hpnN* in hopanoid homeostasis (Doughty *et al.*, 2011). Extracellular sigma factor (ECF) regulates the methylation of hopanoids at C-2 position (Kulkarni *et al.*, 2013). Genome sequence of *Rmi. udaipurense* JA643^T showed that it has two RNA polymerase ECF type sigma factors. Probably these sigma factors may be the regulator for the expression of *hpnP* gene and production of methylated hopanoids in *Rmi udaipurense* JA643^T.

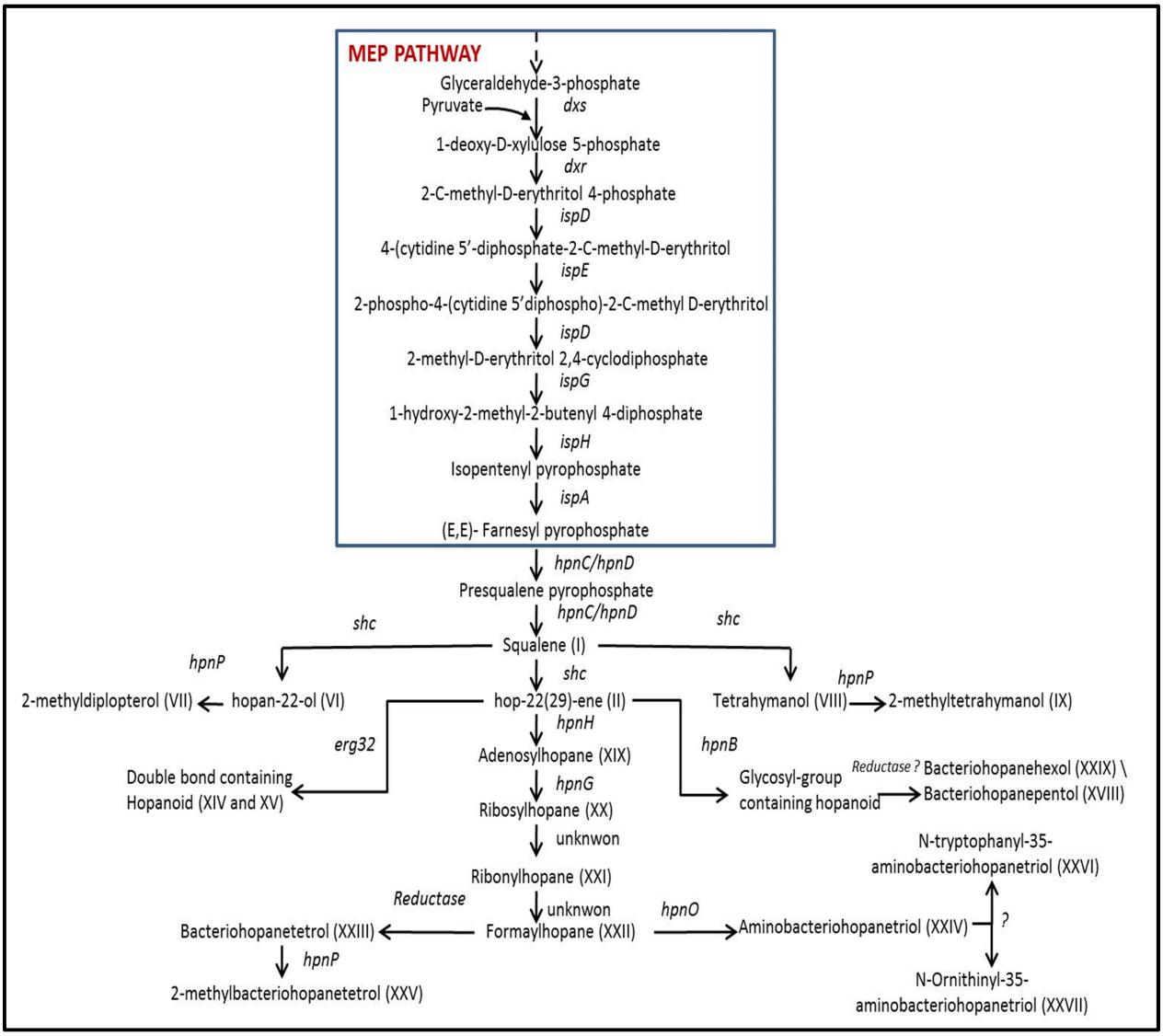

Fig. 26. Schematic representation of hopanoid biosynthetic pathway in *Rmi. udaipurense* JA643^{T} based on genes identified, GC-MS analysis and previous reports.

To understand the physiological functions of hopanoids in photosynthetic bacteria and compare functions to those of sterols in eukaryotes, it was planned to generate a hopanoid deletion mutant of *Rmi. udaipurense* JA643^T. The first step in hopanoid biosynthesis is cyclisation of squalene into diploptene which is catalysed by squalene hopene cyclise (*shc*) gene. Knockout of *shc* gene in *Rmi. udaipurense* JA643^T might be a deficit in synthesizing pentacyclic triterpenoids (especially hopanoids). The desired cassette in which *shc* gene having KAN gene inserted in between was cloned into suicide vector pJQ200SK (another insert where the 1kb flanking regions, upstream and downstream of *shc* gene was cloned into suicidal vector pJQ200SK was also constructed). The insertion of this plasmid into *Rmi. udaipurense* JA643^T was tried using conjugation experiment with a helper strain *Escherichia coli* S-17. Similarly electroporation experiment was also carried out. Inserting a foreign DNA into *Rmi. udaipurense* JA643^T and screening for the transformed colony was found to be difficult because it was not able to grow on Petri plates. Different strategies to overcome the problem like using an anaerobic chamber, growing in slant flashed with argon were tried, but not able to transform plasmid into *Rmi. udaipurense* JA643^T and screened them. Similar studies were conducted by Dr. Paula Welander to delete *shc* in aerobic methanotrophs, but were not successful (unpublished data). The possible explanation might be *shc* gene is essential in some organisms. On request, *Δshc* mutant strain of *Rps. palustris* TIE-1 was shared by Prof. D. K. Newman, California Institute of technology, California, USA. Hence, further study on understanding the physiological function of hopanoids was carried out on *Rps. palustris* TIE-1 wild-type (WT) and *Δshc* mutant.

4.4 Transcriptional response of *Δshc* mutant of *Rps. palustris* TIE-1

All domains of life have ordered cell membrane which is a key factor in the selective fitness of primitive life. The outer membrane serves as the first barrier in Gram-stain-negative bacteria (Silipo *et al.*, 2014). In most of the stress conditions bacteria sense the stress and adopt its plasma membrane in such a way that it can tolerate the stress present in extracellular environment. So ordered membrane is most important part of the cell. Reduced membrane order could lead to lower resistance to bilayer-disrupting agents. It was reported that there is possible interaction between hopanoids and glycolipids in bacterial plasma membrane which results into highly ordered bilayer (Silipo *et al.*, 2014). Hopanoids are known to interact with lipids A to promote order in the outer membrane. This interaction between hopanoids and glycolipids is similar to the

interaction between sterols and sphingolipids in eukaryotic membrane (Silipo *et al.*, 2014). Previously it was reports that, hopanoid-based ordering of lipid bilayer can be improved by structural modification of their ring structure or polar side chains (Silipo *et al.*, 2014). Hopanoid deficiency may leads to weakened structural integrity of cell membrane and may affect the other structures within or spanning cell envelope resulting in impaired lipid ordering which is linked to permeability, fluidity, ion conductivity, cell potential, cell signalling and lateral segregation (Saenz *et al.*, 2015). Hopanoids are involved in antibiotic resistance and tolerance to stress, but the precise understanding is lacking (Schmerk *et al.*, 2011). Understanding the role of hopanoids in shaping membrane properties would provide an important step towards bridging this gap.

Membrane lipid changes the environment of membrane protein which results in alterations of membrane protein activities and there is an effect of the lipid composition on bacterial transport systems. Hopanoids play crucial role in maintaining lipid order in cell which can alter the membrane environment and alter the membrane transport (Saenz *et al.*, 2015). From the transcriptome data it was observed that, 74 genes involved in transport activity were differentially expressed in *Δshc* mutant. In *Streptomyces cremoris*, it was established that the membrane lipid composition affects the transport protein of branched-chain amino acids (Driessen *et al.*, 1988). Twenty-three genes participating in branched chain amino acids (BCAAs) like leucine, isoleucine, valine was differentially expressed in *Δshc* mutant. BCAA transport system (LIV-I and LS system) is a part of osmotic shock-sensitive transporters which rely on periplasmic binding proteins (Quay and Oxender, 1976). This indicates that hopanoid deficiency may lead to osmotic imbalance in *Rps. palustris* TIE-1.

Genes involved in TonB dependent transport system (TBDT) was downregulated in *Δshc* mutant when it was grown in pyruvate. TBDTs catalyses the active transport of iron-siderophore complexes, vitamin B12, nickel complexes, carbohydrates, group B colicins and bacteriophages T1 and ø80 through high affinity transporters in the outer membrane (Noinaj *et al.*, 2010). Two parameters are important in TonB dependent transport process; (1) proton-motive forces of the cytoplasmic membrane; (2) a complex of membrane protein (TonB, ExbB and ExbD). Upon oxidative stress a stronger repression of iron uptake can prevent the formation of hydroxyl radicals by the Fenton reaction (Noinaj *et al.*, 2010). It was observed that with changes in osmolarity there is change in several TBDTs for siderophores (Noinaj *et al.*, 2010). Impaired membrane in

hopanoid mutant may fails to establish proton motive force and imbalanced osmotic balance may leads to downregulation of TBDTs transport system. Seven genes involved in nitrate transport were downregulated. There are two types of transport system for assimilation of nitrate. ABC transporters that are driven by ATP hydrolysis and secondary transporters reliant on proton-motive force. The transport of nitrate might be hampered in *Δshc* mutant which might be effect of defect in proton motive force. Polyamine transport system was also downregulated in *Δshc* mutant. Polyamines are polycationic molecules which interact with negatively charges nucleic acid and linked to protection from oxidative and acid stress (Shah and Swiatlo, 2008).

Similarly, 11 genes subnetwork involved in dipeptide and oligopeptide transport was showing downregulation. Four genes encoding for solute binding proteins (one from family 1 (*Rpal_1663*), one from family 3 (*Rpal_5283*) and two from family 5 (*Rpal_1660* and *Rpal_2941*) were downregulated. Extracellular solute-binding proteins involved in transport system, sensing chemicals (chemoreceptors) and initiators of signal transduction pathway (Tam and Saier, 1993). This gene network triggered the high expression of 33 kDa chaperonin which is redox regulated molecular chaperone. 33 kDa chaperonin plays a crucial role in protection of oxidatively damaged proteins and bacterial defence system in oxidative stress (Jakob *et al.*, 1999). The *fur* gene encodes a regulatory protein got upregulated, which represses genes required for iron uptake, it may be result of impaired membrane in *Δshc* mutant of *Rps. palustris* TIE-1. ATP-dependent zinc metallopeptidase (*Rpal_1317*) was upregulated which is involved into quality control of integral membrane proteins. The transport of polar amino acid was also downregulated in *Δshc* mutant (polar amino acid ABC transporter, inner membrane subunit and extracellular solute binding protein family 3).

Twenty-three ABC transporters were downregulated in *Δshc* mutant. Multidrug transport is impaired in a hopanoid-deficient mutant which gives a clue for the link between membrane order and an energy-dependent, membrane associated functions (Saenz *et al.*, 2015). Impaired multidrug efflux may accounts for sensitivity to chemical stresses. The nonpolar 1-N-phenylnaphthylamine (NPN) is a fluorescent probe which has a property of phospholipid environment sensitive spectral shifts enabling studies of the permeability of outer membrane of Gram-stain-negative bacteria. To test whether hopanoid deficiency leads to defected membrane permeability and transport NPN uptake assay was carried out. In NPN uptake assay it was observed that *Rps. palustris* TIE-1

fluorescence signal increases and again decrease in signal where as in *Δshc* mutant it was increased and get constant with the time, which shows that multidrug transport is impaired (Fig. 15). Multidrug efflux assay was performed to test whether energy dependent multidrug transport was impaired in *Δshc* mutant. After adding pyruvate the fluorescence is increased and subsequently bacteria efflux the dye (H33342) out of the cell, but *Δshc* mutant was not able to efflux dye out using ATP dependent efflux system (Fig. 16). The results showed that the energy-dependent multidrug transport is deficient in the hopanoid *Δshc* mutant.

Twenty-eight genes involved into cellular homeostasis and oxidoreductase activity were upregulated. Bacterial thioredoxins are small redox proteins which linked cellular redox regulation and oxidative stress defence mechanisms. High expression of thioredoxins inturn upregulate *nrdR* transcriptional repressor, glutaredoxin, 30S ribosomal protein S19, ribulose-bisphosphate carboxylase, *BolA* family protein, *OmpA*/*MotB* domain protein, ATP-dependent *clp* protease proteolytic subunit (endopeptidase *clp*) and downregulate uridylate kinase (UK), integrase catalytic region, flagellar hook capping protein, flagellar hook capping protein, *recA* (recombinase A) (Fig. 14). Weekend cell membrane in hopanoid deficiency may create osmotic imbalance and impaired cellular redox potential. To create the cellular homeostasis bacteria may trigger its oxidative stress response machinery to combat stress. Seven monooxygenase genes were upregulated, monooxygenase are the proteins which incorporate oxygen atom in the substrate. Monooxygenase and cytochrome P450 are involved in oxidoreductase activity (Bramkamp and Lopez, 2015). This indicates that hopanoid plays important role in maintaining cellular homeostasis.

From the transcriptome data it was observed that 25 genes involved into the chemotaxis, response to stimuli and flagellar assembly were significantly downregulated (Table S3). The sight of flagellar assembly in a bacterial cell is membrane and in hopanoid deficient mutant membrane is impaired. Eight genes involved in flagellar assembly and motility showed significant downregulation in hopanoid deficient mutant. Therefore swimming assay was carried out to understand the defect in motility. The swimming motility was affected but swarming motility was not affected in *Δshc* mutant (Fig. 17a). Nine genes involved in chemotaxis were downregulated in *Δshc* mutant and 12 genes involved in signal transduction and response to stimuli were also

downregulated. There might be alteration in permeability of cell membrane of hopanoid deficient mutant which affects sensing ability of extracellular ligand.

4.5 Interaction between the proteins and hopanoids

Lipid raft in eukaryotes organize signal transduction proteins and enrich in specific lipids such as cholesterol. Certain proteins of eukaryotic membranes have been consistently described as being present in lipid rafts (Lopez and Kolter, 2010). These proteins involved into various processes such as signal transduction, cytoskeleton rearrangement and vesicle trafficking (Bramkamp and Lopez, 2015; Listowski *et al.*, 2015). Like eukaryotes, prokaryotes do contain lipid rafts which orchestrate proteins involved in protein secretion, transportation and signal transduction (Bramkamp and Lopez, 2015). The discovery of lipid rafts in bacteria reveals a new level of sophistication in signal transduction and membrane organization that was unexpected for bacteria and shows that bacteria are more complex than previously appreciated. There is high possibility that bacterial lipid rafts may comprise of hopanoids as hopanoids are structurally similar to cholesterol. Similarly, hopanoids might be playing crucial role in signal transduction.

Protein-ligand interactions are most important phenomenon which regulates the cellular processes in cell. Extracellular signal stimulate various genes and inturn protein-protein interaction which causes the alteration in cellular process according to signal received. Cell membrane provides platform to form protein complexes, transport system and sensing receptors which controls various cellular process in cell. Hopanoids play crucial role in maintaining integrity (regulating the physical properties) of cell membrane. In eukaryotes it was found that cholesterol regulates the physical properties of cell membrane. Cholesterol plays important role in formation of lipid rafts and regulation of activities of some membrane proteins (Sheng *et al.*, 2012). Cholesterol interacts with PDZ domain-containing proteins and modulates cell signalling and protein network. PDZ domain containing scaffold proteins have been stated to interact with membrane lipids. Many proteins with PDZ domain contain CRAC motif which is present in many proteins known to interact with cholesterol (Sheng *et al.*, 2012). However, it is also possible that hopanoids interact directly with certain proteins, modulating their action. Bacteria also show the presence of various proteins having CRAC motif. The genome of the *Rps. palustris* TIE-1 consist of 34 diguanylate cyclase, organic solvent

tolerant protein (Rpal_3473), serine threonine protein kinase (Rpal_3613) and Proteinase Do (Rpal_2140, Rpal_2105 and Rpal_2705) which has CRAC motif. The genome of *Rps. palustris* TIE-1 consists of 34 genes having PDZ domain out of which three got significantly downregulated. Diguanylate cyclase has a PDZ domain containing CRAC motif which is known to be involved in interaction with cholesterol and controls cell signalling and protein networking (Sheng *et al.*, 2012). So, there might be possible interaction between diguanylate cyclase and hopanoids but interaction study has to be carried out.

Membrane palmitoylated protein 1 (MPP1) from human is known to interact with cholesterol (XXXVI). MPP1 is important in lateral membrane organization in lipid rafts. Cholesterol is analogous to hopanoids; therefore, it is possible that MPP1 can interact with hopanoids. *In silico* docking experiment suggest that diplopterol (VI), diploptene (II) and tetrahymanol (VIII) are able to dock to MPP1 protein similar to cholesterol (XXXVI) does. The MPP1 protein spanning from 258 to 286 amino acids contains 14 possible CRAC motifs. All four cholesterol (XXXVI), diplopterol (VI), diploptene (II) and tetrahymanol (VIII) shows binding affinity for this fragment whereas the binding residues are different. Tetrahymanol (VIII) shows highest binding energy (-9.2kcal/mol) whereas cholesterol (XXXVI) shows least binding energy (-7.6kcal/mol) to this region. According to the Eisenberg scale, this motif is located within a weak hydrophobic region, neighbouring with a region of increased hydrophobicity. This greatly reduces the probability of tested ligand binding. MPP1 protein spanning from 423 to 435 amino acids is located in hydrophobic region, have CRAC motif and shows *in silico* docking for ligands tested. As the CRAC motif occurring within 423-RSQYAHFDLSLV-435 region is a hydrophobic region of protein MPP1, it might be highly possible site of interaction with cholesterol (XXXVI), diplopterol (VI), diploptene (II) and tetrahymanol (VIII). This suggest that hopanoids mimic the cholesterol (XXXVI) molecule and similar to cholesterol (XXXVI), have capability to interact with protein having CRAC motif.

Intracellular secondary messenger c-di-GMP (cyclic diguanylate monophosphate) is important regulator for motile to sessile transition which is crucial lifestyle switch in different bacteria (Paul *et al.*, 2004). C-di-GMP is involved in regulation of number of complex physiological processes such as motility, biofilm formation, bioluminescence, cellulose biosynthesis, secretion, cell-cell signalling, differentiation and virulence (Paul *et al.*, 2004). It was observed that in *Caulobacter crescentus,* the active form of

diguanylate cyclase (PleD) localizes to the stalked pole of differentiating cells. Before genome replication begins PleD inhibits the motility by turning off flagellum rotations (Paul *et al.*, 2004). As two diguanylate cyclases (*Rpal_1916* and *Rpal_2444*) from *Rps. palustris* TIE-1 found to be downregulated in *Δshc* mutant, these were selected for further study.

Docking of ligands with Rpal_1916 protein was carried out and it was observed that protein spanning from 229 to 247 amino acids has 9 CRAC motif and capable to interact with all four ligands [cholesterol (XXXVI), diplopterol (VI), diploptene (II) and tetrahymanol (VIII)] tested. According to hydropathy plot, this motif is located in hydrophobic region and transmembrane helix prediction has showed it as a part of membrane helix (Fig 19). Occurrence of CRAC motif within the transmembrane helix/segment of protein increases the reliability of prediction of interaction with such proteins (Listowski *et al.*, 2015). Similarly, molecular modelling studies have shown that the CRAC motif which belongs to transmembrane domains can have a good fit for cholesterol (XXXVI; Listowski *et al.*, 2015). Therefore, CRAC motif spanning from 229 to 247 amino acids might be the probable site of interaction of hopanoids with Rpal_1916 in *Rps. palustris* TIE-1. Similarly, the stretch spanning from 593 to 714 amino acid has 7 CRAC motifs with some interval in between is a part of hydrophobic region and showed binding affinity for hopanoids (diplopterol (VI), diploptene (II) and tetrahymanol (VIII)) but not for cholesterol (XXXVI). Docking of ligands with Rpal_2444 protein showed that only the stretch spanning from 269 to 296 amino acids had showed binding affinity for both cholesterol (XXXVI) and diplopterol (VI) but not with diploptene (II) and tetrahymanol (VIII). This motif encompasses 6 CRAC motifs and located in hydrophobic region which suggest that it might be possible interaction site. Diploptene (II) and tetrahymanol (VIII) shows binding with Rpal_2444 but in different region of the protein. Still, the validation of this docking experiment needs to be performed to find out the interaction between proteins and hopanoids and outcome of this interaction remains an open question.

MAJOR FINDINGS

5.0 Major findings

- Genomic information and hopanoid screening provided insights of hopanoid biosynthetic capabilities in the domain Bacteria which are highly heterogeneous among the members of different phyla.
- The detailed and systematic investigation is required to use hopanoids as chemotaxonomic markers in bacterial taxonomy.
- Hopanoid biosynthetic pathway is highly conserved in *Cyanobacteria*.
- Some of the endospore producing bacilli produces sporulenes (XXXV) which are associated with endospores.
- *Planctomycetes* are one of the oldest division of the domain Bacteria and harbour hopanoid and sterol biosynthetic pathways. It can be postulated that the cenancestor can synthesize both hopanoids and sterols.
- The heterogeneous and rare distribution of hopanoid biosynthetic pathway in fungal members gives a clue that hopanoid might perform an important biological function in hopanoid producing fungal members.
- Hopanoid biosynthetic pathway is predicted in *Rmi. udaipurense* JA643^{T} which helps in understanding its regulation.
- Hopanoid deficiency can lead to alteration in the transport of branched-chain amino acids, polar amino acids, nitrate, dipeptide and oligopeptide and polyamine in *Rps. palustris* TIE-1.
- Energy-dependent multidrug transport is deficient in *Δshc* mutant of *Rps. palustris* TIE-1.
- Diguanylate cyclase (Rpal_1916 and Rpal_2444) interact with hopanoids [(diploptene (II), diplopterol (VI) and tetrahymanol (VIII)] and play an important role in cell motility and signal transduction in *Rps. palustris* TIE-1.

In a nutshell, this thesis contributes to the state-of-the-art of biohopanoids by providing knowledge about the hopanoid biosynthetic pathway, distribution of hopanoids in the domain bacteria and their role in membrane transport, motility and signal transduction.

SUPPLEMENTARY DATA

6.0 Supplementary data

Table S1. Occurrence of hopanoid biosynthetic pathway proteins in microorganisms. Information was obtained from the NCBI database

	NCBI accession numbers for the proteins							
Organisms	**SHC/hpnF**	**hpnH**	**hpnG**	**hpnO**	**hpnB**	**hpnC**	**hpnE**	**hpnX**
Phylum*: Actinobacteria*								
Acidothermus cellulolyticus 11B	ABK53469	WP011720534	-	WP011719068	ABK53494	WP011720529	WP041835658	-
Actinomadura madurae LIID-AJ290	WP033333971	WP021595756	WP026403258	WP026400385	WP 024935165	WP021592132	WP021595761	WP026314148
Actinospica acidiphila NRRL B-24431	WP033278154	WP034270144	WP034273408	WP033277301	WP 033277635	WP034270146	WP033278152	WP034278673
Amycolatopsis jejuensis NRRL B-24427	WP033289581	WP033289583	WP033295959	WP033294254	WP 033288776	WP033289699	WP033289580	WP038515557
Blastococcus saxobsidens DD2	YP005327239	CCG01189	-	-	CCG02697	CCG01193	CCG01192	WP029431420
Chloracidobacterium thermophilum B	WP014100779	WP014100993	WP014101350	ABV27277	AEP11411	AEP13732	AEP13747	AEP11254
Catenulispora acidiphila DSM44928	WP015795239	WP015795237	-	WP015795765	-	WP015795242	ACU75512	ACU69274
Frankia alni ACN14a	YP711680	WP011604505	WP011435144	WP013423607	CAJ60097	CAJ60803	CAJ60088	WP011607194
Intrasporangium chromatireducens Q5-1	EWT07891	EWT06599	WP013492059	WP034805610	EWT07463	WP034719327	EWT07893	WP034809998
Kitasatospora cheerisanensis KCTC 2395	KDN85988	WP035860865	-	WP035860859	KDN81842	KDN85991	WP035860898	KDN81822
Kutzneria albida DSM 43870	WP030111451	WP025357490	-	WP025356812	WP 030433140	WP025357495	WP025357494	-
Microbispora sp. ATCC PTA-5024	ETK37209	WP036320262	WP036328269	-	ETK37278	ETK30477	WP030508058	-
Microtetraspora glauca ASM72127v1	WP030495674	WP030495676	WP030497174	WP030495677	WP036416525	WP030495671	WP030495672	-
Mycobacterium abscessus 5S-1212	EIU35725	WP016888427	WP014850720	WP030094122	WP036477463	CAB94795	WP030096482	EIU71800
Mycobacterium smegmatis MC2 155	WP003895014	WP003892809	WP011727836	WP011729315	WP036477463	WP015308707	AGB25960	WP003894200
Nocardia sp. NRRL WC-3656	WP030513100	WP030513098	WP030513586	WP020108701	-	WP030513103	WP030515832	WP036525442
Nonomuraea coxensis DSM 45129	WP020540957	WP020540959	WP020543709	-	WP020547027	WP033410665	WP020540955	-
Pseudonocardia dioxanivorans CB1190	YP004333703	WP013675771	WP037046385	WP013672520	WP013672776	WP013674905	WP013675767	WP037068297
Rubrobacter xylanophilus DSM 9941	ABG05671	WP011564003	-	ABG05821	-	ABG03811	ABG03721	-
Saccharomonospora viridis DSM 43017	ACU97316	ACU97314	WP012796063	-	WP015786989	ACU97630	ACU97318	WP005465562
Saccharopolyspora erythraea NRRL 2338	YP001106521	YP001106519	WP010315781	AAQ94256	WP009945061	EQD82226	WP011874306	-
Saccharopolyspora erythraea NRRL 3538	CAM03917	YP001106519	-	AAQ94256	-	WP011874307	WP011874306	-

Organisms	NCBI accession numbers for the proteins							
	SHC/hpnF	hpnH	hpnG	hpnO	hpnB	hpnC	hpnE	hpnX
Sciscionella marina DSM 45152	WP020497097	WP026197179	WP020498515	WP020496121	-	WP020497100	WP020497099	-
Streptosporangium amethystogenes NRRL B-2639	WP030921652	WP030921657	-	WP030906982	WP012894266	WP030923716	WP037971909	WP012891046
Tetrasphaera japonica T1-X7	CCH78703	CCH78276	CCI52140|	CCH80464	-	CCH78401	CCH78402	CCH74132
Thermomonospora curvata DSM 43183	ACY97584	WP012852616	-	WP012851938	-	-	-	-
Phylum: *Cyanobacteria*								
Acaryochloris marina MBIC11017	ABW29816	ABW29989	WP012161264	ABW31361	ABW29550	ABW29825	WP012164067	WP039781860
Anabaena cylindrica PCC 7122	AFZ60533	AFZ61234	WP015214771	WP015215338	AFZ59039	AFZ56043	WP015215871	WP015212423
Anabaena variabilis ATCC 29413	ABA24268	WP011318062	WP011318466	ABA24877	ABA20472	ABA24405	WP011321453	ABA23347
Aphanizomenon flos-aquae NIES-81	WP027403896	WP039200388	WP027403894	WP039199575	WP027403895	WP027402605	WP027402606	WP027401504
Calothrix parietina PCC 7507	WP015199299	WP015199105	WP015199881	WP015199349	WP015199298	WP015201098	WP015201097	WP041739164
"Candidatus Atelocyanobacterium thalassa isolate ALOHA"	ADB95598	-	WP012953610	-	-	WP012953527	-	ADB94930
Chlorogloeopsis fritschii PCC 6912	WP016878379	WP016878349	WP016872624	WP016876908	WP016878378	WP016875938	WP016875939	WP016872796
Crocosphaera watsonii WH 8501	WP021835865	WP021829700	WP021836517	CCQ70944	WP007307835	WP007313064	CCQ69613	WP021835900
Cyanobacterium aponinum PCC 10605	AFZ53755	AFZ54158	WP015218196	AFZ53405	AFZ52214	AFZ53427	WP015218735	AFZ53136
Cyanobacterium endosymbiont of *Epithemia turgida*	BAP17942	BAP18474	BAP17924	BAP18544	BAP18546	BAP17538	BAP17537	BAP17474
Cyanobium sp. CACIAM 14	KEF41830	WP035831683	WP035830182	WP035829587	WP035831673	WP035830590	WP035830466	WP035832402
Cyanothece sp. PCC 7822	ADN12174	WP013320705	WP013324810	ADN13304	WP013321861	WP013321333	WP013321943	WP013323906
Cylindrospermum stagnale PCC 7417	AFZ24663	AFZ27424	WP015208854	AFZ28245	AFZ26450	AFZ24582	WP015208549	AFZ22674
Dolichospermum circinale AWQC310F	WP028088983	WP028085449	WP028091628	WP028091121	WP028084645	WP028082748	WP028091764	WP028091370
Fischerella sp. JSC-11	EHC18779	WP009455668	WP009457244	WP009459173	EHC14068	WP026733654	WP009456906	WP026731345
Geminocystis herdmanii PCC 6308	WP017294326	WP017292986	WP017295347	WP026101850	WP017295536	WP017295865	WP017295864	WP026101884
Gloeobacter kilaueensis JS1	YP008712366	AGY58669	WP023172763	AGY60297	AGY58232	AGY57800	AGY59325	WP023171557
Leptolyngbya boryana PCC 6306	WP017286012	WP017286333	WP017291064	WP026148430	WP017286013	WP017285845	WP017285846	WP017288293
Leptolyngbya sp. *Heron Island J*	WP023070515	WP023075999	WP023074675	WP023074859	WP031291745	WP031291778	WP023076968	WP023075859
Mastigocladopsis repens PCC 10914	WP026082593	WP017316890	WP017316743	WP026082733	WP017316987	WP017314657	WP033365614	WP017316694

Organisms	NCBI accession numbers for the proteins							
	SHC/hpnF	hpnH	hpnG	hpnO	hpnB	hpnC	hpnE	hpnX
Mastigocoleus testarum BC008	WP027840695	WP027840696	WP027843617	WP027846845	WP027840693	WP027842650	WP027840694	WP036265293
Microcoleus sp. PCC 7113	WP017652853	WP015185696	WP015186018	WP015185859	WP041781388	WP015182638	WP015182639	WP015180505
Microcystis aeruginosa SPC777	EPF22558	GAL92560	WP016516712	EPF23810	GAL95763	GAL95682	WP002792672	EPF20272
Moorea producens 3L	EGJ28770	WP008178591	WP009149150	WP008180321	WP008190510	WP008185895	WP008185893	WP008182761
Neosynechococcus sphagnicola sy1	KGF72746	KGF71806	WP036533572	WP036534095	WP036530567	WP036535828	WP036535830	KGF72239
Nodosilinea nodulosa PCC7104	WP017301695	WP017301076	WP017297104	WP017302274	WP026073120	WP017298995	WP017298662	WP040697412
Nostoc punctiforme PCC 73102	ACC84529	ACC79199	WP012412801	ACC81855	ACC84295	WP012409300	ACC82600	ACC79774
Nostoc sp. PCC 7107	AFY41090	WP015114541	WP015115512	WP015115640	WP015111330	WP015114893	WP015114894	WP015113584
Oscillatoriales cyanobacterium JSC-12	EKQ69086	WP009556004	WP009556000	WP009768433	WP009555999	WP009768484	WP036617429	EKQ68782
Planktothrix agardhii NIVA-CYA 126/8	WP027254967	WP042152759	KEI65808	WP042154178	WP042155912	WP042155334	WP042152496	WP027255708
Pleurocapsa minor PCC 7327	WP015144297	WP015144354	WP015143183	WP015144471	WP015144295	WP015141954	WP015141953	WP041392594
Prochlorothrix hollandica PCC 9006	WP026099859	WP016923957	WP026099245	WP017714039	WP017712719	WP026099793	WP017714083	WP017710775
Raphidiopsis brookii D9	EFA72238	EFA74468	WP009342569	EFA74093	WP009343759	EFA73011	EFA72094	EFA72740
Rubidibacter lacunae KORDI 51-2	ERN41784	ERN40437	WP022609034	WP022605172	WP022606372	ERN41782	ERN42097	ERN40115
Scytonema hofmanni PCC 7110	WP029631910	WP017744474	WP038297362	WP026135330	WP017744491	WP029636685	WP017744690	WP017749272
Stanieria cyanosphaera PCC 7437	AFZ37418	AFZ36767	WP015192070	AFZ36011	AFZ35469	AFZ36797	WP015194460	WP015193479
Synechococcus sp. PCC 7502	AFY75324	WP015168690	WP015167344	WP015169353	WP015167247	WP015168912	WP015170063	WP015168992
Synechocystis sp. PCC 6714	AIE72536	WP028948844	AIE76041	WP028946445	WP028946807	AIE74788	WP028947769	AIE75066
Thermosynechococcus elongatus BP-1	NP683099	WP011056444	WP011057121	Q8DLK8.2	WP011056830	WP011057400	WP011057401	WP011057754
Tolypothrix bouteillei VB521301	KGG75707	KIE12304	KIE13465	KIE10707	KIE11982	KIE10445	KIE07965	KIE13550
Trichodesmium erythraeum IMS101	ABG50159	WP011610104	WP011613079	WP011612205	WP011611062	WP011613360	WP011613361	WP011613495
Xenococcus sp. PCC 7305	ELS01058	WP006509463	WP006512357	ELS02431	WP040898968	WP006508810	WP006508811	WP006508751
Phylum: *Firmicutes*								
Alicyclobacillus acidocaldarius subsp. acidocaldarius DSM 446	ACV59449	AEJ44630	-	ACV59672	AEJ44726	4HD1A	WP008337271	WP026961886
Alicyclobacillus acidoterrestris ATCC 49025	CAA61950	WP031218357	-	WP041708259	WP021295886	WP021295960	EPZ48138	WP026961886

Organisms	NCBI accession numbers for the proteins							
	SHC/hpnF	hpnH	hpnG	hpnO	hpnB	hpnC	hpnE	hpnX
Alicyclobacillus hesperidum URH17-3-68	WP006446579	WP040289586	-	WP026174266	EJY57154	WP006447157	WP006447158	WP026961886
Anoxybacillus tepidamans PS2	WP027409037	WP035066879	WP004889336	WP027408941	-	WP027408583	WP035098137	WP027410439
Bacillus anthracis Ames	AIK09633	WP012543542	WP001079707	WP000850974	WP000414318	-	WP000983555	AIM10932
Bacillus cereus ATCC 14579	KFM86789	EEK56781	WP001079706	WP002165093	WP033693187	-	WP002118345	WP000832146
Bacillus cereus group	WP033709363	WP000544614	WP029141135	WP002129009	WP000414321	-	WP001168143	WP000755400
Bacillus lehensis G1	AIC96465	WP038482898	-	WP038484333	-	WP038479156	-	-
Bacillus subtilis E1	CCU58609	BAI87324.2	-	WP013351805	KIN50891	WP019258007	CCU58522	WP038464550
Bacillus thuringiensis BMB171	ADH08042	EEM27863	WP001079714	EEM24522	WP000414316	-	EEM60282	EEM96999
Bacillus toyonensis BCT-7112	AHA06776	-	-	-	-	-	-	-
Brevibacillus laterosporus LMG 15441	WP031415010	WP035311776	WP003342509	WP018669816	WP031411524	WP031414522	WP017250264	WP022586115
Brevibacillus sp. CF112	EJL42438	WP019122294	WP005828140	WP007718241	WP007729883	WP007716554	WP007784709	WP007722371
Cohnella thermotolerans DSM 17683	WP027091823	WP027092034	WP035154429	-	-	WP027093649	WP041064878	WP027092876
Desmospora sp. 8437	WP009708183	-	-	-	-	WP009708529	WP009711277	WP009711237
Desulfotomaculum gibsoniae DSM 7213	AGL02345	WP006522605	-	AGL02153	WP008411256	AGL01513	-	-
Fictibacillus gelatini DSM 15865	WP026677366	-	WP026676611	-	-	-	-	-
Geobacillus caldoxylosilyticus NBRC 107762	WP026078692	WP017436345	-	WP017436335	WP033843655	WP042409791	WP042407798	WP042408542
Geobacillus sp. GHH01	YP007402320	WP015374127	-	WP015374540	WP033018621	WP020960324	AGE20884	EZP76110
Geomicrobium sp. JCM 19038	GAK07843	WP042420976	-	-	-	WP042413693	WP042424299	-
Halobacillus karajensis MA-2	CDQ23781	WP027953986	-	WP035542876	WP035531505	WP027953992	-	-
Halobacillus sp. BBL2006	KHE72190	WP035548589	WP014642699	WP035542876	WP035545565	WP035543776	WP035545149	-
Laceyella sacchari 1-1	WP029071708	-	WP022736870	-	-	WP022738467	WP022735859	WP022737250
Paenibacillus curdlanolyticus YK9	EFM11713	WP006039138	-	-	-	WP013916654	-	WP006040536
Paenibacillus macerans 8244	KFM98440	KFN10687	WP013371880	WP019534875	KFN06538	WP036621930	WP042234218	WP014371055
Paenibacillus sp. P22	CDN45719	CDN45787	-	-	CDN45830	WP017691908	CDN42997	WP041045198
Paenibacillus terrae HPL-003	AET60181	WP014282703	WP014282330	-	WP028543731	WP014282093	WP018756873	WP041045198
Paenisporosarcina sp. HGH0030	WP016427930	-	-	WP017379472	WP036654391	WP016427416	WP017382049	-
Pontibacillus halophilus JSM 076056	KGX92982	KGX91607	-	-	WP026800680	WP026800678	KGX93024	-

Organisms	NCBI accession numbers for the proteins							
	SHC/hpnF	hpnH	hpnG	hpnO	hpnB	hpnC	hpnE	hpnX
Pontibacillus yanchengensis Y32	KGP71583	KGP71008	KGP74117	-	WP036815119	WP036820647	WP036822550	-
Shimazuella kribbensis DSM 45090	WP028778936	-	WP037465375	-	-	WP028775775	WP037463935	-
Terribacillus aidingensis MP602	AIF66556	-	WP026700388	-	AIF66107	WP038565789	WP038559289	-
Thermoactinomyces daqus H-18	WP033101078	-	WP033099084	-	WP037998307	-	WP037994259	-
Virgibacillus sp. Vm-5	CDQ39114	AIF43930	-	WP029267135	WP040956373	WP029267868	WP038245611	CDQ31062
Phylum: *Proteobacteria*								
Acetobacter pasteurianus IFO 3283-01-42C	BAI17744	GAB28380	-	-	WP019088855	-	WP012812362	-
Acetobacter pomorum DM001	KGB23767	WP035365943	WP035352754	-	WP006116771	WP003616600	EGE47483	-
Acetobacteraceae bacterium AT-5844	WP007434563	WP007434561	WP007434562	-	WP007437361	-	WP007434564	-
Acidiphilium angustum ATCC 35903	WP029313818	WP029313167	-	-	WP029314622	-	WP029314626	-
Acidithiobacillus ferrivorans SS3	CDQ11387	WP014028690	WP012536989	-	WP014030079	-	WP014030331	-
Acidocella facilis ATCC35904	WP026440315	WP008492983	WP035178860	-	WP026440319	-	WP026440316	-
Acidomonas methanolica NBRC 104435	GAJ27560	WP042060272	-	-	WP042058194	-	WP042056826	-
Afipia felis ATCC53690	CEG08549	WP002716366	WP002716368	CEG08541	WP002711118	CEG08552	WP048756442	-
Afipia felis B-91-007352	WP024920588	WP024573913	WP024573912	WP029659337	WP024920591	CEG08552	WP002716370	-
Alpha proteobacterium Q-1	GAK33986	WP011440624	-	-	GAK33989	GAK33990	-	WP042085358
Anaeromyxobacter sp. Fw109-5	WP012098896	WP012098900	-	-	-	-	WP011985172	-
Asaia prunellae JCM 25354	WP025885919	WP025884930	-	-	WP035447346	WP035774618	-	-
Azospirillum brasilense Az39	AIB14250	WP014197627	EZQ05511	-	EGY00453	-	WP014197279	WP040843912
Beijerinckia indica ATCC 9039	ACB96717	WP012386067	WP012386066	ACB96775	-	ACB96714	WP012386064	-
Bradyrhizobiaceae bacterium SG-6C	EGP07687	WP009735794	WP009735791	-	WP009735786	WP009735787	WP009735789	-
Bradyrhizobium japonicum USDA 6	KGT78877	WP024339751	WP028135328	WP018648005	WP024508624	WP024339746	WP028176734	WP012042930
Burkholderia rhizoxinica HKI 454	YP004022510	WP013428856	WP013428853	-	CBW76993	WP035502598	-	WP027800221
"Candidatus Burkholderia kirkii"	CCD41342	WP007000145	WP006998781	-	-	-	WP050327732	-
Commensalibacter intestini A911	WP008854779	WP040363620	WP008854780	-	WP040364328	EHD13594	-	-
Corallococcus coralloides ATCC25202	WP014394623	-	-	-	-	WP014393632	WP014399376	-
Cupriavidus metallidurans CH34	WP029310093	WP011518656	WP011518639	WP035869135	WP035883265	WP006578558	-	WP035832607

Organisms	NCBI accession numbers for the proteins							
	SHC/hpnF	hpnH	hpnG	hpnO	hpnB	hpnC	hpnE	hpnX
Cystobacter fuscus DSM 2262	EPX59200	-	-	-	-	-	WP002623474	-
Desulfobacca acetoxidans DSM 11109	YP004369479	WP013705413	-	AEB10298	-	-	AEB08614	-
Desulfovibrio hydrothermalis AM13	CCO25137	WP015334795	WP015334796	WP015334791	WP024825200	-	-	WP018123285
Dongia sp. URHE0060	WP028097266	WP028097264	WP028097265	WP028098410	WP035362741	WP035362743	-	WP028098718
Dyella japonica A8	AIF48050	WP026034273	-	WP026107330	WP019467239	AGW89834	WP019464811	WP035323693
Ensifer sp. TW10	WP026616002	WP034885135	-	-	-	-	WP026616001	WP029959426
Frateuria aurantia DSM6220	WP014404537	WP014404529	-	-	WP041271262	-	WP014402939	-
Geobacter metallireducens GS-15	WP004512391	WP004513981	-	WP004512793	-	-	-	WP012470038
Geobacter sp. OR-1	GAM08906	WP041970595	-	WP041970321	-	-	-	GAM08258
Gluconacetobacter diazotrophicus PA1 5	YP001601866	WP012223346	-	-	CAP55567	WP003616600	-	-
Gluconacetobacter xylinus E25	AHI26287	WP025439451	-	-	WP038508411	-	WP025439931	-
Gluconobacter oxydans 621H	WP029495766	WP011252194	WP015074123	-	WP011253758	WP034953957	WP062448192	-
Granulibacter bethesdensis CGDNIH2	AHJ68032	WP011633106	AHJ69616	-	AHJ68166	AHJ63868	AHJ68033	-
Hyphomicrobium denitrificans ATCC 51888	ADJ22298	WP013214519	WP013214518	-	WP013214513	-	WP013214516	-
Inquilinus limosus MP06	KGM30891	WP034842575	-	-	WP034851374	-	WP034839036	-
Komagataeibacter europaeus LMG 18890	WP029335871	-	WP003616593	-	-	-	WP048852155	-
Kozakia baliensis SR745	WP029605975	WP029604707	-	-	WP029605966	-	WP029605974	-
Legionella fallonii LLAP-10	CEG58976	CEG58980	-	-	-	-	WP045094788	WP028377853
Magnetospira sp. QH-2	CCQ73410	CCQ73412	CCQ73411	-	CCQ73407	CCQ73408	-	-
Magnetospirillum sp. SO-1	EME71971	WP008613015	WP008613018	-	WP008613023	KIL99888	WP008615475	-
Methylobacter tundripaludum SV96	WP031435981	WP006889894	WP006889891	WP006889889	WP027150580	WP010681939	WP006893612	WP028481401
Methylobacterium sp. L2-4	WP029357998	WP043374282	WP026176025	-	-	WP029357994	WP029357789	-
Methylocella silvestris BL2	ACK52150	WP012592221	WP012592220	ACK51802	-	-	-	-
Methylococcus capsulatus Bath	WP017365089	WP010960139	-	WP010960134	WP017365974	-	WP017366337	-
Methylocystis sp. LW5	WP026600054	WP026600052	WP026600053	WP036281436	WP026599945	-	-	WP026016261
Methylocystis sp. SB2	WP029649057	WP029649055	WP029649056	WP029649043	WP029649079	-	WP029649082	WP026016261
Methyloferula stellata AR4	WP026596038	WP026596036	-	WP026595516	-	WP020177156	-	-

Organisms	NCBI accession numbers for the proteins							
	SHC/hpnF	hpnH	hpnG	hpnO	hpnB	hpnC	hpnE	hpnX
Methylomarinum vadi IT-4	WP031432942	WP031432940	-	WP031432945	WP031432939	-	WP031432816	WP031432760
Methylomicrobium alcaliphilum 20Z	YP004917789	WP014149522	WP014149525	WP014149527	-	-	-	-
Methylomicrobium buryatense 5G	WP017842749	WP026130390	WP017842748	WP017842746	-	-	WP026129958	-
Methylomonas sp. LW13	WP033159606	WP033159604	WP033159607	WP033159608	WP033156729	-	-	-
Methylosarcina fibrata AML-C10	WP020562840	WP026223408	WP020562841	WP020562842	-	-	-	-
Methylovulum miyakonense HT12	WP019867050	WP019866209	-	WP019866214	-	-	-	-
Nevskia soli DSM 19509	WP029918711	WP029918736	-	WP029918537	WP029918737	-	-	-
Nitrococcus mobilis Nb-231	WP005002717	WP005002723	-	WP005002617	WP005002725	-	WP005002646	-
Nitrosococcus halophilus Nc 4	YP003526848	WP013032291	WP013032351	-	WP013032290	-	WP013031692	-
Nitrosococcus oceani ATCC19707	KFI22923	WP002811295	WP011330621	-	WP013032290	-	WP036500745	-
Nitrosomonas cryotolerans ATCC 49181	WP028461045	WP028460814	WP028461044	WP013646712	WP036572580	-	-	WP013648969
Nitrosomonas sp. AL212	ADZ25829	WP013646702	WP013965218	WP013646712	WP013646703	-	-	WP013648969
Nitrosospira briensis C-128	WP025041335	WP025041339	WP011381843	WP025042217	-	WP025041665	-	-
Novosphingobium nitrogenifigens DSM 19370	WP008067666	WP008067667	WP018076026	-	WP008067660	-	-	WP008068310
Oligotropha carboxidovorans OM5	WP012563808	WP012563805	WP012563807	WP012563800	-	WP012563811	-	-
Pandoraea pnomenusa ASM76761v3	AHN74606	WP039369899	WP039370011	-	WP025249510	WP039369889	-	-
Pelobacter propionicus DSM2379	WP011734707	WP011735116	WP011341830	WP011736998	WP011341191	-	WP011735975	-
Phaeospirillum molischianum DSM120	WP002725625	WP040566040	-	-	WP040566039	-	WP004156748	-
Pseudoalteromonas sp. Bsw20308	WP007378768	-	WP023399727	WP017216762	-	-	WP007378055	-
Pseudomonas agarici NCPPB2289	WP017133842	WP028241823	-	WP028626375	-	CEA03722	WP060781915	WP021219199
Rhodomicrobium udaipurense JA643	KAI96258	WP037232796	WP037232859	KAI95822	WP013420594	WP037232803	KAI96259	WP037236121
Rhodopseudomonas palustris TIE-1	ACF02757	ACF02752	ACF02758	WP013501376	-	ACF02760	WP012497134	-
Rhodospirillales bacterium URHD0088	WP027300090	WP037263686	-	-	WP027300094	WP027300093	WP027300091	-
Rhodospirillum photometricum DSM122	WP014413697	WP041797168	WP014413696	-	CCG07059	WP011387826	WP014413698	-
Rhodovulum sp. PH10	WP008382850	WP008382870	WP008384799	-	-	EJW13284	WP008382852	-
Roseomonas gilardii ATCC-BAA 691	WP027282198	WP027282196	WP037225720	-	WP027282202	-	WP051418163	-

Organisms	NCBI accession numbers for the proteins							
	SHC/hpnF	hpnH	hpnG	hpnO	hpnB	hpnC	hpnE	hpnX
Rubritepida flocculans DSM 14296	WP027283691	WP027285407	-	-	WP027283690	-	WP037301810	-
Saccharibacter floricola DSM14296	WP026294069	WP018980047	WP018979294	-	WP018979289	WP026294068	WP018979292	-
Salinisphaera hydrothermalis C41B8	KEZ77103	WP037338234	-	WP006914350	WP037338231	-	WP037336309	-
Sinorhizobium fredii NGR234	AAB91964	WP014328554	-	-	-	-	WP041409850	WP014760938
Skermanella stibiiresistens SB22	EWY39469	WP037454687	-	-	-	-	WP051513485	WP037445906
Sphingomonas sp. PR090111-T3T-6A	WP026359781	WP019833943	WP010215762	-	WP019833949	WP019833948	WP051103489	WP009823425
Stigmatella aurantiaca DW4/3-1	WP002615112	-	-	WP002616976	-	WP002611586	-	-
Syntrophobacter fumaroxidans MPOB	ABK18414	WP011697733	-	ABK15766	-	-	-	-
uncultured Desulfobacterium sp.	CBX30849	CBX30852	-	CBX27957	-	-	CBX31046	-
Zeta proteobacterium SCGC AB-604-O16	WP018002756	WP018002755	-	WP026195904	-	WP018286421	CDL72826	WP018287038
Zymomonas mobilis CP4	WP014848478	WP012817100	WP013933694	-	WP011240734	WP011240736	AHB09757	-
Phylum*: Planctomycetes*								
Blastopirellula marina DSM 3645	EAQ81955	EAQ81954	WP002651128	EAQ79288	EAQ82769	WP002652164	EAQ81152	EAQ78619
"Candidatus Scalindua brodae"	KHE93133	WP034405840	WP034410234	WP034402565	WP034407659	-	-	-
Gemmata obscuriglobus UQM 2246	WP010040021	WP010038472	WP010037452	WP010045325	WP010037859	WP033197810	WP033197809	WP010033402
Isosphaera pallida ATCC 43644	YP004179412	WP013565150	WP013565149	WP013565210	WP013564943	WP013564438	WP013566342	-
Pirellula staleyi DSM 6068	ADB16413	WP012910675	WP012910674	WP012910791	WP012910654	WP012909830	WP012909829	-
Planctomyces brasiliensis DSM 5305	ADY57643	WP013628686	WP013626434	ADY59874	ADY57991	WP013629835	ADY59821	-
Planctomyces limnophilus DSM 3776	ADG67734	ADG69174	4M1EA	ADG66978	ADG69736	WP041403544	ADG69018	-
Planctomycete sp. KSU-1	GAB61661	WP007220778	WP007221581	WP007223333	GAB60829	-	-	-
Rhodopirellula baltica SH 1	NP866975	WP007336192	WP011122944	EKJ99584	EKK02762	EKK00815	WP007326464	-
Schlesneria paludicola DSM 18645	WP010588531	WP040594077	WP010583626	WP010584362	WP040593328	WP040593118	WP040591977	WP040593417
Phylum: *Verrucomicrobia*								
Akkermansia muciniphila ATCC BAA-835	ACD04949	ACD04693	WP022397022	ACD04624	ACD04777	-	-	-
bacterium Ellin514	EEF59508	-	EEF60928	-	CDO58319	-	-	-
Chthoniobacter flavus Ellin428	EDY22035	EDY21028	WP006979485	WP006983219	WP006978006	WP006979995	-	WP006981683

Organisms	NCBI accession numbers for the proteins							
	SHC/hpnF	hpnH	hpnG	hpnO	hpnB	hpnC	hpnE	hpnX
Coraliomargarita sp. CAG:312	WP022478061	WP022477972	WP022478222	WP022477344	WP022477998	WP022478223	--	-
Methylacidiphilum infernorum V4	YP001939055	ABX56618	WP012462740	-	WP012463738	WP012464543	WP012464543	-
Pedosphaera parvula Ellin514	WP007418743	WP007416308	EEF60928	WP040548113	WP040549235	WP007415106	-	EEF57674
Verrucomicrobia bacterium LP2A	WP024808711	WP024808154	WP024808712	WP024806846	WP038119173	WP038120517	WP008101007	WP020035672
Verrucomicrobia bacterium SCGC AAA164-E04	WP020148881	WP020146994	WP020148880	WP038142737	WP020148316	WP038132326	-	WP020035672
Phylum: *Nitrospirae*								
"Candidatus Nitrospira defluvii*"*	YP003796553	WP013247482	WP013247454	WP013247084	WP041187291	WP041187121	-	-
Leptospirillum ferrodiazotrophum UBA1	EES53667	EES52785	EES53624	-	-	EES53610	-	-
Leptospirillum ferriphilum ML-04	AFS53090	WP038505592	AIA30407	-	-	-	-	-
Phylum: *Solibacter*								
"Candidatus Solibacter usitatus Ellin6076"	ABJ82180	WP011685281	YP822541	-	WP011685564	ABJ82259	WP011685297	-
Bryobacter aggregatus MPL3	WP031498832	WP035958374	WP031498836	-	WP031497788	WP035957817	WP035957682	-
Miscellaneous								
BRC1 bacterium SCGC AAA257-C11	WP029711460	WP029711461	WP029713023	-	-	WP029712686	WP029712861	-
"Candidatus Chloracidobacterium thermophilum"	WP014100779	WP014100993	WP014101350	ABV27277	AEP11411	AEP13732	AEP13747	AEP11254
"Candidatus Methylomirabilis oxyfera"	YP003205013	-	WP015743775	WP012814328	-	WP006853985	-	-
Capnocytophaga sp. *F0381*	EKY05967		WP009413998	-	EKY08163	-	-	-
Chthonomonas calidirosea T49	YP008089543	WP016481467	WP016481809	WP016482775	WP016481720	WP016482645	WP016482675	-
Fulvivirga imtechensis AK7	WP009577716	WP009581578	WP009581760	WP009578184	WP040497155	WP009581003	-	ELR69794
Nitrospina gracilis 3/211	WP005006766	WP005006939	WP005005611	WP005011772	WP005011646	-	-	WP005005816
Nitrospina sp. AB-629-B18	WP018048288	WP029365609	WP018047946	WP018049361	WP018049594	-	-	WP018049725
Parabacteroides sp. D13	WP005866839	-	WP009275942	-	WP009276591	-	-	-
Prevotella sp. MA2016	WP028911593		WP022480679	-	-	-	-	-
Sphaerobacter thermophilus DSM 20745	YP003320259	WP012873301	WP012871644.	WP012872120	WP012873302	-	-	-

Organisms	NCBI accession numbers for the proteins							
	SHC/hpnF	hpnH	hpnG	hpnO	hpnB	hpnC	hpnE	hpnX
Kingdom*: Fungi*								
Aspergillus fumigatus var. RP-2014	KEY84073	-	-	-	-	-	-	-
Aspergillus fumigatus var. RP-2014	KEY83652	-	-	-	-	-	-	-
Aspergillus parasiticus SU-1	KJK63811	-	-	-	-	-	-	-
Aspergillus ruber CBS 135680	EYE91407	-	-	-	-	-	-	-
Colletotrichum gloeosporioides Nara gc5	XP007277705	-	-	-	-	-	-	-
Colletotrichum orbiculare MAFF 240422	ENH76723	-	-	-	-	-	-	-
Emmonsia crescens UAMH 3008	KKZ63168	-	-	-	-	-	-	-
Endocarpon pusillum Z07020	ERF72956	-	-	-	-	-	-	-
Exophiala aquamarina CBS 119918	KEF56149	-	-	-	-	-	-	-
Fistulina hepatica ATCC 64428	KIY45656	-	-	-	-	-	-	-
Fusarium avenaceum Fave_LH27	KIL86349	-	-	-	-	-	-	-
Fusarium oxysporum f. sp. lycopersici 4287	KNB20458	-	-	-	-	-	-	-
Histoplasma capsulatum H88	EGC48249	-	-	-	-	-	-	-
Magnaporthe oryzae Y34	ELQ43428	-	-	-	-	-	-	-
Metarhizium anisopliae ARSEF 549	KID65327	-	-	-	-	-	-	-
Neosartorya fischeri NRRL 181	EAW20759	-	-	-	-	-	-	-
Neosartorya udagawae IFM 46973	GAO85958	-	-	-	-	-	-	-
Schizosaccharomyces japonicus yFS275	EEB08219	-	-	-	-	-	-	-
Verruconis gallopava CBS 43764	KIW00289	-	-	-	-	-	-	-
Zymoseptoria brevis ASM98365v1	KJY00410	-	-	-	-	-	-	-

Note: The information was mined from the NCBI database. - represents the protein was not observed in the NCBI database for respective bacterial strain

Table S2. Microarray results representing upregulated genes, their mean fold change with standard deviation and p-values. Transcripts with significant fold change (fold change ≥ 0.6 and p-value ≤ 0.05) are included in the table. Fold changes were calculated by comparing *Δshc* mutant with WT strain.

Gene code	Gene description	FC ± SD *	p value
GO:0055114: Oxidation reduction			
Rpal_0804	NADH dehydrogenase (Quinone)	0.84±0.15	**0.04**
Rpal_1155	Nickel-dependent hydrogenase large subunit	1.97±0.53	**0.04**
Rpal_1156	Ni/Fe-hydrogenase, b-type cytochrome subunit	3.14±0.64	**0.03**
Rpal_1398	Iron-containing alcohol dehydrogenase	2.52±0.29	**0.01**
Rpal_1399	Aldehyde Dehydrogenase	2.04±0.26	**0.01**
Rpal_1430	Acyl-CoA dehydrogenase domain protein	0.65±0.04	**0.01**
Rpal_1488	Short-chain dehydrogenase/reductase SDR	1.39±0.10	**0.01**
Rpal_2153	2-dehydropantoate 2-reductase	1.84±0.38	**0.02**
Rpal_2159	Pyrroloquinoline quinone biosynthesis protein C	0.84±0.10	**0.01**
Rpal_2445	Aldehyde Dehydrogenase	1.29±0.03	**0.00**
Rpal_3128	NADH dehydrogenase (Quinone)	0.75±0.05	**0.03**
Rpal_3291	NADH-quinone oxidoreductase subunit H	0.76±0.14	**0.02**
Rpal_3601	PQQ-dependent dehydrogenase, methanol/ethanol family	2.38±0.75	**0.05**
Rpal_3964	Short-chain dehydrogenase/reductase SDR	1.34±0.30	**0.04**
Rpal_4002	Protease Do (EC 1.3.1.74)	0.75±0.02	**0.00**
Rpal_4176	Alcohol dehydrogenase GroES domain protein	0.86±0.00	**0.00**
Rpal_4495	Gluconate 2-dehydrogenase (Acceptor)	1.41±0.20	**0.01**
Rpal_4496	Cytochrome c prime	1.18±0.20	**0.02**
Rpal_5149	Carbon-monoxide dehydrogenase (Acceptor)	1.79±0.04	**0.00**
GO:0009055: Electron carrier activity			
Rpal_0076	Thioredoxin	0.71±0.04	**0.01**
Rpal_0377	Thioredoxin	1.32±0.08	**0.00**
Rpal_0602	Glutaredoxin 3	0.68±0.00	**0.01**
Rpal_0739	4-hydroxybenzoyl-CoA reductase, beta subunit	2.10±0.22	**0.01**
Rpal_0805	Formate dehydrogenase, alpha subunit	1.39±0.25	**0.03**
Rpal_0815	High-potential iron-sulfur protein (HiPIP)	1.71±0.38	**0.04**
Rpal_1796	Glutaredoxin	0.80±0.22	**0.04**
Rpal_4215	Cytochrome c class I	1.39±0.29	**0.05**
Rpal_4502	Oxidoreductase domain protein	0.77±0.09	**0.04**
Rpal_5147	(2Fe-2S)-binding domain protein	1.57±0.28	**0.02**
Rpal_5148	Aldehyde oxidase and xanthine dehydrogenase	1.42±0.21	**0.01**

Gene code	Gene description	FC ± SD *	p value
Rpal_5231	Electron transfer flavoprotein alpha subunit	0.63±0.03	**0.02**
Rpal_5232	Electron transfer flavoprotein alpha/beta-subunit	0.95±0.03	**0.04**
rpt02010: ABC transporters			
Rpal_0735	Extracellular ligand-binding receptor	1.72±0.17	**0.04**
Rpal_1411	Extracellular solute-binding protein family 5	1.07±0.29	**0.04**
Rpal_1424	Inner-membrane translocator	0.74±0.02	**0.00**
Rpal_1940	Inner-membrane translocator	1.21±0.28	**0.03**
Rpal_1941	Extracellular ligand-binding receptor	1.54±0.16	**0.01**
Rpal_2487	Extracellular ligand-binding receptor	0.70±0.06	**0.02**
Rpal_4000	Extracellular ligand-binding receptor	0.89±0.20	**0.05**
Rpal_4024	ABC transporter related	0.84±0.10	**0.01**
Rpal_4568	ABC transporter related	1.34±0.30	**0.04**
Rpal_4576	ABC transporter related	1.06±0.19	**0.04**
rpt00630: Glyoxylate and dicarboxylate metabolism			
Rpal_0005	4-hydroxyphenylpyruvate dioxygenase	2.84±0.39	**0.01**
Rpal_1748	Ribulose-bisphosphate carboxylase	1.27±0.20	**0.04**
Rpal_1942	Tartrate dehydrogenase	0.94±0.00	**0.01**
Rpal_4878	Isocitrate lyase and phosphorylmutase	2.59±0.33	**0.01**
Rpal_5122	Ribulose bisphosphate carboxylase (RuBisCO)	1.14±0.17	**0.01**
GO:0004497: Monooxygenase activity			
Rpal_0425	Cytochrome P450	1.46±0.04	**0.00**
Rpal_1803	Cytochrome P450	1.04±0.04	**0.00**
Rpal_1932	Cytochrome P450	0.66±0.03	**0.03**
Rpal_2511	Putative monooxygenase protein	1.59±0.06	**0.01**
Rpal_4222	Luciferase-like monooxygenase	0.61±0.00	**0.00**
Rpal_5156	Monooxygenase FAD-binding	1.04±0.26	**0.03**
rpt00071:Fatty acid metabolism			
Rpal_0887	3-hydroxyacyl-CoA dehydrogenase NAD-binding	1.29±0.08	**0.00**
Rpal_1903	Acetyl-CoA acetyltransferase	0.76±0.02	**0.04**
Rpal_2014	Enoyl-CoA hydratase/isomerase	2.31±0.56	**0.03**
Rpal_4746	AMP-dependent synthetase and ligase	0.86±0.10	**0.04**
GO:0031975: Envelope			
Rpal_0211	OmpA/MotB domain protein	1.96±0.20	**0.02**
Rpal_0305	Import inner membrane translocase subunit Tim44	0.77±0.07	**0.01**
Rpal_0349	Uncharacterized protein	1.43±0.28	**0.02**
Rpal_1428	Extracellular ligand-binding receptor	1.30±0.14	**0.01**
Rpal_2720	DSBA oxidoreductase	0.82±0.18	**0.02**

Gene code	Gene description	FC ± SD *	p value
Rpal_3853	Porin	1.64±0.45	**0.04**
Rpal_4389	DSBA oxidoreductase	1.38±0.44	**0.05**
Rpal_4404	Import inner membrane translocase subunit Tim44	2.16±0.21	**0.01**
GO:0006508: Proteolysis			
Rpal_0310	ATP-dependent protease subunit HslV	0.97±0.10	**0.05**
Rpal_0892	Signal peptidase I	1.30±0.08	**0.02**
Rpal_0940	Peptidyl-dipeptidase Dcp	0.65±0.02	**0.02**
Rpal_1235	Peptidase S49	1.49±0.10	**0.01**
Rpal_1317	ATP-dependent zinc metalloprotease FtsH	1.33±0.16	**0.02**
Rpal_3309	ATP-dependent Clp protease proteolytic subunit	0.92±0.16	**0.02**
Rpal_3737	Peptidase M50	1.15±0.35	**0.05**
Rpal_4857	Peptidase M16 domain protein	1.54±0.14	**0.00**
GO:0004872: Receptor activity			
Rpal_0409	TRAP transporter solute receptor, TAXI family	0.96±0.13	**0.03**
Rpal_0583	Extracellular ligand-binding receptor	1.42±0.27	**0.03**
Rpal_4246	Extracellular ligand-binding receptor	1.60±0.14	**0.01**
Miscellaneous			
Rpal_0003	DNA replication and repair protein RecF	0.77±0.07	**0.03**
Rpal_0008	KaiB domain protein	1.33±0.27	**0.04**
Rpal_0031	Fmu (Sun) domain protein	0.78±0.09	**0.02**
Rpal_0054	PTS IIA-like nitrogen-regulatory protein PtsN	1.24±0.08	**0.04**
Rpal_0074	Acetyl-coenzyme A carboxylase carboxyl transferase subunit beta	0.74±0.15	**0.04**
Rpal_0175	Rare lipoprotein A	1.18±0.37	**0.05**
Rpal_0183	2-oxoglutarate dehydrogenase complex component E2	1.15±0.32	**0.05**
Rpal_0191	ABC transporter related	1.35±0.19	**0.04**
Rpal_0251	Diaminopimelate epimerase	1.32±0.17	**0.04**
Rpal_0286	Two component transcriptional regulator, winged helix family	1.21±0.25	**0.04**
Rpal_0379	ChaB family protein	1.22±0.10	**0.00**
Rpal_0462	AMP-dependent synthetase and ligase	0.91±0.04	**0.05**
Rpal_0463	Beta-lactamase	1.44±0.21	**0.01**
Rpal_0572	von Willebrand factor type A	1.67±0.20	**0.03**
Rpal_0587	RNA binding S1 domain protein	0.98±0.14	**0.03**
Rpal_0809	Putative glucose/sorbosone dehydrogenase	2.40±0.30	**0.01**
Rpal_0817	Cytochrome C family protein (PioA)	1.11±0.30	**0.04**
Rpal_0889	Transcriptional regulator, MarR family	0.95±0.14	**0.02**
Rpal_0891	Apple	1.37±0.01	**0.00**
Rpal_0937	GCN5-related N-acetyltransferase	1.33±0.24	**0.02**

Gene code	Gene description	FC ± SD *	p value
Rpal_0938	Ornithine decarboxylase	1.42±0.20	**0.01**
Rpal_0942	High-affinity nickel-transporter	1.09±0.08	**0.00**
Rpal_1019	MATE efflux family protein	0.79±0.03	**0.03**
Rpal_1158	HupE/UreJ protein	2.15±0.24	**0.03**
Rpal_1197	NUDIX hydrolase	1.57±0.05	**0.00**
Rpal_1230	Tetratricopeptide TPR_2 repeat protein	0.74±0.00	**0.00**
Rpal_1255	DNA-3-methyladenine glycosylase I	0.79±0.05	**0.02**
Rpal_1308	Protein TolQ	1.08±0.31	**0.04**
Rpal_1376	ATPase associated with various cellular activities AAA_3	0.82±0.00	**0.01**
Rpal_1413	Putative signal-transduction protein with CBS domains	0.96±0.27	**0.04**
Rpal_1433	TonB system transport protein ExbD	1.43±0.20	**0.02**
Rpal_1477	N-formylglutamate amidohydrolase	1.98±0.35	**0.03**
Rpal_1683	FAD dependent oxidoreductase	1.28±0.11	**0.01**
Rpal_1702	UspA domain protein	1.12±0.07	**0.02**
Rpal_1742	5-aminolevulinate synthase	1.28±0.06	**0.01**
Rpal_1747	Ribulose bisphosphate carboxylase large chain (RuBisCO large subunit)	0.78±0.00	**0.00**
Rpal_1749	CbbX protein	1.08±0.29	**0.03**
Rpal_1789	BolA family protein	1.01±0.08	**0.02**
Rpal_1805	Methyltransferase type 11	1.30±0.03	**0.00**
Rpal_1807	ErfK/YbiS/YcfS/YnhG family protein	0.77±0.01	**0.01**
Rpal_1882	Glucose-methanol-choline oxidoreductase	1.18±0.23	**0.02**
Rpal_2010	Efflux transporter, RND family, MFP subunit	1.19±0.19	**0.01**
Rpal_2126	Two component transcriptional regulator, winged helix family	1.20±0.09	**0.00**
Rpal_2131	Cytochrome c-type biogenesis protein CcmE	0.90±0.25	**0.04**
Rpal_2132	Cytochrome c-type biogenesis protein CcmF	1.13±0.10	**0.02**
Rpal_2153	2-dehydropantoate 2-reductase	1.84±0.38	**0.02**
Rpal_2155	Formyl-CoA:oxalate CoA-transferase	1.99±0.55	**0.04**
Rpal_2159	Pyrroloquinoline quinone biosynthesis protein C	0.84±0.10	**0.01**
Rpal_2186	6-phosphogluconate dehydrogenase NAD-binding	0.74±0.06	**0.01**
Rpal_2191	Cyclic pyranopterin monophosphate synthase	0.69±0.04	**0.02**
Rpal_2204	Ribonuclease VapC (Toxin VapC)	1.25±0.03	**0.03**
Rpal_2205	Cupin 2 conserved barrel domain protein	1.42±0.06	**0.01**
Rpal_2218	CDP-diacylglycerol/serine O-phosphatidyltransferase	0.85±0.20	**0.04**
Rpal_2419	TonB system transport protein ExbD	1.50±0.05	**0.02**
Rpal_2434	AMP-dependent synthetase and ligase	1.31±0.29	**0.03**
Rpal_2445	Aldehyde Dehydrogenase	1.29±0.03	**0.00**

Gene code	Gene description	FC ± SD *	p value
Rpal_2494	Uncharacterized protein	1.28±0.36	**0.04**
Rpal_2532	Tetratricopeptide TPR_2	0.97±0.17	**0.01**
Rpal_2576	Nuclease (SNase domain protein)	0.78±0.02	**0.00**
Rpal_2612	Two component transcriptional regulator, winged helix family	0.84±0.21	**0.03**
Rpal_2698	Uncharacterized protein	2.80±0.42	**0.01**
Rpal_2702	Beta-agarase	0.98±0.12	**0.04**
Rpal_2710	Signal transduction histidine kinase	0.78±0.07	**0.01**
Rpal_2747	Glyoxalase/bleomycin resistance protein/dioxygenase	1.41±0.21	**0.02**
Rpal_2748	Iron-sulfur cluster assembly accessory protein	1.15±0.12	**0.02**
Rpal_2767	Beta-lactamase domain protein	1.21±0.33	**0.04**
Rpal_2810	Pyruvate carboxyltransferase	1.13±0.34	**0.04**
Rpal_2814	Pentapeptide MXKDX repeat protein	0.95±0.28	**0.04**
Rpal_2823	Alpha-2-macroglobulin domain protein	0.87±0.03	**0.00**
Rpal_2825	Glycosyl transferase family 39	0.83±0.19	**0.04**
Rpal_2865	Two component, sigma54 specific, Fis family	0.74±0.04	**0.00**
Rpal_2921	Uncharacterized protein	1.48±0.00	**0.00**
Rpal_2922	Uncharacterized protein	1.42±0.22	**0.04**
Rpal_2928	Glycosyl transferase family 2	1.30±0.22	**0.01**
Rpal_2946	Ubiquinone biosynthesis hydroxylase,	0.87±0.23	**0.03**
Rpal_2987	RDD domain containing protein	1.47±0.40	**0.04**
Rpal_2995	Globin	0.96±0.00	**0.01**
Rpal_3173	Preprotein translocase, YajC subunit	0.72±0.03	**0.03**
Rpal_3180	Response regulator receiver protein	1.38±0.30	**0.05**
Rpal_3190	Segregation and condensation protein B	1.38±0.21	**0.05**
Rpal_3192	Beta-N-acetylhexosaminidase	0.76±0.05	**0.03**
Rpal_3203	Sel1 domain protein repeat-containing protein	1.90±0.03	**0.03**
Rpal_3211	NADPH-dependent FMN reductase	0.71±0.03	**0.02**
Rpal_3242	Type IV pilus assembly PilZ	1.25±0.19	**0.04**
Rpal_3322	Amidase (EC 3.5.1.4)	1.10±0.02	**0.01**
Rpal_3447	CreA family protein	1.73±0.42	**0.04**
Rpal_3464	Putative transcriptional regulator, Crp/Fnr family	1.46±0.18	**0.01**
Rpal_3474	SurA domain	1.21±0.14	**0.01**
Rpal_3479	Guanylate kinase	0.69±0.10	**0.02**
Rpal_3622	ATP12 ATPase	0.93±0.09	**0.02**
Rpal_3647	Protein translocase subunit SecY	0.73±0.13	**0.05**
Rpal_3651	50S ribosomal protein L18	1.04±0.08	**0.01**
Rpal_3652	50S ribosomal protein L6	0.94±0.25	**0.04**

Gene code	Gene description	FC ± SD *	p value
Rpal_3653	30S ribosomal protein S8	1.10±0.16	**0.01**
Rpal_3659	50S ribosomal protein L29	0.78±0.24	**0.05**
Rpal_3660	50S ribosomal protein L16	1.11±0.13	**0.01**
Rpal_3661	30S ribosomal protein S3	1.15±0.25	**0.02**
Rpal_3663	30S ribosomal protein S19	1.25±0.31	**0.03**
Rpal_3684	ABC transporter related	1.27±0.02	**0.01**
Rpal_3686	Transcriptase subunit beta'	0.90±0.23	**0.05**
Rpal_3717	Inner-membrane translocator	0.85±0.05	**0.00**
Rpal_3722	Propanoyl-CoA C-acyltransferase	1.05±0.24	**0.03**
Rpal_4084	ErfK/YbiS/YcfS/YnhG family protein	1.61±0.20	**0.01**
Rpal_4096	Phosphomethylpyrimidine synthase	1.06±0.03	**0.01**
Rpal_4115	SOUL heme-binding protein	1.24±0.07	**0.04**
Rpal_4125	UPF0114 protein Rpal_4125	1.45±0.06	**0.00**
Rpal_4267	Putative RND superfamily transporter	0.87±0.26	**0.04**
Rpal_4327	Carbon monoxide dehydrogenase subunit G	0.96±0.20	**0.03**
Rpal_4411	Flagellar basal body rod protein FlgB	0.95±0.06	**0.00**
Rpal_4468	Uncharacterized protein	1.13±0.10	**0.05**
Rpal_4499	Carbamoyltransferase	1.08±0.31	**0.04**
Rpal_4502	Oxidoreductase domain protein	0.77±0.09	**0.04**
Rpal_4611	Cobyrinic acid ac-diamide synthase	1.18±0.05	**0.02**
Rpal_4619	Rv0623 family protein transcription factor	1.28±0.35	**0.04**
Rpal_4620	Ribonuclease VapC (RNase VapC)	1.04±0.05	**0.03**
Rpal_4636	AsmA family protein	1.22±0.04	**0.01**
Rpal_4650	putative branched-chain amino acid transporter	0.79±0.10	**0.01**
Rpal_4659	Glyoxalase/bleomycin resistance protein/dioxygenase	0.66±0.06	**0.01**
Rpal_4674	OsmC family protein	1.61±0.43	**0.04**
Rpal_4681	Uncharacterized protein	3.80±0.82	**0.02**
Rpal_4689	SCP-like extracellular	0.79±0.10	**0.03**
Rpal_4720	CBS domain containing membrane protein	0.65±0.07	**0.02**
Rpal_4749	Ribonuclease H (RNase H)	1.11±0.23	**0.03**
Rpal_4812	Glucose sorbosone dehydrogenase	1.46±0.08	**0.01**
Rpal_4889	Putative periplasmic binding ABC transporter protein	2.01±0.12	**0.02**
Rpal_4895	Glycerol-3-phosphate dehydrogenase	1.99±0.12	**0.04**
Rpal_4920	NHL repeat containing protein	1.76±0.23	**0.01**
Rpal_5008	Diguanylate phosphodiesterase	0.88±0.00	**0.00**
Rpal_5163	Efflux transporter, RND family, MFP subunit	1.15±0.26	**0.03**
Rpal_5187	DedA	0.73±0.15	**0.02**

Gene code	Gene description	FC ± SD *	p value
Rpal_5192	Uncharacterized protein	1.13±0.06	**0.00**
Rpal_5252	Lipolytic protein G-D-S-L family	0.84±0.15	**0.05**
Rpal_5255	Protein ApaG	0.95±0.07	**0.00**
Rpal_5257	33 kDa chaperonin	1.39±0.05	**0.03**

* FC is $\log_2$ (fold change) calculated for *Δshc* mutant with respect to WT and SD is standard deviation.

Table S3. Microarray results representing downregulated genes, their mean fold change with standard deviation and p-values. Transcripts with significant fold change (fold change ≤ -0.6 and p-value ≤ 0.05) are included in the table. Fold changes were calculated by comparing *Δshc* mutant with WT strain.

Gene code	Gene description	FC ± SD*	p value
GO:0006810: Transport			
rpt02010: ABC transporters			
Rpal_0104	Binding-protein-dependent transport systems inner membrane component	-0.80±0.01	**0.00**
Rpal_0767	Phosphonate ABC transporter, periplasmic phosphonate binding protein	-1.57±0.42	**0.03**
Rpal_1178	Inner-membrane translocator	-1.12±0.21	**0.03**
Rpal_1593	ABC transporter periplasmic binding protein, urea carboxylase region	-1.11±0.02	**0.00**
Rpal_1660	Extracellular solute-binding protein family 5	-2.01±0.51	**0.03**
Rpal_1840	Uncharacterized protein	-1.31±0.02	**0.00**
Rpal_2405	Nitrate ABC transporter, ATPase subunits C and D	-1.87±0.08	**0.01**
Rpal_2673	Molybdate ABC transporter, inner membrane subunit	-1.04±0.05	**0.01**
Rpal_2901	Polar amino acid ABC transporter, inner membrane subunit	-0.88±0.03	**0.04**
Rpal_2903	Binding-protein-dependent transport systems inner membrane component	-0.77±0.15	**0.04**
Rpal_2904	ABC transporter related	-1.16±0.01	**0.03**
Rpal_2915	ABC transporter related	-1.02±0.17	**0.02**
Rpal_2941	Extracellular solute-binding protein family 5	-0.97±0.06	**0.03**
Rpal_2952	NMT1/THI5 like domain protein	-2.93±0.70	**0.03**
Rpal_2953	Binding-protein-dependent transport systems inner membrane component	-2.57±0.56	**0.02**
Rpal_4191	Urea ABC transporter, urea binding protein	-2.25±0.34	**0.02**
Rpal_4556	ABC transporter related	-0.84±0.00	**0.02**
Rpal_4557	Inner-membrane translocator	-0.79±0.09	**0.02**
Rpal_4558	Inner-membrane translocator	-0.90±0.01	**0.05**
Rpal_4583	Glycosyl transferase group 1	-1.02±0.24	**0.05**
Rpal_4884	ABC transporter related	-0.69±0.02	**0.00**
Rpal_5197	Molybdate ABC transporter, inner membrane subunit	-0.78±0.07	**0.02**
Rpal_5264	Phosphate ABC transporter, inner membrane subunit PstA	-1.26±0.09	**0.01**
GO:0006811: Ion transporter			
Rpal_0767	Phosphonate ABC transporter, periplasmic phosphonate binding protein	-1.57±0.42	**0.03**
Rpal_0914	ATP synthase subunit a (ATP synthase F0 sector subunit a)	-1.51±0.30	**0.04**
Rpal_1997	Sodium/hydrogen exchanger	-0.70±0.02	**0.04**
Rpal_2300	Heavy metal efflux pump, CzcA family	-0.98±0.08	**0.01**

Gene code	Gene description	FC ± SD*	p value
Rpal_2405	Nitrate ABC transporter, ATPase subunits C and D	-1.87±0.08	**0.01**
Rpal_2673	Molybdate ABC transporter, inner membrane subunit	-1.04±0.05	**0.01**
Rpal_3436	Probable potassium transport system protein kup	-0.78±0.19	**0.03**
Rpal_3823	Sodium/hydrogen exchanger	-1.22±0.03	**0.00**
Rpal_5197	Molybdate ABC transporter, inner membrane subunit	-0.78±0.07	**0.02**
Rpal_5264	Phosphate ABC transporter, inner membrane subunit PstA	-1.26±0.09	**0.01**
Rpal_2635	Ferric iron reductase	-1.21±0.00	**0.00**
Rpal_0147	Anti-sigma-factor antagonist	-1.51±0.07	**0.01**
GO:0022890: Inorganic cation transmembrane transporter activity			
Rpal_0278	Ammonium transporter	-2.79±0.29	**0.01**
Rpal_0900	Cytochrome c oxidase, subunit I	-0.78±0.08	**0.01**
Rpal_0914	ATP synthase subunit a (ATP synthase F0 sector subunit a)	-1.51±0.30	**0.04**
Rpal_2049	TonB-dependent siderophore receptor	-1.21±0.28	**0.03**
Rpal_2237	TonB-dependent siderophore receptor	-0.81±0.02	**0.05**
Rpal_3436	Probable potassium transport system protein kup	-0.78±0.19	**0.03**
Rpal_4917	TonB-dependent siderophore receptor	-0.60±0.01	**0.04**
Other transporter			
Rpal_0278	Ammonium transporter	-2.79±0.29	**0.01**
Rpal_1090	Outer membrane efflux protein	-1.14±0.13	**0.01**
Rpal_1593	ABC transporter periplasmic binding protein, urea carboxylase region	-1.11±0.02	**0.00**
Rpal_1663	Extracellular solute-binding protein family 1	-0.78±0.17	**0.02**
Rpal_1984	TRAP dicarboxylate transporter-DctP subunit	-0.75±0.09	**0.03**
Rpal_2300	Heavy metal efflux pump, CzcA family	-0.98±0.08	**0.01**
Rpal_3012	K(+)-insensitive pyrophosphate-energized proton pump	-0.96±0.18	**0.03**
Rpal_3305	Transporter, hydrophobe/amphiphile efflux-1 (HAE1) family	-1.26±0.35	**0.04**
Rpal_3614	Formate/nitrite transporter	-3.04±0.46	**0.02**
Rpal_3866	ABC transporter related	-1.90±0.33	**0.02**
Rpal_4377	Outer membrane autotransporter barrel domain protein	-1.22±0.10	**0.01**
Rpal_5283	Extracellular solute-binding protein family 3	-0.79±0.03	**0.02**
Chemotaxis, response to stimulus and flagellar assembly			
GO:0071973: bacterial-type flagellum assembly			
Rpal_1457	Flagellar M-ring protein	-1.06±0.12	**0.04**
Rpal_1458	Flagellar motor switch protein FliG	-1.60±0.21	**0.01**
Rpal_1459	Flagellar assembly protein H	-1.14±0.10	**0.01**
Rpal_1460	Flagellar motor switch protein FliN	-1.09±0.05	**0.02**
Rpal_2294	Flagellar basal body rod protein	-0.77±0.10	**0.01**
Rpal_2540	Uncharacterized protein	-1.70±0.11	**0.00**
Rpal_4452	Uncharacterized protein	-1.44±0.09	**0.02**

Gene code	Gene description	FC ± SD*	p value
rpt02030: Bacterial chemotaxis			
Rpal_0140	Chemotaxis response regulator protein-glutamate methylesterase	-0.85±0.11	**0.02**
Rpal_0141	Chemotaxis protein methyltransferase	-1.34±0.26	**0.03**
Rpal_0143	CheW protein	-1.20±0.21	**0.02**
Rpal_0144	CheW protein	-1.52±0.10	**0.01**
Rpal_0145	Histidine kinase	-1.56±0.31	**0.03**
Rpal_0146	Response regulator receiver protein	-1.73±0.18	**0.01**
Rpal_0148	Response regulator receiver modulated metal dependent phosphohydrolase	-0.89±0.01	**0.00**
Rpal_0147	Anti-sigma-factor antagonist	-1.51±0.07	**0.01**
Rpal_1871	Methyl-accepting chemotaxis sensory transducer with Pas/Pac sensor	-1.18±0.22	**0.02**
Rpal_0435	Methyl-accepting chemotaxis sensory transducer with Pas/Pac sensor	-0.62±0.13	**0.02**
GO:0007165: Signal transduction			
Rpal_0845	Diguanylate cyclase/phosphodiesterase with PAS/PAC sensor(S)	-0.92±0.13	**0.01**
Rpal_1487	Diguanylate cyclase	-1.00±0.04	**0.00**
Rpal_1916	Diguanylate cyclase	-1.48±0.27	**0.02**
Rpal_2444	Diguanylate cyclase/phosphodiesterase with PAS/PAC sensor(S)	-1.03±0.07	**0.00**
Rpal_2754	Diguanylate cyclase	-1.26±0.10	**0.00**
Rpal_4646	Diguanylate cyclase/phosphodiesterase with PAS/PAC sensor(S)	-0.72±0.14	**0.02**
Rpal_5015	Response regulator receiver protein	-0.87±0.22	**0.05**
Rpal_3600	Histidine kinase	-0.86±0.23	**0.04**
Rpal_2863	Nitrogen metabolism transcriptional regulator, NtrC, Fis Family	-1.08±0.07	**0.01**
Rpal_2862	Histidine kinase	-1.62±0.35	**0.04**
Rpal_2651	TonB-dependent receptor	-1.56±0.40	**0.04**
Rpal_2049	TonB-dependent siderophore receptor	-1.21±0.28	**0.03**
Rpal_1726	Putative PAS/PAC sensor protein	-0.81±0.24	**0.05**
Rpal_2237	TonB-dependent siderophore receptor	-0.81±0.02	**0.05**
Rpal_1176	Glutamine synthetase catalytic region	-0.84±0.26	**0.05**
Rpal_1956	Acetyl-CoA acetyltransferase	-1.02±0.30	**0.05**
Rpal_2862	Histidine kinase	-1.62±0.35	**0.04**
Rpal_2863	Nitrogen metabolism transcriptional regulator, NtrC, Fis Family	-1.08±0.07	**0.01**
Rpal_3314	Nitrogen regulatory protein P-II	-0.97±0.31	**0.05**
Rpal_3315	Glutamine synthetase	-1.62±0.29	**0.02**
Rpal_4690	Glutamine synthetase	-3.82±0.47	**0.01**
Metabolic process			
Rpal_0061	L-carnitine dehydratase/bile acid-inducible protein F	-0.75±0.03	**0.02**
Rpal_0071	N-(5'-phosphoribosyl)anthranilate isomerase (PRAI)	-0.68±0.02	**0.00**

Gene code	Gene description	FC ± SD*	p value
Rpal_0120	dTDP-glucose 4,6-dehydratase	-0.96±0.12	**0.02**
Rpal_0123	Glucose-1-phosphate thymidylyltransferase	-0.70±0.03	**0.02**
Rpal_0138	FAD-dependent pyridine nucleotide-disulphide oxidoreductase	-0.82±0.21	**0.03**
Rpal_0169	RNA pyrophosphohydrolase	-0.79±0.05	**0.03**
Rpal_0186	Succinyl-CoA ligase [ADP-forming] subunit beta	-1.04±0.15	**0.02**
Rpal_0436	Polyribonucleotide nucleotidyltransferase	-1.75±0.47	**0.04**
Rpal_0718	Cyclohexanecarboxylate-CoA ligase	-3.14±0.64	**0.02**
Rpal_0720	1,4-dihydroxy-2-naphthoyl-CoA synthase	-5.83±1.68	**0.04**
Rpal_0723	Alcohol dehydrogenase zinc-binding domain protein	-1.02±0.14	**0.03**
Rpal_0726	Benzoyl-CoA reductase, subunit A	-1.30±0.17	**0.01**
Rpal_0727	Benzoyl-CoA reductase, subunit D	-2.71±0.08	**0.00**
Rpal_0728	Benzoate-CoA ligase family	-0.72±0.01	**0.00**
Rpal_0729	4Fe-4S ferredoxin iron-sulfur binding domain protein	-1.15±0.28	**0.03**
Rpal_0744	Benzoyl-CoA oxygenase, B subunit	-0.85±0.02	**0.00**
Rpal_1270	Amidohydrolase 2	-1.35±0.01	**0.01**
Rpal_1349	3-deoxy-D-manno-octulosonic-acid transferase domain protein	-0.93±0.24	**0.04**
Rpal_1608	Cysteine desulfurase	-1.15±0.10	**0.01**
Rpal_1641	Nitric-oxide reductase, small subunit	-2.64±0.56	**0.04**
Rpal_1780	Glutamate racemase	-0.80±0.04	**0.02**
Rpal_1862	Coproporphyrinogen-III oxidase	-0.92±0.15	**0.02**
Rpal_1863	Bacteriochlorophyll 4-vinyl reductase	-1.49±0.14	**0.01**
Rpal_1959	Aminoglycoside phosphotransferase	-0.85±0.17	**0.03**
Rpal_2042	2-amino-4-hydroxy-6-hydroxymethyldihydropteridine pyrophosphokinase	-0.79±0.16	**0.05**
Rpal_2228	Lipid A biosynthesis acyltransferase	-0.72±0.10	**0.01**
Rpal_2291	SNARE associated Golgi protein	-0.66±0.03	**0.02**
Rpal_2831	Cystathionine beta-lyase	-0.85±0.00	**0.02**
Rpal_2846	Membrane bound O-acyl transferase MBOAT family protein	-0.91±0.17	**0.04**
Rpal_2847	Alginate O-acetyltransferase AlgJ	-1.15±0.10	**0.00**
Rpal_2861	tRNA-dihydrouridine synthase	-0.94±0.22	**0.04**
Miscellaneous			
Rpal_0030	Heparinase II/III family protein	-0.71±0.04	**0.01**
Rpal_0259	HemY domain protein	-0.71±0.04	**0.04**
Rpal_0307	Smr protein/MutS2	-0.78±0.03	**0.01**
Rpal_0616	PfkB domain protein	-0.71±0.09	**0.02**
Rpal_0621	Recombination protein RecR	-0.68±0.06	**0.04**
Rpal_1044	Transposase and inactivated derivatives-like protein	-1.30±0.00	**0.00**

Gene code	Gene description	FC ± SD*	p value
Rpal_1289	Crossover junction endodeoxyribonuclease RuvC	-0.77±0.10	**0.03**
Rpal_1291	CMP/dCMP deaminase zinc-binding	-1.10±0.27	**0.03**
Rpal_1292	Holliday junction ATP-dependent DNA helicase RuvB	-0.99±0.08	**0.01**
Rpal_1928	RES domain protein	-0.82±0.01	**0.00**
Rpal_1947	UPF0317 protein Rpal_1947	-2.11±0.12	**0.01**
Rpal_2201	Transcriptional regulator, AraC family	-1.20±0.10	**0.01**
Rpal_2446	Acyltransferase 3	-0.96±0.06	**0.00**
Rpal_2530	TPR repeat-containing protein	-0.73±0.18	**0.05**
Rpal_2705	Peptidase S1 and S6 chymotrypsin/Hap	-1.02±0.08	**0.00**
Rpal_2868	GTPase HflX (GTP-binding protein HflX)	-0.80±0.08	**0.02**
Rpal_3030	NinB family protein	-2.96±0.70	**0.04**
Rpal_3032	Exonuclease, phage-type	-4.44±0.82	**0.02**
Rpal_3075	Putative phage tail collar domain	-5.37±1.18	**0.02**
Rpal_3077	Lysozyme	-3.98±1.23	**0.05**
Rpal_3138	Pyridoxal kinase	-0.90±0.00	**0.01**
Rpal_3231	CTP synthase	-1.33±0.35	**0.03**
Rpal_3253	Citrate synthase	-0.68±0.02	**0.03**
Rpal_3266	Uridylate kinase (UK)	-0.73±0.11	**0.01**
Rpal_3509	NnrUfamily protein	-0.64±0.06	**0.01**
Rpal_3617	NAD-dependent epimerase/dehydratase	-1.29±0.01	**0.01**
Rpal_3758	4'-phosphopantetheinyl transferase	-0.89±0.01	**0.04**
Rpal_3762	Amino acid adenylation domain protein	-0.95±0.04	**0.01**
Rpal_3764	Uncharacterized protein	-0.74±0.15	**0.02**
Rpal_3765	Glycosyl transferase group 1	-0.88±0.11	**0.01**
Rpal_3769	Glycosyl transferase group 1	-1.12±0.08	**0.00**
Rpal_3773	Glycosyl transferase family 25	-1.50±0.31	**0.04**
Rpal_3774	Glycosyl transferase group 1	-1.16±0.31	**0.04**
Rpal_3777	Capsular exopolysaccharide family	-0.87±0.14	**0.02**
Rpal_3780	Transglutaminase family protein cysteine peptidase BTLCP	-0.91±0.08	**0.01**
Rpal_3836	Alpha,alpha-trehalose-phosphate synthase (UDP-forming)	-1.25±0.05	**0.00**
Rpal_3894	PepSY-associated TM helix domain protein	-1.04±0.28	**0.04**
Rpal_3975	Phage portal protein, HK97 family	-1.13±0.21	**0.04**
Rpal_4062	Transcriptional regulator, TetR family	-0.67±0.03	**0.05**
Rpal_4217	Prephenate dehydratase	-0.67±0.09	**0.01**
Rpal_4224	Methionine synthase	-1.46±0.25	**0.02**
Rpal_4231	Precorrin-3B synthase	-2.86±0.67	**0.03**
Rpal_4260	Hopanoid-associated phosphorylase	-2.09±0.32	**0.03**

Gene code	Gene description	FC ± SD*	p value
Rpal_4376	Protein RecA (Recombinase A)	-1.32±0.33	**0.04**
Rpal_4470	Glycosyl transferase group 1	-0.90±0.12	**0.01**
Rpal_4476	Thioesterase superfamily protein	-0.67±0.06	**0.01**
Rpal_4546	S-adenosylmethionine synthase	-1.02±0.06	**0.03**
Rpal_4577	Glycosyl transferase group 1	-1.06±0.08	**0.01**
Rpal_4599	Acyltransferase 3	-0.71±0.04	**0.00**
Rpal_4793	GCN5-related N-acetyltransferase	-0.89±0.02	**0.01**
Rpal_4844	Laccase domain protein	-1.01±0.05	**0.02**
Rpal_4862	Transferase hexapeptide repeat containing protein	-0.77±0.13	**0.01**
Rpal_4863	Riboflavin biosynthesis protein	-1.04±0.08	**0.02**
Rpal_4883	ABC transporter related	-0.90±0.17	**0.03**
Rpal_5014	HAD-superfamily hydrolase, subfamily IA, variant 3	-0.65±0.03	**0.01**
Rpal_5020	Protein tyrosine phosphatase	-0.77±0.11	**0.02**
Rpal_5086	Electron transfer flavoprotein alpha/beta-subunit	-1.71±0.46	**0.04**
Rpal_5092	NifQ family protein	-1.27±0.26	**0.03**
Rpal_5093	Ferredoxin III, nif-specific	-1.40±0.22	**0.03**
Rpal_5097	Nitrogenase molybdenum-iron cofactor biosynthesis protein NifN	-1.01±0.26	**0.04**
Rpal_5112	4Fe-4S ferredoxin iron-sulfur binding domain protein	-0.96±0.24	**0.04**
Rpal_5115	Uncharacterized protein	-1.45±0.12	**0.00**
Rpal_5178	Amidohydrolase 2	-2.35±0.27	**0.01**
Rpal_5179	4-carboxy-4-hydroxy-2-oxoadipate aldolase/oxaloacetate decarboxylase	-1.64±0.36	**0.02**
Rpal_5180	Phosphogluconate dehydrogenase	-1.53±0.03	**0.00**
Rpal_5181	Amidohydrolase 2	-1.46±0.36	**0.04**
Rpal_5208	Alpha-1,4 glucan phosphorylase	-0.79±0.16	**0.04**
Rpal_5249	Metallophosphoesterase	-1.64±0.35	**0.02**
Rpal_5263	Phosphate import ATP-binding protein PstB	-1.24±0.33	**0.04**

* FC is $\log_2$ (fold change) calculated for *Δshc* mutant with respect to WT and SD is standard deviation.

Table S4. Microarray results representing uncharacterised genes showing upregulation, their mean fold change with standard deviation and p-values. Transcripts with significant fold change (fold change ≥0.6 and p-value ≤ 0.05) are included in the table. Fold changes were calculated by comparing *Δshc* mutant with WT strain.

Gene Code	FC ± SD*	P value
Rpal_0149	0.81±0.17	**0.02**
Rpal_0178	1.14±0.04	**0.01**
Rpal_0179	0.97±0.06	**0.04**
Rpal_0197	0.73±0.01	**0.00**
Rpal_0237	3.51±0.43	**0.01**
Rpal_0238	1.41±0.25	**0.02**
Rpal_0239	2.07±0.08	**0.01**
Rpal_0249	0.75±0.21	**0.04**
Rpal_0321	0.69±0.02	**0.03**
Rpal_0335	1.32±0.38	**0.04**
Rpal_0402	1.34±0.15	**0.03**
Rpal_0407	1.64±0.47	**0.04**
Rpal_0466	0.71±0.01	**0.00**
Rpal_0493	1.10±0.14	**0.04**
Rpal_0541	1.28±0.30	**0.03**
Rpal_0816	2.45±0.62	**0.03**
Rpal_0843	1.52±0.06	**0.00**
Rpal_0894	1.02±0.16	**0.02**
Rpal_0958	2.46±0.52	**0.02**
Rpal_0965	0.95±0.24	**0.03**
Rpal_1012	1.09±0.15	**0.01**
Rpal_1070	0.84±0.07	**0.01**
Rpal_1196	1.58±0.16	**0.01**
Rpal_1236	1.72±0.17	**0.01**
Rpal_1249	1.79±0.22	**0.01**
Rpal_1254	2.54±0.58	**0.02**
Rpal_1302	0.97±0.04	**0.04**
Rpal_1343	0.78±0.01	**0.03**
Rpal_1351	1.09±0.13	**0.01**
Rpal_1373	1.34±0.25	**0.02**
Rpal_1377	0.82±0.15	**0.02**
Rpal_1402	1.01±0.13	**0.01**
Rpal_1414	0.98±0.22	**0.03**
Rpal_1606	0.75±0.02	**0.04**
Rpal_1765	1.11±0.27	**0.03**
Rpal_1775	1.45±0.43	**0.05**
Rpal_2015	3.78±0.49	**0.01**
Rpal_2047	0.88±0.20	**0.03**
Rpal_2069	0.79±0.24	**0.05**
Rpal_2157	0.84±0.08	**0.03**
Rpal_2206	1.42±0.14	**0.01**
Rpal_2207	0.85±0.09	**0.03**
Rpal_2297	0.77±0.22	**0.04**
Rpal_2426	1.71±0.24	**0.01**
Rpal_2536	1.50±0.10	**0.00**
Rpal_2538	0.78±0.00	**0.00**
Rpal_2539	0.85±0.04	**0.00**
Rpal_3143	0.73±0.15	**0.04**
Rpal_3152	1.09±0.23	**0.03**
Rpal_3163	1.37±0.24	**0.02**
Rpal_3214	1.20±0.11	**0.04**
Rpal_3240	1.15±0.17	**0.03**
Rpal_3301	1.00±0.10	**0.01**
Rpal_3443	1.81±0.19	**0.01**
Rpal_3478	2.55±0.22	**0.00**
Rpal_3507	1.12±0.04	**0.01**
Rpal_3545	1.07±0.06	**0.02**
Rpal_3546	1.09±0.12	**0.01**
Rpal_3561	1.21±0.17	**0.03**
Rpal_3565	1.45±0.44	**0.04**
Rpal_3587	2.41±0.17	**0.02**
Rpal_3610	3.15±0.37	**0.01**
Rpal_3854	3.18±0.51	**0.01**
Rpal_3855	4.40±0.65	**0.01**
Rpal_3891	1.12±0.18	**0.01**
Rpal_3921	1.45±0.23	**0.02**
Rpal_3852	1.40±0.11	**0.00**
Rpal_4030	1.04±0.06	**0.04**
Rpal_4116	2.95±0.02	**0.00**
Rpal_4117	2.10±0.42	**0.04**
Rpal_4122	2.33±0.43	**0.02**
Rpal_4123	1.73±0.32	**0.02**
Rpal_4359	1.05±0.14	**0.02**
Rpal_4394	0.98±0.02	**0.01**
Rpal_4396	0.98±0.29	**0.04**
Rpal_4521	1.10±0.21	**0.03**
Rpal_4580	1.39±0.01	**0.01**
Rpal_4612	2.42±0.37	**0.02**
Rpal_4671	1.59±0.52	**0.05**
Rpal_4703	1.57±0.22	**0.01**
Rpal_4704	1.42±0.42	**0.05**
Rpal_4772	1.79±0.12	**0.02**
Rpal_4829	0.94±0.26	**0.04**
Rpal_4837	1.31±0.28	**0.03**
Rpal_4859	1.14±0.20	**0.03**
Rpal_4866	1.05±0.25	**0.04**
Rpal_4890	0.81±0.20	**0.03**
Rpal_4918	2.15±0.36	**0.01**
Rpal_5028	0.95±0.03	**0.00**
Rpal_5030	0.63±0.01	**0.04**
Rpal_5050	1.90±0.51	**0.04**
Rpal_5268	0.68±0.06	**0.01**
Rpal_5306	0.73±0.12	**0.03**

* FC is $\log_2$ (fold change) calculated for *Δshc* mutant with respect to WT and SD is standard deviation.

Table S5. Microarray results representing uncharacterised genes showing downregulation, their mean fold change with standard deviation and p-values. Transcripts with significant fold change (fold change ≤ -0.6 and p-value ≤ 0.05) are included in the table. Fold changes were calculated by comparing *Δshc* mutant with WT strain.

Gene Code	FC ± SD*	P value
Rpal_0091	-1.57±0.26	**0.02**
Rpal_0092	-1.16±0.09	**0.04**
Rpal_0167	-0.85±0.02	**0.02**
Rpal_0258	-0.73±0.15	**0.05**
Rpal_0354	-0.98±0.12	**0.01**
Rpal_0364	-1.16±0.17	**0.01**
Rpal_0624	-1.07±0.24	**0.03**
Rpal_0846	-0.76±0.18	**0.03**
Rpal_0860	-0.92±0.21	**0.04**
Rpal_0962	-0.91±0.29	**0.05**
Rpal_1064	-0.82±0.11	**0.04**
Rpal_1083	-0.87±0.08	**0.01**
Rpal_1086	-0.80±0.24	**0.04**
Rpal_1104	-1.38±0.16	**0.01**
Rpal_1121	-1.02±0.07	**0.02**
Rpal_1135	-0.79±0.08	**0.03**
Rpal_1145	-1.39±0.37	**0.03**
Rpal_1204	-0.97±0.15	**0.02**
Rpal_1224	-1.66±0.11	**0.02**
Rpal_1507	-1.38±0.10	**0.00**
Rpal_1844	-1.84±0.23	**0.01**
Rpal_1845	-1.85±0.16	**0.01**
Rpal_1960	-1.61±0.03	**0.05**
Rpal_1979	-0.70±0.13	**0.03**
Rpal_2089	-0.95±0.01	**0.01**
Rpal_2118	-0.69±0.03	**0.00**
Rpal_2239	-4.18±0.04	**0.00**
Rpal_2256	-0.73±0.02	**0.01**
Rpal_2266	-0.76±0.04	**0.01**
Rpal_2307	-1.21±0.18	**0.01**
Rpal_2325	-1.36±0.12	**0.01**
Rpal_2328	-1.36±0.16	**0.01**
Rpal_2335	-0.74±0.02	**0.01**
Rpal_2338	-1.12±0.14	**0.01**
Rpal_2470	-0.70±0.03	**0.02**
Rpal_2471	-0.76±0.15	**0.02**
Rpal_2503	-1.06±0.21	**0.04**
Rpal_2512	-1.57±0.18	**0.01**
Rpal_2515	-0.66±0.06	**0.00**
Rpal_2516	-0.86±0.05	**0.01**
Rpal_2540	-1.70±0.11	**0.00**
Rpal_2643	-0.83±0.10	**0.01**
Rpal_2727	-0.92±0.09	**0.01**
Rpal_3023	-5.56±1.39	**0.03**
Rpal_3024	-4.85±0.45	**0.00**
Rpal_3026	-4.68±1.33	**0.04**
Rpal_3028	-1.99±0.18	**0.02**
Rpal_3033	-2.65±0.63	**0.03**
Rpal_3035	-3.16±0.21	**0.02**
Rpal_3037	-3.53±0.88	**0.03**
Rpal_3038	-2.00±0.00	**0.01**
Rpal_3040	-5.29±0.35	**0.01**
Rpal_3042	-5.98±0.30	**0.00**
Rpal_3043	-7.51±0.37	**0.00**
Rpal_3045	-1.68±0.08	**0.03**
Rpal_3046	-2.74±0.36	**0.01**
Rpal_3047	-2.37±0.40	**0.03**
Rpal_3051	-4.15±0.62	**0.02**
Rpal_3053	-2.62±0.24	**0.03**
Rpal_3054	-2.53±0.50	**0.03**
Rpal_3058	-2.86±0.80	**0.05**
Rpal_3059	-3.88±1.18	**0.05**
Rpal_3061	-2.35±0.61	**0.03**
Rpal_3062	-6.66±0.01	**0.00**
Rpal_3064	-3.89±0.98	**0.04**
Rpal_3065	-3.02±0.63	**0.04**
Rpal_3066	-3.56±0.64	**0.02**
Rpal_3067	-2.25±0.65	**0.05**
Rpal_3068	-3.97±0.75	**0.03**
Rpal_3069	-2.49±0.06	**0.01**
Rpal_3070	-3.37±1.07	**0.05**
Rpal_3072	-5.19±0.23	**0.00**
Rpal_3074	-5.00±0.40	**0.01**
Rpal_3080	-3.97±0.90	**0.03**
Rpal_3081	-3.53±0.50	**0.01**
Rpal_3082	-4.82±1.33	**0.04**
Rpal_3103	-0.74±0.13	**0.02**
Rpal_3118	-1.01±0.08	**0.02**
Rpal_3181	-0.95±0.24	**0.04**
Rpal_3199	-0.98±0.24	**0.03**
Rpal_3332	-1.33±0.16	**0.01**
Rpal_3416	-0.90±0.25	**0.05**
Rpal_3533	-1.37±0.43	**0.05**
Rpal_3562	-0.89±0.24	**0.05**
Rpal_3596	-1.19±0.13	**0.01**
Rpal_3790	-0.83±0.16	**0.03**
Rpal_3807	-1.00±0.00	**0.00**
Rpal_3808	-0.78±0.03	**0.05**
Rpal_3820	-1.34±0.13	**0.01**
Rpal_3822	-1.41±0.23	**0.04**
Rpal_3887	-1.42±0.08	**0.04**
Rpal_3905	-1.09±0.10	**0.00**
Rpal_3907	-1.03±0.29	**0.05**
Rpal_3994	-0.82±0.05	**0.00**
Rpal_4032	-1.75±0.21	**0.01**
Rpal_4099	-0.80±0.06	**0.03**
Rpal_4452	-1.44±0.09	**0.02**

* FC is $\log_2$ (fold change) calculated for *Δshc* mutant with respect to WT and SD is standard deviation.

REFERENCES

0.7 References

Aziz R.K., Bartels D., Best A.A., DeJongh M., Disz T., Edwards R.A., Formsma K., Gerdes S., Glass E.M., Kubal M., Meyer F., Olsen G.J., Olson R., Osterman A.L., Overbeek R.A., McNeil L.K., Paarmann D., Paczian T., Parrello B., Pusch G.D., Reich C., Stevens R., Vassieva O., Vonstein V., Wilke A. and Zagnitko O. 2008. The RAST server: rapid annotations using subsystems technology. *BMC Genomics* **9**, 75-89.

Banerjee A. and Sharkey T.D., 2014. Methylerythritol 4-phosphate (MEP) pathway metabolic regulation. *Nat Prod Rep* **31**, 1043-1055.

Barak I. and Muchova K. 2013. The role of lipid domains in bacterial cell processes. *Int J Mol Sci* **14**, 4050-4065.

Belin G.K. 2009. Investigation of hopanoid biomarkers in lake sediments by GC-MS and RP-HPLC-APCI-MS. *E-Journal of Chemistry* **6**, 77-88.

Benz R., Hallmann D., Poralla K. and Eibl H. 1983. Interaction of hopanoids with phosphatidylcholines containing oleic and omega-cyclohexyldodecanoic acid in lipid bilayer membranes. *Chem Phys Lipids* **34**, 7-24.

Berry A.M., Harriott O.T., Moreau R.A., Osman S.F., Benson D.R. and Jones A.D. 1993. Hopanoid lipids compose the *Frankia* vesicle envelope, presumptive barrier of oxygen diffusion to nitrogenase. *PNAS* **90**, 6091-6094.

Blumenberg M., Hoppert M., Krüger M., Dreier A. and Thiel V. 2012. Novel findings on hopanoid occurrences among sulfate reducing bacteria: Is there a direct link to nitrogen fixation? *Organic Geochemistry* **49**, 1-5.

Blumenberg M., Mollenhauer G., Zabel M., Reimer A. and Thiel V. 2010. Decoupling of bio- and geohopanoids in sediments of the Benguela Upwelling System (BUS). *Organic Geochemistry* **41**, 1119-1129.

Blumenberg M., Oppermann B.I., Guyoneaud R. and Michaelis W. 2009. Hopanoid production by *Desulfovibrio bastinii* isolated from oilfield formation water. *FEMS Microbiol Lett* **293**, 73-78.

Blumenberg M., Kruger M., Nauhaus K., Talbot H.M., Oppermann B.I., Seifert R., Pape T. and Michaelis W. 2006. Biosynthesis of hopanoids by sulfate-reducing bacteria (genus *Desulfovibrio*). *Environ Microbiol* **8**, 1220-1227.

Bode H.B., Zeggel B., Silakowski B., Wenzel S.C., Reichenbach H. and Muller R. 2003. Steroid biosynthesis in prokaryotes: identification of myxobacterial steroids and

cloning of the first bacterial 2,3(S)-oxidosqualene cyclase from the myxobacterium *Stigmatella aurantiaca*. *Mol Microbiol* **47**, 471-481.

Bramkamp M. and Lopez D. 2015. Exploring the existence of lipid rafts in bacteria. *Microbiology and molecular biology reviews* **79**, 81-100.

Brocks J.J., Buick R., Summons R. and Logan G.A. 2003. A reconstruction of Archean biological diversity based on molecular fossils from the 2.78 to 2.45 billion-year-old Mount Bruce Supergroup, Hamersley Basin, Western Australia. *Geochimica et Cosmochimica Acta* **67**, 4321-4335.

Brocks J.J., Logan G.A., Buick R. and Summons R.E. 1999. Archean molecular fossils and the early rise of eukaryotes. *Science* **285**, 1033-1036.

Cantera J.J., Kawasaki H. and Seki T. 2002. Farnesyl diphosphate synthase gene of three phototrophic bacteria and its use as a phylogenetic marker. *Int J Syst Evol Microbiol* **52**, 1953-1960.

Cronan J.E. and Thomas J. 2009. Bacterial fatty acid synthesis and its relationships with polyketide synthetic pathways. *Methods in enzymology* **459**, 395-433.

Cvejic J.H., Bodrossy L., Kovacs K.L. and Rohmer M. 2000. Bacterial triterpenoids of the hopane series from the methanotrophic bacteria *Methylocaldum* spp.: phylogenetic implications and first evidence for an unsaturated aminobacteriohopanepolyol. *FEMS Microbiol Lett* **182**, 361-365.

Damsté J.S., Rijpstra W.I.C., Schouten S., Fuerst J.A., Jetten M.S.M. and Strous M. 2004. The occurrence of hopanoids in *Planctomycetes*: implications for the sedimentary biomarker record. *Organic Geochemistry* **35**, 561-566.

Doughty D.M., Coleman M.L., Hunter R.C., Sessions A.L., Summons R.E. and Newman D.K. 2011. The RND-family transporter, HpnN, is required for hopanoid localization to the outer membrane of *Rhodopseudomonas palustris* TIE-1. *PNAS* **108**, 1045-1051.

Doughty D.M., Hunter R.C., Summons R.E. and Newman D.K. 2009. 2-Methyl-hopanoids are maximally produced in akinetes of *Nostoc punctiforme*: geobiological implications. *Geobiology* **7**, 524-532.

Driessen A.J., Zheng T., In't Veld G., Opden Kamp J.A. and Konings W.N. 1988. Lipid requirement of the branched-chain amino acid transport system of *Streptococcus cremoris*. *Biochemistry* **27**, 865-872.

Duvold T. and Rohmer M. 1999. Synthesis of ribosylhopane, the putative biosynthetic precursor of bacterial triterpenoids of the hopane series. *Tetrahedron* **55**, 9847-9858.

Eickhoff M., Birgel D., Talbot H.M., Peckmann J. and Kappler A. 2013. Bacteriohopanoid inventory of *Geobacter sulfurreducens* and *Geobacter metallireducens*. *Organic Geochemistry* **58**, 107-114.

Fahy E., Subramaniam S., Brown H.A., Glass C.K., Merrill A.H., Murphy R.C., Raetz C.R., Russell D.W., Seyama Y., Shaw W., Shimizu T., Spener F., van Meer G., VanNieuwenhze M.S., White S.H., Witztum J.L. and Dennis E.A. 2005. A comprehensive classification system for lipids. *J Lipid Res* **46**, 839-861.

Fahy E., Subramaniam S., Murphy R.C., Nishijima M., Raetz C.R., Shimizu T., Spener F., van Meer G., Wakelam M.J. and Dennis E.A. 2009. Update of the LIPID MAPS comprehensive classification system for lipids. *J Lipid Res* **50**, 9-14.

Fischer W.W., Summons R.E. and Pearson A. 2005. Targeted genomic detection of biosynthetic pathways: anaerobic production of hopanoid biomarkers by a common sedimentary microbe. *Geobiology* **3**, 33-40.

Forster H.J., Biemann K., Haigh W.G., Tattrie N.H. and Colvin J.R. 1973. The structure of novel C_{35} pentacyclic terpenes from *Acetobacter xylinum*. *Biochemical Journal* **135**, 133-143.

Garcia Costas A.M., Tsukatani Y., Rijpstra W.I., Schouten S., Welander P.V., Summons R.E. and Bryant D.A. 2012. Identification of the bacteriochlorophylls, carotenoids, quinones, lipids, and hopanoids of "*Candidatus* Chloracidobacterium thermophilum". *J Bacteriol* **194**, 1158-1168.

Hannich J.T., Umebayashi K. and Riezman H. 2011. Distribution and functions of sterols and sphingolipids. *Cold Spring Harbor perspectives in biology* **3,** 4762-4776

Hartner T., Straub K.L. and Kannenberg E. 2005. Occurrence of hopanoid lipids in anaerobic *Geobacter* species. *FEMS Microbiol Lett* **243**, 59-64.

Harwood C.S., Burchhardt G., Herrmann H. and Fuchs G. 1999. Anaerobic metabolism of aromatic compounds via the benzoyl-CoA pathway. *FEMS Microbiol. Rev.* **22**, 439-458.

Heuston S., Begley M., Gahan C.G. and Hill C. 2012. Isoprenoid biosynthesis in bacterial pathogens. *Microbiology* **158**, 1389-1401.

Hiraishi A. and Ueda Y. 1994. *Rhodoplanes* gen. nov., a new genus of phototrophic bacteria including *Rhodopseudomonas rosea* as *Rhodoplanes roseus* comb. nov. and *Rhodoplanes elegans* sp. nov. *Int J Syst Bacteriol* **44**, 665–673.

Hunter W.N. 2007. The non-mevalonate pathway of isoprenoid precursor biosynthesis. *J Biol Chem* **282**, 21573-21577.

Jakob U., Muse W., Eser M. and Bardwell J.C. 1999. Chaperone activity with a redox switch. *Cell* **96**, 341-352.

Kannenberg E.L. and Poralla K. 1999. Hopanoid biosynthesis and function in bacteria. *Naturwissenschaften* **86**, 168–176.

Kannenberg E.L., Perzl M. and Hartner T. 1995. The occurrence of hopanoid lipids in *Bradyrhizobium* bacteria. *FEMS Microbiol Lett* **127**, 255-262.

Kannenberg E., Blume A., Geckeler K. and Poralla K. 1985. Properties of hopanoids and phosphatidylcholines containing ω-cyclohexane fatty acid in monolayer and liposome experiments. *Biochimica et biophysica acta* **814**, 179-185.

Kathiravan R., Jegan S., Ganga V., Prabavathy V.R., Tushar L., Sasikala C. and Ramana Ch.V. 2013. *Ciceribacter lividus* gen. nov., sp. nov., isolated from rhizosphere soil of chick pea (*Cicer arietinum* L.). *Int J Syst Evol Microbiol* **63**, 4484-4488.

Kontnik R., Bosak T., Butcher R.A., Brocks J.J., Losick R., Clardy J. and Pearson A. 2008. Sporulenes, heptaprenyl metabolites from *Bacillus subtilis* spores. *Org Lett* **10**, 3551-3554.

Kulkarni G., Busset N., Molinaro A., Gargani D., Chaintreuil C., Silipo A., Giraud E. and Newman D.K. 2015. Specific hopanoid classes differentially affect free-living and symbiotic states of *Bradyrhizobium diazoefficiens*. *mBio* **6**, e01251-01215.

Kulkarni G., Wu H.G. and Newman D.K. 2013. The general stress response factor EcfG regulates expression of the C_2 hopanoid methylase *hpnP* in *Rhodopseudomonas palustris* TIE-1. *J. Bacteriol*. **195**, 2490-2498.

Lakshmi K.V.N.S., Sasikala Ch. and Ramana Ch.V. 2009. *Rhodoplanes pokkaliisoli* sp. nov., a phototrophic alphaproteobacterium isolated from a waterlogged brackish paddy soil. *Int. J. Syst. Evol. Microbiol.* **59**, 2153-2157.

Lingwood D., Kaiser H.J., Levental I. and Simons K. 2009. Lipid rafts as functional heterogeneity in cell membranes. *Biochemical Society transactions* **37**, 955-960.

Listowski M.A., Leluk J., Kraszewski S. and Sikorski A.F. 2015. Cholesterol interaction with the MAGUK protein family member, MPP1, via CRAC and CRAC-like motifs: an *in silico* docking analysis. *PLoS One* **10**, e0133141.

Lombard J. and Moreira D. 2011. Origins and early evolution of the mevalonate pathway of isoprenoid biosynthesis in the three domains of life. *Mol Biol Evol* **28**, 87-99.

Lopez D. and Kolter R. 2010. Functional microdomains in bacterial membranes. *Genes and development* **24**, 1893-1902.

Lopez-Lara I.M. and Geiger O. 2016. Bacterial lipid diversity. *Biochimica et biophysica acta.* dx.doi.org/10.1016/j.bbalip.2016.10.007

Malott R.J., Steen-Kinnaird B.R., Lee T.D. and Speert D.P. 2012. Identification of hopanoid biosynthesis genes involved in polymyxin resistance in *Burkholderia multivorans*. *Antimicrob Agents Chemother* **56**, 464-471.

McGarvey D.J. and Croteau R. 1995. Terpenoid metabolism. *Plant Cell* **7**, 1015-1026.

Meikle P.J. and Summers S.A. 2017. Sphingolipids and phospholipids in insulin resistance and related metabolic disorders. *Nature reviews: Endocrinology* **13**, 79-91.

Mende D.R., Sunagawa S., Zeller G. and Bork P. 2013. Accurate and universal delineation of prokaryotic species. *Nat Methods* **10**, 881-884.

Methe B.A., Nelson K.E., Eisen J.A., Paulsen I.T., Nelson W., Heidelberg J.F., Wu D., Wu M., Ward N., Beanan M.J., Dodson R.J., Madupu R., Brinkac L.M., Daugherty S.C., DeBoy R.T., Durkin A.S., Gwinn M., Kolonay J.F., Sullivan S.A., Haft D.H., Selengut J., Davidsen T.M., Zafar N., White O., Tran B., Romero C., Forberger H.A., Weidman J., Khouri H., Feldblyum T.V., Utterback T.R., van Aken S.E., Lovley D.R. and Fraser C.M. 2003. Genome of *Geobacter sulfurreducens*: metal reduction in subsurface environments. *Science* **302**, 1967-1969.

Miziorko H.M. 2011. Enzymes of the mevalonate pathway of isoprenoid biosynthesis. *Arch Biochem Biophys* **505**, 131-143.

Nalin R., Putra S.R., Domenach A.M., Rohmer M., Gourbiere F. and Berry A.M. 2000. High hopanoid/total lipids ratio in *Frankia* mycelia is not related to the nitrogen status. *Microbiology* **146**, 3013-3019.

Neunlist S., Holst O. and Rohmer M. 1985. Prokaryotic triterpenoids. The hopanoids of the purple non-sulphur bacterium *Rhodomicrobium vannielii*: an aminotriol and

its aminoacyl derivatives, N-tryptophanyl and N-ornithinyl aminotriol. *Eur J Biochem* **147**, 561-568.

Neunlist S. and Rohmer M. 1985a. A novel hopanoid, 30-(5'-adenosyl)hopane, from the purple non-sulphur bacterium *Rhodopseudomonas acidophila*, with possible DNA interactions. *Biochem J* **228**, 769-771.

Neunlist S. and Rohmer M. 1985b. Novel hopanoids from the methylotrophic bacteria *Methylococcus capsulatus* and *Methylomonas methanica*. (22S)-35-aminobacteriohopane-30,31,32,33,34-pentol and (22S)-35-amino-3 beta-methylbacteriohopane-30,31,32,33,34-pentol. *Biochem J* **231**, 635-639.

Noinaj N., Guillier M., Barnard T.J. and Buchanan S.K. 2010. TonB-dependent transporters: regulation, structure, and function. *Annual review of microbiology* **64**, 43-60.

Ourisson G., Albrecht P. and Rohmer M. 1979. The hopanoids: Palaeochemistry and biochemistry of a group of natural products. *Pure and Appl. Chem* **51**, 709-729.

Ourisson G., Rohmer M. and Poralla K. 1987. Prokaryotic hopanoids and other polyterpenoid sterol surrogates. *Annual review of microbiology* **41**, 301-333.

Paul R., Weiser S., Amiot N.C., Chan C., Schirmer T., Giese B. and Jenal U. 2004. Cell cycle-dependent dynamic localization of a bacterial response regulator with a novel di-guanylate cyclase output domain. *Genes and development* **18**, 715-727.

Pearson A., Page S.R.F., Jorgenson T.L., Fischer W.W. and Higgins M.B. 2007. Novel hopanoid cyclases from the environment. *Environ Microbiol* **9**, 2175-2188.

Pearson A., Budin M. and Brocks J.J. 2003. Phylogenetic and biochemical evidence for sterol synthesis in the bacterium *Gemmata obscuriglobus*. *PNAS* **100**, 15352–15357.

Perzl M., Muller P., Poralla K. and Kannenberg E.L. 1997. Squalene-hopene cyclase from *Bradyrhizobium japonicum*: cloning, expression, sequence analysis and comparison to other triterpenoid cyclases. *Microbiology* **143**, 1235-1231.

Perzl M., Reipen I.G., Schmitz S., Poralla K., Sahm H., Sprenger G.A. and Kannenberg E.L. 1998. Cloning of conserved genes from *Zymomonas mobilis* and *Bradyrhizobium japonicum* that function in the biosynthesis of hopanoid lipids. *Biochimica et biophysica acta* **1393**, 108-118.

Poralla K., Muth G. and Hartner T. 2000. Hopanoids are formed during transition from substrate to aerial hyphae in *Streptomyces coelicolor* A3(2). *FEMS Microbiol Lett* **189**, 93-95.

Poralla K., Härtner T. and Kannenberg E. 1984. Effect of temperature and pH on the hopanoid content of *Bacillus acidocaldarius*. *FEMS Microbiology Letters* **23**, 253-256.

Quay S.C. and Oxender D.L. 1976. Regulation of branched-chain amino acid transport in *Escherichia coli*. *Journal of bacteriology* **127**, 1225-1238.

Rahul K., Sasikala Ch., Tushar L., Debadrita R. and Ramana Ch.V. 2014. *Alcanivorax xenomutans* sp. nov., a hydrocarbonoclastic bacterium isolated from a shrimp cultivation pond. *Int J Syst Evol Microbiol* **64**, 3553-3558.

Ramana Ch.V., Srinivas A., Subhash Y., Tushar L., Mukherjee T., Kiran P.U. and Sasikala Ch. 2013a. *Salinicoccus halitifaciens* sp. nov., a novel bacterium participating in halite formation. *Antonie Van Leeuwenhoek* **103**, 885-898.

Ramana V.V., Raj P.S., Tushar L., Sasikala Ch. and Ramana Ch.V. 2013b. *Rhodomicrobium udaipurense* sp. nov., a psychrotolerant, phototrophic alphaproteobacterium isolated from a freshwater stream. *Int J Syst Evol Microbiol* **63**, 2684-2689.

Ramaprasad E.V., Tushar L., Dave B., Sasikala Ch. and Ramana Ch.V. 2016. *Rhodovulum algae* sp. nov., isolated from an algal mat. *Int J Syst Evol Microbiol* **66**, 3367-3371.

Reipen I.G., Poralla K., Sahm H. and Sprenger G.A. 1995. *Zymomonas mobilis* squalene-hopene cyclase gene (*shc*): cloning, DNA sequence analysis, and expression in *Escherichia coli*. *Microbiology* **141**, 155-161.

Ricci J.N., Michel A.J. and Newman D.K. 2015. Phylogenetic analysis of *HpnP* reveals the origin of 2-methylhopanoid production in alphaproteobacteria. *Geobiology* **13**, 267-277.

Rodier C., Llopiz, P. and Neunlist S. 1999. C_{32} and C_{34} hopanoids in recent sediments of European lakes: novel intermediates in the early diagenesis of biohopanoids. *Organic Geochemistry* **30**, 713-716.

Rohmer M. 2008. From molecular fossils of bacterial hopanoids to the formation of isoprene units: discovery and elucidation of the methylerythritol phosphate pathway. *Lipids* **43**, 1095-1107.

Rohmer M. 1999. The discovery of a mevalonate-independent pathway for isoprenoid biosynthesis in bacteria, algae and higher plants. *Nat Prod Rep* **16**, 565-574.

Rohmer M. 1993. The biosynthesis of triterpenoids of the hopane series in the eubacteria: a mine of new enzyme reactions. *Pure Appl. Chem.* **65**, 1293-1298.

Rohmer M., Bouvier-Navez P. and Ourisson G.P. 1984. Distribution of hopanoid triterpenes in prokaryotes. *Journal of Microbiology* **130**, 1137-1150.

Rosa-Putra S., Nalin R., Domenach A.M. and Rohmer M. 2001. Novel hopanoids from *Frankia* spp. and related soil bacteria. Squalene cyclization and significance of geological biomarkers revisited. *Eur J Biochem* **268**, 4300-4306.

Saenz J.P., Grosser D., Bradley A.S., Lagny T.J., Lavrynenko O., Broda M. and Simons K. 2015. Hopanoids as functional analogues of cholesterol in bacterial membranes. *PNAS* **112**, 11971-11976.

Saenz J.P., Sezgin E., Schwille P. and Simons K. 2012a. Functional convergence of hopanoids and sterols in membrane ordering. *PNAS* **109**, 14236-14240.

Saenz J.P., Waterbury J.B., Eglinton T.I. and Summons R.E. 2012b. Hopanoids in marine cyanobacteria: probing their phylogenetic distribution and biological role. *Geobiology* **10**, 311-319.

Schmerk C.L., Bernards M.A. and Valvano M.A. 2011. Hopanoid production is required for low-pH tolerance, antimicrobial resistance, and motility in *Burkholderia cenocepacia*. *J Bacteriol* **193**, 6712-6723.

Seeman M., Bisseret P., Tritz J.P., Hooper A.B. and Rohmer M. 1999. Novel bacterial triterpenoids of the hopane series from *Nitrosomonas europaea* and their significance for the formation of the C_{35} bacteriohopane skeleton. *Tetra. Lett.* **40**, 1681-1684.

Seipke R.F. and Loria R. 2009. Hopanoids are not essential for growth of *Streptomyces scabies* 87-22. *J Bacteriol* **191**, 5216-5223.

Sessions A.L., Zhang L., Welander P.V., Doughty D., Summons R.E. and Newman D.K. 2013. Identification and quantification of polyfunctionalized hopanoids by high temperature gas chromatography-mass spectrometry. *Organic Geochemistry* **56**, 120-130.

Shah P. and Swiatlo E. 2008. A multifaceted role for polyamines in bacterial pathogens. *Molecular microbiology* **68**, 4-16.

Sheng R., Chen Y., Yung Gee H., Stec E., Melowic H.R., Blatner N.R., Tun M.P., Kim Y., Kallberg M., Fujiwara T.K., Hye Hong J., Pyo Kim K., Lu H., Kusumi A., Goo Lee M. and Cho W. 2012. Cholesterol modulates cell signaling and protein networking by specifically interacting with PDZ domain-containing scaffold proteins. *Nat Commun* **3**, 1249-1258.

Shivani Y., Subhash Y., Tushar L., Sasikala Ch. and Ramana Ch.V. 2015. *Spirochaeta lutea* sp. nov., isolated from marine habitats and emended description of the genus *Spirochaeta*. *Syst Appl Microbiol* **38**, 110-114.

Shunthirasingham C. and Simpson M.J. 2006. Investigation of bacterial hopanoid inputs to soils from Western Canada. *Applied Geochemistry* **21**, 964-976.

Siedenburg G. and Jendrossek D. 2011. Squalene-Hopene Cyclases. *Applied and Environmental Microbiology* **77**, 3905-3915.

Silipo A., Vitiello G., Gully D., Sturiale L., Chaintreuil C., Fardoux J., Gargani D., Lee H.I., Kulkarni G., Busset N., Marchetti R., Palmigiano A., Moll H., Engel R., Lanzetta R., Paduano L., Parrilli M., Chang W.S., Holst O., Newman D.K., Garozzo D., D'Errico G., Giraud E. and Molinaro A. 2014. Covalently linked hopanoid-lipid A improves outer-membrane resistance of a *Bradyrhizobium* symbiont of legumes. *Nat Commun* **5**, 5106-5117.

Simonin P., Jurgens U.J. and Rohmer M. 1996. Bacterial triterpenoids of the hopane series from the prochlorophyte *Prochlorothrix hollandica* and their intracellular localization. *Eur J Biochem* **241**, 865-871.

Simonin P., Tindall B. and Rohmer M. 1994. Structure elucidation and biosynthesis of 31-methylhopanoids from *Acetobacter europaeus*. Studies on a new series of bacterial triterpenoids. *Eur J Biochem* **225**, 765-771.

Sohlenkamp C. and Geiger O. 2016. Bacterial membrane lipids: diversity in structures and pathways. *FEMS microbiology reviews* **40**, 133-159.

Srinivas A., Vinay Kumar B., Divya Sree B., Tushar L., Sasikala Ch. and Ramana Ch.V. 2014. *Rhodovulum salis* sp. nov. and *Rhodovulum viride* sp. nov., phototrophic alphaproteobacteria isolated from marine habitats. *Int J Syst Evol Microbiol* **64**, 957-962.

Stanier R.Y. and Cohen-Bazire G. 1977. Phototrophic prokaryotes: the cyanobacteria. *Annual review of microbiology* **31**, 225-274.

Street I.P. and Poulter C.D. 1990. Isopentenyldiphosphate:dimethylallyldiphosphate isomerase: construction of a high-level heterologous expression system for the gene from *Saccharomyces cerevisiae* and identification of an active-site nucleophile. *Biochemistry* **29**, 7531-7538.

Subhash Y., Tushar L., Sasikala Ch. and Ramana Ch.V. 2013a. *Erythrobacter odishensis* sp. nov. and *Pontibacter odishensis* sp. nov. isolated from dry soil of a solar saltern. *Int J Syst Evol Microbiol* **63**, 4524-4532.

Subhash Y., Tushar L., Sasikala Ch. and Ramana Ch.V. 2013b. *Falsirhodobacter halotolerans* gen. nov., sp. nov., isolated from dry soils of a solar saltern. *Int J Syst Evol Microbiol* **63**, 2132-2137.

Subhash Y., Tushar L., Sasikala Ch. and Ramana Ch.V. 2013c. *Mongoliicoccus alkaliphilus* sp. nov. and *Litoribacter alkaliphilus* sp. nov., isolated from salt pans. *Int J Syst Evol Microbiol* **63**, 3457-3462.

Subhash Y., Tushar L., Sasikala Ch. and Ramana Ch.V. 2013d. *Vogesella alkaliphila* sp. nov., isolated from an alkaline soil, and emended description of the genus Vogesella. *Int J Syst Evol Microbiol* **63**, 2338-2343.

Summons R.E., Jahnke L.L., Hope J.M. and Logan G.A. 1999. 2-Methylhopanoids as biomarkers for cyanobacterial oxygenic photosynthesis. *Nature* **400**, 554-557.

Swan T.M. and Watson K. 1998. Stress tolerance in a yeast sterol auxotroph: role of ergosterol, heat shock proteins and trehalose. *FEMS Microbiol Lett* **169**, 191-197.

Talbot H.M., Summons R., Jahnke L., Cockell C.S., Rohmer M. and Farrimond P. 2008. Cyanobacterial bacteriohopanepolyol signatures from cultures and natural environmental settings. *Organic Geochemistry* **39**, 232-263.

Talbot H.M. and Farrimond P. 2007. Bacterial populations recorded in diverse sedimentary biohopanoid distributions. *Organic Geochemistry* **38**, 1212-1225.

Talbot H.M., Rohmer M. and Farrimond P. 2007a. Rapid structural elucidation of composite bacterial hopanoids by atmospheric pressure chemical ionisation liquid chromatography/ion trap mass spectrometry. *Rapid Commun Mass Spectrom* **21**, 880-892.

Talbot H.M., Rohmer M. and Farrimond P. 2007b. Structural characterisation of unsaturated bacterial hopanoids by atmospheric pressure chemical ionisation liquid chromatography/ion trap mass spectrometry. *Rapid Commun Mass Spectrom* **21**, 1613-1622.

Tam R. and Saier M.H. 1993. Structural, functional, and evolutionary relationships among extracellular solute-binding receptors of bacteria. *Microbiol Rev* **57**, 320-346.

Tank M. and Bryant D.A. 2015. *Chloracidobacterium thermophilum* gen. nov., sp. nov.: an anoxygenic microaerophilic chlorophotoheterotrophic acidobacterium. *Int J Syst Evol Microbiol* **65**, 1426-1430.

Tritza J.P., Herrmannb D., Bisseretb P., Connanc J. and Rohmera M. 1999. Abiotic and biological hopanoid transformation: towards the formation of molecular fossils of the hopane series. *Organic Geochemistry* **30**, 499-514.

Tushar L., Sasikala Ch. and Ramana Ch.V. 2014. Draft genome sequence of *Rhodomicrobium udaipurense* JA643^{T} with special reference to hopanoid biosynthesis. *DNA Res* **21**, 639-647.

Tushar L., Srinivas A., Sasikala Ch. and Ramana Ch.V. 2015. Hopanoid inventory of *Rhodoplanes* spp. *Arch Microbiol* **197**, 861-867.

van Dongen B.E., Talbot H.M., Schouten S. and Pancost R.D. 2006. Well preserved Paleogene and Cretaceous biomarkers from the Kilwa area, Tanzania. *Organic Geochemistry* **37**, 539-557.

van Meer G., Voelker D.R. and Feigenson G.W. 2008. Membrane lipids: where they are and how they behave. *Nature reviews:Molecular cell biology* **9**, 112-124.

Ventura M., Canchaya C., Tauch A., Chandra G., Fitzgerald G.F., Chater K.F. and van Sinderen D. 2007. Genomics of *Actinobacteria*: tracing the evolutionary history of an ancient phylum. *Microbiology and molecular biology reviews* **71**, 495-548.

Vilcheze C., Pierre L., Neunlist S., Poralla K. and Rohmer M. 1994. Prokaryotic triterpenoids: new hopanoids from the nitrogen-fixing bacteria *Azotobacter vinelandii*, *Beijerinckia indica* and *Beijerinckia mobilis*. *Microbiology* **140**, 2749-2753.

Vishnuvardhan R.S., Tushar L., Ramana Ch.V. and Sasikala Ch. 2013a. *Cohaesibacter haloalkalitolerans* sp. nov., isolated from a soda lake, and emended description of the genus *Cohaesibacter*. *Int J Syst Evol Microbiol* **63**, 4271-4276.

Vishnuvardhan R.S., Aspana S., Tushar L., Sasikala Ch. and Ramana Ch.V. 2013b. *Spirochaeta sphaeroplastigenens* sp. nov., a halo-alkaliphilic, obligately anaerobic spirochaete isolated from soda lake Lonar. *Int J Syst Evol Microbiol* **63**, 2223-2228.

Volkman J.K. 2003. Sterols in microorganisms. *Appl Microbiol Biotechnol* **60**, 495-506.

Wang W.Z., Morohoshi T., Ikenoya M., Someya N. and Ikeda T. 2010. *AiiM*, a novel class of N-acylhomoserine lactonase from the leaf-associated bacterium *Microbacterium testaceum*. *Appl Environ Microbiol* **76**, 2524-2530.

Wayne L.G., Brenner D.J., Colwell R.R., Grimont P.A.D., Kandler O., Krichevsky M.I., Moore L.H., Moore W.E.C., Murray R.G.E., Stackebrandt E., Starr M.P. and

Truper H.G. 1987. Report of the Ad Hoc committee on reconciliation of approaches to bacterial systematics. *Int J Syst Evol Microbiol* **37**, 463-464.

Wei J.H., Yin X. and Welander P.V. 2016. Sterol synthesis in diverse bacteria. Front *Microbiol* **7**, 990-1009.

Welander P.V., Doughty D.M., Wu C.H., Mehay S., Summons R. and Newman D.K. 2012. Identification and characterization of *Rhodopseudomonas palustris* TIE-1 hopanoid biosynthesis mutants. *Geobiology* **10**, 163-177.

Welander P.V., Hunter R.C., Zhang L., Sessions A.L., Summons R.E. and Newman D.K. 2009. Hopanoids Play a Role in Membrane Integrity and pH Homeostasis in *Rhodopseudomonas palustris* TIE-1. *Journal of Bacteriology* **191**, 6145–6156.

Zhang Y.M. and Rock C.O. 2008. Membrane lipid homeostasis in bacteria. *Nature reviews*: *Microbiology* **6**, 222-233.

PUBLICATIONS

8.0 Publications

1. Ramaprasad E.V.V., **Tushar L.,** Bharti D., Sasikala Ch. and Ramana Ch.V. 2016. *Rhodovulum algae* sp. nov., isolated from an algal mat. *Int J Syst Evol Microbiol,* **66**, 3367-3371
2. Srinivas A., Divyasree B., Sasikala Ch., **Tushar L.,** Bharti D. and Ramana Ch.V. 2016. Description of *Jeotgalibacillus alkaliphilus* sp. nov., isolated from a solar salt pan, and *Jeotgalibacillus terrae* sp. nov., a name to replace '*Jeotgalibacillus soli'* Chen et al. 2010 *Int J Syst Evol Microbiol,* **66**, 5167-5172
3. Srinivas A., Divyasree B., **Tushar L.,** Sasikala Ch. and Ramana Ch.V. 2016. *Salinicoccus amylolyticus* sp. nov., isolated from a saltern. *Int J Syst Evol Microbiol,* **66**, 3814-3820
4. Sadaf K., **Tushar L.,** Nirosha P., Appa Rao P., Sasikala Ch. and Ramana Ch.V. 2016. *Paenibacillus arachidis* sp. nov., isolated from groundnut seeds. *Int J Syst Evol Microbiol* **66**, 2923-2928
5. Sasijyotsana T. S., **Tushar L.,** Sasikala Ch. and Ramana Ch.V. 2016. *Paraclostridium benzoelyticum* gen. nov. sp. nov., isolated from marine sediment and reclassification of *Clostridium bifermentans* as *Paraclostridium bifermentans* comb. nov. Proposal of a new genus *Paeniclostridium* gen. nov. to accommodate *Clostridium sordellii* and *Clostridium ghonii*. *Int J Syst Evol Microbiol.* **66**, 1268-1274
6. Sravanthi T., **Tushar L.,** Sasikala Ch. and Ramana Ch.V. 2015. *Alkalispirochaeta cellulosivorans* gen. nov., sp. nov., a novel cellulose hydrolyzing, alkaliphilic, halotolerant bacterium isolated from the gut of wood eating cockroach (*Cryptocercus*) and reclassification of four Spirochaeta spp. *Int J Syst Evol Microbiol.* **66**,1612-9
7. Sravanthi T., **Tushar L.,** Sasikala Ch. and Ramana Ch.V. 2015. *Spirochaeta odontotermitis* sp. nov., a novel obligately anaerobic, cellulolytic, halotolerant, alkaliphilic spirochaete isolated from the termite, *Odontotermes obesus* (Rambur) gut. *Int J Syst Evol Microbiol.* **65,** 4589-94.
8. **Tushar L.,** Sasi Jyothsna T.S., Sasikala Ch. and Ramana Ch.V. 2015. Draft Genome Sequence of Antimicrobial-Producing *Clostridium* sp. JC272, Isolated from Marine Sediment. *Genome Announc*. **3**, e00650-15
9. **Tushar L.,** Srinivas A., Sasikala Ch. and Ramana Ch.V. 2015. Hopanoid inventory of the genus *Rhodoplanes. Archieves of Microbiology.* **197,** 861-867.

10. **Tushar L.**, Sravanthi T., Sasikala Ch. and Ramana Ch.V. 2015. Draft Genome Sequence of *Spirochaeta sp*. Strain JC202, an Endosymbiont of the Termite (*Isoptera*) Gut. *Genome Announc*. 3, e01481-14
11. Shivani Y., Subhash Y., **Tushar L.**, Sasikala Ch. and Ramana Ch.V. 2015. *Spirochaeta lutea* sp. nov., isolated from marine habitats and emended description of the genus Spirochaeta. *Syst Appl Microbiol*. **38**, 110-114
12. **Tushar L.**, Sasikala Ch. and Ramana Ch.V. 2014. Draft genome sequence of *Rhodomicrobium udaipurense* JA643^T with special reference to hopanoid biosynthesis. *DNA Research.* **21**, 639-47
13. Rahul D., Sasikala Ch., **Tushar L.**, Roy D. and Ramana Ch.V. 2014. *Alcanivorax xenomutans* sp. nov., a hydrocarbonoclastic bacterium isolated from a shrimp pond. *Int J Syst Evol Microbiol.* **64**, 3553-8.
14. Srinivas A., Vinay Kumar B., Divya Sree B., **Tushar L.**, Sasikala Ch. and Ramana Ch. V. 2014. *Rhodovulum salis* sp. nov. and *Rhodovulum viride* sp. nov., phototrophic Alphaproteobacteria isolated from marine habitats. *Int J Syst Evol Microbiol*, **64,** 957–962
15. Kathiravan R., Jegan S., Ganga V., Prabavathy V.R., **Tushar L.**, Sasikala Ch. and Ramana Ch.V. 2013. *Ciceribacter lividus* gen. nov., sp. nov., isolated from rhizosphere soil of chick pea (*Cicer arietinum* L.). *Int J Syst Evol Microbiol,* **63**, 4484-8
16. Subhash Y., **Tushar L.**, Sasikala Ch. and Ramana ChV. (2013). *Erythrobacter odishensis* sp. nov. and *Pontibacter odishensis* sp. nov. isolated from a dry soil of a solar saltern. *Int J Syst Evol Microbiol,* **63,** 4524-32
17. Ramana Ch.V., Srinivas A., Subhash Y., **Tushar L.**, Mukharjee T., Usha Kiran P. and Sasikala Ch. (2013). *Salinicoccus halitifaciens* sp. Nov., a novel bacterium participating in halite formation. *Antonie van Leeuwenhoek.,* **103**, 885-98
18. Vishnuvardhan S. R., **Tushar L.**, Sasikala Ch. and Ramana Ch.V. 2013. *Cohaesibacter haloalkalitolerans* sp. nov., isolated from Lonar soda lake, India and emended description of the genus Cohaesibacter. *Int J Syst Evol Microbiol,* **63**, 4271-6.
19. Subhash Y., **Tushar L.**, Sasikala Ch. and Ramana Ch.V. 2013. *Mongoliicoccus alkaliphilus* sp. nov. and *Litoribacter alkaliphilus* sp. nov. isolated from salt pans. *Int J Syst Evol Microbiol,* **63,** 3457-62
20. Ramana V.V., Shalem Raj P., **Tushar L.**, Sasikala Ch. and Ramana Ch.V. 2013. *Rhodomicrobium udaipurense* sp. Nov., a psychrotolerant phototrophic alphaproteobacterium isolated from a fresh water stream. *Int J Syst Evol Microbiol,* **63**, 2684-9

21. Subhash Y., **Tushar L.**, Sasikala Ch. and Ramana Ch.V. 2013. *Vogesella alkaliphila* sp. nov., isolated from an alkaline soil, and emended description of the genus *Vogesella*. *Int J Syst Evol Microbiol,* **63,** 2338-43
22. Vishnuvardhan S.R., Aspana S., **Tushar L.**, Sasikala Ch. and Ramana Ch.V. 2013. *Spirochaeta sphaeroplastigenens* sp. nov., a novel halo-alkaliphilic, obligately anaerobic spirochaete isolated from soda lake Lonar, India. *Int J Syst Evol Microbiol,* **63,** 2223-8
23. Subhash Y., **Tushar L.**, Sasikala Ch. and Ramana Ch.V. 2013. *Falsirhodobacter halotolerans* gen. nov., sp. nov., isolated from a dry soil of a solar saltern. *Int J Syst Evol Microbiol,* **63**, 2132-7

International Journal of Systematic and Evolutionary Microbiology (2016), **66**, 3367–3371 **DOI** 10.1099/ijsem.0.001203

Rhodovulum algae sp. nov., isolated from an algal mat

E. V. V. Ramaprasad,[1] L. Tushar,[1] Bharti Dave,[2] Ch. Sasikala[3] and Ch. V. Ramana[1]

Correspondence
Ch. Sasikala
sasi449@yahoo.ie
Ch. V. Ramana
cvr449@gmail.com

[1]Department of Plant Sciences, School of Life Sciences, University of Hyderabad, P.O. Central University, Hyderabad 500 046, India

[2]Department of Life Sciences, Maharaja Krishnakumarsinhji Bhavnagar University, Bhavnagar 364002, Gujarat, India

[3]Bacterial Discovery Laboratory, Centre for Environment, IST, JNT University Hyderabad, Kukatpally, Hyderabad-500 085, India

A reddish-brown-pigmented, phototrophic bacterium, designated strain JA877^T, was isolated from a brown algae mat sample collected from Jalandhar beach, Gujarat, India. On the basis of the 16S rRNA gene sequence, strain JA877^T belongs to the class *Alphaproteobacteria* and is closely related to the type strains *Rhodovulum viride* JA756^T (99.0 %), *Rhodovulum sulfidophilum* Hansen W4^T (98.9 %), *Rhodovulum visakhapatnamense* JA181^T (98.8 %), *Rhodovulum kholense* JA297^T (97.5 %) and *Rhodovulum salis* JA746^T (97.0). However, strain JA877^T showed only 20–45 % relatedness with its phylogenetic neighbours and had a ΔT_m between 5.8 and 7.0 °C. The major respiratory quinone was ubiquinone-10 (Q10), and the polar lipid profile was composed of the major components phosphatidylglycerol, phosphatidylethanolamine, an unidentified phospholipid, two unidentified sulfolipids and five unidentified lipids. The major fatty acids were $C_{18:1}\omega5c$, $C_{18:1}\omega7c/C_{18:1}\omega6c$, $C_{16:0}$ and $C_{18:0}$. The DNA G+C content was 64.5 mol%. On the basis of 16S rRNA gene sequence analysis, physiological data, and chemotaxonomic and molecular differences, strain JA877^T is significantly different from other species of the genus *Rhodovulum* and represents a novel species, for which the name *Rhodovulum algae* sp. nov. is proposed. The type strain is JA877^T (=LMG 29228^T= KCTC 42963^T).

Members of genus *Rhodovulum (Rdv.)* are phototrophic, isolated from marine habitats and form a distinct monophyletic 16S rRNA gene cluster with no interspersing chemotrophs. At the time of writing, there were 19 species with validly published names assigned to this genus (Divyasree *et al.,* 2016). In this study, we isolated a strain (JA877^T) from a brown algae mat sample and found that the 16S rRNA gene sequence of the isolate was related to those of species of the genus *Rhodovulum*. Here we describe the phenotypic, physiological and chemotaxonomic features of this isolate.

Abbreviations: ML, maximum-likelihood; MP, maximum-parsimony; NJ, neighbour-joining.

The GenBank/EMBL/DDBJ accession number for the 16S rRNA gene sequence of strain JA877^T is LN908891.

Five supplementary figures and two supplementary tables are available with the online Supplementary Material.

Strain JA877^T was isolated from a brown algae mat sample collected from Jalandhar beach, Gujarat, India (GPS positioning of the sample collection site: 20° 709′ N 70° 985′ E), on 21 December 2014. One gram brown algae mat was serially diluted [10-fold dilution in saline (0.9 % NaCl)] and plated on a Zobell's marine agar (MA) medium (Himedia, India, cat no. M384). Three distinct colony morphologies were observed from plates incubated at 30 °C for 6 days. Reddish-brown-pigmented colonies were purified by subsequent streaking on the same medium. The purified isolate was designated strain JA877^T and further the strain was preserved as glycerol stocks and stored at 4 °C. For routine culturing and for physiological tests, strain JA877^T was grown in a medium described previously (Srinivas *et al.,* 2014) in 50 ml fully filled, screw-capped bottles incubated at 30 °C under 200 W m^{-2} of illumination by a tungsten lamp for 7 days under anaerobic conditions.

Genomic DNA was isolated and purified by the method described by Marmur (1961), and the G+C content (mol%)

International Journal of Systematic and Evolutionary Microbiology (2016), **66**, 5167–5172 **DOI** 10.1099/ijsem.0.001491

Description of *Jeotgalibacillus alkaliphilus* sp. nov., isolated from a solar salt pan, and *Jeotgalibacillus terrae* sp. nov., a name to replace '*Jeotgalibacillus soli*' Chen *et al.* 2010

A. Srinivas,[1] B. Divyasree,[1] Ch. Sasikala,[1] L. Tushar,[2] Dave Bharti[3] and Ch. V. Ramana[2]

Correspondence
Ch. Sasikala
sasi449@yahoo.ie
Ch. V. Ramana
cvr449@gmail.com

[1]Bacterial Discovery Laboratory, Center for Environment, Institute of Science and Technology, J.N.T. University Hyderabad, Kukatpally, Hyderabad 500085, India

[2]Department of Plant Sciences, School of Life Sciences, University of Hyderabad, PO Central University, Hyderabad 500046, India

[3]Department of Life Sciences, Majaraja Krishnakumarsinhji Bhavnagar University, Bhavnagar, Gujarat 364002, India

A Gram-stain-positive, non-motile, rod-shaped bacterium (strain JC303^T) isolated from a salt pan was identified based on 16S rRNA gene sequence analysis as a member of the genus *Jeotgalibacillus*. It was related most closely to *Jeotgalibacillus salarius* ASL-1^T (99.1 % similarity), *Jeotgalibacillus alimentarius* YKJ-13^T (97.9 %), *Jeotgalibacillus soli* JSM 081008 (97.9 %), *Jeotgalibacillus malaysiensis* D5^T (97.8 %), *Jeotgalibacillus marinus* DSM 1297^T (96.3 %), *Jeotgalibacillus campisalis* SF-57^T (96.1 %) and *J. soli* P9^T (94.9 %). Genomic relatedness based on DNA–DNA hybridization of strain JC303^T with the type strains of the closest related species was less than 40 %. Diphosphatidylglycerol, three aminophospholipids, an unidentified aminoglycolipid, two unidentified phospholipids and an unidentified lipid were the polar lipids of strain JC303^T. Major (>10 %) fatty acids were anteiso-$C_{15:0}$, iso-$C_{15:0}$ and iso-$C_{14:0}$. Cell-wall amino acids contained peptidoglycan with L-lysine as the diagnostic diamino acid. Strain JC303^T contained MK-7 as the predominant (96 %) menaquinone with the presence of a significant amount (4 %) of MK-8. The DNA G+C content was 43 mol%. On the basis of morphological, physiological, genotypic, phylogenetic and chemotaxonomic analyses, strain JC303^T is considered to represent a novel species of the genus *Jeotgalibacillus,* for which the name *Jeotgalibacillus alkaliphilus* sp. nov. is proposed. The type strain is JC303^T (=KCTC 33662^T=LMG 28756^T). In addition, we propose to rename *J. soli* (Chen *et al.*, 2010), an illegitimate homonym of the validly published name *Jeotgalibacillus soli* (Cunha *et al.*, 2012) as *Jeotgalibacillus terrae* sp. nov. with type strain JSM 081008^T (=DSM 22174^T=KCTC 13528^T).

The genus *Jeotgalibacillus*, which belongs to the family *Planococcaceae*, a member of the phylum *Firmicutes*, was first proposed by Yoon *et al.* (2001). The genus includes six species with validly published names: *Jeotgalibacillus alimentarius* (Yoon *et al.*, 2001), *J. soli* (Cunha *et al.*, 2012), *J. salarius* (Yoon *et al.*, 2010), *J. marinus* (Rüger, 1983; Rüger & Richter, 1979), *J. campisalis* (Yoon *et al.*, 2004) and *J. malaysiensis* (Yaakop *et al.*, 2015). The name '*Jeotgalibacillus soli*' previously published by Chen *et al.* (2010) represented by isolate JSM 081008 (=DSM 22174=KCTC 13528) did not appear on a validation list and thus currently has no standing in the nomenclature. It should not be confused with *Jeotgalibacillus soli* described by Cunha *et al.* (2012). Thus, the effectively but not validly published name *Jeotgalibacillus soli* (Chen *et al.*, 2010) is illegitimate (Rule 53; Parker *et al.*, 2016) because

Abbreviations: ME, minimum-evolution; ML, maximum-likelihood; NJ, neighbour-joining.

The GenBank/EMBL/DDBJ accession number for the 16S rRNA gene sequence of strain JC303^T is LN866628.

Four supplementary figures and one supplementary table are available with the online Supplementary Material.

International Journal of Systematic and Evolutionary Microbiology (2016), **66**, 3814–3820 **DOI** 10.1099/ijsem.0.001270

Salinicoccus amylolyticus sp. nov., isolated from a saltern

A. Srinivas,[1] B. Divyasree,[1] L. Tushar,[2] G. Suresh,[2] Ch. Sasikala[1] and Ch. V. Ramana[2]

Correspondence
Ch. Sasikala
sasi449@yahoo.ie
Ch. V. Ramana
cvr449@gmail.com

[1]Bacterial Discovery Laboratory, Center for Environment, Institute of Science and Technology, J. N. T. University Hyderabad, Kukatpally, Hyderabad 500085, India

[2]Department of Plant Sciences, School of Life Sciences, University of Hyderabad, P. O. Central University, Hyderabad 500046, India

A Gram-stain-positive coccus, strain JC304^T, was isolated from a saltern of Nari along the Bhavnagar Coast, Gujarat, India. The 16S rRNA gene sequence analysis and sequence comparison data indicated that JC304^T represented a member of the genus *Salinicoccus* and was most closely related to *Salinicoccus roseus* 9^T (99.6 %), *Salinicoccus luteus* YIM 70202^T (97.0 %), *Salinicoccus hispanicus* J-82^T (97.0 %) and the remaining species of the genus *Salinicoccus* (<97 %). Genome relatedness based on DNA–DNA hybridization of JC304^T with the type strains of the most closely related species was less than 46 % and the ΔT_m was >5 °C indicating that the strain represents a novel species of the genus *Salinicoccus*. Independent and concatenated phylogenetic analysis of *recA*/*fusA* gene translated product showed a clear distinction of JC304^T from its phylogenetic neighbors. Diphosphotidylglycerol, phosphatidylglycerol, an unidentified glycolipid and three unidentified lipids (L1, L2 and L3) were the polar lipids of JC304^T. Iso-$C_{15:0}$ and anteiso-$C_{15:0}$ were the major (>10 %) fatty acids in strain JC304^T. The cell-wall amino acids were L-lysine and D-glycine. Hopanoids were not detected. The major isoprenoid quinone was menaquinone (MK-6). The DNA G+C content of JC304^T was 48 mol%. On the basis of physiological, genotypic, phylogenetic and chemotaxonomic analyses, strain JC304^T is considered to represent a novel species of the genus *Salinicoccus*, for which the name *Salinicoccus amylolyticus* sp. nov. is proposed. The type strain is JC304^T (=KCTC 33661^T=LMG 28757^T).

The genus *Salinicoccus* was first proposed by Ventosa *et al.* (1990) and belongs to the family *Staphylococcaceae*, a member of the phylum Firmicutes. Species of the genus *Salinicoccus* have been isolated from salt mines (Chen *et al.*, 2007, 2009; Franca *et al.*, 2006; Wang *et al.*, 2008; Ramana *et al.*, 2013), soda lake (Zhang *et al.*, 2002), fermented foods (Aslam *et al.*, 2007; Pakdeeto *et al.*, 2007; Jung *et al.*, 2010), desert soil (Zhang *et al.*, 2007), sea water (Qu *et al.*, 2012), waste waters (Amoozegar *et al.*, 2008) and rhizosphere soil (Kämpfer *et al.*, 2011). The genus *Salinicoccus* includes 15 species with validly published names (http://www.bacterio.net/salinicoccus.html). Members of the genus *Salinicoccus* are moderately halophilic, aerobic, Gram-stain-positive cocci, which are chemotaxonomically characterized by having menaquinone-6 (MK-6) as the predominant isoprenoid quinone, a cell wall peptidoglycan type based on L-Lys-D-Gly_5 and a DNA G+C content of 46–51 mol% (Ventosa *et al.*, 1992). '*Salinicoccus kekensis*' (Gao *et al.*, 2010) and '*Salinicoccus salitudinis*' (Chen *et al.*, 2007) are later additions to the genus whose names have not been validly published at the time of writing.

During our studies on bacterial diversity of hypersaline habitats of India, strain JC304^T was isolated from soil collected from a salt pan at Nari along the Bhavnagar Coast, Gujarat, India (GPS position of sampling site: 21°78′ N 72°08′ E) after serial dilution (in 0.8 % w/v NaCl) and plating on marine agar 2216 (MA, pH 9; Himedia). Several different colony morphologies were observed on plates that had been incubated at 30 °C for 2 weeks. A pink–red colored colony was purified by repeated streaking and the the purified isolate was designated as JC304. On MA medium, colonies of JC304^T were circular, smooth, slightly elevated, approximately 2 mm in diameter and pink–red. JC304^T cells were observed after Gram-staining (protocol of Norrell & Messley, 1997) using a BH-2 phase contrast microscope (Olympus). Cells were coccus shaped (1.0–2.5 μm; Fig. S1, available in the online

Abbreviation: MLSA, multilocus sequence analysis.

The Genbank/EMBL/DDBJ accession number for the 16S rRNA gene sequences of strain JC304^T is LN866629.

One supplementary table and seven supplementary figures are available with the online Supplementary Material.

Paenibacillus arachidis sp. nov., isolated from groundnut seeds

K. Sadaf,[1] L. Tushar,[1] P. Nirosha,[1] A. R. Podile,[1] Ch. Sasikala[2] and Ch. V. Ramana[1]

Correspondence
A. R. Podile
podilerao@gmail.com
Ch. V. Ramana
cvr449@gmail.com

[1]Department of Plant Sciences, School of Life Sciences, University of Hyderabad, P.O. Central University, Hyderabad 500046, India

[2]Bacterial Discovery Laboratory, Centre for Environment, Institute of Science and Technology, J. N. T. University Hyderabad, Kukatpally, Hyderabad 500 085, India

A Gram-stain-positive, endospore-forming, rod-shaped, facultatively anaerobic bacterium, designated as strain E3^T, was isolated from groundnut seeds. Based on the 16S rRNA gene sequence analysis, strain E3^T belongs to the genus *Paenibacillus* with P*aenibacillus thailandensis* S3-4A^T (96.0 %), *Paenibacillus xanthinilyticus* 11N27^T (95.7 %), *Paenibacillus mendelii* C/2^T (95.7 %) and other members of the genus *Paenibacillus* (<95.5 %) as its closest phylogenetic neighbours. The DNA G+C content of strain E3^T was 53 mol%. Strain E3^T was positive for gelatin hydrolysis, ammonification, catalase, chitinase production, 1-aminocyclopropane-1-carboxylate (ACC) deaminase activity, HCN production, siderophore production, biofilm formation, and urea and starch hydrolysis. Strain E3^T had phosphatidylethanolamine, diphosphotidylglycerol, phosphatidylcholine, an unidentified aminophospholipid, two unidentified aminolipids and two unidentified lipids as polar lipids. Strain E3^T had diploptene, deplopterol and bacteriohopaneterol as major hopanoids. anteiso-$C_{15:0}$ was the predominant cellular fatty acid with significant proportions of iso-$C_{16:0}$, $C_{16:0}$, $C_{17:0}$, anteiso-$C_{17:0}$, $C_{18:1}\omega9c$ and iso-$C_{14:0}$. Strain E3^T had *meso*-diaminopimelic acid as the diagnostic diamino acid in the cell-wall peptidoglycan. On the basis of physiological, biochemical, chemotaxonomic and molecular analysis, strain E3^T represents a novel species of the genus *Paenibacillus*, for which the name *Paenibacillus arachidis* sp. nov. is proposed. The type strain is E3^T (=KCTC 33574^T=LMG 28417^T).

The genus *Paenibacillus* is a group of Gram-stain-positive, endospore-forming, rod-shaped, facultatively anaerobic bacteria, which branched off from the genus *Bacillus* (Ash *et al.*, 1993; Shida *et al.*, 1997; Achouak *et al.*, 1999). Plant-associated species of the genus *Paenibacillus* have been isolated from roots (Nielsen & Sorensen, 1997; Berge *et al.*, 2002), leaves (De Oliveira Costa *et al.*, 2012) or seeds (Liu *et al.*, 2010). During a survey on the bacteria associated with groundnut seeds, we isolated a strain (E3^T) which belongs to the genus *Paenibacillus* based on 16S rRNA gene sequence analysis, and characterized it using a polyphasic taxonomic analysis as described by Heyndrickx *et al.* (1996). Species of the genus *Paenibacillus* are widely recognized as plant growth promoting rhizobacteria, which promote plant growth through an array of mechanisms and are thus exploited in agricultural practices (Oedjijono & Dragar, 1993; Lebuhn *et al.*, 1997; Weid *et al.*, 2002; Cheong *et al.*, 2005; da Mota *et al.*, 2008; Das *et al.*, 2010a; Ghazalibiglar *et al.*, 2015).

Strain E3^T was isolated from groundnut seed. Briefly, seed coat was removed and the seeds surface sterilized with 2.5 % (w/v) sodium hypochlorite (NaOCl) for 5 min, followed by washing with sterile double-distilled water. The washed seeds were triturated (using a mortar and pestle in a small volume of 1× PBS buffer, pH 7) and diluted to 15 ml with 1× PBS buffer and incubated at 37 °C for 15 min to maintain osmolarity. Two percent of the diluted triturate was added to Luria Bertani (LB) agar and incubated at 37 ±2 °C until colonies appeared. Only one type of colony appeared after 5 days of incubation. The culture was further purified by repeated streaking. The purified culture was

Abbreviations: ACC, 1-aminocyclopropane-1-carboxylate; ME, minimum-evolution; ML, maximum-likelihood; NJ, neighbour-joining.

The GenBank/EMBL/DDBJ accession number for the 16S rRNA gene sequence of strain E3^T is KJ572789.

Two supplementary figures and one supplementary table are available with the online Supplementary Material.

Paraclostridium benzoelyticum gen. nov., sp. nov., isolated from marine sediment and reclassification of *Clostridium bifermentans* as *Paraclostridium bifermentans* comb. nov. Proposal of a new genus *Paeniclostridium* gen. nov. to accommodate *Clostridium sordellii* and *Clostridium ghonii*

T. S. Sasi Jyothsna,[1] L. Tushar,[1] Ch. Sasikala[2] and Ch. V. Ramana[1]

[1]Department of Plant Sciences, School of Life Sciences, University of Hyderabad, P.O. Central University, Hyderabad 500 046, India

[2]Bacterial Discovery Laboratory, Centre for Environment, Institute of Science and Technology, J. N. T. University Hyderabad, Kukatpally, Hyderabad 500 085, India

Correspondence
Ch. Sasikala
sasi449@yahoo.ie
Ch. V. Ramana
cvr449@gmail.com

Twenty-three rod-shaped, endospore-forming, Gram-stain-positive, obligately anaerobic bacteria were isolated from different marine sediment samples of Gujarat. All 23 strains shared 16S rRNA gene sequence similarity of ~100 %. Strain JC272^T was designated the type strain and shared highest sequence similarity with *Clostridium bifermentans* ATCC 638^T (99.8 %), *Clostridium ghonii* JCM 1400^T (98.0 %), *Clostridium sordellii* ATCC 9714^T (97.9 %) and other members of the genus *Clostridium* (<96.4 %). $C_{16:0}$, $C_{18:0}$, $C_{17:0}$, $C_{16:1}\omega 9c$ and iso-$C_{16:0}$ were the major (>5 %) fatty acids. Strain JC272^T contained diphosphatidylglycerol, phosphatidylglycerol, phosphatidylethanolamine, phosphatidylcholine and two unidentified amino lipids. Genome-based analysis of average nucleotide identity (ANI) and *in silico* DNA–DNA hybridization (DDH) of strain JC272^T with *C. bifermentans* ATCC 638^T yielded values of 94.35 and 58.5 ± 2.8 %, respectively. The DNA G+C content of strain JC272^T was 28.3 mol%. Strain JC272^T together with *C. bifermentans* were found to fall outside *Clostridium* rRNA cluster I considered as *Clostridium senso stricto*. Based on ANI value, *in-silico* DDH, and distinct morphological and physiological differences from the previously described taxa, we suggest that strain JC272^T represents a novel species of a new genus in the family *Clostridiaceae*, for which the name *Paraclostridium benzoelyticum* gen. nov., sp. nov. is proposed. The type strain is JC272^T (=KCTC 15476^T=LMG 28745^T). It is also proposed to transfer *C. bifermentans* to this new genus, as *Paraclostridium bifermentans* comb. nov. (type strain ATCC 638^T=DSM 14991^T=JCM 1386^T). The genus *Paeniclostridium* gen. nov. is proposed to accommodate *C. sordellii* and *C. ghonii* as *Paeniclostridium sordellii* comb. nov. (type strain ATCC 9714^T=LMG 15708^T=JCM 3814^T) and *Paeniclostridium ghonii* comb. nov. (type strain ATCC 25757^T=DSM 15049^T=JCM 1400^T).

1

In an attempt to discover antibiotics from obligately anaerobic bacteria, we have isolated a large number of these organisms from marine habitats of India which belong to the genus *Clostridium*. Based on 16S rRNA gene sequence analysis, the majority of these strains shared highest 16S rRNA gene sequence similarity (>99 %) with *Clostridium bifermentans* ATCC 638^T. *C. bifermentans* and *Clostridium sordellii* are phylogenetically closely related (Nisida *et al.*, 1964; Brooks *et al.*, 1969). Although the type strain *C. bifermentans* ATCC

Abbreviations: ANI, average nucleotide identity; DDH, DNA–DNA hybridization; ME, minimum-evolution; ML, maximum-likelihood; NJ, neighbour-joining.

The GenBank/EMBL accession numbers for the 16S rRNA gene sequence and the draft genome sequence of strain JC272^T are LN846800 and LBBT00000000 (Version LBBT01000000), respectively.

Two supplementary figures and four supplementary tables are available with the online Supplementary Material.

International Journal of Systematic and Evolutionary Microbiology (2016), **66**, 1612–1619 **DOI** 10.1099/ijsem.0.000865

Alkalispirochaeta cellulosivorans gen. nov., sp. nov., a cellulose-hydrolysing, alkaliphilic, halotolerant bacterium isolated from the gut of a wood-eating cockroach (*Cryptocercus punctulatus*), and reclassification of four species of *Spirochaeta* as new combinations within *Alkalispirochaeta* gen. nov.

T. Sravanthi,[1]† L. Tushar,[2]† Ch. Sasikala[1] and Ch. V. Ramana[2]

Correspondence
Ch. Sasikala
sasi449@yahoo.ie
Ch. V. Ramana
cvr449@gmail.com

[1]Bacterial Discovery Laboratory, Centre for Environment, Institute of Science and Technology, J. N. T. University Hyderabad, Kukatpally, Hyderabad 500 085, India

[2]Department of Plant Sciences, School of Life Sciences, University of Hyderabad, P.O. Central University, Hyderabad 500 046, India

An obligately anaerobic spirochaete designated strain JC227^T was isolated from the gut of a wood-eating cockroach, *Cryptocercus punctulatus* (Scudder), from the Rann of Kutch, Gujarat, India. Strain JC227^T was Gram-stain-negative, mesophilic, halotolerant and alkaliphilic. Based on 16S rRNA gene sequence analysis, strain JC227^T belongs to the genus *Spirochaeta*, with *Spirochaeta sphaeroplastigenens* JC133^T (99.51 %), *S. odontotermitis* JC202^T (99.30 %), *S. alkalica* Z-7491^T (99.10 %), *S. americana* (98.54 %) and other members of the genus *Spirochaeta* (<92.7 %) as its closest phylogenetic neighbours. However, DNA–DNA hybridization between strain JC227^T and *S. sphaeroplastigenens* JC133^T, *S. odontotermitis* JC202^T, *S. alkalica* DSM 8900^T and *S. americana* DSM 14872^T was 62±2, 63, 58±2 and 48±4 %, respectively. Strain JC227^T contained phosphatidylglycerol, diphosphatidylglycerol, an unidentified glycolipid and six unidentified lipids. Summed feature $C_{18:1}\omega7c/C_{18:1}\omega6c$ was the predominant cellular fatty acid, with significant proportions of $C_{16:0}$, $C_{14:0}$, $C_{12:0}$, $C_{15:1}\omega6c$, $C_{16:1}\omega5c$, $C_{16:1}\omega6c/C_{16:1}\omega7c$ and $C_{17:0}$ 2-OH. The DNA G+C content of strain JC227^T was 55.5 mol%. On the basis of physiological, biochemical, chemotaxonomic (including metabolomic) and genomic differences from previously described taxa, strain JC227^T can be differentiated from members of the genus *Spirochaeta* and represents a novel species of a new genus, for which the name *Alkalispirochaeta cellulosivorans* gen. nov., sp. nov. is proposed. The type strain of *Alkalispirochaeta cellulosivorans* is JC227^T (=KCTC 15343^T=NBRC 110105^T). We also propose the reclassification of *Spirochaeta sphaeroplastigenens*, *Spirochaeta odontotermitis*, *Spirochaeta alkalica* and *Spirochaeta americana* as *Alkalispirochaeta sphaeroplastigenens* comb. nov. (type strain JC133^T=KCTC 15220^T=NBRC 109056^T), *Alkalispirochaeta odontotermitis* comb. nov. (type strain JC202^T=KCTC 15324^T=NBRC 110104^T), *Alkalispirochaeta alkalica* comb. nov. (type strain Z-7491^T=DSM 8900^T=ATCC 700262^T) and *Alkalispirochaeta americana* comb. nov. (type strain ASpG1^T=ATCC BAA-392^T=DSM 14872^T). The type species of *Alkalispirochaeta* gen. nov. is *Alkalispirochaeta alkalica* comb. nov.

Symbiotic spirochaetes are interesting for two major reasons. First, they are key players in carbon recycling, particularly in the degradation of lignocellulose along with other gut micro-organisms (Berlanga *et al.*, 2007), and second, they are not well characterized taxonomically, since the majority are putative taxa identified through metagenomics (Ohkuma *et al.*, 1999; Shivani *et al.*, 2015;

†These authors contributed equally to this work.

The GenBank/EMBL/DDBJ accession number for the 16S rRNA gene sequence of strain JC227^T is HG531387.

Four supplementary figures and a supplementary table are available with the online Supplementary Material.

Spirochaeta odontotermitis sp. nov., an obligately anaerobic, cellulolytic, halotolerant, alkaliphilic spirochaete isolated from the termite *Odontotermes obesus* (Rambur) gut

T. Sravanthi,[1] L. Tushar,[2] Ch. Sasikala[1] and Ch. V. Ramana[2]

[1]Bacterial Discovery Laboratory, Centre for Environment, Institute of Science and Technology, J. N. T. University Hyderabad, Kukatpally, Hyderabad 500085, India

[2]Department of Plant Sciences, School of Life Sciences, University of Hyderabad, P.O. Central University, Hyderabad 500046, India

Correspondence
Ch. Sasikala
sasi449@yahoo.ie
Ch. V. Ramana
cvr449@gmail.com

A Gram-stain-negative spirocaete (strain JC202^T) was isolated from the gut of the termite *Odontotermes obesus* (Rambur) from Rann of Kutch, Gujarat, India. This strain was obligately anaerobic, mesophilic, halotolerant and required alkaline conditions for growth. Strain JC202^T was resistant to rifampicin and kanamycin, but sensitive to gentamicin, tetracycline, ampicillin and chloramphenicol. Strain JC202^T possessed phosphatidylglycerol, diphosphatidylglycerol, glycolipid and six unidentified lipids. $C_{18:1}\omega7c$ was the predominant cellular fatty acid with significant proportions of $C_{16:0}$, $C_{18:1}\omega9c$, $C_{14:0}$, $C_{18:0}$, $C_{16:1}\omega5c$, $C_{18:1}\omega5c$ and $C_{20:1}\omega9c$. The DNA G+C content of strain JC202^T was 59 mol%. Based on 16S rRNA gene sequence analysis, strain JC202^T is considered to belong to the genus *Spirochaeta* with *Spirochaeta sphaeroplastigenens* JC133^T (100 % similarity), *Spirochaeta alkalica* Z-7491^T (99.92 %), *Spirochaeta americana* ATCC BAA-392^T (99.47 %) and other members of the genus *Spirochaeta* (<93.83 %) as the closest phylogenetic neighbours. However, mean DNA–DNA hydridization values between strain JC202^T and *S. sphaeroplastigenens* JC133^T, *S. alkalica* DSM 8900^T (=Z-7491^T) and *S. americana* DSM 14872^T (=ASpG1^T) were 55±2, 22±3 and 32±1 %, respectively. On the basis of physiological, biochemical, chemotaxonomic (including metabolome) and genomic differences from the previously described taxa, strain JC202^T is differentiated from other members of the genus *Spirochaeta* and is considered to represent a novel species, for which the name *Spirochaeta odontotermitis* sp. nov. is proposed. The type strain is JC202^T (=KCTC 15324^T=NBRC 110104^T).

The genus *Spirochaeta* consists of free-living, saccharolytic, obligately or facultatively anaerobic, helical-shaped bacteria (Paster, 2010). Members of the genus *Spirochaeta* are widely distributed (Canale-Parola, 1992) in aquatic habitats (Breznak & Canale-Parola, 1975), freshwater mud (Canale-Parola, 1980), marine mud (Hespell & Canale-Parola, 1970; Harwood & Canale-Parola, 1983), oilfields (Magot *et al.*, 1997), microbial mats (Teal *et al.*, 1996; Breznak & Warnecke, 2008), termite hindgut (Dröge *et al.*, 2006) and alkaline hypersaline sediments/lakes (Zhilina *et al.*, 1996; Pikuta *et al.*, 2009; Dubinina *et al.*, 2011). Seven of 21 species reported so far in the genus *Spirochaeta* (http://www.bacterio.cict.fr/s/spirochaeta.html), namely *Spirochaeta alkalica*, *Spirochaeta africana*, *Spirochaeta asiatica* (Zhilina *et al.*, 1996), *Spirochaeta americana* (Hoover *et al.*, 2003), *Spirochaeta dissipatitropha* (Pikuta *et al.*, 2009), *Spirochaeta halophila* (Greenberg & Canale-Parola, 1976) and *Spirochaeta perfilievii* (Dubinina *et al.*, 2011), are halo-/alkaliphilic. Through this communication, we add one more halotolerant, alkaliphilic species (represented by strain JC202^T) to the genus *Spirochaeta* isolated from the hindgut of a termite. The genome sequence of strain JC202^T was published recently (Tushar *et al.*, 2015).

Strain JC202^T was isolated from the hindgut of *Odontotermes obesus* (Rambur) from Rann of Kutch (GPS, 23° 12′ 45.77″ N 69° 39′ 20.73″ E) after enrichment in alkaline medium II (Zhilina & Zavarzin, 1994) containing (g l^{-1}) $NaHCO_3$

Abbreviations: ME, minimum-evolution; ML, maximum-likelihood; NJ, neighbour-joining.

1 The GenBank/EMBL/DDBJ accession numbers for the 16S rRNA gene sequence and the draft genome sequence of strain JC202^T are HF968430 and JRAS00000000 (version JRAS01000000), respectively.

2 One supplementary table and three supplementary figures are available with the online Supplementary Material.

genomeA
Journals.ASM.org

Draft Genome Sequence of Antimicrobial-Producing *Clostridium* sp. JC272, Isolated from Marine Sediment

L. Tushar,[a] T. S. Sasi Jyothsna,[a] C. Sasikala,[b] C. V. Ramana[a]

Department of Plant Sciences, School of Life Sciences, University of Hyderabad, Hyderabad, India[a]; Centre for Environment, Bacterial Discovery Laboratory, Institute of Science and Technology, J. N. T. University Hyderabad, Hyderabad, India[b]

We announce the draft genome sequence of *Clostridium* sp. JC272, isolated from a sediment sample collected from marine habitats of Gujarat, India. *Clostridium* sp. JC272 is an obligate anaerobe and has the ability to produce antimicrobial compounds. The genome sequence indicates the strain's capability of producing small peptides (microcins), which are potential novel antibiotics.

Received 15 May 2015 **Accepted** 18 May 2015 **Published** 11 June 2015

Citation Tushar L, Sasi Jyothsna TS, Sasikala C, Ramana CV. 2015. Draft genome sequence of antimicrobial-producing *Clostridium* sp. JC272, isolated from marine sediment. Genome Announc 3(3):e00650-15. doi:10.1128/genomeA.00650-15.

Address correspondence to C. Sasikala, sasi449@yahoo.ie.

There is limited information about antibiotics and secondary metabolites produced by obligate anaerobic bacteria. Whole-genome sequences of *Clostridium* spp. have revealed the wide occurrence of biosynthetic gene clusters coding for polyketide synthases (PKS) and nonribosomal peptide synthases (NRPs) involved in antibiotic biosynthesis (1, 2). The discovery of closthioamide, a polythioamide antibiotic from *Clostridium cellulolyticum* (3) widens the search for novel antibiotics from other members of the genus.

Clostridium sp. JC272 was isolated from a sediment sample collected from Gujrat, India (23°8′82″N and 69°74′E). Genome sequencing was carried out using the Illumina HiSeq 2000 (Illumina, Inc.) platform. Assembly of the raw sequencing data was performed using MaSuRCA (de Bruijn graph and overlap-layout-consensus). Annotation of the assembled data was performed using the Rapid Annotations using Subsystem Technology (RAST) server (4). For antibiotics and secondary metabolites analysis, the antiSMASH (http://antismash.secondarymetabolites.org) server was used. The proposal of strain JC272 as a new species to the genus *Clostridium* is also evidenced from the species identification tool *SpecI*, which is based on core genome analysis and the results supported strain JC272 as a novel species (5).Whole-genome sequencing of strain JC272 yielded a genome of 3,568,807 bp in length. The calculated G+C mol% of the bacterium was 28.3%. Annotation of the genome consisted of 2,174 coding sequences that included 105 RNA genes. Only one copy of the 16S rRNA gene (1,530 bp) was identified in strain JC272. Annotation reveals the presence of 60 genes related to motility and chemotaxis and 149 genes related to cell wall and capsule formation. Eighty-two genes are involved in the biosynthesis of fatty acid, lipids, and isoprenoids. Based on a KEGG analysis using the RAST server, the genome of strain JC272 showed the presence of 11 genes related to nitrogen metabolism, 54 genes related to phosphorus metabolism, and 6 genes related to potassium metabolism. Moreover, 82 genes related to membrane transport and 66 genes related to respiration are also present in the genome of strain JC272. Isoprenoid biosynthesis occurred through the 2-C-methyl-D-erythritol 4-phosphate (MEP) pathway in strain JC272. Hopanoid biosynthetic pathway genes were not found in the draft genome sequence of strain JC272 or in the available 190 genomes of *Clostridium*.

Strain JC272 has gene clusters responsible for the production of microcins, which are responsible for antimicrobial activity (6, 7). Four small peptides (45, 64, 77, and 66 amino acids) were predicted to be microcins from the draft genome of strain JC272, whereas the nearest genome of *C. bifermentans* ATCC 638 has only two sets of genes producing two small peptides (37 and 77 amino acids). These microcins have a two-component system that comprises a sensory histidine kinase (HK) and its cognate response regulator (RR). The HK gets autophosphorylated followed by phosphorylation of the receiver domain of RR (8). Methanolic extracts of strain JC272 show good antimicrobial activity against *E. coli*, *S. aureus*, and *Bacillus* spp., and work is in progress to validate the microcins.

Nucleotide sequence accession numbers. This whole-genome shotgun project has been deposited at DDBJ/EMBL/GenBank under the accession number LBBT00000000. The version described in this paper is the first version, LBBT01000000.

ACKNOWLEDGMENTS

C.S. acknowledges the MoES, Government of India, for financial support. T.S.S.J. acknowledges UGC for a D. S. Kothari postdoctoral fellowship. L.T. acknowledges CSIR-UGC for a fellowship.

REFERENCES

1. **Behnken S, Hertweck C.** 2012. Cryptic polyketide synthase genes in nonpathogenic *Clostridium* spp. PLoS One **7**:e29609. http://dx.doi.org/10.1371/journal.pone.0029609.
2. **Letzel AC, Pidot SJ, Hertweck C.** 2014. Genome mining for ribosomally synthesized and post-translationally modified peptides (RiPPs) in anaerobic bacteria. BMC Genomics **15**:983. http://dx.doi.org/10.1186/1471-2164-15-983.
3. **Lincke T, Behnken S, Ishida K, Roth M, Hertweck C.** 2010. Closthioamide: an unprecedented polythioamide antibiotic from the strictly anaerobic bacterium *Clostridium cellulolyticum*. Angew Chem Int Ed Engl **49**:2011–2013. http://dx.doi.org/10.1002/anie.200906114.
4. **Aziz RK, Bartels D, Best AA, DeJongh M, Disz T, Edwards RA, Formsma**

Arch Microbiol (2015) 197:861–867
DOI 10.1007/s00203-015-1112-5

SHORT COMMUNICATION

Hopanoid inventory of *Rhodoplanes* spp.

Tushar Dilipchand Lodha[1] · Are Srinivas[2] · Chintalapati Sasikala[2] · Chintalapati Venkata Ramana[1]

Received: 9 January 2015 / Revised: 16 April 2015 / Accepted: 17 April 2015 / Published online: 3 May 2015

Abstract Hopanoids are pentacyclic triterpenoid lipids and are important for bacterial membrane stability and functioning. These pentacyclic triterpenoids of hopane series are biomarkers for eubacteria and can be used as chemotaxonomic markers. Anoxygenic phototrophic bacteria are good producers of hopanoids, and their inventory to date is restricted to a few members. *Rhodoplanes* spp. are phototrophic prokaryotes which grow and thrive in subsurface and sediment environments. A study on the diversity of hopanoids of several species of *Rhodoplanes* revealed a rich diversity of hopanoids with carbon length of C_{30}/C_{31} and C_{35}. Hop-22(29)-ene (II), diplopterol (V), tetrahymanol (VII), 2-methyldiplopterol (VI), 2-methyltetrahymanol (VIII), bacteriohopanetetrol (IX), bacteriohopaneaminotriol (X) and bacteriohopanepolyols [BHP-492 (XIII), BHP-550 (XIV), BHP-508 (XII)] are the major hopanoids of the genus *Rhodoplanes*. Tetrahymanol (VII) content is high (38–60 %) among all the members, except for *Rhodoplanes elegans*. Hopanoid fingerprints allowed differentiation of species of the genus *Rhodoplanes*. Statistical analyses also indicate hopanoids as good chemotaxonomic markers to distinguish species of the genus *Rhodoplanes*.

Keywords *Rhodoplanes* spp. · Hopanoids · Biomarker · Chemotaxonomy

Communicated by Erko Stackebrandt.

Electronic supplementary material The online version of this article (doi:10.1007/s00203-015-1112-5) contains supplementary material, which is available to authorized users.

✉ Chintalapati Venkata Ramana
cvr449@gmail.com; cvr449@yahoo.com

[1] Department of Plant Sciences, School of Life Sciences, University of Hyderabad, P.O. Central University, Hyderabad 500 046, India

[2] Bacterial Discovery Laboratory, Centre for Environment, IST, JNT University Hyderabad, Kukatpally, Hyderabad 500 085, India

Introduction

Hopanoids are pentacyclic triterpenoids biosynthesized by bacteria, ferns, fungi, plants, mosses, protists and lichens (Rohmer et al. 1984; Ourisson et al. 1987). They represent the oldest chemofossils or molecular fossils dating back to late Archean times (2.77 billion tears Ga; Blumenberg et al. 2006), to which a discrete biological source can be attributed (Summons et al. 1999). More than 200 hopanoids are identified from both biological and geological sources (Ourisson and Albrech 1992). Biohopanoids are buried in the phospholipid bilayer of bacteria and have function similar to steroids of eukaryotic cells playing key role in regulating and rigidifying the membranes (Talbot et al. 2007). Hopanoids were initially considered to be components of membranes of aerobic bacteria; however, hopanogenesis was independent of oxygen (Blumenberg et al. 2006) and were discovered among many anaerobic bacteria also (Hermans et al. 1991; Talbot et al. 2007; Garcia Costas et al. 2012; Tushar et al. 2014; Tank and Bryant 2015). Even though hopanoids were reported from some phylogenetically related members of cyanobacteria, purple non-sulfur bacteria, acetic acid bacteria, *Alicyclobacillus* sp., nitrogen-fixing bacteria, methylotrophs, methanotrophs and sulfate-reducing bacteria (SRB), no definitive taxonomic conclusions were drawn from their distribution (Rohmer et al. 1984; Neunlist and Rohmer 1985; Neunlist et al. 1988; Hermans et al. 1991; Hartner et al. 2005; Talbot et al. 2007; Blumenberg et al. 2009; Tushar et al. 2014). There are no reports of hopanoids from *Archaea.*

genomeA
Journals.ASM.org

Draft Genome Sequence of *Spirochaeta* sp. Strain JC202, an Endosymbiont of the Termite (*Isoptera*) Gut

L. Tushar,[a] T. Sravanthi,[b] C. Sasikala,[b] C. V. Ramana[a]

Department of Plant Sciences, School of Life Sciences, University of Hyderabad, P. O. Central University, Hyderabad, India[a]; Centre for Environment, Bacterial Discovery Laboratory, IST, JNT University, Hyderabad, Kukatpally Hyderabad, India[b]

We announce here the draft genome sequence of *Spirochaeta* sp. strain JC202 isolated from gut of a termite (*Isoptera*). The genome suggests that *Spirochaeta* sp. JC202 has the capability for natural conjugation with the help of fimbriae and pili. Experimental evidence and the genome sequence suggest that strain JC202 is capable of producing colicin V and a bacteriocin group of peptides in a specific interaction.

Received 9 December 2014 **Accepted** 9 December 2014 **Published** 22 January 2015

Citation Tushar L, Sravanthi T, Sasikala C, Ramana CV. 2015. Draft genome sequence of *Spirochaeta* sp. strain JC202, an endosymbiont of the termite (*Isoptera*) gut. Genome Announc 3(1):e01481-14. doi:10.1128/genomeA.01481-14.

Address correspondence to C. Sasikala, sasi449@yahoo.ie.

Members of the genus *Spirochaeta* are free living or live in association with insects and animals. The termite (*Isoptera*)-*Spirochaeta* association is a good example of symbiosis, in which the host (termite) provides shelter by creating an anaerobic niche and supplements the complex carbon (cellulose) required for the growth of *Spirochaeta* (1). The interactions of *Spirochaeta* with other bacterial systems has not studied to date, with the only exception of *Spirochaeta-Clostridium* enhancing cellulose degradation (2). *Spirochaeta* sp. strain JC202 was isolated from the termite gut and was grown in alkaline medium (3). Sequencing was carried out using Illumina Miseq 2 × 300-bp paired end chemistry. The sequence data were *de novo* assembled using the ABySS assembly software. Annotations were performed with 275 *de novo*-assembled contigs using the Rapid Annotations using Subsystems Technology (RAST) server (4).

The draft genome sequence of *Spirochaeta* sp. JC202 is 3,826,243 bp (3.82 Mb), with a G+C content of 59 mol%. The protein-coding bases total 3,190,883 bp, covering 83.39% of the total bases determined. The protein-coding genes of *Spirochaeta* sp. JC202 have an average length of 871.82 bases, ranging from 70 to 4,796 bases. Out of 3,660 open reading frames (ORFs) identified, 2,299 (62.81%) were functionally annotated, with 1,361 (37.18%) being hypothetical genes. The proposal of strain JC202 being a new species of the genus *Spirochaeta* is also evidenced from the species identification tool SpecI, which is based on core genome analysis, and the results support strain JC202 as a novel species (5).

Strain JC202 has a bacteroides aerotolerance operon (*batABDE*) and all the machinery to derive energy under anaerobic conditions (6). It has all the genes that are involved in periplasmic flagellar synthesis. The late competence protein *comEC* related to DNA transport is present in the genome, which suggests that the genome of strain JC202 is capable of natural competence (7). The draft genome of strain JC202 has around 11 genes involved in chitin and *N*-acetyl glucose amine utilization. Various stress response genes are present in the genome of strain JC202, which are involved mainly in oxidative, metal, temperature, and salt stress. The draft genome of strain JC202 has a HD-Gyp domain-containing gene, which is responsible for signaling and bacterial virulence to plants (8). Although the genomes of several spirochaetas have revealed the presence of genes for bacteriocins, these were never isolated and characterized.

The draft genome of strain JC202 has genes coding for phage terminase, prophage protein, phage capsid, scaffold Psp operon transcriptional activator, phage shock protein, hemagglutinin-like protein, prevent-host-death protein, mobile element protein, and phage peptidoglycan hydrolase. The presence of these viral genes in the genome of *Spirochaeta* sp. JC202 suggests that it is a carrier of prophage. Nuromedin U (*NmU*), coding for a peptide that stimulates the contraction of muscles in rats, is present in the genome of strain JC202, and this gene probably plays an important role in the elasticity of the cell (9).

Nucleotide sequence accession numbers. This whole-genome shotgun project has been deposited at DDBJ/EMBL/GenBank under the accession numbers JRAS00000000 and SRR1562012. The version described in this paper is version JRAS01000000.

ACKNOWLEDGMENTS

This work was funded by Department of Biotechnology (DBT) project. L.T. is supported by a research fellowship from the University Grants Commission (UGC).

We acknowledge Ashwin Kumar Mishra for help with annotations and other related work.

REFERENCES

1. **Graber JR, Leadbetter JR, Breznak JA.** 2004. Description of *Treponema azotonutricium* sp. nov. and *Treponema primitia* sp. nov., the first *Spirochetes* isolated from termite guts. Appl Environ Microbiol **70:**1315–1320. http://dx.doi.org/10.1128/AEM.70.3.1315-1320.2004.
2. **Pohlschroeder M, Leschine SB, Canale-Parola E.** 1994. *Spirochaeta caldaria* sp. nov., a thermophilic bacterium that enhances cellulose degradation by *Clostridium thermocellum*. Arch Microbiol **161:**17–24. http://dx.doi.org/10.1007/BF00248889.

Systematic and Applied Microbiology 38 (2015) 110–114

Contents lists available at ScienceDirect

Systematic and Applied Microbiology

journal homepage: www.elsevier.de/syapm

Spirochaeta lutea sp. nov., isolated from marine habitats and emended description of the genus *Spirochaeta*☆

Y. Shivani[a], Y. Subhash[b], L. Tushar[b], Ch. Sasikala[a], Ch.V. Ramana[b,*]

[a] *Bacterial Discovery Laboratory, Centre for Environment, Institute of Science and Technology, J. N. T. University, Kukatpally, Hyderabad 500 085, India*
[b] *Department of Plant Sciences, School of Life Sciences, University of Hyderabad, P.O. Central University, Hyderabad 500 046, India*

ARTICLE INFO

Article history:
Received 15 July 2014
Received in revised form 5 November 2014
Accepted 17 November 2014

Keywords:
Spirochaeta lutea
Spirochaetes
Whole genome sequencing
Chemotaxonomic analysis

ABSTRACT

Metagenome analysis of forty samples indicated a rich diversity of free living spirochaetes among Indian habitats. Only 2–3% of the total bacterial diversity was represented by spirochaetes with five distinct phylogenetic OTUs. A strain (JC230^T) was brought to cultivation and its 16S rRNA gene sequence showed highest sequence similarity with that of *Spirochaeta asiatica* Z-7591^T (90.78%). Genome sequence analysis of strain JC230^T indicates the presence of 117 genes related to motility and chemotaxis. Strain JC230^T is an obligate anaerobe. It is helical shaped, Gram-stain-negative and catalase and oxidase negative. Strain JC230^T produces carotenoids and have all the genes related to carotenogenesis of spirilloxanthin series. Isoprenoid biosynthesis occurs through HMG-CoA (3-hydroxy-3-methylglutaryl-coenzyme A) pathway. Twelve bacterial haemoglobin and one flavohaemoglobin related genes are present in the genome of strain JC230^T. The genome of strain JC230^T showed the presence of heavy metal resistance related genes of cobalt, zinc, cadmium and arsenic. Six genes related to colicin V and bacteriocin production cluster are present. Major (>2%) fatty acids were $C_{12:0}$, $C_{14:0}$, *iso*-$C_{14:0}$, *iso*-$C_{15:1}$H/$C_{13:0}$3OH, *anteiso*-$C_{15:0}$, $C_{16:0}$, and *iso*-$C_{16:0}$. Strain JC230^T contains diphosphatylglycerol, phosphatydilglycerol, phosphatydilethanolamine, unidentified phospholipid (PL1) and unidentified lipids (L1-7). G + C mol% of strain JC230^T was 54.1%. Distinct morphological, physiological and genotypic differences from the previously described taxa support the classification of strain JC230^T as a representative of a new species in the genus *Spirochaeta*, for which the name *Spirochaeta lutea* sp. nov. is proposed. The type strain is JC230^T (=KCTC 15387^T = DSM 29074^T).

The genus *Spirochaeta* is represented by a large number of free living non-pathogenic, helical shaped bacteria commonly found in the anoxic mud, marshes, marine sediments, soda lakes and microbial mats [1,2,4,8,9,13,17,25]. The genus *Spirochaeta* currently has 17 validly published species names (including the recently described *Spirochaeta psychrophila* [16]) of which, genome sequences for 9 type strains are available. Only one species name added to the genus *Spirochaeta* was based on a strain isolated from India [26]. During a survey of free living spirochaetes, we have analyzed a large number of samples from a few coastal habitats of India and isolated an obligately anaerobic spirochaete, designated it as strain JC230^T which was characterized using polyphasic taxonomy and through genome sequence.

Soil samples collected from Gujarat (GPS positioning of the sample collection site; 23°8′82″N and 69°74′E), Tamil Nadu (GPS positioning of the sample collection site is 9°06′24″N, 79°31′28″E; 8°04′42″N, 77°32′30″E) during December, 2012 were used for metagenome analysis. A total of 40 composite samples were made from the samples collected and soil DNA was extracted from all the samples using HiPurA^{TM} soil DNA isolation kit (Himedia Laboratories Pvt. Ltd, Mumbai, India) according to the manufacturer's protocol, with 0.25 g of soil (dry wt.). An average of 7 ng of DNA was recovered from 1 g of soil sample. The extracted DNA samples were stored at −20 °C. DNA samples were sent for bacterial tag-encoded FLX 454 pyrosequencing to Research and Testing Laboratory LLC (Lubbock, TX, USA). The samples underwent partial amplification of the V1–V3 region of the 16S rRNA gene as described previously [6]. The sequence data obtained after pyrosequencing were processed as described previously [7,19,20]. All taxonomic classification was performed using Mothur's version of the RDP Bayesian classifier, using a RDP training dataset number 9 (available at http://www.mothur.org/wiki/RDP_reference_files). All sequence data are available under the following NCBI SRA accession nos. SRP034851, SRP040491 and SRP034851.

☆ The GenBank/EMBL/DDBJ accession numbers for the 16S rRNA gene sequence and the draft genome sequence of strain JC230^T are HG965770 and JNUP00000000 (version JNUP01000000), respectively.

* Corresponding author. Tel.: +91 8179724006.
E-mail addresses: sasi449@yahoo.ie (Ch. Sasikala), cvr449@yahoo.com, cvr449@gmail.com (Ch.V. Ramana).

http://dx.doi.org/10.1016/j.syapm.2014.11.002
0723-2020/

DNA Research Advance Access published August 12, 2014

DNA Research pp. 1–9, (2014) doi:10.1093/dnares/dsu026

Draft Genome Sequence of *Rhodomicrobium udaipurense* JA643^T with Special Reference to Hopanoid Biosynthesis

L. Tushar[1], Ch. Sasikala[2], and Ch. V. Ramana[1,*]

Department of Plant Sciences, School of Life Sciences, University of Hyderabad, P.O. Central University, Hyderabad 500 046, India[1] and Bacterial Discovery Laboratory, Centre for Environment, IST, JNT University, Hyderabad, Kukatpally, Hyderabad 500 085, India[2]

*To whom correspondence should be addressed. Tel. +91 40-23-134-502. Fax. +91 40-23-010-120. Email: cvr449@yahoo.com

Edited by Dr Naotake Ogasawara
(Received 29 January 2014; accepted 4 July 2014)

Abstract

Hopanoids are present in vast amounts as integral components of bacteria and plants with their primary function to strengthen rigidity of the plasma membrane. To establish their roles more precisely, we conducted sequencing of the whole genome of *Rhodomicrobium udaipurense* JA643^T isolated from a fresh water stream of Udaipur in Himachal Pradesh, India, by using the Illumina HiSeq pair end chemistry of 2 × 100 bp platform. Determined genome showed a high degree of similarity to the genome of *R. vannielii* ATCC17100^T and the 13.7 million reads generated a sequence of 3,649,277 bp possessing 3,611 putative genes. The genomic data were subsequently investigated with respect to genes involved in various features. The machinery required for the degradation of aromatic compounds and resistance to solvents as well as all that required for photosynthesis are present in this organism. Also, through extensive functional annotation, 18 genes involved in the biosynthesis of hopanoids are predicted, namely those responsible for the synthesis of diploptene, diplopterol, adenosylhopane, ribosylhopane, aminobacteriohopanetriol, glycosyl group containing hopanoids and unsaturated hopanoids. The hopanoid biosynthetic pathway was then inferred based on the genes identified and through experimental validation of individual hopanoid molecules. The genome data of *R. udaipurense* JA643^T will be useful in understanding the functional features of hopanoids in this bacterium.

Key words: *Rhodomicrobium udaipurense* JA643^T; genome sequence; Illumina Hiseq; hopanoid biosynthesis pathway

1. Introduction

Hopanoids are a group of natural pentacyclic triterpenoid lipids widely distributed in plant and bacterial systems, act as cell membrane rigidifiers, analogues to sterols present in eukaryotes which have tetracyclic rings. Apart from their biological occurrence, hopanoids were also observed in geo-sediments (geohopanoids) formed due to diagenetic processes and are considered as 'molecular fossils' for ancient bacteria.[1] Till date, ~200 structures of hopanoids are identified from bio-/geo-sources.[2] Hopanoids play a key role in conferring membrane integrity under extreme conditions of stress and any loss in hopanoids makes the bacterium sensitive due to weakening of outer membrane integrity.[3,4] Hopanoids are synthesized from six isopentenyl units forming squalene, an immediate precursor in hopanoid synthesis.[5] In a highly complex cyclization reaction which is similar to oxido squalene to sterols conversion, the hopane skeleton is formed from squalene by the squalene hopene cyclase coded by the gene *shc*.[5] Though the occurrence of *shc* gene is widespread among bacteria, there is limited information on the hopanoids identified from different members.[1]

Among the hopanoids of phototrophic bacteria, much of the work was focused on *Rhodopseudomonas palustris* TIE-1, which accumulates substantial amounts of diploptene, diplopterol, aminobacteriohopanetriol and 2β-methyl-bacteriohopanepoyol.[6] A large diversity

Alcanivorax xenomutans sp. nov., a hydrocarbonoclastic bacterium isolated from a shrimp cultivation pond

K. Rahul,[1] Ch. Sasikala,[1] L. Tushar,[2] R. Debadrita[2] and Ch. V. Ramana[2]

Correspondence
Chintalapati Sasikala
cvr449@gmail.com *or* sasi449@yahoo.ie

[1]Bacterial Discovery Laboratory, Centre for Environment, Institute of Science and Technology, J.N.T. University Hyderabad, Kukatpally, Hyderabad 500 085, India

[2]Department of Plant Sciences, School of Life Sciences, University of Hyderabad, P.O. Central University, Hyderabad 500 046, India

Two bacterial strains (JC109^T and JC261) were isolated from a sediment sample collected from a shrimp cultivation pond in Tamil Nadu (India). Cells were Gram-stain-negative, motile rods. Both strains were positive for catalase and oxidase, hydrolysed Tween 80, and grew chemo-organoheterotrophically with an optimal pH of 6 (range pH 4–9) and at 30 °C (range 25–40 °C). Based on 16S rRNA gene sequence analysis, strains JC109^T and JC261 were identified as belonging to the genus *Alcanivorax* with *Alcanivorax dieselolei* B-5^T (sequence similarity values of 99.3 and 99.7 %, respectively) and *Alcanivorax balearicus* MACL04^T (sequence similarity values of 98.8 and 99.2 %, respectively) as their closest phylogenetic neighbours. The 16S rRNA gene sequence similarity between strains JC109^T and JC261 was 99.6 %. The level of DNA–DNA relatedness between the two strains was 88 %. Strain JC109^T showed 31 ± 1 and 26 ± 2 % DNA–DNA relatedness with *A. dieselolei* DSM 16502^T and *A. balearicus* DSM 23776^T, respectively. The DNA G+C content of strains JC109^T and JC261 was 54.5 and 53.4 mol%, respectively. Polar lipids of strain JC109^T included diphosphatidylglycerol, phosphatidylglycerol, phosphatidylethanolamine, two unidentified aminophospholipids, two unidentified phospholipids and two unidentified lipids. The major fatty acids were $C_{10:0}$, $C_{12:0}$, $C_{16:0}$, $C_{12:0}$ 3-OH, $C_{16:1}\omega7c$, $C_{18:1}\omega7c$ and $C_{19:0}$ cyclo $\omega8c$. Both strains could utilize diesel oil and a variety of xenobiotics as carbon and energy sources. The results of physiological, biochemical, chemotaxonomic and molecular analyses allowed the clear differentiation of strains JC109^T and JC261 from all other members of the genus *Alcanivorax*. Strains JC109^T and JC261 are thus considered to represent a novel species, for which the name *Alcanivorax xenomutans* sp. nov. is proposed. The type strain is JC109^T (=KCTC 23751^T=NBRC 108843^T).

Millions of litres of diesel and petroleum oil enter the environment from natural and, more prominently, via anthropogenic sources, which introduces problems for a diverse range of ecosystems (Ryerson *et al.*, 2012). Unearthing novel hydrocarbon-degrading micro-organisms is imperative in the bioremediation processes of hydrocarbon-contaminated sites (Chandran & Das, 2010; Atlas & Hazen, 2011). In this paper, we report two novel strains belonging to the genus *Alcanivorax* which were isolated from a sediment sample of a shrimp cultivation pond and are able to degrade diesel oil.

The genus *Alcanivorax* was first proposed by Yakimov *et al.* (1998) with *Alcanivorax borkumensis* as the type species and the description of the genus was later amended by Fernández-Martínez *et al.* (2003). At the time of writing, the genus *Alcanivorax* comprised eight recognized species (http://www.bacterio.net/a/alcanivorax.html): *A. borkumensis* (Yakimov *et al.*, 1998), *Alcanivorax jadensis* (Bruns & Berthe-Corti, 1999), *Alcanivorax venustensis* (Fernández-Martínez *et al.*, 2003), *Alcanivorax dieselolei* (Liu & Shao, 2005), *Alcanivorax balearicus* (Rivas *et al.*, 2007), *Alcanivorax hongdengensis* (Wu *et al.*, 2009), *Alcanivorax pacificus* (Lai *et al.*, 2011) and *Alcanivorax marinus* (Lai *et al.*, 2013) were isolated from marine sediment/water samples. *Alcanivorax dieselolei* was specifically isolated from a hydrocarbon-contaminated site (Liu & Shao, 2005). Members of the genus

Abbreviations: DPG, diphosphatidylglycerol; ME, minimum-evolution; ML, maximum-likelihood; NJ, neighbour-joining; PE, phosphatidylethanolamine; PG, phosphatidylglycerol.

The GenBank/EMBL/DDBJ accession numbers for the 16S rRNA gene sequences of strains JC109^T and JC261 are HE601937 and HG974551, respectively.

One supplementary table and two supplementary figures are available with the online version of this paper.

International Journal of Systematic and Evolutionary Microbiology (2014), **64**, 957–962 **DOI** 10.1099/ijs.0.058974-0

Rhodovulum salis sp. nov. and *Rhodovulum viride* sp. nov., phototrophic *Alphaproteobacteria* isolated from marine habitats

A. Srinivas,[1] B. Vinay Kumar,[1] B. Divya Sree,[1] L. Tushar,[2] Ch. Sasikala[1] and Ch. V. Ramana[2]

Correspondence
Ch. Sasikala
sasi449@yahoo.ie *or* r449@sify.com

[1]Bacterial Discovery Laboratory, Centre for Environment, IST, JNT University Hyderabad, Kukatpally, Hyderabad 500 085, India

[2]Department of Plant Sciences, School of Life Sciences, University of Hyderabad, P.O. Central University, Hyderabad 500 046, India

Two strains (JA746^T and JA756^T) having yellowish brown-to-green pigment were isolated from a solar saltern and a pink pond, respectively. While both strains were non-motile and shared the presence of bacteriochlorophyll-*a*, major cellular fatty acids ($C_{18:1}\omega7c$, $C_{16:0}$, $C_{18:0}$), quinone (Q-10), polar lipids and hopanoids, they differed from each other in their carotenoid composition. The G+C content of genomic DNA of strains JA746^T and 756^T was 62.4 and 63.3 mol%, respectively. The 16S rRNA gene-based EzTaxon-e BLAST search analysis of strains JA746^T and 756^T indicated highest sequence similarity with members of the genus *Rhodovulum* in the family *Rhodobacteraceae* of the class *Alphaproteobacteria*. Strain JA746^T has high sequence similarities with *Rhodovulum visakhapatnamense* JA181^T (97.3 %), *Rhodovulum steppense* A-20s^T (97.3 %), *Rhodovulum phaeolacus* JA580^T (97 %), *Rhodovulum strictum* MB-G2^T (97 %) and other members of the genus *Rhodovulum* (<97 %). Strain JA756^T has high sequence similarities with *Rhodovulum visakhapatnamense* JA181^T (99.8 %), *Rhodovulum sulfidophilum* Hansen W4^T (99.1 %), *Rhodovulum kholense* JA297^T (97.9 %) and other members of the genus *Rhodovulum* (<97 %). The sequence similarity between strains JA746^T and JA756^T was 97.5 %. However, these strains are not closely related to each other or to their phylogenetic neighbours since the DNA–DNA reassociation values were less than 56 %. The genomic information was also supported by phenotypic and chemotaxonomic results, leading us to classify strains JA746^T (=NBRC 108898^T=KCTC 15180^T) and JA756^T (=NBRC 109122^T=KCTC 15223^T) as the type strains of two novel species of the genus *Rhodovulum*, for which the names *Rhodovulum salis* sp. nov. and *Rhodovulum viride* sp. nov. are proposed, respectively.

Members of the genus *Rhodovulum* are widely distributed in marine habitats and are phototrophic. At the time of writing, there are 15 species with validly published names affiliated to this genus, and through this communication, we add two novel species which were isolated from different marine habitats. Strain JA746^T was isolated from a solar saltern, near Humma, Odisha, India on 5 January 2012 (GPS position 15° 29′ N 78° 26′ E) while, strain JA756^T was isolated from a water sample collected from a pink pond at Chirala, Andhra Pradesh, India on 19 May 2011 (GPS position 15° 50′ N 80° 21′ E). Both the strains were isolated from enrichment cultures obtained in a medium described previously (Lakshmi *et al.*, 2009), in 50 ml fully filled screw-capped bottles incubated at 2400 lx and 30±2 °C for 7 days under anaerobic conditions. Cultures were purified by repeated streaking on agar slants (Srinivas *et al.*, 2007) and were maintained in pure culture under refrigeration at 4 °C and preserved as lyophilized vials.

Genomic DNA was extracted and purified according to the method of Marmur (1961) and the G+C content of the DNA of strains JA746^T and JA756^T, as determined by HPLC (Mesbah *et al.*, 1989), was 62.4 and 63.3 mol%, respectively. Well isolated colonies were used for 16S rRNA gene amplification by using PCR master mix (GeNei) as described previously (Subhash *et al.*, 2013b). 16S rRNA gene sequencing was performed on a 3130xl ABI prism automated

Abbreviations: ML, maximum-likelihood, MP, maximum-parsimony, NJ, neighbour-joining.

The GenBank/EMBL/DDBJ accession numbers for the 16S rRNA gene sequences of strains JA746^T and JA756^T are HE680093 and HE983843, respectively.

Four supplementary figures are available with the online version of this paper.

International Journal of Systematic and Evolutionary Microbiology (2013), **63**, 4484–4488 **DOI** 10.1099/ijs.0.049726-0

Ciceribacter lividus gen. nov., sp. nov., isolated from rhizosphere soil of chick pea (*Cicer arietinum* L.)

R. Kathiravan,[1] S. Jegan,[1] V. Ganga,[1] V. R. Prabavathy,[1] L. Tushar,[2] Ch. Sasikala[3] and Ch. V. Ramana[2]

Correspondence
V. R. Prabavathy
prabavathyvr@mssrf.res.in *or*
Microbiology@mssrf.res.in

[1]Microbiology Department, M. S. Swaminathan Research Foundation, 3rd Cross street, Taramani institutional area, Chennai 600113, India

[2]Department of Plant Sciences, School of Life Sciences, University of Hyderabad, PO Central University, Gachibowli, Hyderabad 500046, India

[3]Bacterial Discovery laboratory, Centre for Environment, Institute of Science and Technology, JNT University Hyderabad, Kukatpally, Hyderabad 500085, India

The taxonomic position of strain MSSRFBL1^T, isolated from chickpea rhizosphere soil from Kannivadi, India, was determined. Strain MSSRFBL1^T formed bluish black colonies, stained Gram-negative and was motile, aerobic, capable of fixing dinitrogen, oxidase-negative and catalase-positive. Q-10 was the major respiratory quinone. Major fatty acids of strain MSSRFBL1^T were $C_{18:1}\omega7c$ and $C_{19:0}$cyclo$\omega8c$. Minor amounts of $C_{18:0}$, $C_{12:0}$, $C_{14:0}$ 3-OH, $C_{18:0}$ 3-OH, $C_{16:0}$, $C_{16:1}\omega6c$/$C_{16:1}\omega7c$, $C_{17:0}$ 3-OH and $C_{20:1}\omega7c$ were also present. Polar lipids included diphosphatidylglycerol, phosphatidylethanolamine, phosphatidylmethylethanolamine, phosphatidylcholine and two unidentified glycolipids. Bacteriohopane derivatives (BHD1 and 2), diplopterol, diploptene, bishomohopanediol, adenosylhopane and 2β-methyl bacteriohopanetetrol were the major hopanoids of strain MSSRFBL1^T. The genomic DNA G+C content was 71 mol%. EzTaxon-e-based BLAST analysis of the 16S rRNA gene indicated the highest similarity of strain MSSRFBL1^T to *Ensifer adhaerens* LMG 20216^T (97.3 %) and other members of the genus *Ensifer* (<96.9 %) in the family *Rhizobiaceae* of the class *Alphaproteobacteria*. However, phylogenetic analysis based on 16S rRNA, *recA*, *thrC* and *dnaK* gene sequences showed distinct out-grouping from the recognized genera of the family *Rhizobiaceae*. Based on phenotypic, genotypic and chemotaxonomic characters, strain MSSRFBL1^T represents a novel species in a new genus in the family *Rhizobiaceae* for which the name *Ciceribacter lividus* gen. nov., sp. nov. is proposed. The type strain of *Ciceribacter lividus* is MSSRFBL1^T (=DSM 25528^T=KCTC 32403^T).

While understanding the rhizosphere bacterial diversity of chick pea (*Cicer arietinum* L.) we came across bluish black colonies which happened to be a close relative of the genus *Ensifer* based on 16S rRNA gene sequence analysis. The family *Rhizobiaceae* comprises the genera *Ensifer*, *Shinella*, *Kaistia* and *Rhizobium*. Except for the members of the genus *Kaistia*, all other members of the family *Rhizobiaceae* are dinitrogen fixers and are associated with plants. Through this study, we propose a novel genus in the family *Rhizobiaceae* for strain MSSRFBL1^T isolated from the rhizosphere soil of *C. arietium* L.

Rhizosphere soils of *C. arietium* L. collected from Kannivadi (GPS position of the sample collection site is 10° 22′ 44.40″ N 77° 49′ 48.0″ E), Tamil Nadu, India, were serially diluted and plated on yeast malt agar (no. M424; HiMedia) and incubated at 28 °C for 7 days. Bluish black colonies appeared along with other white colonies and these were of particular interest because of the unique colony colour; they were purified and maintained on yeast malt agar. The purified isolate was designated MSSRFBL1^T and preserved at −80 °C in 20 % (v/v) glycerol.

Genomic DNA was extracted and purified from strain MSSRFBL1^T according to the method of Marmur (1961). G+C content of the DNA as determined by reversed-phase HPLC (Mesbah *et al.*, 1989) was 71±0.5 mol% for strain

The GenBank/EMBL/DDBJ accession numbers for the 16S rRNA, *recA*, *dnaK*, *thrC* and *nifH* gene sequences of strain MSSRFBL1^T are JQ230000, KC189949, KC189950, KC189951 and KC189952, respectively.

Five supplementary figures are available with the online version of this paper.

International Journal of Systematic and Evolutionary Microbiology (2013), **63**, 4524–4532 **DOI** 10.1099/ijs.0.052183-0

Erythrobacter odishensis sp. nov. and *Pontibacter odishensis* sp. nov. isolated from dry soil of a solar saltern

Y. Subhash,[1] L. Tushar,[1] Ch. Sasikala[2] and Ch. V. Ramana[1]

Correspondence
Ch. V. Ramana
r449@sify.com *or*
sasi449@yahoo.ie

[1]Department of Plant Sciences, School of Life Sciences, University of Hyderabad, P.O. Central University, Hyderabad 500046, India

[2]Bacterial Discovery Laboratory, Centre for Environment, Institute of Science and Technology, J.N.T. University Hyderabad, Kukatpally, Hyderabad 500085, India

Two bacterial strains (JC130^T and JA747^T) were isolated from dry soils of a solar saltern. Phylogenetic analysis showed that strain JA747^T clustered with species of the genus *Erythrobacter* belonging to the family *Erythrobacteraceae* of the class *Alphaproteobacteria* in the phylum *Proteobacteria*, while strain JC130^T clustered with species of the genus *Pontibacter* belonging to the family *Cytophagaceae* of the phylum *Bacteroidetes*. Based on 16S rRNA gene sequence analysis, strain JA747^T had highest similarity with *Erythrobacter gangjinensis* K7-2^T (96.7 %) and other members of the genus *Erythrobacter* (<96 %). Strain JC130^T had highest sequence similarity with *Pontibacter korlensis* X14-1^T (98.1 %), *Pontibacter actiniarum* KMM 6156^T (96.9 %) and other members of the genus *Pontibacter* (<96 %). However, strain JC130^T showed less than 32 % DNA reassociation value (based on DNA–DNA hybridization) with *Pontibacter korlensis* NRRL B-51097^T (=X14-1^T) and *Pontibacter actiniarum* LMG 23027^T (=KMM 6156^T). Strain JA747^T was positive for catalase and oxidase activity and negative for nitrate reduction, and hydrolysis of starch and casein. Phosphatidylglycerol, diphostatidylglycerol, phosphatidylethanolamine and phosphatidylcholine were the major polar lipids for strain JA747^T. $C_{18:1}\omega7c$, $C_{16:1}\omega6c/C_{16:1}\omega7c$, $C_{17:1}\omega6c$ and $C_{16:0}$ were the major fatty acids of strain JA747^T. Strain JC130^T was positive for catalase and oxidase, and negative for gelatinase and nitrate reduction. Phosphatidylethanolamine was the major polar lipid of strain JC130^T. Major fatty acids of strain JC130^T were iso-$C_{15:0}$ and summed feature 4 (anteiso-$C_{17:1}$B/iso I). Based on the phenotypic, chemotaxonomic and molecular evidence presented, strains JA747^T and JC130^T are considered to represent two novel species of the genera *Erythrobacter* and *Pontibacter*, for which the names *Erythrobacter odishensis* sp. nov. (type strain JA747^T=KCTC 23981^T=NBRC 108930^T) and *Pontibacter odishensis* sp. nov. (type strain JC130^T=KCTC 23982^T=LMG 26962^T), respectively, are proposed. Emended descriptions of the genera *Erythrobacter* and *Pontibacter* are provided.

India is one of the major producers of natural salt, having a large number of solar salterns. Solar salterns are major niches for many salt-loving bacteria, although only a few novel species have been recorded so far from Indian solar salterns (Kumar *et al.*, 2007; Kalyan Chakravarthy *et al.*, 2007; Ritika *et al.*, 2012; Srinivas *et al.*, 2007; Venkata Ramana *et al.*, 2010). Here we report the description of two novel strains recovered from a solar saltern in Odisha, eastern India. Based on 16S rRNA gene sequence analysis, the two novel strains (designated JA747^T and JC130^T) are shown to represent novel species of the genera *Erythrobacter* and *Pontibacter*, respectively.

Ten soil samples were collected randomly from an unused (at the time of sample collection) solar saltern at Humma, Odisha, India (GPS positioning of the sample collection site 19° 25′ N 85° 04′ E) during December 2011. These different samples collected from the same site were pooled together. One gram of air-dried soil was serially diluted to 10^{-4} dilution and 100 µl was spread on three different

Abbreviations: Bchl-*a*, bacteriochlorophyll-*a*; DPG, diphosphatidylglycerol; ML, maximum-likelihood; MP, maximum-parsimony; NJ, neighbour-joining; PC, phosphatidylcholine; PE, phosphatidylethanolamine; PG, phosphatidylglycerol.

The GenBank/EMBL/DDBJ accession numbers for the 16S rRNA gene sequences of strains JA747^T and JC130^T are HE680094 and HE681883, respectively.

Five supplementary figures are available with the online version of this paper.

Antonie van Leeuwenhoek (2013) 103:885–898
DOI 10.1007/s10482-012-9870-4

ORIGINAL PAPER

Salinicoccus halitifaciens sp. nov., a novel bacterium participating in halite formation

Chintalapati Venkata Ramana · Are Srinivas · Yadav Subhash · Lodha Tushar · Tapas Mukherjee · Pemmaraju Usha Kiran · Chintalapati Sasikala

Received: 18 October 2012 / Accepted: 22 December 2012 / Published online: 10 January 2013

Abstract Strain JC90^T was isolated from a soda lake in Lonar, India. Strain JC90^T maintains its external pH to 8.5 and participates in halite formation. Based on 16S rRNA gene sequence similarity studies, strain JC90^T was found to belong to the genus *Salinicoccus* and is most closely related to "*Salinicoccus kekensis*" K164^T (99.3 %), *Salinicoccus alkaliphilus* T8^T (98.4 %) and other members of the genus *Salinicoccus* (<96.5 %). However Strain JC90^T is <36 % related (based on DNA–DNA hybridization) with the type strains of "*S. kekensis*" K164^T and *S. alkaliphilus* T8^T. The DNA G+C content of strain JC90^T was determined to be 46 mol %. The cell-wall amino acids were identified as lysine and glycine. Polar lipids were found to include diphosphatidylglycerol, phosphatidylglycerol, phosphatidyl ethanolamine, an unidentified glycolipid and unidentified lipids (L1,2). Major hopanoids of strain JC90^T were determined to be bacterial hopane derivatives (BHD1,2), diplopterol, diploptene and two unidentified hopanoids (UH1,2). The predominant isoprenoid quinone was identified as menaquinone (MK-6). *Ante-iso*-$C_{15:0}$ was determined to be the predominant fatty acid and significant proportions of *iso*-$C_{14:0}$, $C_{14:0}$, *iso*-$C_{15:0}$, $C_{16:0}$, *iso*-$C_{16:0}$, *iso*-$C_{17:0}$, *anteiso*-$C_{17:0}$ and $C_{18:0}$2OH were also detected. The results of physiological and biochemical tests support the molecular evidence and allowed a clear phenotypic differentiation of strain JC90^T from all other members of the genus *Salinicoccus*. Strain JC90^T is therefore considered to represent a novel species, for which the name *Salinicoccus halitifaciens* sp. nov. is proposed. The type strain is JC90^T (=KCTC 13894^T =DSM 25286^T).

Keywords *Salinicoccus* · sp. nov. · Haloalkaliphile · Halite formation · Polyphasic taxonomy

Electronic supplementary material The online version of this article (doi:10.1007/s10482-012-9870-4) contains supplementary material, which is available to authorized users.

C. V. Ramana · Y. Subhash · L. Tushar · T. Mukherjee · P. U. Kiran
Department of Plant Sciences, School of Life Sciences, University of Hyderabad, P.O. Central University, Hyderabad 500 046, India
e-mail: chvrsl@uohyd.ernet.in

A. Srinivas · C. Sasikala (✉)
Bacterial Discovery Laboratory, Centre for Environment, Institute of Science and Technology, J.N.T. University Hyderabad, Kukatpally, Hyderabad 500 085, India
e-mail: r449@sify.com; sasi449@yahoo.ie

Introduction

Lonar meteor crater lake in India is one of the most important soda lakes in the world. We serendipitously observed salt crystals in a 20 % NaCl medium enriched with soil samples from this lake. A newly isolated strain (JC90^T) from the salt crystal participated in halite formation and was identified based on its 16S rRNA gene sequence as belonging to the genus *Salinicoccus*. The genus *Salinicoccus* was first described by Ventosa

Cohaesibacter haloalkalitolerans sp. nov., isolated from a soda lake, and emended description of the genus *Cohaesibacter*

Vishnuvardhan Reddy Sultanpuram,[1] Tushar Dilipchand Lodha,[2] Venkata Ramana Chintalapati[2] and Sasikala Chintalapati[1]

Correspondence
Sasikala Chintalapati
sasi449@yahoo.ie; r449@sify.com

[1]Bacterial Discovery Laboratory, Centre for Environment, Institute of Science and Technology, Jawaharlal Nehru Technological University, Kukatpally, Hyderabad 500085, India

[2]Department of Plant Sciences, School of Life Sciences, University of Hyderabad, P.O. Central University, Hyderabad 500046, India

Two novel Gram-stain-negative, motile, catalase-negative and oxidase-positive strains of bacteria (JC131^T and JC112) were isolated from Lonar, a soda lake in India. Based on 16S rRNA gene sequence similarity studies, strains JC131^T and JC112 belong to the family *Cohaesibacteraceae* of the class *Alphaproteobacteria* and were most closely related to *Cohaesibacter marisflavi* DQHS21^T (98.0 %) and *Cohaesibacter gelatinilyticus* CL-GR15^T (96.0 %). Polar lipids of strains JC131^T and JC112 include phosphatidylglycerol, phosphatidylethnolamine, phosphatidylmonomethylethanolamine, diphosphatidylglycerol and two unidentified lipids (L1 and L2). Both strains have diplopterol, diploptene, an unidentified hopane (UH) and bacteriohopane derivatives (BHD1 and 2) as major hopanoids and an unidentified pigment (P1). The predominant isoprenoid quinone of both strains was ubiquinone-10 (Q10). Whole-cell fatty acid analysis of both strains revealed that $C_{18:1}\omega7c$ was the predominant cellular fatty acid and significant proportions of $C_{16:0}$, summed feature 3 ($C_{16:1}\omega7c$ and/or iso-$C_{15:0}$ 2-OH), 11-methyl $C_{18:1}\omega7c$, $C_{18:1}\omega9c$, $C_{18:0}$ and $C_{20:1}\omega7c$ were also detected. The DNA G+C content of strains JC131^T and JC112 was 54.6 and 53.8 mol%, respectively. The genome reassociation (based on DNA–DNA hybridization) of strains JC131^T and JC112 with *Cohaesibacter marisflavi* NCCB 100300^T (=DQHS21^T) was about 58 %, while between JC131^T and JC112 it was about 87 %. On the basis of physiological, biochemical and chemotaxonomical properties, strains JC131^T and JC112 are differentiated from the other two members of the genus *Cohaesibacter*. Strains JC131^T and JC112 represent a novel species of the genus *Cohaesibacter*, for which the name *Cohaesibacter haloalkalitolerans* sp. nov. is proposed. The type strain is JC131^T (=KCTC 32038^T=NBRC 109022^T). An emended description of the genus *Cohaesibacter* is presented.

The family *Cohaesibacteraceae* in the order *Rhizobiales* consists of only one genus, *Cohaesibacter* described by Hwang & Cho (2008). Presently the genus consists of two species with validly published names. *Cohaesibacter gelatinilyticus* CL-GR15^T, is a facultatively anaerobic rod isolated from seawater with positive oxidase and catalase activities. *C. gelatinilyticus* CL-GR15^T forms circular, entire, convex and creamy white colonies 2 mm in diameter on marine agar supplemented with 3 % NaCl. Optimal growth occurs at 25–30 °C (range 15–31 °C), pH 8 (range pH 6–9) and at 3 % (w/v) NaCl (range 2–5 %) (Hwang & Cho, 2008). *Cohaesibacter marisflavi* DQHS21^T is also a facultatively anaerobic rod isolated from coastal pond sediment showing catalase-negative and oxidase-positive phenotypes. It forms white, smooth, circular, translucent colonies of 1–2 mm diameter. Optimal growth is at 25–30 °C (range 10–38 °C), pH 7–8 (range pH 4–9) and 3 % (w/v) NaCl (range 0.5–15 %) (Qu *et al.*, 2011). In this paper, we describe the polyphasic studies of two strains isolated from Lonar soda lake, India and propose that these strains are representatives of a novel species of the genus *Cohaesibacter*.

Two strains designated JC131^T and JC112 were isolated from sediment samples of the Lonar soda lake

Abbreviations: BHD, bacteriohopane derivative; MR/VP, methyl red/Voges–Proskauer.

The GenBank/EMBL/DDBJ accession numbers for the 16S rRNA gene sequence of strains JC131^T and JC112 are HE774678 and HE647713, respectively.

A supplementary figure and a supplementary table are available with the online version of this paper.

Mongoliicoccus alkaliphilus sp. nov. and *Litoribacter alkaliphilus* sp. nov., isolated from salt pans

Y. Subhash,[1] L. Tushar,[1] Ch. Sasikala[2] and Ch. V. Ramana[1]

[1]Department of Plant Sciences, School of Life Sciences, University of Hyderabad, P.O. Central University, Hyderabad 500046, India

[2]Bacterial Discovery Laboratory, Centre for Environment, Institute of Science and Technology, J.N.T. University Hyderabad, Kukatpally, Hyderabad 500085, India

Correspondence
Ch. V. Ramana
r449@sify.com *or* sasi449@yahoo.ie

Four bacterial strains (JC165^T, JC166^T, JC169 and JC170) were isolated from salt pan soils from a coastal region of Tamilnadu, India. They were obligately aerobic, pink- to red-pigmented, mesophilic, haloalkaliphiles having chemoorganoheterotrophic growth on various carbon sources and were catalase- and oxidase-positive. Phototrophic growth and bacteriochlorophyll *a* were absent in all four strains. Major carotenoids present were β-carotene and rhodoxanthin. The main fatty acid in all strains was iso-$C_{15:0}$. The main polar lipids were phosphatidylethanolamine (PE) and phosphatidylcholine (PC) as well as a few unidentified lipids. Bacterial hopane derivatives and diplopterol (DPL) were detected in all four strains. Based on the 16S rRNA gene sequences, all four strains belong to the family *Cyclobacteriaceae* in the phylum *Bacteroidetes*. Strains JC165^T and JC169 had a sequence similarity of 97.2 % with *Mongoliicoccus roseus* MIM28^T, while strains JC166^T and JC170 had a sequence similarity of 99.5 % with *Litoribacter ruber* YIM CH208^T. Strains JC165^T/JC169 and JC166^T/JC170 had genomic DNA reassociation values (based on DNA–DNA hybridization) of 21 ± 2 % and 23 ± 1 % with *M. roseus* KCTC 19808^T (=MIM28^T) and *L. ruber* KCTC 22899^T (=YIM CH208^T), respectively, suggesting that they represented novel species. The reassociation values of >85 % between strains JC165^T and JC169, and JC166^T and JC170 suggested they were strains of the same species. The genomic information was supported by phenotypic observations leading to the proposal of two novel species, *Mongoliicoccus alkaliphilus* sp. nov. (type strain, JC165^T=KCTC 32210^T=LMG 27255^T) and *Litoribacter alkaliphilus* sp. nov. (type strain, JC166^T=KCTC 32217^T=LMG 27256^T).

While studying pigmented bacteria from coastal regions of Tamilnadu, India, through cultivable approaches, bacteria were isolated that form distinct pink- to red-coloured colonies. Based on the 16S rRNA gene sequence data, the new isolates were identified as members of the genus *Mongoliicoccus* and *Litoribacter* in the family *Cyclobacteriaceae* of the phylum *Bacteroidetes*. Members of the phylum *Bacteroidetes* are a diverse group of bacteria and play an important role in the environment through degradation of complex organic compounds (Cottrell & Kirchman, 2000; Nedashkovskaya *et al.*, 2003). At the time of writing the manuscript, only one species name has been validly published in each of the genera *Mongoliicoccus* (Liu *et al.*, 2012) and *Litoribacter* (Tian *et al.*, 2010). Here we describe a novel species of each of these genera, both of which possess β-carotene and rhodoxanthin as major carotenoides.

Strains JC165^T and JC170 were isolated from dried soil samples collected from Kanyakumari, Tamilnadu, India (GPS position of the sample collection site is 8° 04′ 42″ N 77° 32′ 30″ E). Strains JC166^T and JC169 were isolated from dry soils of Rameshwaram, Tamilnadu, India (GPS position of the sample collection site is 9° 06′ 24″ N 79° 31′ 28″ E) during June 2012. Dry soil was serially diluted 10-fold in 0.6 % (w/v) saline and plated on a medium with pH 9.0 that contained (g l^{-1}): KH_2PO_4 (0.2), NH_4Cl (0.25), KCl (0.5), $CaCl_2.2H_2O$ (0.15), NaCl (1), $MgCl_2.6H_2O$ (0.62), Na_2SO_4 (2.84), HEPES (2.83), yeast extract (3.0), peptone (3), Casamino acids (0.5), glucose (0.5) and sodium pyruvate (3.0). Four distinct pink to red colony morphologies were observed from plates incubated at 30 °C for three days. All four

The GenBank/EMBL/DDBJ accession numbers for the 16S rRNA gene sequences of strains JC165^T, JC166^T, JC169 and JC170 are HE996970, HE996966, HE996971 and HE996967, respectively.

Four supplementary figures are available with the online version of this paper.

International Journal of Systematic and Evolutionary Microbiology (2013), **63**, 2684–2689 **DOI** 10.1099/ijs.0.046409-0

Rhodomicrobium udaipurense sp. nov., a psychrotolerant, phototrophic alphaproteobacterium isolated from a freshwater stream

V. Venkata Ramana,[1] P. Shalem Raj,[2] L. Tushar,[1] Ch. Sasikala[2] and Ch. V. Ramana[1]

Correspondence
Ch. V. Ramana
r449@sify.com *or*
sasi449@yahoo.ie

[1]Department of Plant Sciences, School of Life Sciences, University of Hyderabad, P.O. Central University, Hyderabad 500 046, India

[2]Bacterial Discovery Laboratory, Centre for Environment, Institute of Science and Technology, J.N.T.University Hyderabad, Kukatpally, 500085, India

Two strains (JA643^T and JA755) of Gram-stain-negative, facultatively anaerobic phototrophic, bacteria capable of growth at low temperatures (10–15 °C) were isolated from freshwater streams from different geographical regions of India. Both strains contain bacteriochlorophyll *a* and carotenoids of the spirilloxanthin series. Phosphatidylethanolamine, phosphatidylcholine, phosphatidylglycerol, diphosphatidylglycerol, an unidentified phospholipid (PL), unidentified amino lipids (AL1–AL6, AL9) and an unidentified lipid (L1) were the polar lipids present in both strains. The major cellular fatty acid was $C_{18:1}\omega7c$ (76–79 % of the total). Bacteriohopane derivatives (BHD1,2), unidentified hopanoids (UH1–5), diplopterol (DPL) and diploptene (DPE) were the major hopanoids of both strains. The DNA G+C content was 64.2–64.5 mol%. 16S rRNA gene sequence-based phylogenetic analysis showed that both strains are closely related to the genus *Rhodomicrobium* and clustered with *Rhodomicrobium vannielii* DSM 162^T (99 % sequence similarity). However, both strains exhibited only 46.1 % DNA–DNA hybridization with *R. vannielii* DSM 162^T. Strains JA643^T and JA755 shared >99 % 16S rRNA gene sequence similarity and were >85 % related on the basis of DNA–DNA hybridization; they are therefore considered to represent a novel species in the genus *Rhodomicrobium*, for which the name *Rhodomicrobium udaipurense* sp. nov. is proposed. The type strain is JA643^T (=KCTC 15219^T=NBRC 109057^T).

The family *Hyphomicrobiaceae* in the class *Alphaproteobacteria* contains three phototrophic genera: *Blastochloris*, *Rhodomicrobium* and *Rhodoplanes*. The genus *Rhodomicrobium* can be distinguished from *Blastochloris* and *Rhodoplanes* mainly on the basis of cell morphology, including long prosthecae and a characteristic vegetative growth cycle. *Rhodomicrobium vannielii* (Duchow & Douglas, 1949) is the single recognized species of the genus *Rhodomicrobium*; in the present communication, we propose a novel species based on two strains (JA643^T and JA755) isolated from different geographical locations in India.

Abbreviation: FT-IR, Fourier transform infrared.

The GenBank/EMBL/DDBJ accession numbers for the 16S rRNA gene sequence of strains JA643^T and JA755 are FN995218 and HE863941, respectively.

Five supplementary figures are available with the online version of this paper.

Strain JA643^T was isolated from a freshwater stream sample collected from Udaipur in Himachal Pradesh [GPS of the sampling site is 32° 43′ 30.55″ N 76° 39′ 55.45″ E; altitude of 8970 feet (2734 m) above sea level], in the western Himalayas, India. Strain JA755 was isolated from a freshwater stream sample collected from Rottikadai town near the Annamalai hills [10° 35′ N 76° 97′ E; altitude of 3500 feet (1067 m) above sea level] in the Western Ghats, Tamil Nadu, India. Both strains were isolated after enrichment in PE medium (Hanada *et al.*, 1995) at pH 7.0, in fully filled 50 ml screw-capped bottles incubated under phototrophic (2500 lx) conditions at 30±2 °C for 15 days. Purification of the isolates and the media used for growth of the organisms are as previously described (Lakshmi *et al.*, 2011a, b).

Genomic DNA was extracted and purified according to the method of Marmur (1961) and the DNA G+C content of strains JA643^T and JA755 was 62.4 and 62.8 mol% as determined by HPLC (Mesbah *et al.*, 1989). Cell material

International Journal of Systematic and Evolutionary Microbiology (2013), **63**, 2338–2343 **DOI** 10.1099/ijs.0.046300-0

Vogesella alkaliphila sp. nov., isolated from an alkaline soil, and emended description of the genus *Vogesella*

Y. Subhash,[1] L. Tushar,[1] Ch. Sasikala[2] and Ch. V. Ramana[1]

Correspondence
Ch. V. Ramana
r449@sify.com *or*
sasi449@yahoo.ie

[1]Department of Plant Sciences, School of Life Sciences, University of Hyderabad, P.O. Central University, Hyderabad 500 046, India

[2]Bacterial Discovery Laboratory, Centre for Environment, Institute of Science and Technology, J. N. T. University, Kukatpally, Hyderabad 500 085, India

Strain JC141^T was isolated from an alkaline soil (pH 8.8) at Mau, Uttar Pradesh, India. Colonies were blue with a metallic sheen; cells stained Gram-negative, and were oxidase- and catalase-positive, but chitinase-negative. Major fatty acids were $C_{16:1}\omega7c$/$C_{16:1}\omega6c$, $C_{16:0}$ and $C_{18:0}$ with minor amounts of $C_{10:0}$, $C_{10:0}$ 3-OH, $C_{12:0}$, $C_{14:0}$ and $C_{18:1}\omega7c$. Strain JC141^T contained phosphatidylethanolamine and phosphatidylglycerol as major polar lipids, with minor amounts of diphosphatidylglycerol, unidentified aminolipids (AL1–3) and unidentified lipids (L1–4). A bacterial hopane derivative (BHD1) was the major hopanoid. Genomic DNA G+C content was 62.5 mol%. 16S rRNA gene sequence comparisons indicated that strain JC141^T represents a member of the genus *Vogesella* within the family *Neisseriaceae* of the class *Betaproteobacteria*. Strain JC141^T had a 16S rRNA gene sequence similarity of 98 % with *Vogesella indigofera* ATCC 19706^T and <96.5 % with other members of the genus *Vogesella*. However, strain JC141^T showed 45.8 % relatedness (based on DNA–DNA hybridization) with *V. indigofera* LMG 6867^T (=ATCC 19706^T). Distinct morphological, physiological and genotypic differences from previously described taxa support the classification of strain JC141^T as a representative of a novel species in the genus *Vogesella*, for which the name *Vogesella alkaliphila* sp. nov. is proposed. The type strain is JC141^T (=KCTC 32041^T=LMG 27066^T). An emended description of the genus *Vogesella* is also proposed.

The genus *Vogesella* was proposed by Grimes *et al.* (1997) to accommodate bacteria which have blue-pigmented colonies with a metallic copper-coloured sheen. The blue pigment was due to the presence of indigoidine (5,5′-diamino-4,4′-dihydroxy-3,3′-diazadiphenoquinone-[2,2′]), and at higher concentrations of this pigment the colonies appear with a metallic copper sheen (Kuhn *et al.*, 1965). At the time of writing, the genus *Vogesella* comprises four recognized species. However, except for the blue colonies of the type species (*Vogesella indigofera*; Grimes *et al.*, 1997), colonies of the remaining three species, *Vogesella lacus* (Chou *et al.*, 2009), *Vogesella mureinivorans* (Jørgensen *et al.*, 2010) and *Vogesella perlucida* (Chou *et al.*, 2008), are colourless. Here we describe a novel species of the genus *Vogesella* for a blue colony-coloured bacterium.

Strain JC141^T was isolated from a soil sample collected from an alkaline soil (pH 8.8) at Mau, Uttar Pradesh, India (GPS position of the sample collection site, 26°7′ 44.13″ N 83° 32′ E) on 6 March 2012. One gram of air-dried soil was serially diluted up to 10^{-4} dilution and 100 µl was spread on an agar (1.5 %) medium (pH 8.0) containing (g l^{-1}): KH_2PO_4 (0.2), NH_4Cl (0.25), KCl (0.5), $CaCl_2.2H_2O$ (0.15), NaCl (1), $MgCl_2.6H_2O$ (0.62), Na_2SO_4 (2.84), HEPES (2.83), yeast extract (3.0), peptone (3), Casamino acids (0.5), glucose (0.5) and sodium pyruvate (3.0). Purification was done by repeated streaking on agar plates and the purified culture was preserved by lyophilization. Purified cultures were grown in a conical flask (500 ml) with shaking (160 r.p.m.) in the above described medium (pH 8.0). For routine culturing and for physiological tests, strain JC141^T was grown at pH 8.0 and at 30 °C. *V. indigofera* LMG 6867^T (=ATCC 19706^T) was used for comparative taxonomic analysis.

Morphological properties (cell shape, cell division, cell size, motility) were observed by light microscopy (with an

Abbreviations: DPG, diphosphatidylglycerol; ME, minimum-evolution; MP, maximum-parsimony; NJ, neighbour-joining; PE, phosphatidylethanolamine; PG, phosphatidylglycerol; PHA, poly-hydroxyalkanoate.

The GenBank/EMBL/DDBJ accession number for the 16S rRNA gene sequence of strain JC141^T is HE819389.

A supplementary table and a supplementary figure are available with the online version of this paper.

Spirochaeta sphaeroplastigenens sp. nov., a halo-alkaliphilic, obligately anaerobic spirochaete isolated from soda lake Lonar

S. Vishnuvardhan Reddy,[1] S. Aspana,[2] D. L. Tushar,[1] Ch. Sasikala[2] and Ch. V. Ramana[1]

Correspondence
Ch. Sasikala
sasi449@yahoo.ie
or r449@sify.com

[1]Department of Plant Sciences, School of Life Sciences, University of Hyderabad, P.O. Central University, Hyderabad 500046, India

[2]Bacterial Discovery Laboratory, Centre for Environment, Institute of Science and Technology, J. N. T. University, Kukatpally, Hyderabad, 500085, India

Two helical-shaped bacteria (strains JC133^T and JC143), which stain Gram-negative, were isolated from an alkaline soda lake, Lonar, India. Both strains were obligate anaerobes, mesophilic and required halo-alkaline conditions for growth. Both strains were resistant to rifampicin and kanamycin, but sensitive to gentamicin, tetracycline, ampicillin and chloramphenicol. Both strains had phosphatidylglycerol (PG), diphosphotidylglycerol (DPG), glycolipid (GL) and four unidentified lipids (L1–4) as the major polar lipids. $C_{18:1}\omega7c$ was the predominant cellular fatty acid with significant proportions of $C_{16:0}$, $C_{18:1}\omega9c$, $C_{14:0}$, $C_{18:0}$, $C_{16:1}\omega5c$, $C_{18:1}\omega5c$ and $C_{20:1}\omega9c$. The DNA G+C contents of strain JC131^T and JC143 were 58.2 and 58.5 mol%, respectively, and the two strains showed DNA reassociation >85 % (based on DNA–DNA hybridization). Based on the 16S rRNA gene sequence analysis, both strains were identified as belonging to the genus *Spirochaeta* with *Spirochaeta alkalica* Z-7491^T (99.6 % sequence similarity), *Spirochaeta americana* ASpG1^T (99 %) and other members of the genus *Spirochaeta* (<93 %) as their closest phylogenetic neighbours. However, strain JC133^T and JC143 displayed less than 53.5 % binding (based on DNA–DNA hybridization) with *S. alkalica* Z-7491^T and *S. americana* ASpG1^T. On the basis of physiological, biochemical, chemotaxonomic and molecular properties, strains JC133^T and JC143 can be differentiated from other members of the genus *Spirochaeta* and represent a novel species of the genus *Spirochaeta*, for which the name *Spirochaeta sphaeroplastigenens* sp. nov. is proposed. The type strain is JC133^T (=KCTC 15220^T=NBRC 109056^T).

The genus *Spirochaeta* represents free-living, saccharolytic, obligate or facultative anaerobic, helical shaped bacteria (Paster, 2010). Members of the genus *Spirochaeta* are widely distributed (Canale-Parola, 1992) in aquatic habitats (Breznak & Canale-Parola, 1975), freshwater mud (Canale-Parola, 1980), marine mud (Hespell & Canale-Parola, 1970; Harwood & Canale-Parola, 1983), oilfields (Magot *et al.*, 1997), microbial mats (Teal *et al.*, 1996; Breznak & Warnecke, 2008), termite hindgut (Dröge *et al.*, 2006) and alkaline hypersaline sediments/lakes (Zhilina *et al.*, 1996; Pikuta *et al.*, 2009; Dubinina *et al.*, 2011). Seven [*Spirochaeta alkalica*, *Spirochaeta africana*, *Spirochaeta asiatica* (Zhilina *et al.*, 1996), *Spirochaeta americana* (Hoover *et al.*, 2003), *Spirochaeta dissipatitropha* (Pikuta *et al.*, 2009), *Spirochaeta halophila* (Greenberg & Canale-Parola, 1976) and *Spirochaeta perfilievii* (Dubinina *et al.*, 2011)] out of 19 species reported to date in the genus *Spirochaeta* (http://www.bacterio.cict.fr/s/spirochaeta.html) represent halophilic members. In this paper, we describe halo-alkaliphilic strains of the genus *Spirochaeta* isolated from a soda lake, Lonar, India.

Strain JC133^T and JC143 were isolated from a sediment sample collected from Lonar lake (Latitude 19° 58′, Longitude 76° 36′) after performing an enrichment in an alkaline medium II (Zhilina & Zavarzin, 1994) containing (g l^{-1}) $NaHCO_3$ (15); Na_2CO_3 (10); NaCl (10); $MgCl_2.6H_2O$ (0.2) and starch (5). Isolation and pure culture maintenance were done in an alkaline basic medium (Zhilina *et al.*, 1996) under strict anaerobic conditions and subjected to a polyphasic analysis. The

Abbreviations: BHD, bacteriohopane derivative; DPE, diploptene; DPL, diplopterol; MP, maximum-parsimony; NJ, neighbour-joining.

The GenBank/EMBL/DDBJ accession numbers for the 16S rRNA gene sequences of strains JC133^T and JC143 are HE806187 and HE962136, respectively.

Four supplementary figures are available with the online version of this paper.

International Journal of Systematic and Evolutionary Microbiology (2013), **63**, 2132–2137 **DOI** 10.1099/ijs.0.044107-0

Falsirhodobacter halotolerans gen. nov., sp. nov., isolated from dry soils of a solar saltern

Y. Subhash,[1] L. Tushar,[1] Ch. Sasikala[2] and Ch. V. Ramana[1]

Correspondence
Ch. V. Ramana
r449@sify.com *or*
sasi449@yahoo.ie

[1]Department of Plant Sciences, School of Life Sciences, University of Hyderabad, PO Central University, Hyderabad 500046, India

[2]Bacterial Discovery Laboratory, Centre for Environment, Institute of Science and Technology, J.N.T. University Hyderabad, Kukatpally, Hyderabad 500085, India

Two bacterial strains (JA744^T and JA745) were isolated from dry soil samples collected from solar salterns at Humma, Odisha, India. Both strains were Gram-stain-negative, catalase- and oxidase-positive, motile rods. Major fatty acids in both strains included $C_{18:1}\omega7c$, $C_{18:0}$ and $C_{16:0}$, while minor amounts of $C_{10:0}$ 3-OH, $C_{12:0}$, $C_{12:0}$ 3-OH, $C_{14:0}$ and $C_{16:0}$ were also present. Diphosphatidylglycerol, phosphatidylethanolamine, phosphatidylcholine, phosphatidylglycerol, an unidentified glycolipid, five unidentified lipids, an unidentified aminolipid and an unidentified phospholipid made up the polar lipids of both strains. Both strains had bacteriohopane derivatives (BHD1,2) and diploptene as major hopanoids. Mean genomic DNA G+C content was 75±1 mol% and the two strains were closely related (mean DNA–DNA hybridization >90 %). Phylogenetic analysis based on the 16S rRNA gene sequence showed that the two strains clustered with species of the genus *Rhodobacter* belonging to the family *Rhodobacteraceae* of the class *Alphaproteobacteria*. The highest sequence similarity was observed with *Rhodobacter sphaeroides* ATH2.4.1^T (96 %) and other members of the genera *Rhodobacter* and *Pseudorhodobacter* (<96 %). However, the two strains were positioned distinctly outside the group formed by the other genera of the family *Rhodobacteraceae*. Distinct morphological, physiological and genotypic differences from previously described taxa support the classification of these isolates as representatives of a novel species in a new genus, for which the name *Falsirhodobacter halotolerans* gen. nov., sp. nov. is proposed. The type strain of *Falsirhodobacter halotolerans* is JA744^T (=KCTC 32158^T =NBRC 108897^T).

Phototrophy is considered to be an important character in differentiating genera of phototrophs and chemotrophs (Imhoff & Caumette, 2004). Such a distinction is particularly clear for members of the family *Rhodobacteraceae*, where the phototrophic genera are distinguished from the nearest interspersed chemotrophs. A good example is the transfer of *Rhodobacter massiliensis* (Greub & Raoult, 2003) to a new genus, as *Haematobacter massiliensis* (Helsel *et al.*, 2007). In this communication, we report two novel non-phototrophic members of a new genus associated with the family *Rhodobacteraceae*, isolated from a solar saltern.

Strains JA744^T and JA745 were isolated from dry soils of an unused solar saltern at Humma, Odisha, India (GPS positioning of the sample collection site is 19° 25′ N 85° 04′ E), in December 2011. One gram dry soil was serially diluted [10-fold dilution in saline (0.6 % NaCl)] and plated on a medium (pH 7.0) containing (g l^{-1}) KH_2PO_4 (0.2), NH_4Cl (0.25), KCl (0.5), $CaCl_2.2H_2O$ (0.15), NaCl (1), $MgCl_2.6H_2O$ (0.62), Na_2SO_4 (2.84), HEPES (2.83), yeast extract (3.0), peptone (3), Casamino acids (0.5), glucose (0.5) and sodium pyruvate (3.0). Three distinct colony morphologies were observed from plates incubated at 30 °C for 3 days. Two pale-yellow colonies were selected for further purification and the purified isolates were designated strains JA744^T and JA445. Both cultures were preserved as glycerol stocks and by lyophilization and stored at 4 °C.

Genomic DNA was extracted and purified according to the method of Marmur (1961) and the G+C content of the DNA as determined by reversed-phase HPLC (Mesbah *et al.*, 1989) was 75±1 mol% for both strains JA744^T and JA745. Cell material for 16S rRNA gene sequencing was taken from a colony. DNA was extracted and purified by using a Qiagen genomic DNA extraction kit. Recombinant *Taq* polymerase (Genei) was used for PCR. The almost-complete 16S rRNA gene sequence was obtained using

Abbreviation: BChl, bacteriochlorophyll.

The GenBank/EMBL/DDBJ accession numbers for the 16S rRNA gene sequences of strains JA744^T and JA745 are HE662814 and HE662815.

Four supplementary figures and a supplementary table are available with the online version of this paper.

MINING BACTERIA FOR HOPANOIDS & GENOMIC INSIGHT OF HOPANOGENESIS : A CRITICAL ANALYSIS OF GLOBAL TRANSCRIPTIONAL RESPONSE OF SHC MUTANT OF RHODOPSEUDOMANU PALUSTRIS TIE - I

ORIGINALITY REPORT

%18	%9	%16	%3
SIMILARITY INDEX	INTERNET SOURCES	PUBLICATIONS	STUDENT PAPERS

PRIMARY SOURCES

1	Tushar, L., C. Sasikala, and C. V. Ramana. "Draft Genome Sequence of Rhodomicrobium udaipurense JA643T with Special Reference to Hopanoid Biosynthesis", DNA Research, 2014. Publication	%4
2	Lodha, Tushar Dilipchand, Are Srinivas, Chintalapati Sasikala, and Chintalapati Venkata Ramana. "Hopanoid inventory of Rhodoplanes spp.", Archives of Microbiology, 2015. Publication	%1
3	www.pnas.org Internet Source	%1
4	brcdownloads.vbi.vt.edu Internet Source	%1
5	transterm.cbcb.umd.edu Internet Source	%1